[redacted]

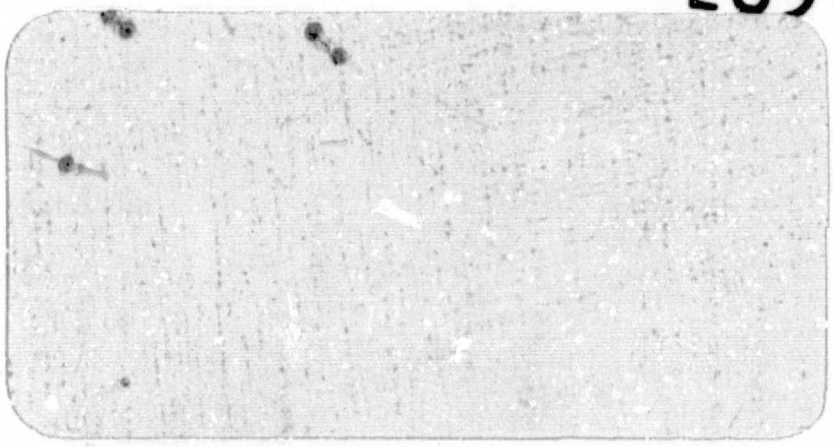

CRinc

THE UNIVERSITY of KANSAS CENTER for RESEARCH, INC.

2291 Irving Hill Drive-Campus West Lawrence, Kansas 66045

MODELING THE BACKSCATTERING AND TRANSMISSION PROPERTIES OF VEGETATION CANOPIES

FINAL REPORT

C. T. Allen*
F. T. Ulaby**

February 1984

Prepared for:

NASA Johnson Space Flight Center
Houston, Texas 77058

Contract NAS 9-15421

*C. T. Allen is presently affiliated with Sandia Corporation, Sandia Base, Albuquerque, New Mexico.

**F. T. Ulaby is presently with the Department of Electrical Engineering and Computer Science, University of Michigan, Ann Arbor, Michigan, 48109.

1. Report No.	2. Government Accession No.	3. Recipient's Catalog No.

4. Title and Subtitle
MODELING THE BACKSCATTERING AND TRANSMISSION PROPERTIES OF VEGETATION CANOPIES

5. Report Date
February 1985

6. Performing Organization Code

7. Author(s)
C. T. Allen, F. T. Ulaby

8. Performing Organization Report No.
RSL TR 360F

9. Performing Organization Name and Address
Remote Sensing Laboratory
University of Kansas Center for Research, Inc.
2291 Irving Hill Drive - Campus West
Lawrence, Kansas 66045-2969

10. Work Unit No.

11. Contract or Grant No.
NAS 9-15421

12. Sponsoring Agency Name and Address
David Pitts
NASA - Johnson Space Center
Houston, Texas 77058

13. Type of Report and Period Covered
Final Report

14. Sponsoring Agency Code

15. Supplementary Notes

16. Abstract

This investigation includes experimental measurements of canopy attenuation at 10.2 GHz (X-band) for canopies of wheat and soybeans, experimental observations of the effect upon the microwave backscattering coefficient (σ°) of free water in a vegetation canopy, and experimental measurements of σ° (10.2 GHz, 50°, VV and VH polarization) of 30 agricultural fields over the growing season of each crop. The measurements of the canopy attenuation through wheat independently determined the attenuation resulting from the wheat heads and that from the stalks. An experiment conducted to simulate the effects of rain or dew on σ° showed that σ° increases by about 3 dB as a result of spraying a vegetation canopy with water. The temporal observations of σ° for the 30 agricultural fields (10 each of wheat, corn, and soybeans) indicated that fields of the same crop type exhibit similar temporal patterns. Models previously reported were tested using these multitemporal σ° data, and a new model for each crop type was developed and tested. The new models proved to be superior to the previous ones.

17. Key Words (Suggested by Author(s))	18. Distribution Statement
Radar, Remote Sensing, Crops, Leaf-Area Index	

19. Security Classif. (of this report)	20. Security Classif. (of this page)	21. No. of Pages	22. Price*
Unclassified	Unclassifed	341	

*For sale by the National Technical Information Service, Springfield, Virginia 22161

NASA Form 1424 (Rev Nov 75)

NASA — JSC

TABLE OF CONTENTS

ACKNOWLEDGEMENT

This research is supported by NASA/GSFC Grant No. 923-677-24-01-16 92-2511, and is a continuation of work that was conducted at the University of Kansas under Grant NAG5-272.

LIST OF FIGURES

LIST OF TABLES

ABSTRACT

This investigation includes experimental measurements of canopy attenuation at 10.2 GHz (X-band) for canopies of wheat and soybeans, experimental observations of the effect upon the microwave backscattering coefficient (σ°) of free water in a vegetation canopy, and experimental measurements of σ° (10.2 GHZ, 50°, VV and VH polarization) of 30 agricultural fields over the growing season of each crop. The measurements of the canopy attenuation through wheat independently determined the attenuation resulting from the wheat heads and that from the stalks. An experiment conducted to simulate the effects of rain or dew on σ° showed that σ° increases by about 3 dB as a result of spraying a vegetation canopy with water. The temporal observations of σ° for the 30 agricultural fields (10 each of wheat, corn, and soybeans) indicated that fields of the same crop type exhibit similar temporal patterns. Models previously reported were tested using these mutlitemporal σ° data, and a new model for each crop type was developed and tested. The new models proved to be superior to the previous ones.

1.0 INTRODUCTION

A remote-sensing instrument--such as radar--mounted on a spaceborne platform offers enormous scientific and nonscientific potential. Tasks heretofore thought impossible now are becoming feasible on a global scale because of such systems. One of the applications for which spaceborne remote sensing seems custom-made is environmental monitoring. This includes but is not limited to monitoring snow coverage, sea-ice coverage, and land-use patterns, as well as determining the areal extent of vegetated land.

Sensors operating in various parts of the electromagnetic spectrum have been utilized for various applications. The more common sensors operate in the optical, thermal-infrared, millimeter, and microwave regions of the electromagnetic spectrum. Each sensor band or channel operates at a different wavelength and receives new information about the target by virtue of its spectral properties. Hence, an optical sensor operating alongside a microwave sensor can provide helpful supplementary data about the target being observed.

1.1 Radar as a Remote Sensing Tool

A sensor operating in the microwave region has certain advantages over one operating in the optical/thermal infrared region. The most widely known advantage is exemplified by the all-weather capability of radar sensors, i.e., the capacity of microwaves to penetrate clouds and precipitation without much attenuation. While this is certainly useful, there are other reasons that radars are good remote-sensing instruments. Because

of the wavelengths involved, microwaves can penetrate a variety of land-cover types to some extent, thus providing information on cover height or thickness, background material, etc. In addition, because radar provides its own source of illumination, both incidence angle and polarization can be regarded as free parameters to be optimized along with frequency or wavelength for a specific application.

The application to be investigated in this study is the use of radar as a remote sensor of vegetation, specifically, agricultural crops.

1.2 Agricultural Monitoring

From the standpoint of the user, desirable radar capabilities include the identification of crop type, the determination of where and to what extent plants within a given field are undergoing stresses that may have an impact on yield, and finally, the prediction of final yield. In order to provide such information, an understanding of the physical parameters affecting the quantity representing the sensor's output, σ^o, is needed.

Investigators (Brisco and Protz, 1980; Bush and Ulaby, 1978) have examined the effectiveness of microwave remote sensors (primarily radar) as target discriminators, i.e., the ability of radar to distinguish urban areas from forest from farmland. Further breakdown into crop types is possible in some cases, as a result of a crop's temporal "signature" (not to be confused with spectral signature). As examples of these "signatures," Figures 1.1 and 1.2 show temporal histories of σ^o from wheat. Figure 1.1

shows the temporal variation of σ^o from a winter wheat field in Manhattan, Kansas as measured at 13 GHz with a 50° incidence angle and VV polarization. For comparison purposes, the temporal behavior of the green leaf area index (LAI) is presented in the same plot. Figure 1.2 shows the temporal variation of σ^o from a spring wheat field in France as measured at 9 GHz with a 40° incidence angle and VV polarization. Again the accompanying LAI is presented as well. Note the similarities in the temporal behavior of σ^o, i.e., both exhibit an early peak followed by a low period followed by an increase in σ^o. Notice also the coincident increase in LAI followed by its decrease, which corresponds to a similar behavior in σ^o. Differences are also apparent, e.g., whereas the peak level of LAI from the Kansas field is about 8, the peak from the French field is only about 4. Yet the peak in σ^o from Kansas is about 0.23 $m^2\ m^{-2}$ or -6.4 dB, whereas the peak in σ^o from France is about +2 dB or 1.6 $m^2\ m^{-2}$. This difference may be a real one, although some of it is certainly due to calibration differences. Overall, it may be shown that wheat has a definite temporal signature, although at this point it is not known whether it is a unique one.

Another example of a crop's temporal signature is depicted in Figure 1.3. The temporal behavior of σ^o of corn for two consecutive years (1975 and 1976) at 14.2 GHz, 50° and 60° incidence angles, and HH polarization is shown. If we ignore the difference in incidence angles and proceed with our comparison, we see strikingly similar patterns, though some differences are also

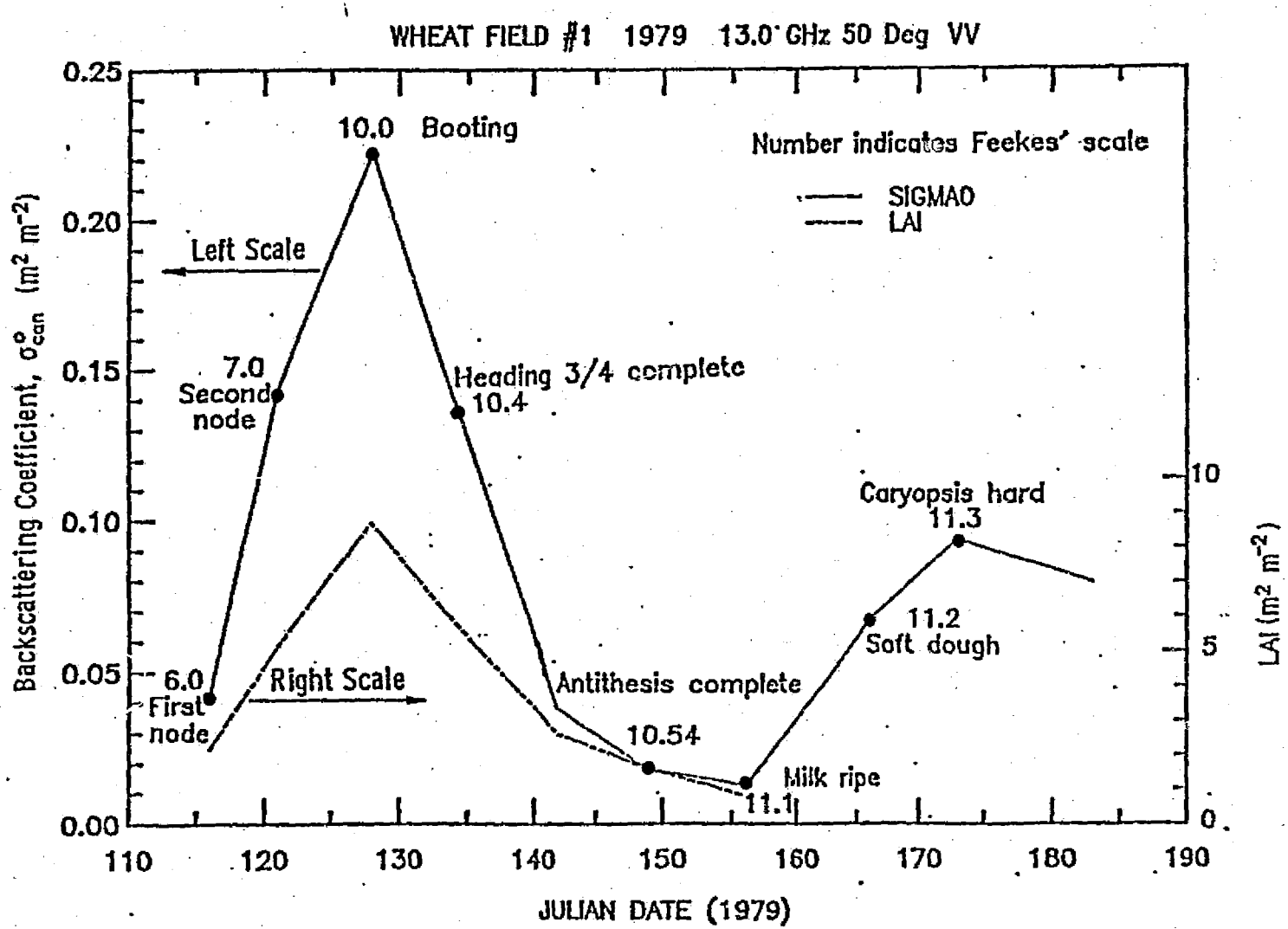

Figure 1.1 Temporal history of σ°_{VV} (13 GHz, 50°) and LAI from Manhattan, Kansas, as reported by Ulaby, et al. (1984). Stage of growth is indicated by Feekes' scale (Large, 1954).

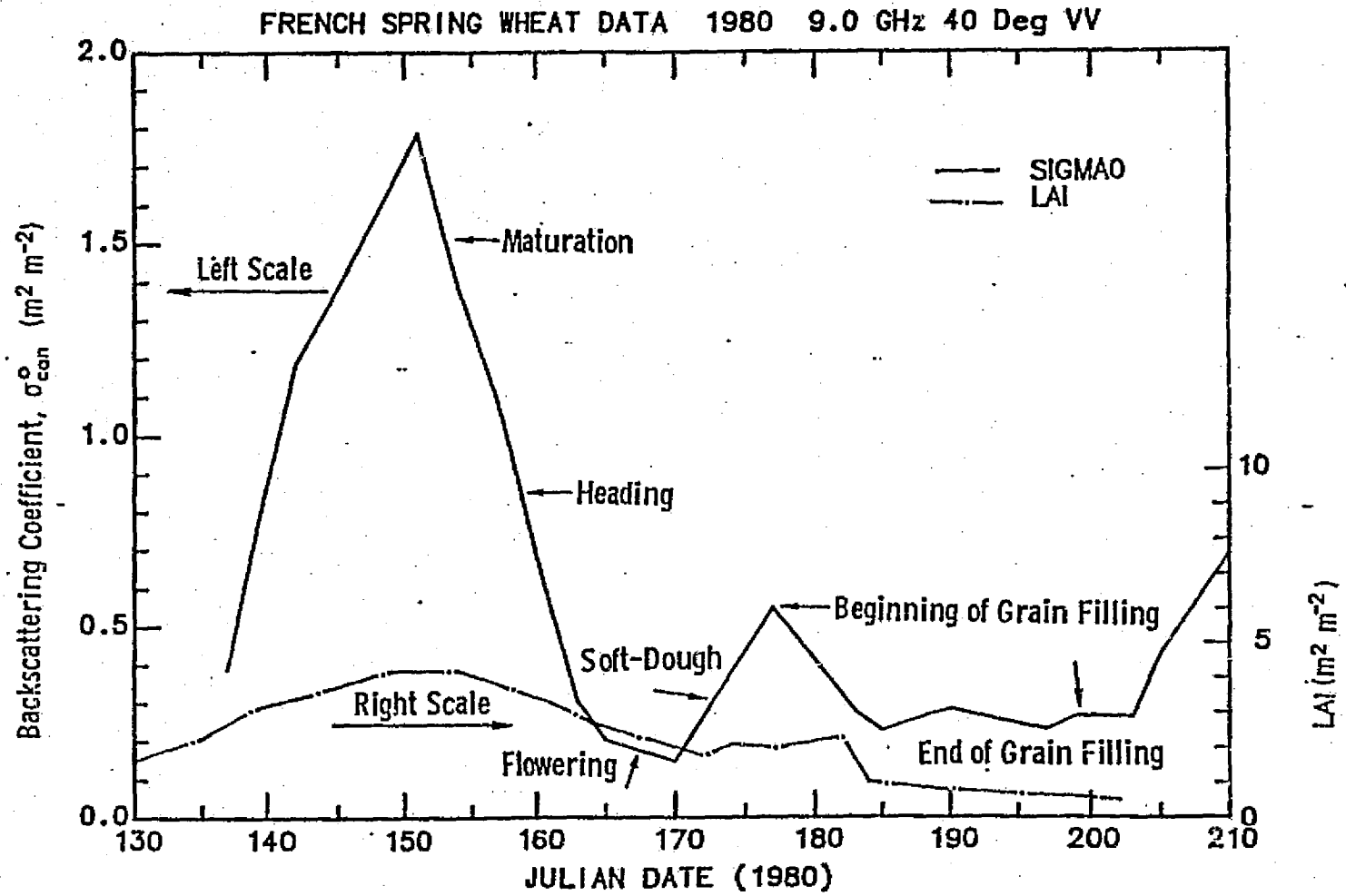

Figure 1.2 Temporal history of σ^o_{VV} (9 GHz, 40°) and LAI measurements made in France (from Huet, 1983).

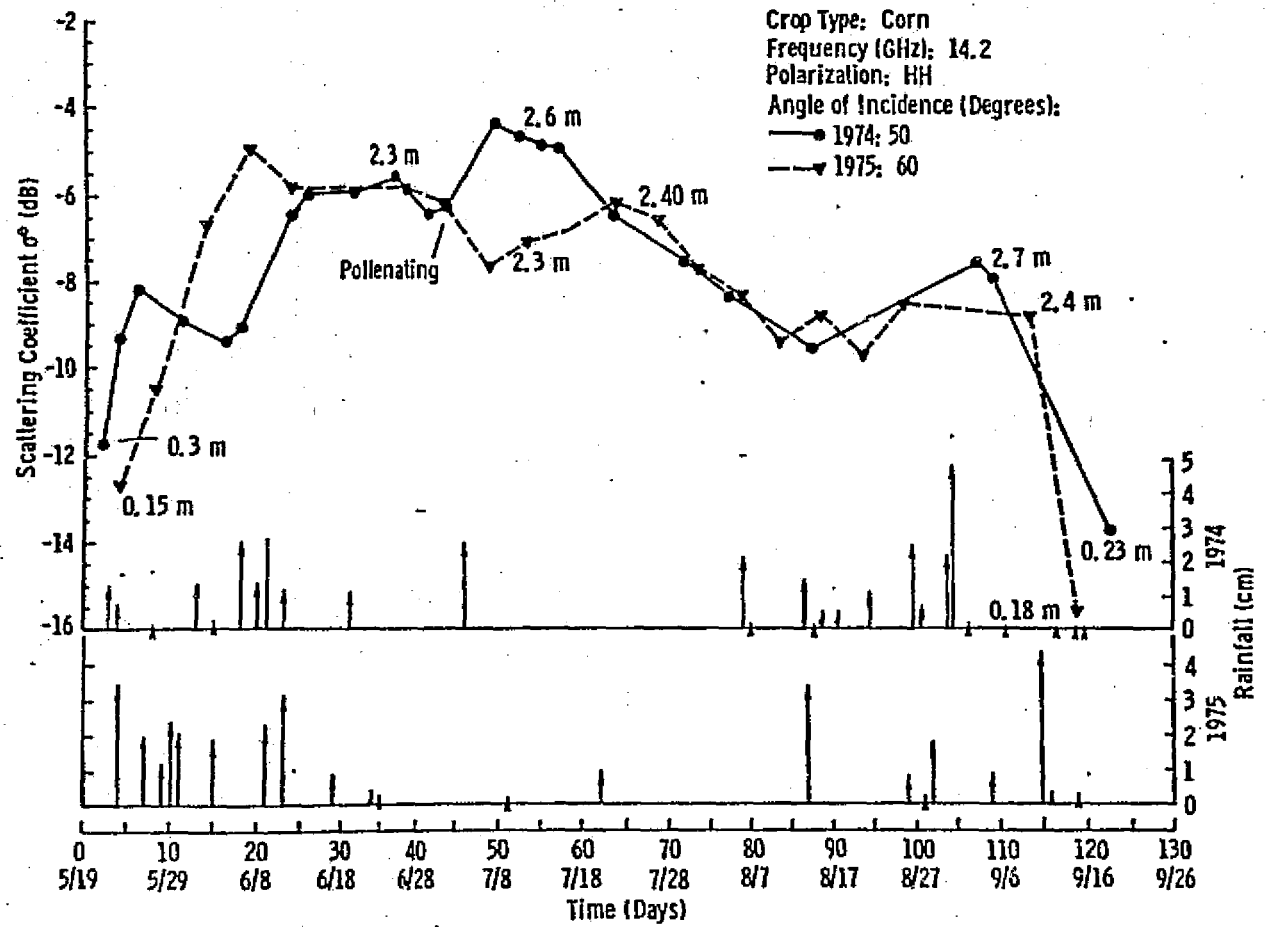

Figure 1.3 Comparison of 1974 and 1975 temporal variations of σ^o of corn over a period of four months. Also shown are the rainfall histories for the two years; the numbers next to the points on the graphs refer to canopy height (from Ulaby and Burns, 1976).

apparent. In view of these observations, it seems apparent that indeed there are temporal signatures which may be used in discrimination analyses.

1.3 The Need for Models

In order to use radar effectively as a remote sensing tool, the physics of the sensing process must first be understood. Such an understanding can be gained by investigations into theoretical electromagnetics and through extensive experimentation. The former provides explanations for certain observations in the experiments, whereas the latter verifies or refutes the proposed theories. Through these efforts, theoretical models are evolved; yet these models can also be considered empirical because they can be "fitted" to experimental data. As the models become more accurate, specific information about the physical properties of the target is needed to serve as input to the models.

When agricultural fields are used as targets, properties useful as inputs to these models include soil conditions, canopy attenuation, and plant dielectric constant. The role of the soil background in radar backscattering (σ^o) has been studied extensively both experimentally (Batlivala and Ulaby, 1977) and theoretically (Eom and Fung, 1982; Ulaby et al., 1982, Chapter 12). Data on canopy attenuation are very limited, although this state of affairs is changing (Ulaby and Jedlicka, 1983; Van Kasteren and Smit, 1977). Similarly, the dielectric properties of plant parts are only now being extensively studied. Theoretical models that incorporate these data have been

developed to varying degrees of complexity. For example, some treat the entire canopy as a homogeneous layer with inclusions that provide a suitable albedo (related to backscattering or σ^o) and attenuation, whereas others model a volume of leaves as having specific shapes and angular distributions. Clearly, the former model is more easily tested given the limited information about plant parameters (ground truth), whereas the latter requires extensive measurements and has therefore not been tested fully.

1.4 Scope of the Investigation

To further this line of research, this investigation included experimental data on canopy attenuation and σ^o from various canopies and attempted to extend current models in order to yield superior fits. An attempt to relate the temporal behavior of σ^o to harvested yield was made, using purely empirical approaches as well as other appropriate methods currently in use. Finally, this investigation extended its findings to examine the effects of varying sensor properties, i.e., the effects of frequency, incidence angle, and polarization, on σ^o.

developed to varying degrees of complexity. For example, some treat the entire canopy as a homogeneous layer with inclusions that provide a suitable albedo (related to backscattering or σ^o) and attenuation, whereas others model a volume of leaves as having specific shapes and angular distributions. Clearly, the former model is more easily tested given the limited information about plant parameters (ground truth), whereas the latter requires extensive measurements and has therefore not been tested fully.

1.4 Scope of the Investigation

To further this line of research, this investigation included experimental data on canopy attenuation and σ^o from various canopies and attempted to extend current models in order to yield superior fits. An attempt to relate the temporal behavior of σ^o to harvested yield was made, using purely empirical approaches as well as other appropriate methods currently in use. Finally, this investigation extended its findings to examine the effects of varying sensor properties, i.e., the effects of frequency, incidence angle, and polarization, on σ^o.

2.0 CANOPY ATTENUATION MEASUREMENTS

2.1 Introduction

Using the microwave spectrum to monitor agricultural targets shows significant potential (Brisco and Protz (1980); Bush and Ulaby (1978)). In order to utilize this potential to its fullest extent, an understanding of the interaction between electromagnetic energy and a crop canopy is necessary.

The backscattering from a vegetation canopy consists of scattering from three sources: the direct backscattering from plants, the direct backscattering from soil (including the two-way attenuation by the canopy), and multiple scattering from plants/soil. A visual interpretation of these three scattering sources is presented in Figure 2.1a. Due to the fact that the multiple scattering term involves two (or more) reflections, it is generally considered to be insignificant when compared to the sum of the direct backscattering terms. For this reason, most models attempting to predict the magnitude of the backscattered energy ignore the multiple scattering term. Hence, the backscattering process may be visualized as depicted in Figure 2.1b.

Empirical models with a theoretical basis, but incorporating measured data, have been developed by Attema and Ulaby (1978), Hoekman et al. (1982), and Ulaby et al. (1984), among others. These models all have the same basic structure, i.e., the backscattered energy received by the receiver is composed primarily of two components: (1) vegetation backscattering and (2) soil backscattering attenuated by vegetation. Mathematically, the models may be written in the form

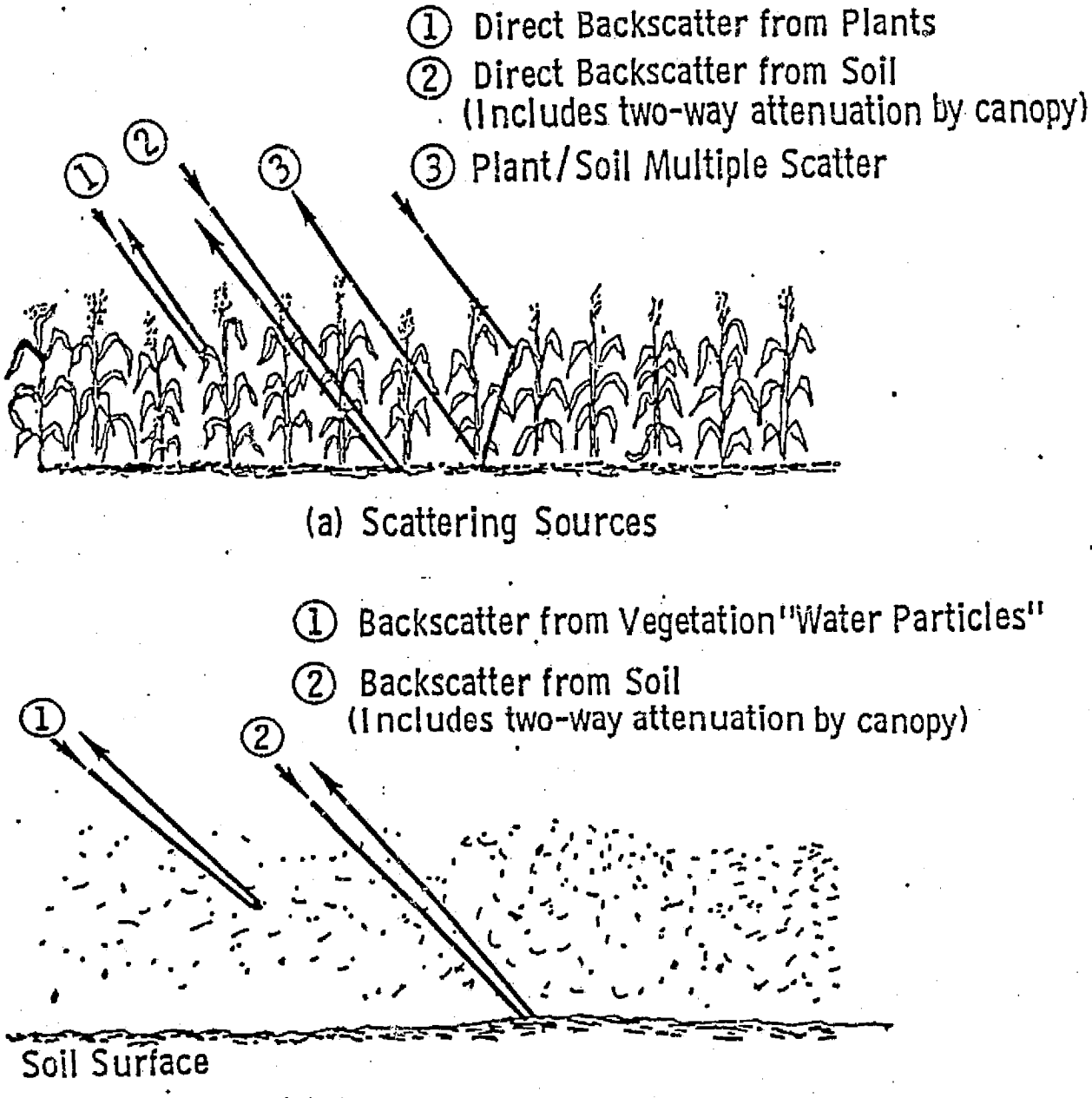

Figure 2.1 Backscattering contributions from a vegetation canopy: (a) scattering sources and (b) equivalent "cloud" representation in terms of water scatterers.

$$\sigma^o_{can} = \sigma^o_{veg} + \sigma^o_{soil}/L^2, \qquad (2.1)$$

where σ^o_{can} is the total backscattering coefficient reaching the receiver, σ^o_{veg} is that part of σ^o_{can} due entirely to backscattering by plant parts, and σ^o_{soil} is that part of σ^o_{can} due to backscattering from the underlying soil surface attenuated twice by the vegetation canopy (hence the L^2 term).

The part of σ^o_{can} resulting from soil backscattering has been investigated previously (Batlivala and Ulaby 1977; Dobson and Ulaby 1979) and was found to be dependent on three soil parameters: (1) surface roughness, which may be characterized by an effective RMS height and correlation length, (2) soil texture, and (3) soil moisture. For a given field, the first two should not change appreciably over the growing season. The third parameter, however, changes on an almost daily basis. Models characterizing the effect of moisture changes on σ^o_{soil} (for a given frequency, polarization, and incidence angle) take the form (Ulaby et al., 1982)

$$\sigma^o_{soil} = A \cdot \exp(B \cdot m_s) \quad (m^2m^{-2}), \qquad (2.2)$$

where A and B are constants that incorporate the roughness and texture factors, and m_s is the soil moisture content of the surface layer.

Thus, the soil component of σ^o_{can} is predictable, leaving σ^o_{veg} and L as unknowns. In attempting to model these components it is

helpful to establish reasonable values for each. Since σ^o_{can} can be measured directly, and σ^o_{soil} can be estimated, knowledge of one component yields knowledge of the other.

2.2 Review of Past Results

In the past, a number of people have attempted to measure the attenuation of microwave energy by plants. In 1974, Attema and Kuilenburg (1974) reported two-way attenuation coefficients for potatoes, oats, barley, and wheat ranging from 30 dB m^{-1} for potatoes to 12 dB m^{-1} for wheat. The measurements were made at X-band, using a 45° incidence angle and VV polarization. In 1977, van Kastern and Smit (1977) reported one-way attenuation coefficients for potatoes at six locations within a single field on a single day at X-band. Their values ranged from 25.4 dB m^{-1} to 63.6 dB m^{-1}. They attributed this variability to the number of leaves present between the transmitter and receiver.

In 1970, Story, Johnson, and Stewart (1970) reported one-way attenuation through wheat at 16 GHz with a 90° incidence angle through a canopy 5 feet wide (152 cm). From their data, which were acquired using wheat at the harvest point, i.e., having about 10% moisture content (wet basis), one-way attenuation coefficients were computed to be 1.1 dB m^{-1} and 0.43 dB m^{-1} through stalks (900 stalks per m^{-2}) at V and H polarizations, respectively, and between 7.8 and 12.8 dB m^{-1} through the heads (900 heads per m^{-2}). In 1984, Ulaby and Jedlicka (1984) reported one-way attenuation values through corn and soybean canopies on a temporal basis at 10.2 GHz with a 52° incidence angle and V polarization.

For corn, their values ranged from about 8 dB m^{-1} early in the season to about 5.8 dB m^{-1} at full canopy height (2.7 m). For soybeans, their values ranged from about 6.9 dB m^{-1} early in the season (height = 20 cm) to about 22.6 dB m^{-1} at full canopy height (102 cm).

Lopes (1983) reported one-way attenuation through wheat stalks at 9 GHz with a 90° incidence angle as a function of polarization. The values ranged from about 23 dB for purely vertical polarization to about 1 dB for horizontal.

2.3 Experiment Description

In order to determine values for head attenuation and stalk attenuation in wheat under natural field conditions, measurements were made on 23 June 1983 on a winter wheat field in the north Lawrence (Kansas) area. See Table 2.1 for crop and field parameters.

The equipment used in making these measurements included the Mobile Agricultural Radar Sensor (MARS), which is a truck-mounted FM-CW X-band scatterometer that operates at 10.2 GHz. The system is described in Gable et al. (1981) and a summary of its parameters are presented in Table 2.2. Also used in these experiments was a small (7- x 5-cm aperture) X-band horn antenna connected via a detector to a logarithmic power scope comprising the receiver. The experiment consisted of the following steps: with the transmitting antenna approximately 10 m above the soil and transmitting at 10.2 GHz (60° incidence angle, vertically

Table 2.1

Winter Wheat Attenuation Experiment

Ground-Truth Data

Measured σ^o (50° Incidence Angle, 10.2 GHz)

σ^o_{VV} = -15.14 dB

σ^o_{VH} = -20.74 dB

Canopy height:	105 cm
Head length:	8 cm
Plant density:	900 plants m^{-2}
Row spacing:	20 cm
Head moisture:	45% (wet basis, gravimetric)
Leaf moisture:	16% (wet basis, gravimetric)
Stalk moisture:	63% (wet basis, gravimetric)
Soil moisture:	20.9% (dry basis, gravimetric, 0-2 cm)
Head water content:	0.437 kg m^{-2}
Leaf water content:	0.034 kg m^{-2}
Stalk water content:	1.173 kg m^{-2}

TABLE 2.2

MARS System Parameters

Type	FM-CW
Modulation	Triangular
Frequency: f_o	10.2 GHz
RF Bandwidth: Δf	420 MHz
Transmitter Power	60 mW
IF Frequency: f_{IF}	22 KHz
Antennas:	
Height above ground	9.3 m
Transmit-antenna diameter	30 cm
Cross-polarization antenna	standard gain horn
Transmit feed	dual dipole
Beamwidths of product patterns $(G_T(\theta,\phi) \cdot G_R(\theta,\phi))$	
VV Elevation:	3.96°
Azimuth :	4.31°
VH Elevation:	5.44°
Azimuth :	5.14°
Look-Angle Range: θ	20° - 80° from vertical
Dynamic Range:	50 dB

polarized) the receiving antenna was placed in the field, within the main beam of the transmitting antenna. This receiving antenna was mounted on a structure that enabled the operator to continuously vary its height above the soil from 132 cm down to 23 cm. The height of the receiving antenna was output as a voltage via a potentiometer. Thus, by monitoring the output of both the power meter and the height-voltage, information about attenuation versus height was available. To remove any effects due to antenna gain variations, the system was also calibrated without a canopy between the antennas at the same range and incidence angle. The result of this calibration was then removed from the data, thus leaving only the effects of the canopy.

2.4 Results

From six locations within the same field, separated by approximately one meter, canopy attenuation profiles were recorded under two conditions. First a profile was made under normal conditions. Then, from the same position, another profile was made of the same area, but with the wheat heads removed. A sample plot is shown in Figure 2.2. Notice that the profile of the canopy with the heads intact shows higher attenuation than the profile with the heads removed. Also note the strong oscillations in the profile that includes the heads. To examine the effect of the heads alone, the difference between the two curves was plotted against the height of the receiving antenna. By multiplying the height scale by $\tan\theta$, the x-scale was converted into horizontal distance from the receiving antenna in the direction towards the

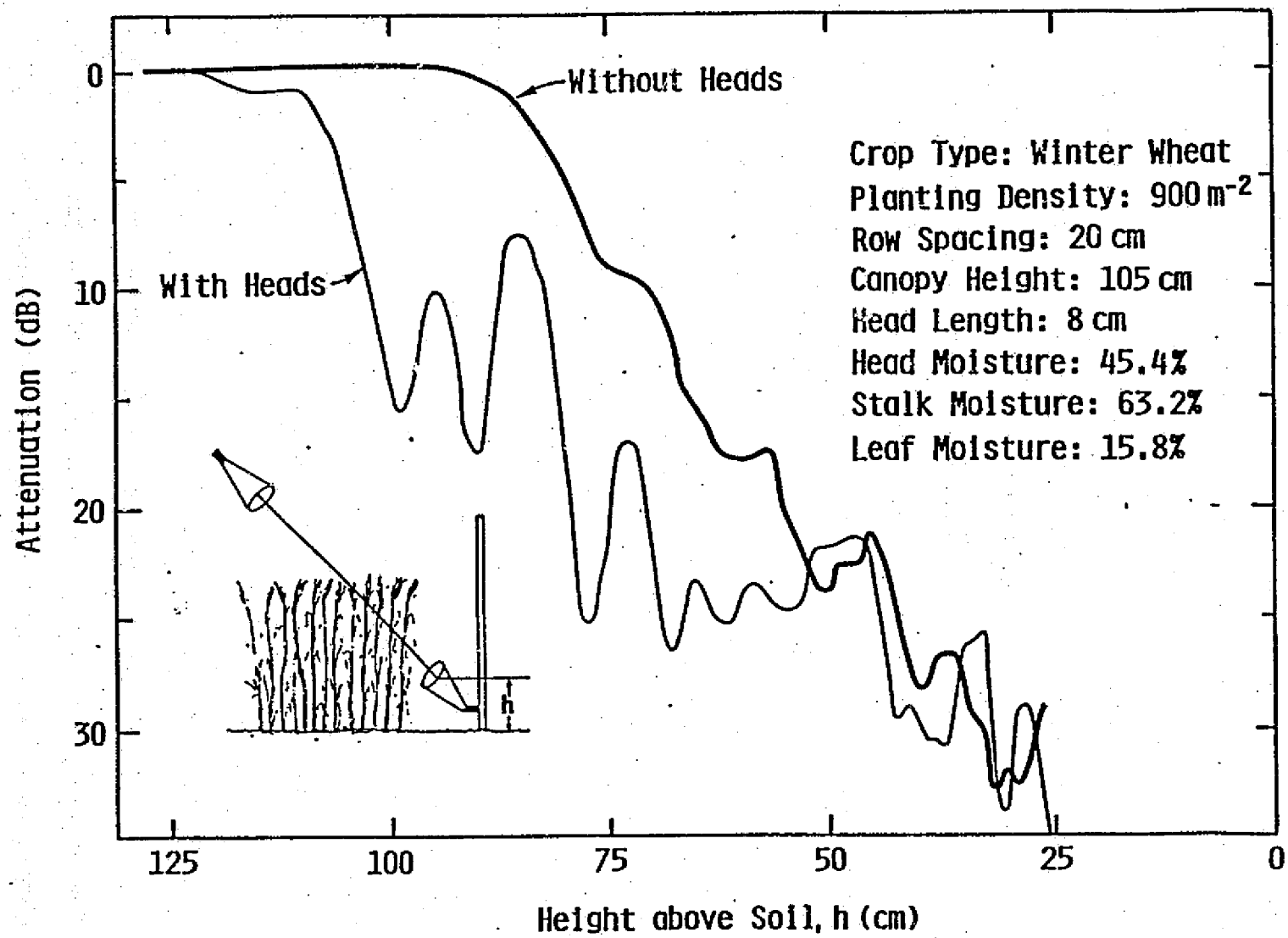

Figure 2.2 Example of data acquired using the vertical attenuation device.

transmitting antenna. A sample plot, as described, for one of the six locations is shown in Figure 2.3. In addition to the overall level of approximately 11 dB, notice the oscillatory behavior indicated in Figure 2.3. The spacing between peaks is roughly 20 cm, which corresponds to the row spacing. This may be explained as a clustering of the heads every 20 cm, whereas in between, the density drops. Based on such head-attenuation values from all six locations, a histogram of the head attenuations was produced and is shown in Figure 2.4. From these data the mean head attenuation under these conditions was found to be approximately 8.3 dB, which corresponds to an attenuation coefficient of 52 dB m^{-1}. If we assume that the attenuation coefficient is proportional to the imaginary part of the refractive index of the heads, n''_{head}, comparisons with Story's data are possible. At 10% moisture, $n''_{head} \simeq 0.16$ at 12.2 GHz (Nelson and Stetson, 1976) and at 24% moisture $n''_{head} \simeq 0.48$. In obtaining these values, a correction for bulk densities was made in accordance with Nelson (1976). By extrapolating in a linear fashion, at 45% moisture $n''_{head} \simeq 0.95$. Thus had Story et al. measured heads with 45% moisture, they might have seen attenuation coefficients ranging from 45 to 74 dB m^{-1} at 900 heads m^{-2}, which was the head density in the RSL experiment. Thus the numbers obtained here seem appropriate.

In addition to information about head attenuation, stalk attenuation data are also available from this series of measurements. By taking the overall attenuation due to the stalks (the leaves are neglected, as they contain only 16% moisture,

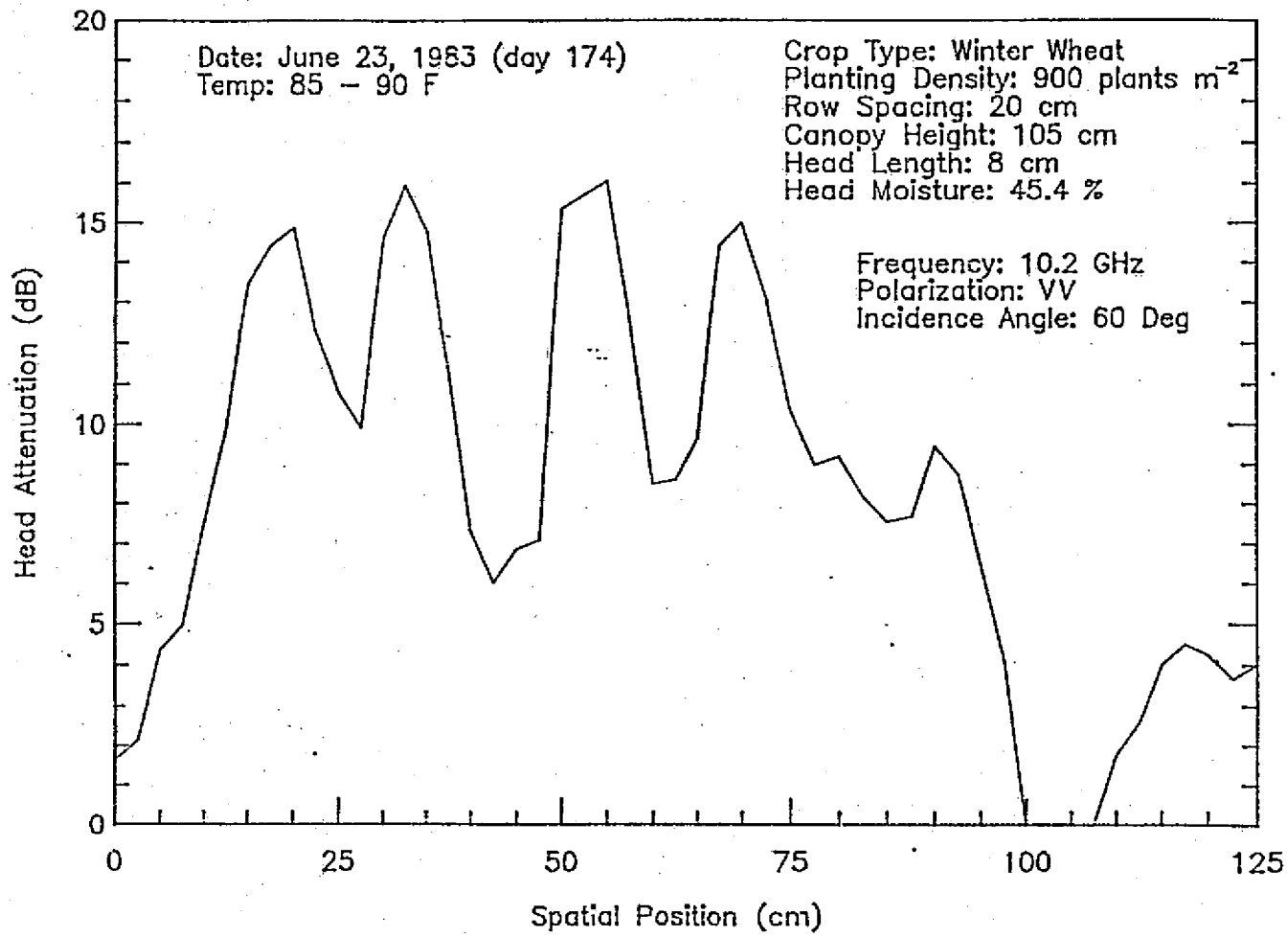

Figure 2.3 Plot of head attenuation as a function of horizontal position.

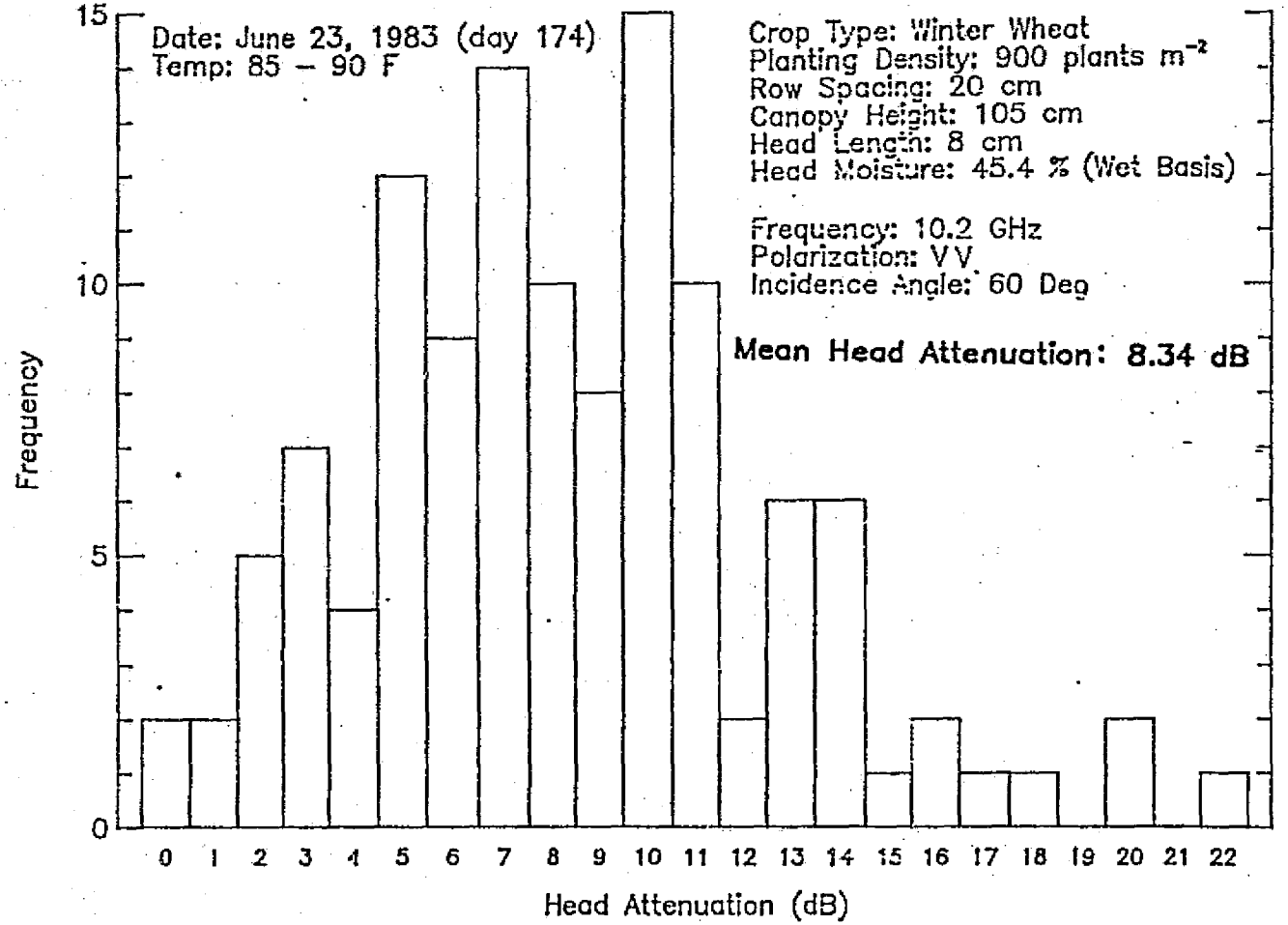

Figure 2.4 Histogram of head attenuation from all six locations.

whereas the stalks contain 63%) and dividing by the height of the stalks determined from each plot of attenuation versus height, an attenuation coefficient due to stalks is obtained for each location; Figure 2.5 shows these values. In addition to the overall magnitude, notice also the variability between locations. This is attributed to within-field variability in plant moisture and density, the latter being the more dominant factor.

An identical experiment was tried on a spring wheat field, also in the North Lawrence area, on July 29, 1983. Table 2.3 gives the crop and field parameters. By this date the canopy was ready for harvest, with all plant parts having moisture contents of only 8% (wet basis). Attenuation profiles were made under three conditions: full canopy, canopy without heads, and no canopy. Under all three conditions, at two locations, no difference was seen in the profiles, i.e., no measurable attenuation due to the canopy was taking place.

2.4.1 Absorption Loss Factor of Canopy Stalks

This section provides an approximate method for computing the absorption loss factor $L_a^{st}(\theta,p)$ for a canopy of thin vertical stalks of height h. The major requirement of the method is that the stalk's diameter be much smaller than the wavelength λ, where $\lambda = \lambda_0/\sqrt{\epsilon_v'}$ is the wavelength in the stalk material with relative permittivity ϵ_v'. Thus, the size condition depends on the stalk diameter d, the water content of the stalk material (which in turn determines ϵ_v), and the signal wavelength λ_0. This means that the

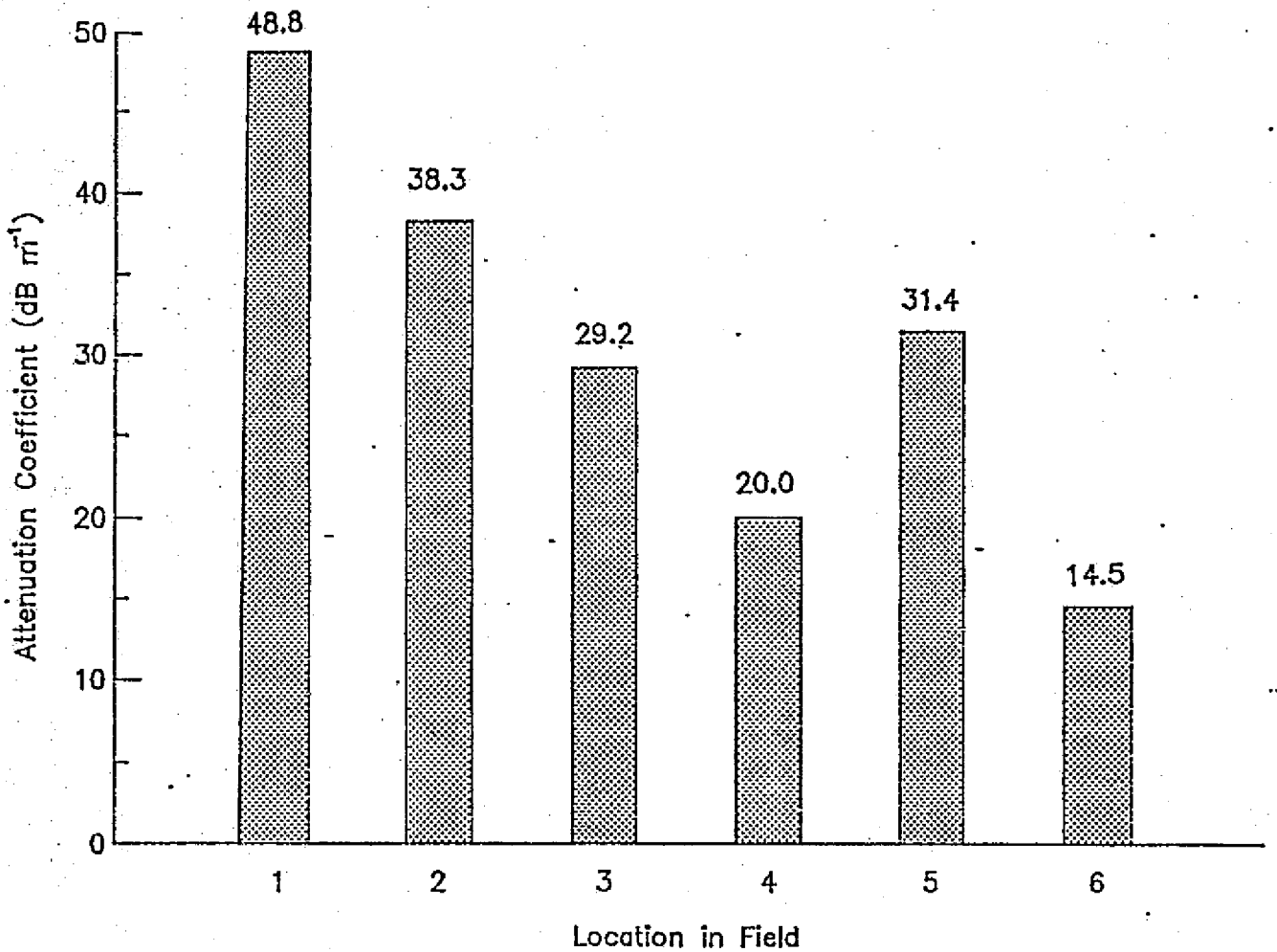

Figure 2.5 Graphic display of the way in which the stalk attenuation coefficient varies.

Table 2.3

Spring Wheat Attenuation Experiment
Ground-Truth Data

Measured σ^o (50° Incidence Angle, 10.2 GHz)

$$\sigma^o_{VV} = -12.53 \text{ dB}$$

$$\sigma^o_{VH} = -20.83 \text{ dB}$$

Canopy height:	70 cm
Head moisture:	8.6% (wet basis, gravimetric)
Stalk moisture:	8.1% (wet basis, gravimetric)
Soil moisture:	2.5% (dry basis, gravimetric)

condition is easily met for wheat stalks ($d \simeq 0.2$ cm) at 10 GHz ($\lambda_0 = 3$ cm), even for very moist stalks ($\varepsilon_v' \simeq 30$). When the size condition is violated, the loss value obtained may still prove to be a useful estimate, albeit a rough one, of the true loss attributed to stalks.

Parts (a) and (b) of Figure 2.6 depict, respectively, a horizontally polarized wave and a vertically polarized wave incident upon the upper surface of a dielectric slab consisting of thin parallel cylinders oriented along the z-axis. The parallel orientation of the cylinders leads to the characterization of the slab as an anisotropic dielectric medium with

$$\overset{\leftrightarrow}{\varepsilon} = \hat{x}\,\varepsilon^x + \hat{y}\,\varepsilon^y + \hat{z}\,\varepsilon^z \,. \tag{2.3}$$

Because of azimuthal symmetry, $\varepsilon^x = \varepsilon^y$. Such a medium is called a uniaxial crystal in optics (Born and Wolf, 1965, Ch. 14) and the direction of orientation of the cylinders is referred to as the optic axis. In the present treatment, the optic axis is parallel to the surface normal of the slab (z-direction).

The dielectric components ε^x and ε^z can be related to the relative dielectric constants of the inclusion (stalk) and host materials, ε_v and ε_h, respectively, and the inclusion volume fraction (volume of stalks per unit volume of canopy) v_{st} by the dielectric mixing formulas given by Polder and Van Santen. Specifically, for v_{st} small (typically, $v_{st} \simeq 10^{-3}$ to 10^{-2}) and $\varepsilon_h = 1$ (air), they become

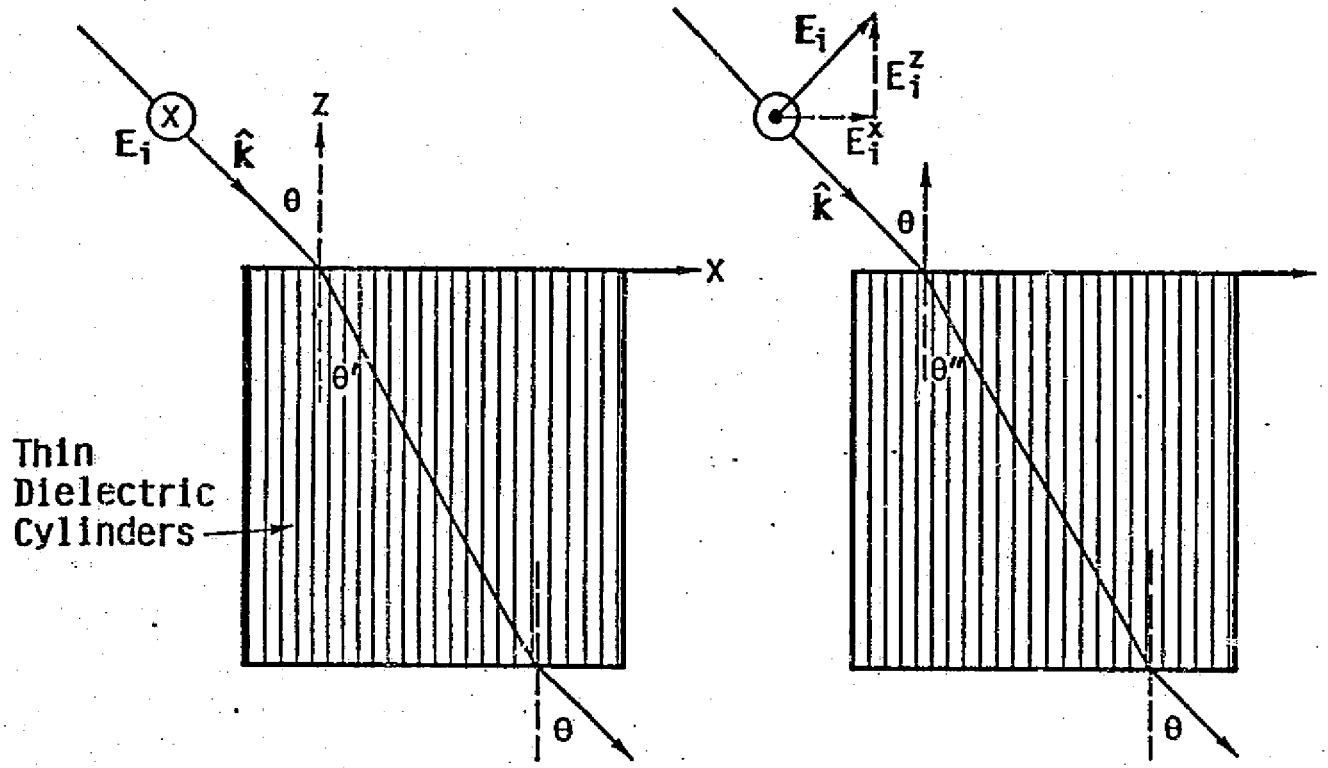

(a) Horizontal Polarization (b) Vertical Polarization

Figure 2.6 A depiction of how a number of thin, parallel cylinders behave as a uniaxial crystal.

$$\varepsilon^x = \varepsilon^y = 1 + 2\, v_{st}\left(\frac{\varepsilon_v - 1}{\varepsilon_v + 1}\right) \tag{2.4}$$

and

$$\varepsilon^z = 1 + v_{st}(\varepsilon_v - 1). \tag{2.5}$$

Each of the above relative dielectric constants is in general a complex quantity, $\varepsilon = \varepsilon' - j\varepsilon''$. Also, as we shall see below, ε^x and ε^y are associated with the propagation of an "ordinary" wave, and ε^z is associated with the propagation of an "extraordinary" wave through the crystal (dielectric slab). Hence, we shall use the notation $\varepsilon^x = \varepsilon^y = \varepsilon_o$ and $\varepsilon^z = \varepsilon_e$, where the subscripts "o" and "e" denote ordinary and extraordinary, respectively. These substitutions lead to

$$\varepsilon_o' = 1 + 2\, v_{st}\left[\frac{(\varepsilon_v' - 1)(\varepsilon_v' + 1) + (\varepsilon_v'')^2}{(\varepsilon_v' + 1)^2 + (\varepsilon_v'')^2}\right] \tag{2.6}$$

$$\varepsilon_o'' = \frac{4\, v_{st}\, \varepsilon_v''}{(\varepsilon_v' + 1)^2 + (\varepsilon''_v)^2} \tag{2.7}$$

$$\varepsilon_e' = 1 + v_{st}(\varepsilon_v' - 1) \tag{2.8}$$

$$\varepsilon_e'' = v_{st}\, \varepsilon_v''\,. \tag{2.9}$$

For stalks with a high moisture content, ε_v' and ε_v'' are each larger than 10, in which case ε_0' and ε_0'' can be simplified to

$$\varepsilon_0' \simeq 1 + 2\, v_{st} \tag{2.10}$$

$$\varepsilon_0'' \simeq \frac{4\, v_{st}\, \varepsilon_v''}{(\varepsilon_v')^2 + (\varepsilon_v'')^2} . \tag{2.11}$$

Since ε_v' and ε_v'' increase with increasing moisture content at comparable rates, the above expression for ε_0'' leads to the result that ε_0'' decreases with increasing moisture content of the stalks. In the limit where the stalks are "perfect conductors" with $\varepsilon_v'' = \infty$, we have $\varepsilon_0'' = 0$. This implies that ordinary waves propagate through such a uniaxial crystal with no dielectric loss. Since the electric field for an ordinary wave is in the x-y plane, it cannot induce currents in vertical wires if the diameter of wire is sufficiently small relative to λ to be considered zero. Hence, there is no absorption and no conduction, i.e., there is no dielectric loss.

According to the treatment of wave propagation in uniaxial crystals given by Born and Wolf (1965, Ch. 14), the results given below apply to the configurations shown in Figure 2.6.

Horizontal Polarization

The attenuation coefficient for a horizontally polarized wave (Figure 2.6(a)) is given by

$$\alpha_h = \frac{2\pi}{\lambda_0} n''_o \ , \tag{2.12}$$

where

$$n''_o = |\mathrm{Im}\ \{\sqrt{\varepsilon_o}\}|. \tag{2.13}$$

Since v_{st} is very small, $\varepsilon''_o \ll 1$ and

$$\alpha_h \simeq \frac{\pi}{\lambda_0} \varepsilon''_o \ . \tag{2.14}$$

The stalk's dielectric loss factor for canopy height h is

$$L_a^{st}(\theta,h) = \exp(2\ \alpha_h\ h\ \sec\theta). \tag{2.15}$$

Vertical Polarization

Although in the general case $\theta'' \neq \theta' \neq \theta$, these three angles are approximately equal for a stalk canopy because ε'_o and ε'_e are each only slightly larger than 1. This is a consequence of having air as the background material in the canopy and of the fact that the volume fraction of stalks, v_{st}, is of the order of 10^{-2} or smaller.

The attenuation coefficient for a vertically polarized wave (Figure 2.6(b)) is

$$\alpha_v = \frac{2\pi}{\lambda_0} n''_v \ , \tag{2.16}$$

where

$$n''_v = n''_o \cos^2 \theta + n''_e \sin^2 \theta, \tag{2.17}$$

$$n''_e = |\mathrm{Im}\ \{\sqrt{\varepsilon_e}\}|, \tag{2.18}$$

and n''_o is given by (2.13). Finally, the dielectric loss factor for canopy height h is given by

$$L_a^{st}(\theta,v) = \exp(2\ \alpha_v\ h\ \sec\theta). \tag{2.19}$$

Application to Experimental Data

This model may be applied to all three sets of data mentioned earlier concerning wheat stalks: (1) this data set, (2) Story's data, and (3) Lopes' data.

In the first set, wheat stalks were observed at 10.2 GHz with an incidence angle of 60°. The mean of measurements from six locations is 30.4 dB m^{-1} with a standard deviation of 12.4 dB m^{-1}. From the measured plant parameters, a volumetric water content of 35% was computed. Based on measurements made by Ulaby and Jedlicka (1983) of wheat stalks at 8 GHz, the stalks were found to have a dielectric of 10.81 -j4.53. By applying the mixing formulas reported by Polder and Van Santen (1946) and de Loor (1968) for needle-like inclusions comprising a volume fraction of 0.00363, the dielectric along the vertical or z-direction was computed to be 1.036 - j0.01644, whereas the

horizontal or x- or y-direction was 1.006 - j0.00042. Based on these values, the model for uniaxial media gives an index of refraction for a vertically polarized wave propagating at an angle of 60° from the optical axis of 1.014 - j0.00611, which corresponds to a one-way attenuation of 21.1 dB m^{-1}. The measured value of 30.4 dB m^{-1} is within one standard deviation (12.4 dB m^{-1}) of the computed value.

The next set, Story's data at 16 GHz, is for dry stalks. He reports the vertical attenuation coefficient to be 0.55 dB m^{-1}, whereas the horizontal coefficient is 0.22 dB m^{-1} through a planting density of about 900 plants m^{-2}. Using stalk dielectric data at 8 GHz, modified to fit the vertical polarization data (0.54 dB m^{-1}), the horizontal attenuation coefficient was computed using the technique described above. It was found to be 0.25 dB m^{-1}, which yields a ratio of 2.2:1 (dB) relative to the measured ratio of 2.5:1 (dB). It would seem that this model again proves satisfactory.

Finally, a plot of Lopes' data along with the modeled fit is shown in Figure 2.7. His $\alpha_{||}$ and $\alpha_{\perp}$ correspond to extraordinary and ordinary wave attenuation. Clearly, the model provides close agreement to the measured data. Since the wave's direction of propagation is orthogonal to the optical axis of the uniaxial medium, the wave is simply decomposed into extraordinary (V polarization) and ordinary (H polarization) components, attenuated appropriately, added once again, and then squared to yield the power. The ratio here between vertical and horizontal attenuation is about 20:1 (dB) or about 100:1 in real units, which is higher

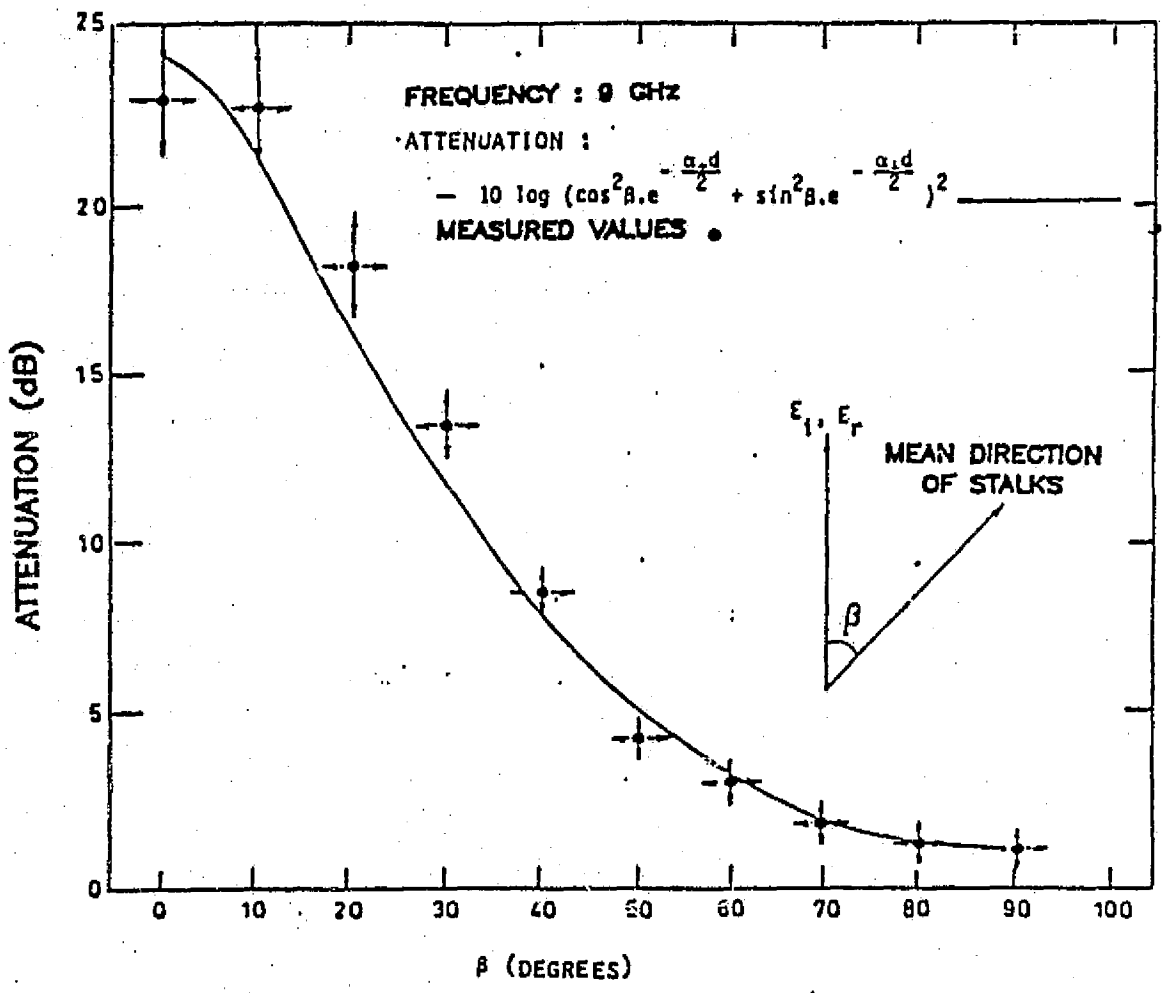

Figure 2.7 Data and model reported by Lopes (1983) showing how attenuation through wheat stalks is dependent on polarization.

than Story's data by two orders of magnitude. This is due to the higher stalk moisture content.

2.4.2 Absorption Loss Factor for Wheat Heads

A similar situation is seen in the wheat-head absorption data. The measurements by Lopes (1983) shown in Figure 2.8 indicate unequal attenuation through the heads at 9 GHz at a 90° incidence angle for V and H polarizations. This again implies a uniaxial-like behavior yielding a larger absorption factor for vertical polarization than for horizontal. Further complicating the situation is the fact that the heads are not as uniformly vertical as the stalks, and due to their larger dimensions (comparable to a wavelength at X-band), a substantial part of the attenuation may be due to scattering. Accurate measurements have yet to be devised to quantify the latter effect.

Ignoring these added complexities, a computation of the loss due to absorption is possible. The heads may be modeled as prolate spheroids whose major axes are all vertically parallel. Again, the de Loor formula applies with the following results:

$$\varepsilon_m = 1 + \frac{v_h\,(\varepsilon_h - 1)}{1 + A_u\,(\varepsilon_h - 1)}, \qquad u = a,\ b,\ \text{or}\ c \qquad (2.20)$$

where

$$A_c = \frac{1 - e^2}{2\,e^3}\left[\ln\left(\frac{1 + e}{1 - e}\right) - 2e\right] \qquad (2.21)$$

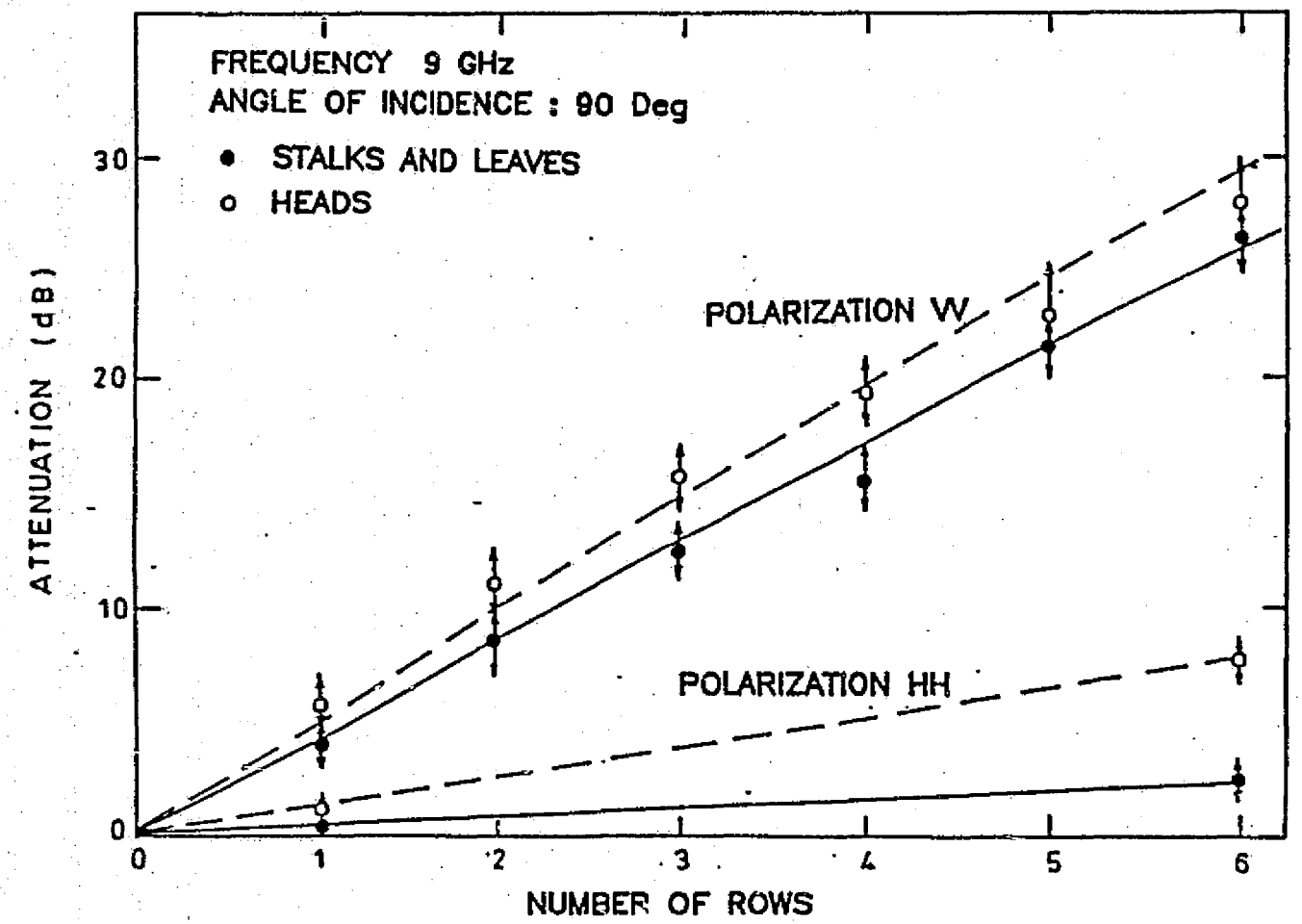

Figure 2.8 Data reported by Lopes (1983) showing a polarization dependence in the attenuation through wheat heads.

$$A_a = A_b = (1 - A_c)/2 \tag{2.22}$$

and

$$e = [1 - (a/c)^2]^{1/2}; \quad c > a = b \tag{2.23}$$

where a and b represent the x- and y-directions, and c denotes the z- or vertical direction. Also, v_h and ε_h are the volume fraction and dielectric constant of the inclusion material (heads) and the dielectric of the host medium (air) is 1. Eccentricity, e, is given in terms of the ratio of the minor axes (a and b) to the major axis (c).

In applying these formulas to the 1983 experiment reported earlier, first it is necessary to obtain a value for ε_{head}. Nelson and Stetson (1976) reported values for the dielectric constant of winter wheat grain as a function of gravimetric moisture (wet basis) up to 24% over a frequency range from 250 Hz to 12.1 GHz. From their findings it is possible to extrapolate a moisture of 45% and correct for the difference in bulk density using the results given by Nelson (1976). From this we obtain a value for the head dielectric of 6.92 - j4.74. The ground-truth data permit calculation of the volume fraction and this is found to be 0.01016. Now the only variable left unknown is the eccentricity. Physically, the head measures about 8 cm in length and about 1 cm in diameter, yielding a value for a/c of 1/8. This variety of wheat is characterized by awns, i.e., it has hairlike

fibers extending from the heads in a vertical direction. If we include the awns in the length measurement, the a/c term is 1/15. Using these two values, we compute values for n''_z and n''_x of 0.0169 and 0.0012 for the awnless case and 0.0206 and 0.0011 for the case with awns.

These values, when figured for a frequency of 10.2 GHz and an incidence angle of 60°, yield values of vertical attenuation through an 8-cm layer of heads of 3.86 dB and 4.86 dB for the awnless case and the case with awns. The uniaxial crystal properties have been included in the above calculations. The reported value for measured attenuation is 8.3 dB with a standard deviation of about 3.5 dB. As neither the non-vertical head distribution nor the loss due to scattering has been accounted for a definite conclusion cannot be drawn.

2.5 SUMMARY

To aid in the understanding of the interaction between microwave energy and a vegetation canopy, measurements were made on a winter wheat field which demonstated that under the conditions described, one-way attenuation due to the heads when moist is approximately 8 dB at 60°, 10.2 GHz, vertical polarization, and attenuation due to the stalks when moist ranges from 15 to 48 dB m^{-1}. The value of the head attenuation agrees with values reported previously by Story et al., after adjustment for moisture differences are made. The variability in the stalk attenuation is similar to that seen by van Kastern and Smit, which they attributed to the variations in the biomass between

antennas. Also, for a dry canopy (8% moisture content) no significant attenuation was found.

A model that treats the stalks (and later the heads) as uniaxial crystals was applied to the measured data as well as to previously reported data. Good agreement was shown, indicating that a similar mechanism may be in action.

2.6 Sliding-Horn Experiment

In this section, the details and results of a sliding-horn experiment are presented. The methodology is similar to that used by Ulaby and Jedlicka (1983).

The major advantage of the sliding-horn experiment is that it yields a large number of independent samples, which when combined, provide a good estimate of the average and standard deviation for canopy attenuation, as shown by Ulaby and Jedlicka (1984).

Another advantage of the sliding-horn technique is that attenuation can be measured as a function of horizontal position, which means that autocorrelation and associated statistics become available. This is important for applications to theoretical models.

2.6.1 Experiment Statistics

The one-way attenuation through a lossy vegetation canopy has been modeled by Attema and Ulaby (1976) as

$$L = \exp(k_e \cdot h \cdot \sec\theta), \tag{2.24}$$

where θ is the incidence angle relative to nadir, h is the canopy height, and k_e is the extinction coefficient. For a lossy canopy with a small albedo, extinction is dominated by absorption, hence $k_e \approx k_a$, where k_a is the absorption coefficient.

Electromagnetic theory tells us that for a dielectric

$$k_a = 2\alpha, \tag{2.25}$$

where

$$\alpha = k_o |\mathrm{Im}\{\sqrt{\varepsilon_r}\}|$$

$$= k_o\, n'', \tag{2.26}$$

where α is the field absorption coefficient, k_o is the free-space wave number, ε_r is the complex relative dielectric constant of the medium, and n" is the imaginary part of the index of refraction of the medium.

The received power through a vegetation canopy at position x is therefore

$$P_r(x) = P_o \exp(-2\, k_o\, n''(x) \cdot h(x) \sec\theta), \tag{2.27}$$

where P_o is the signal strength that would be received without an intervening canopy, and n" and h are canopy parameters that are dependent upon location. When the received power is expressed in

dB and canopy height is assumed to be independent of location, we obtain

$$P_r(x) = k_1 + k_2\, n''(x), \quad \text{dB} \tag{2.28}$$

where k_1 and k_2 are constants for a given transmitter power level, incidence angle, canopy height, and frequency.

Given the magnitude of the transmitter power, k_1 may be determined, leaving $k_2\, n''(x)$, attenuation in dB, as the measured quantity. Based on this knowledge, statistics for $k_2\, n''$ may be determined.

The autocorrelation for a stationary, stochastic process is computed as follows

$$A(\tau) = \frac{1}{A(0)} \int W(x)\, W(x + \tau)\, dx, \tag{2.29}$$

where $W(x)$ is the function for which the autocorrelation is to be computed, and τ is the displacement or lag. $A(\tau)$ is normalized by the $A(0)$ factor, the autocorrelation with zero lag.

2.7 Soybean Attenuation Experiment

On July 20, 1983, the sliding-horn experiment as described above was conducted in a fully-developed soybean canopy. Table 2.4 lists the measured ground-truth conditions for this field on this day, as well as measured σ^o data. Figure 2.9 shows

TABLE 2.4

Soybean Attenuation Experiment
Ground-Truth Data

DATE: July 20, 1983 (Day 201)
TEMPERATURE: 95 - 100°F

Crop Type:	Soybeans
Canopy Height:	82 cm
Planting Density:	26 plants m^{-2}
Plant Spacing:	5 cm
Row Spacing:	74 cm
Percent Cover:	90 - 95%
Soil Moisture:	3.7% (0 - 2 cm, gravimetric)
Leaf Moisture:	76.4% (Fresh Basis)
Stalk Moisture:	81.2% (Fresh Basis)
Leaf Fresh Biomass:	0.590 kg m^{-2}
Stalk Fresh Biomass:	0.970 kg m^{-2}

Measured σ^0 (50° Incidence Angle, 10.2 GHz, 2 Trials)

VV Polarization	VH Polarization
-7.26	-16.36
-6.80	-16.30

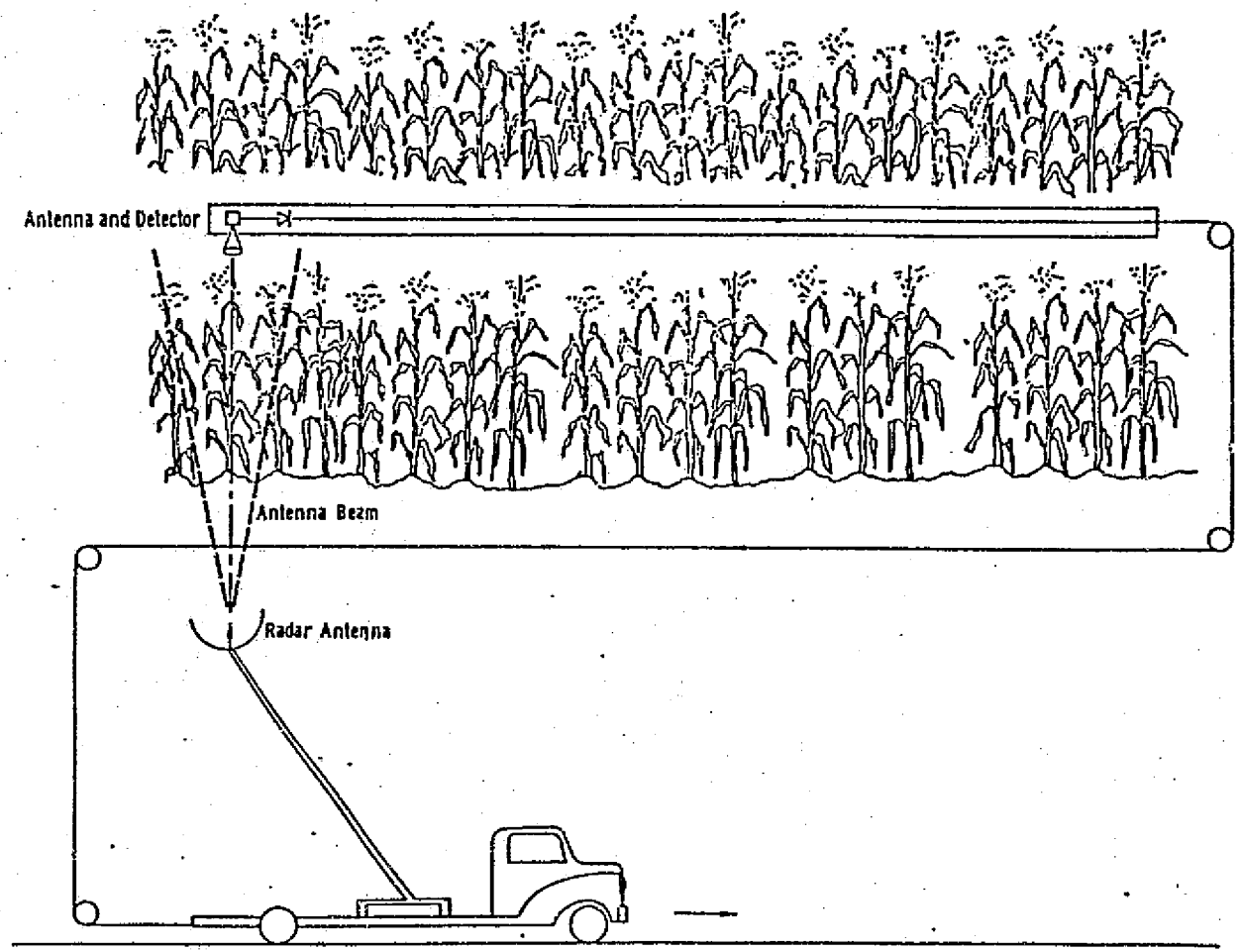

Figure 2.9 Plan of the experiment setup for measuring soybean-canopy attenuation by using the sliding-horn technique.

a plan of the experiment arrangement. The experiment was performed three times to improve the statistical quality of the data. Figure 2.10 shows the recorded data in its raw form.

Two problems immediately appear. First the power level at the beginning and end are not equal, although neither suffers any attenuation due to the "cleared" areas shown in Figure 2.9. Second, the record length for a known distance is different from one trial to the next. The first problem is caused by the fact that the transmitter is supported and transported by a truck. If the motion of the truck is not exactly parallel to the motion of the receiving antenna, the antenna pattern causes a reduction in signal strength. This may be corrected if it is assumed that the signal loss is a linear process as a function of position. The second problem is also truck-related. The recording mechanism records signal strength versus time; thus, although the truck maintains a near-constant speed during the pass, its speed varies between trials. This too may be corrected, since the length of the canopy section is known and shows up clearly in the record. The edges were defined as the point at which the signal drops 3 dB from the power received at that end.

Based upon these corrections, Figure 2.11 was generated, excluding the regions outside the canopy. One significant error remains however, and it cannot be corrected. In trial 3, the signal level dropped because of truck drift, and it is possible that the signal strength became comparable to the noise-floor level, thus corrupting the results. Hence, this data set may produce inconsistent results, as discussed below.

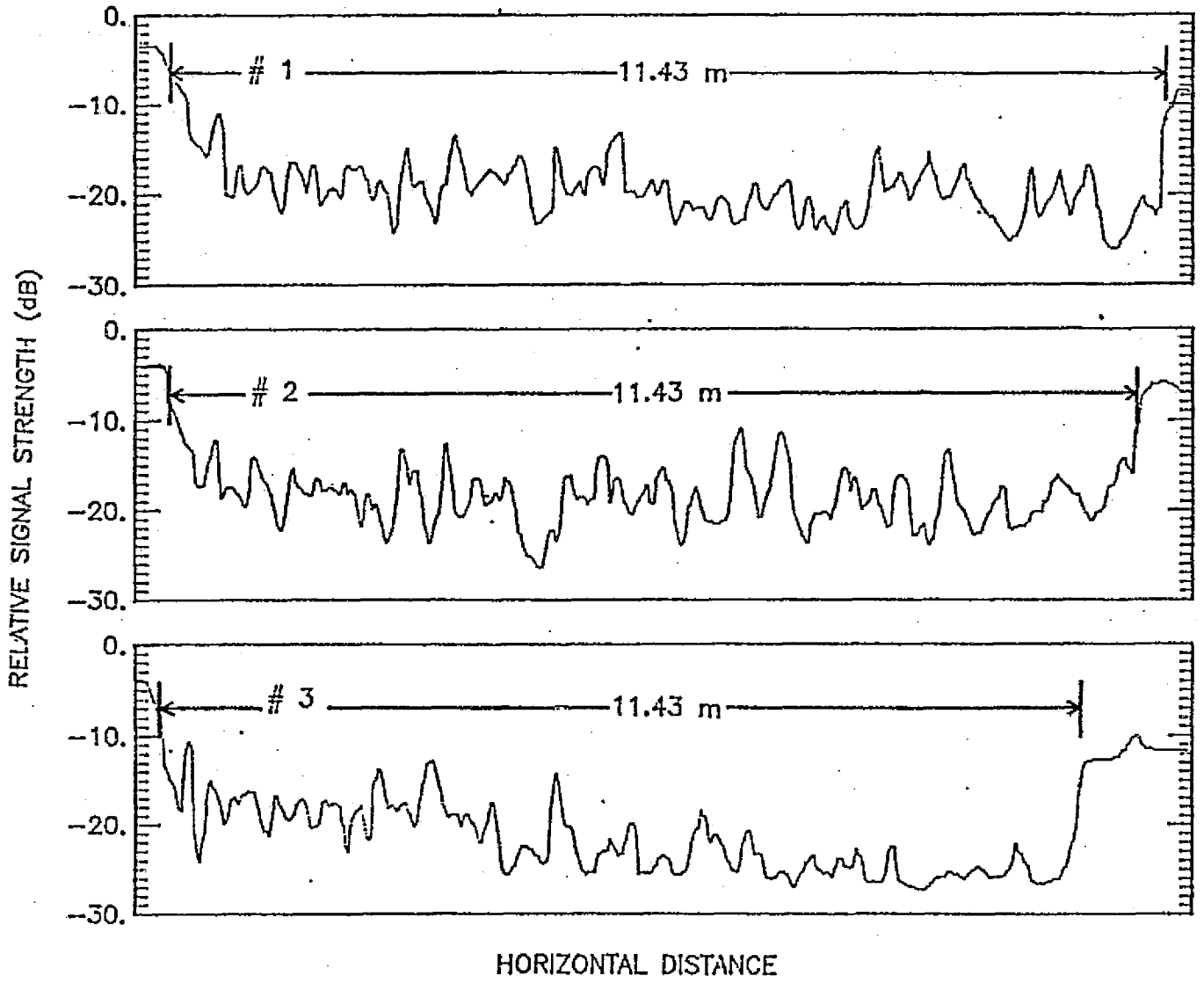

Figure 2.10 Measured power through a soybean canopy as a function of position, based on three trials.

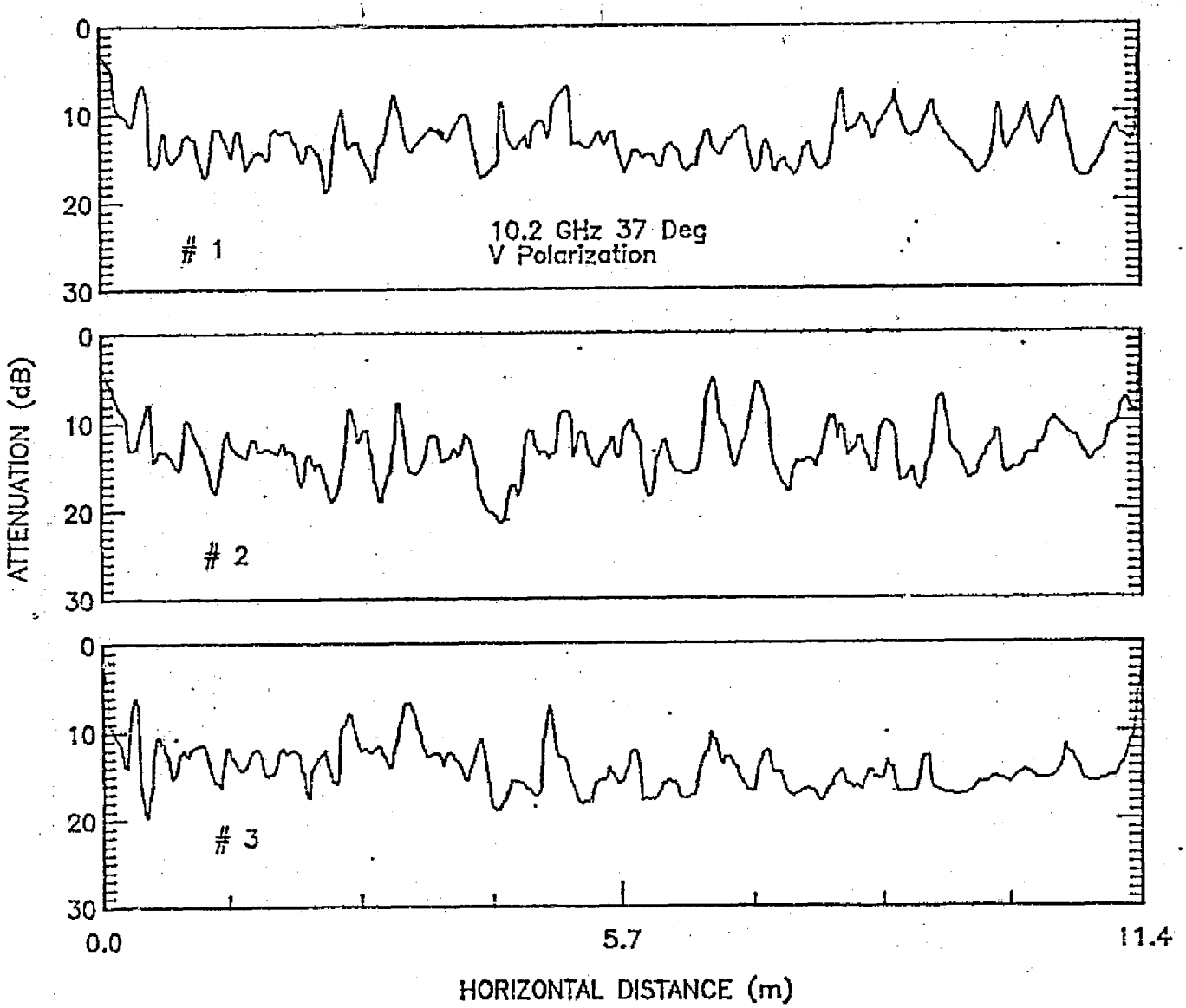

Figure 2.11 Refined version of data presented in Figure 2.10.

2.7.1 Experiment Results

Both the mean and the standard deviation of one-way canopy attenuation were computed for the three trials after excluding 0.5 m from either end due to possible edge effects. These results are shown in Table 2.5, along with the number of discrete samples or elements into which the data were segmented, and the distance each element represents, as well as the offset needed to correct the raw data. The means for trials 1 and 2 were quite consistent, whereas that for trial 3 was off by about one decibel.

A histogram was computed for each trial, and the results are shown in Table 2.6. A plot of the histogram computed for all three trials combined is shown in Figure 2.12. The distribution is seen to approximate a normal or Gaussian distribution and has a mean of 13.6 dB and a standard deviation of 2.6 dB.

The correlation length at various points within the record was also computed for each trial. The results are shown in Table 2.7. Again, the results for trials 1 and 2 agree, whereas trial 3 results do not. The offset in element is the number of elements from the left edge in Figure 2.11, at which point the computation starts. As an example of the shape of this autocorrelation, a plot of the computed autocorrelation is shown in Figure 2.13 from trial 2, with an offset of 200 elements.

Figure 2.13 shows what appears to be a consistent period of about 50 cm. The cause underlying this cyclical behavior is not known; the plant spacing is approximately 5 cm.

TABLE 2.5

Sliding Horn - Soybean Data, July 20, 1983
10.2 GHz, 37°, V-Polarization

Trial	Slope Correction (dB)	Total No. of Elements	Mean Attenuation (dB)	Std. Dev. (dB)	No. of Elements Used	Element Size (cm)
1	5	479	13.2	2.36	438	2.39
2	3	469	13.4	2.89	428	2.44
3	8	448	14.4	2.40	409	2.55
			13.8	2.61	1275	

TABLE 2.6

Histogram Data - Soybean Data
Number of Data Points Exceeding α-1 but Not α

α(dB)

Trial	5	6	7	8	9	10	11	12	13	14	15	16	17	18	19	20	21
1	0	0	6	8	20	23	31	75	71	65	57	52	26	2	2	0	0
2	2	6	7	6	15	32	39	41	65	77	43	39	25	15	7	4	5
3	0	0	6	5	6	7	14	57	45	46	71	65	63	20	3	1	0
Total	2	6	19	19	41	62	84	173	181	188	171	156	114	37	12	5	5

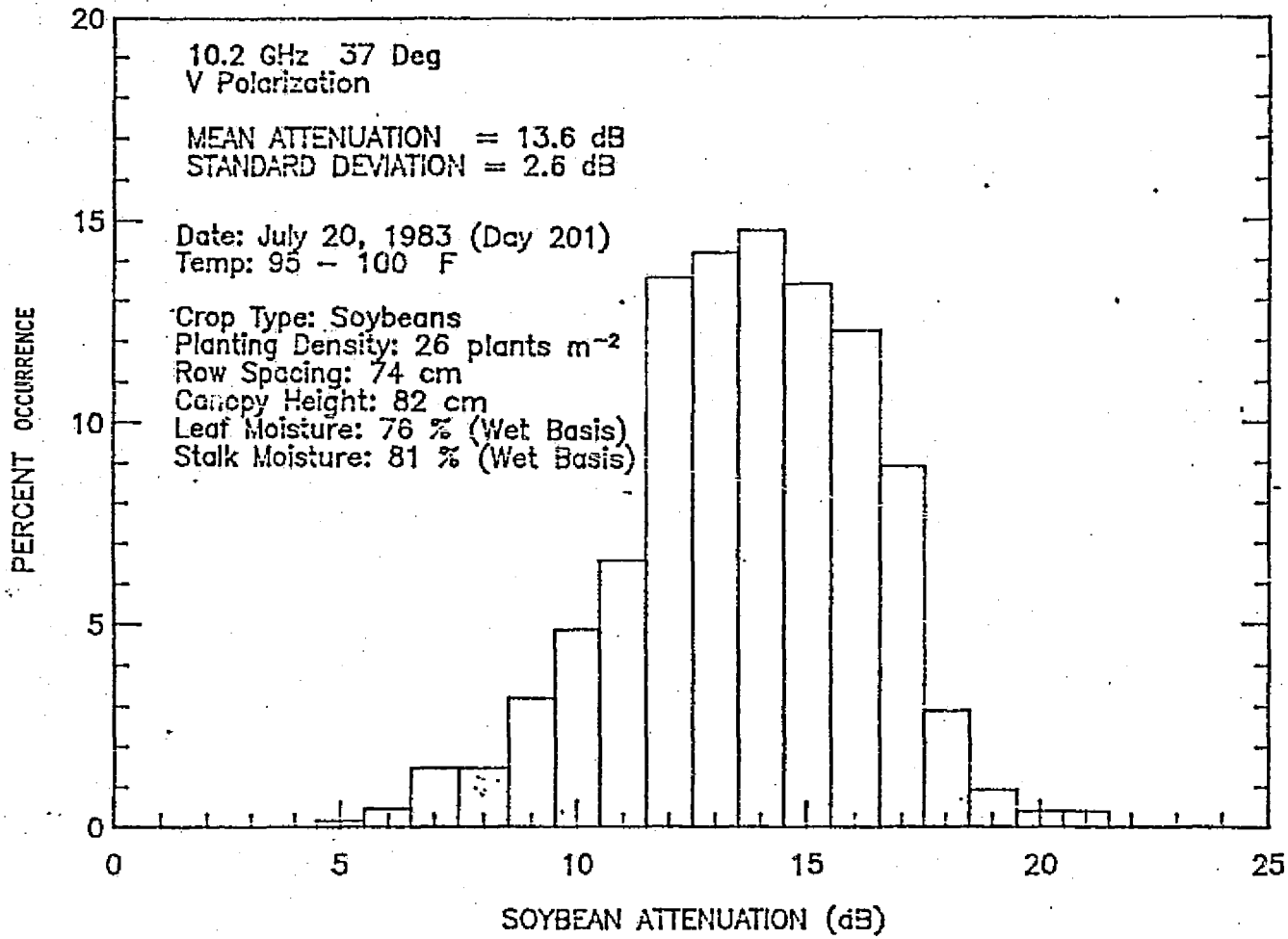

Figure 2.12 Histogram of one-way attenuation through the soybean canopy.

TABLE 2.7

Autocorrelation Length (cm)

Offset (Elements)

Trial	50	100	150	200	250	Mean
1	8.4	10.7	12.8	13.2	13.2	11.6
2	7.9	13.1	15.2	11.0	11.9	11.8
3	41.1	15.0	11.6	13.5	80.8	32.4

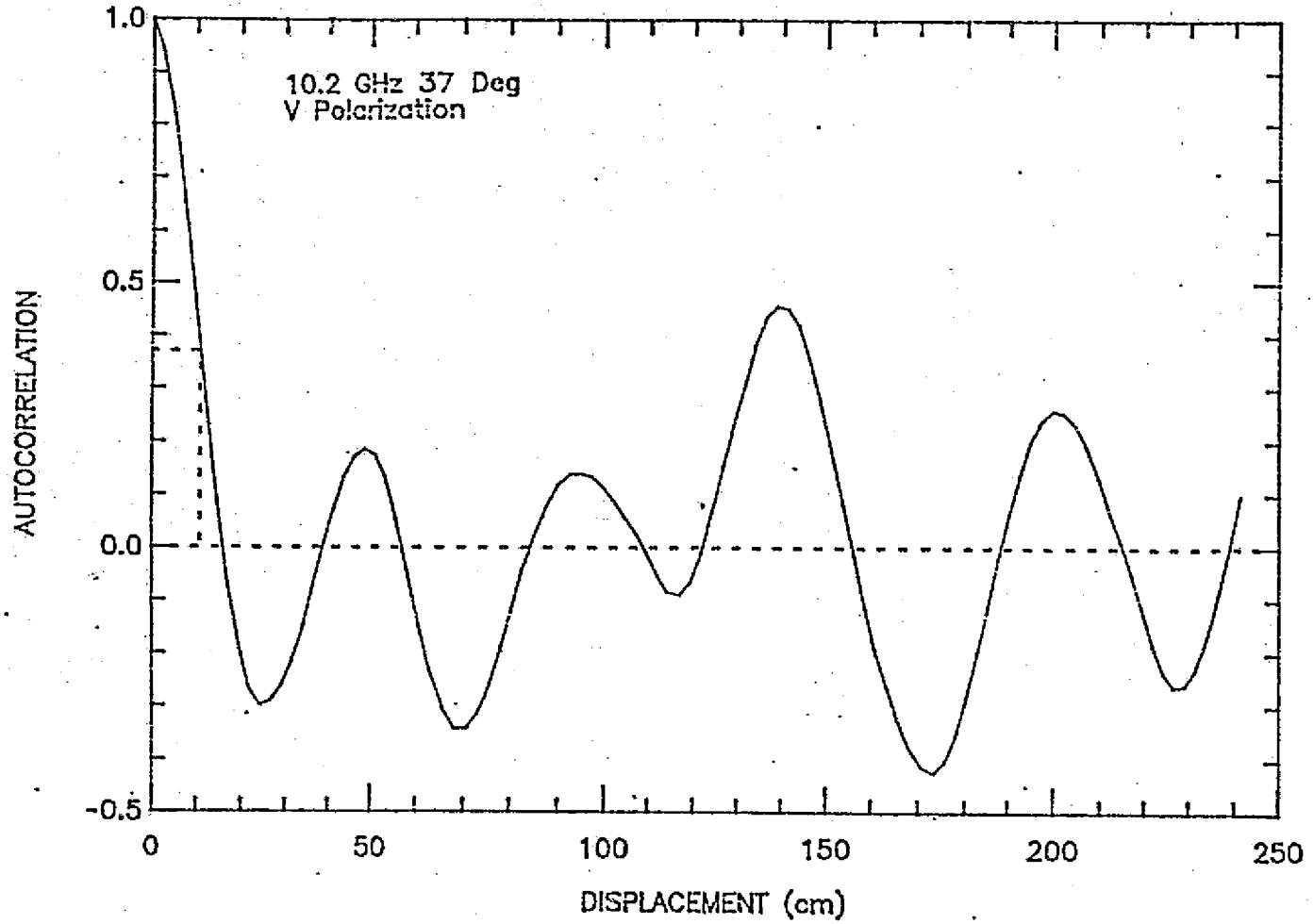

Figure 2.13 Example of the computed autocorrelation from the attenuation plots.

2.8 Vertical Attenuation Profile Experiment

Immediately after the three sliding-horn trials were performed, vertical attenuation profiles were produced for nine locations within the same canopy. From these profiles, total one-way attenuation was determined by subtracting the power measured in dB at the bottom of the canopy from that measured above it. Since the height of the receiving antenna in this case was the same as that for the sliding-horn experiment, i.e., about 23 cm, the estimates of attenuation should agree. For calibration purposes, one additional vertical-attenuation profile was made without any canopy obstruction.

The resulting attenuation estimates for the nine locations are shown in Table 2.8. The mean, 15.9 dB, although high, when taken in conjunction with the associated standard deviation, overlaps the estimate yielded by the sliding-horn data. The increased standard deviation is a result of the limited sample size (9) as compared to over 400 samples for trials with the sliding horn.

2.9 Summary

An estimate of the one-way soybean canopy attenuation was arrived at by two methods. The sliding-horn method yielded an estimate of 13.8 ± 2.6 dB, whereas the vertical attenuation profile yielded 15.9 ± 7.5 dB, at 10.2 GHz, 37° incidence angle, and V-polarization. Hence, the sliding-horn method seems to be much more accurate than the vertical attenuation profile.

TABLE 2.8

Vertical-Attenuation Profile Data, Soybeans, July 20, 1983
10.2 GHz, 37° Incidence Angle, V-Polarization

Location No.	One-Way Attenuation (dB)
1	18.63
2	17.23
3	25.62
4	21.79
5	17.20
6	5.22
7	21.79
8	3.94
9	11.60

Mean: 15.89 dB
Std. Dev.: 7.5 dB

A histogram of attenuation was also obtained from the data, which revealed a near-normal distribution. Further analysis yielded correlation-length estimates of about 22 cm and cyclic structures in autocorrelation with a period of roughly 50 cm.

2.10 Comparison with Past Results and Models

The experiment described above is a repetition of a series of similar measurements made in 1982 at the University of Kansas (Ulaby and Jedlicka, 1984). Those results are presented for comparison in Figure 2.14. On Day 201, the one-way attenuation was of the order of 9 dB through a soybean canopy about 58-cm tall at an incidence angle of 52°. On Day 215 the canopy height was comparable to that used in this report, i.e., about 85 cm, and one-way attenuation of about 15 dB was reported.

It is assumed the attenuation follows a $\sec\theta$ behavior, i.e.,

$$\alpha(\theta;\text{dB}) = \alpha(0;\text{dB}) \cdot \sec\theta, \tag{2.30}$$

where θ is the incidence angle, and $\alpha(\theta;\text{dB})$ is the attenuation in dB at an angle θ. Using this model, the data obtained at 37° may be computed for an angle of 52°; the result is a one-way attenuation of 17.7 dB. Assuming a standard deviation of about 2.5 dB (from the 37° data) and a comparable standard deviation in Jedlicka's data, the measurements agree. Unfortunately, Jedlicka did not report canopy biomass data, so variations may also contribute to differences.

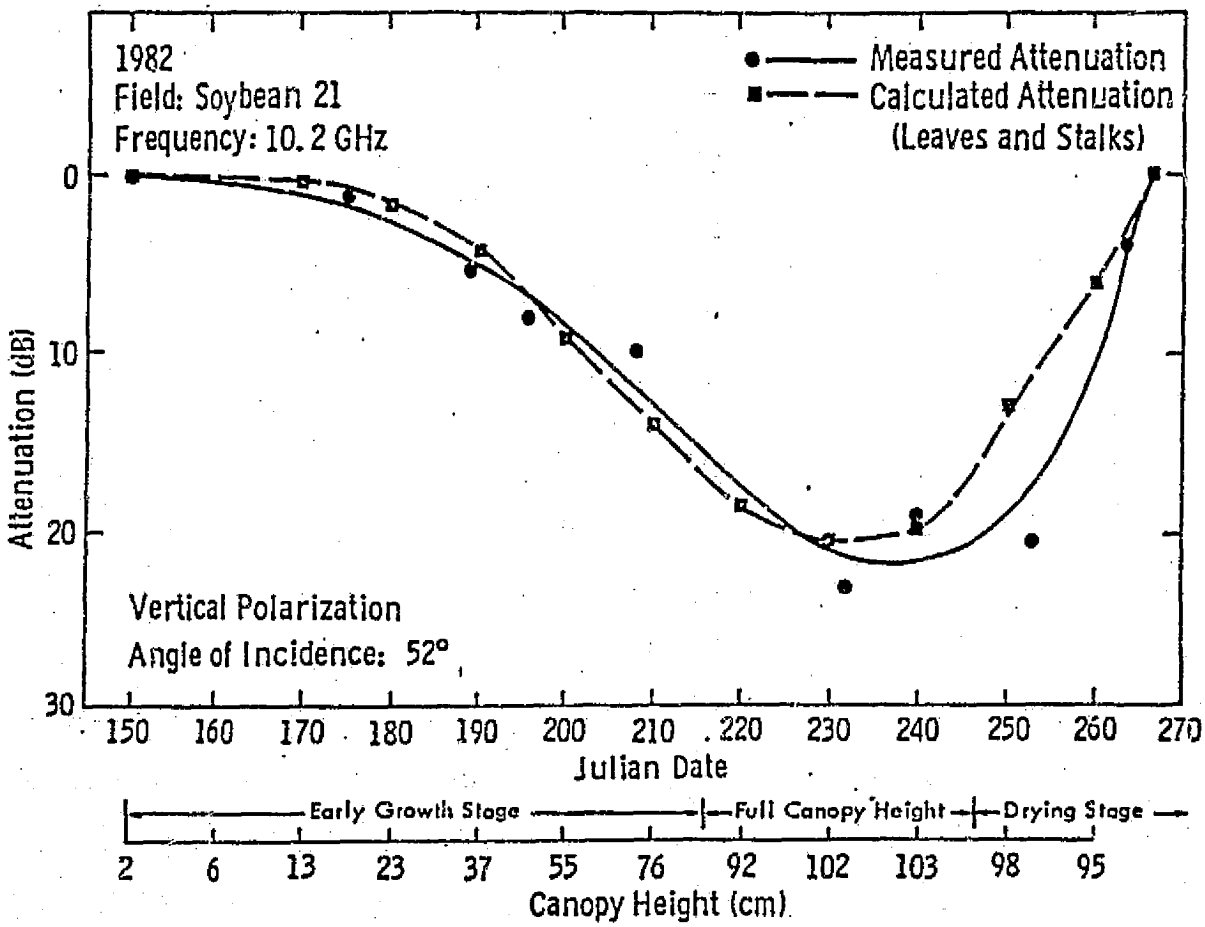

Figure 2.14 Temporal variation of the measured one-way attenuation at 10.2 GHz for a soybean canopy, and calculated attenuation due to absorption by leaves and stalks (from Ulaby and Jedlicka, 1983).

If the vegetation canopy is modeled as a collection of randomly oriented discs (not a bad approximation for a soybean canopy because of leaf shape), a comparison with a theoretical model is possible. The model proposed by Polder and Van Santen (1946) and de Loor (1968) considers the case of ellipsoidal inclusions suspended in a host medium. In this case, the ellipsoids are compressed into discs and the host medium is air. The equivalent dielectric of such a medium is

$$\varepsilon_m = \varepsilon_h + \frac{V_i}{3}(\varepsilon_i - \varepsilon_h)(2 + \frac{\varepsilon^*}{\varepsilon_i}), \qquad (2.31)$$

where ε_m is the equivalent dielectric constant of the medium, the subscript h denotes host, the subscript i denotes inclusion, and V_i is the inclusion volume fraction. Also, ε^* is usually replaced by ε_m however when V_i is quite small, ε_h and ε_m are fairly close, therefore, ε_h is chosen.

Jedlicka also reported measurements of ε for corn and wheat leaves as a function of volumetric water content at around 8 GHz. Using the value reported for corn leaves and a computed volumetric water content of 54%, a dielectric of 20.6 - j9.1 was obtained for the leaves. A volume fraction of the canopy material (leaves and stalks) was computed to be 0.00282. This yields an equivalent dielectric of the medium of 1.038 - j0.01707. From this, the one-way attenuation may be computed using an expression from electromagnetic theory

$$\alpha(\text{dB}) = 2 \cdot 4.34 \cdot \frac{2\pi}{\lambda} \cdot n'' \cdot h \sec\theta, \qquad (2.32)$$

where λ is the free-space wavelength, n'' is the imaginary part of the index of refraction, and h is the thickness of the medium. As $n^2 = \varepsilon$, $n'' = |\mathrm{Im}\sqrt{\varepsilon}|$. Here $n'' = 0.00838$. At 10.2 GHz, $\theta = 37°$, a one-way attenuation of 15.95 dB is predicted, whereas 13.67 dB is the mean attenuation measured. Again, an uncertainty of the order of $\pm$ 2.5 dB is associated with the measurement.

3.0 EFFECTS OF FREE WATER IN A VEGETATION CANOPY

3.1 Introduction

One advantage of microwave systems over optical systems is that microwave systems (radars, radiometers) are "all weather," i.e., sun position, clouds, fog, snow, and rain have negligible affects on microwave propagation. This means that remotely sensed data can be acquired at any time.

The weather may affect the characteristics of the target, however. Backscattering from water will be different depending on wind speed and direction (Bradley, 1971) as well as on whether or not it is raining, for example. A snow layer's backscattering may be different in the daytime and at night due to the change of phase of the water (Stiles and Ulaby, 1980).

Another possible weather influence upon target characteristics is the presence of free water in a vegetation canopy. The water may be present for a number of reasons: condensation or dew, rain, or irrigation. The presence of free water in a vegetation canopy should influence the way it appears to microwave sensors, as water has a much larger dielectric constant than vegetation matter, i.e., between 40 and 80 depending on frequency (see Figure 3.1) for water versus between 10 and 30 for fresh leaves, stalks, and grain (Carlson, 1967; Ulaby and Jedlicka, 1983; Nelson and Stetson, 1976) at X-band and below.

The backscattering coefficient from a vegetation canopy may be written (Ulaby et al., 1982)

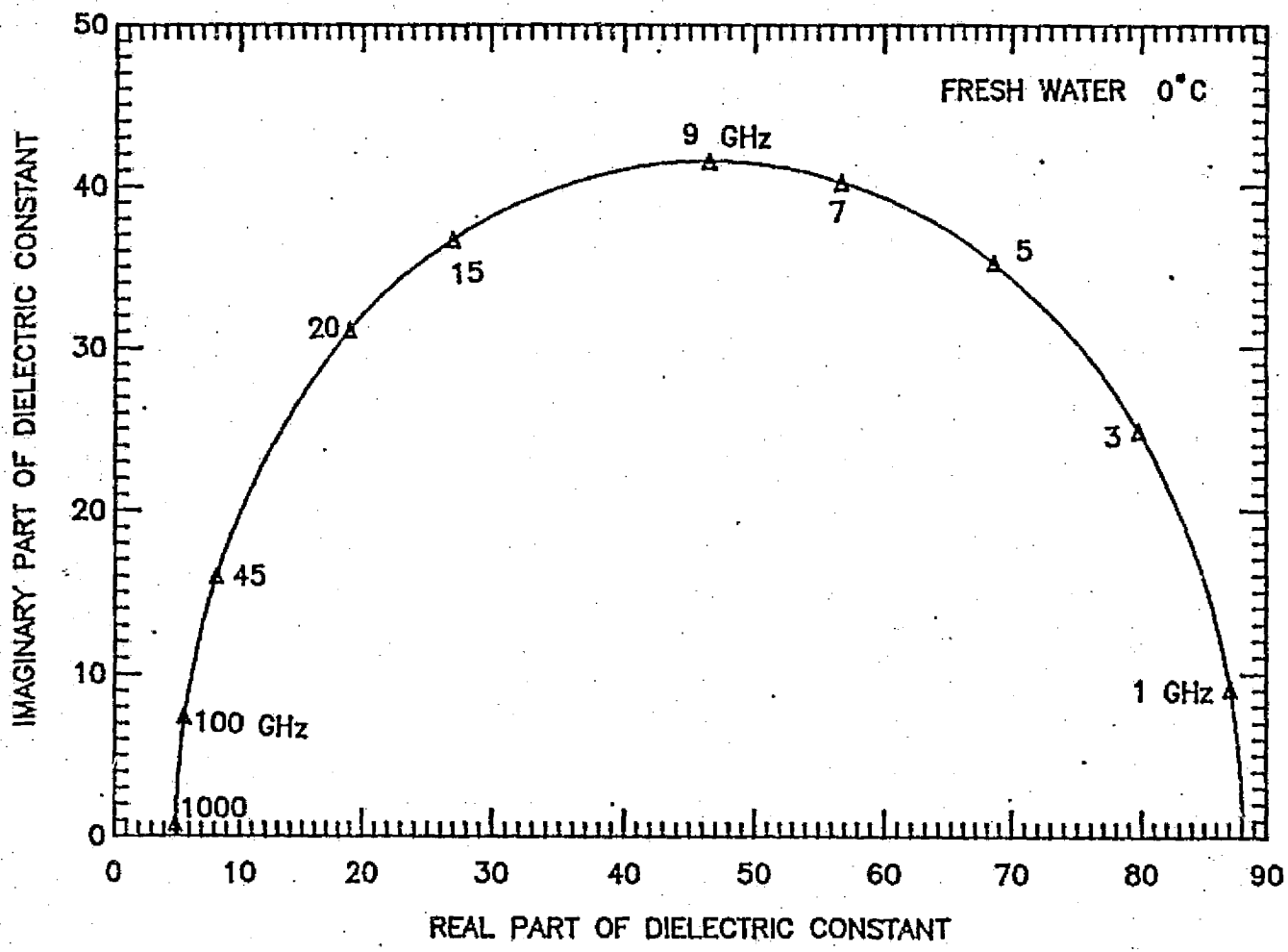

Figure 3.1 Cole-Cole diagram showing how the real and imaginary parts of the dielectric constant of water vary as a function of frequency.

$$\sigma^o_{can} = \sigma^o_{veg} + \sigma^o_{soil}/L^2, \qquad (3.1)$$

where σ^o_{veg} is the backscattering due to the vegetation and σ^o_{soil} is the backscattering due to the soil. The soil term is attenuated twice by the vegetation layer, hence the L^2 term. Therefore, even though σ^o_{soil} increases with water content, its influence may be ignored if $\sigma^o_{veg} >> \sigma^o_{soil}/L^2$, i.e., if L^2 is large and σ^o_{veg} is sufficient. Ulaby and Jedlicka (1983) reported values for L of more than 10 dB for corn and more than 20 dB for soybeans at 10.2 GHz, at 50° incidence angle with vertical polarization at full canopy height. In Chapter 2, values for L in excess of 30 dB for wheat at 10.2 GHz, 60°, and vertical polarization at full height were shown. Hence, when the observed σ^o is sufficiently large, the soil component may be ignored for wheat and soybean canopies, and perhaps also for corn. Based on this information the influence of free water on σ^o_{can} was investigated.

3.2 Experiment Description

On June 14, 1983 a small section (approximately 40 feet by 15 feet) of a winter wheat field was observed by the MARS X-band scatterometer (Gable et al., 1981). Water was applied twice by a water truck in a fashion to simulate a rain. Altogether, approximately two inches of water was uniformly distributed over the area. Logistical problems necessitated a second spraying to permit observation of rapid dry-down. The weather, which was clear with a temperature in the 70's and a wind speed of

10-15 mph, aided the dry-down process. Two moisture sensors were placed in the canopy to qualitatively monitor the presence of free water. Table 3.1 lists the measured ground-truth data.

On August 1, 1983, comparable areas of a soybean and corn field were also observed by the MARS X-band scatterometer. Approximately 1.5 inches of water was uniformly distributed over both areas to simulate rainfall. The weather, which was clear with a temperature of about 85°F and a windspeed of 5 to 10 mph, aided the dry-down process. One moisture sensor was located in each field to qualitatively monitor the presence of free water. Tables 3.2 and 3.3 list the measured ground-truth data.

3.3 Results

3.3.1 Wheat

Plots of σ^o_{VV} and σ^o_{VH} versus time, acquired on June 14, 1983 for winter wheat are shown in Figures 3.2 and 3.3. Also indicated are the spraying events, along with the moisture sensor data. No scale is given for the moisture sensor data, as it is included for qualitative value only. It is proportional to -log of the sensor resistance measured, which varied from > 20 MΩ when dry to about 35 kΩ when moist.

Notice in both figures an overall increase of σ^o of about 3 dB between wet and dry canopy conditions. Also in both cases, a steady dry-down is observed in σ^o, which tracks the sensor data well. There is more scattering in σ^o_{VH} than σ^o_{VV} around 1500 hours, but a definite trend is apparent.

TABLE 3.1

Winter Wheat Ground-Truth Data

Canopy Height:	109 cm
Head Length:	8 cm
Planting Density:	900 plants m^{-2}
Ground Cover:	100%
Head Moisture:	53% (fresh basis)
Leaf Moisture:	22% (fresh basis)
Stalk Moisture:	62% (fresh basis)
Head Water Content:	0.821 kg m^{-2}
Leaf Water Content:	0.071 kg m^{-2}
Stalk Water Content:	1.858 kg m^{-2}

TABLE 3.2

Soybean Ground-Truth Data

Canopy Height:	85 cm
Planting Density:	27 plants m^{-2}
Ground Cover:	90 to 95%
Leaf Moisture:	75% (fresh basis)
Stalk Moisture:	77% (fresh basis)
Leaf Water Content:	0.479 kg m^{-2}
Stalk Water Content:	0.910 kg m^{-2}
Soil Moisture (0 - 2 cm, gravimetric)	
Before Spraying:	3.3% (dry basis)
After Spraying:	18.2% (dry basis)

TABLE 3.3

Corn Ground-Truth Data

Canopy Height:	267 cm
Planting Density:	3.2 plants m^{-2}
Ground Cover:	70 - 80%
Cob Moisture:	76% (fresh basis)
Leaf Moisture:	73% (fresh basis)
Stalk Moisture:	68% (fresh basis)
Cob Water Content:	1.238 kg m^{-2}
Leaf Water Content:	0.488 kg m^{-2}
Stalk Water Content:	0.985 kg m^{-2}
Soil Moisture (0-2 cm, gravimetric)	
Before Spraying:	2.7% (dry basis)

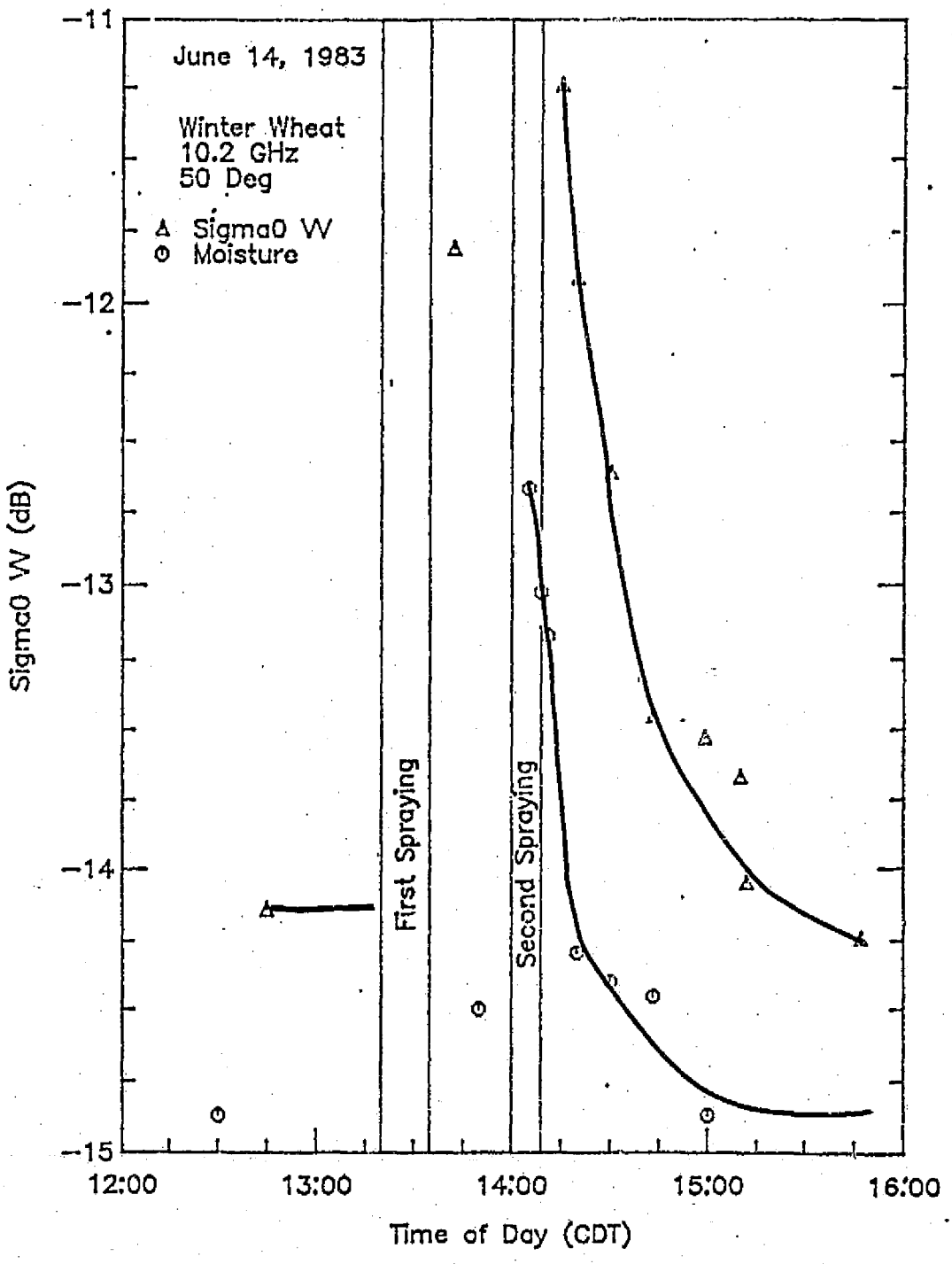

Figure 3.2 Effects on σ^{o}_{VV} of spraying water on a wheat canopy. Also shown is the response of a moisture sensor.

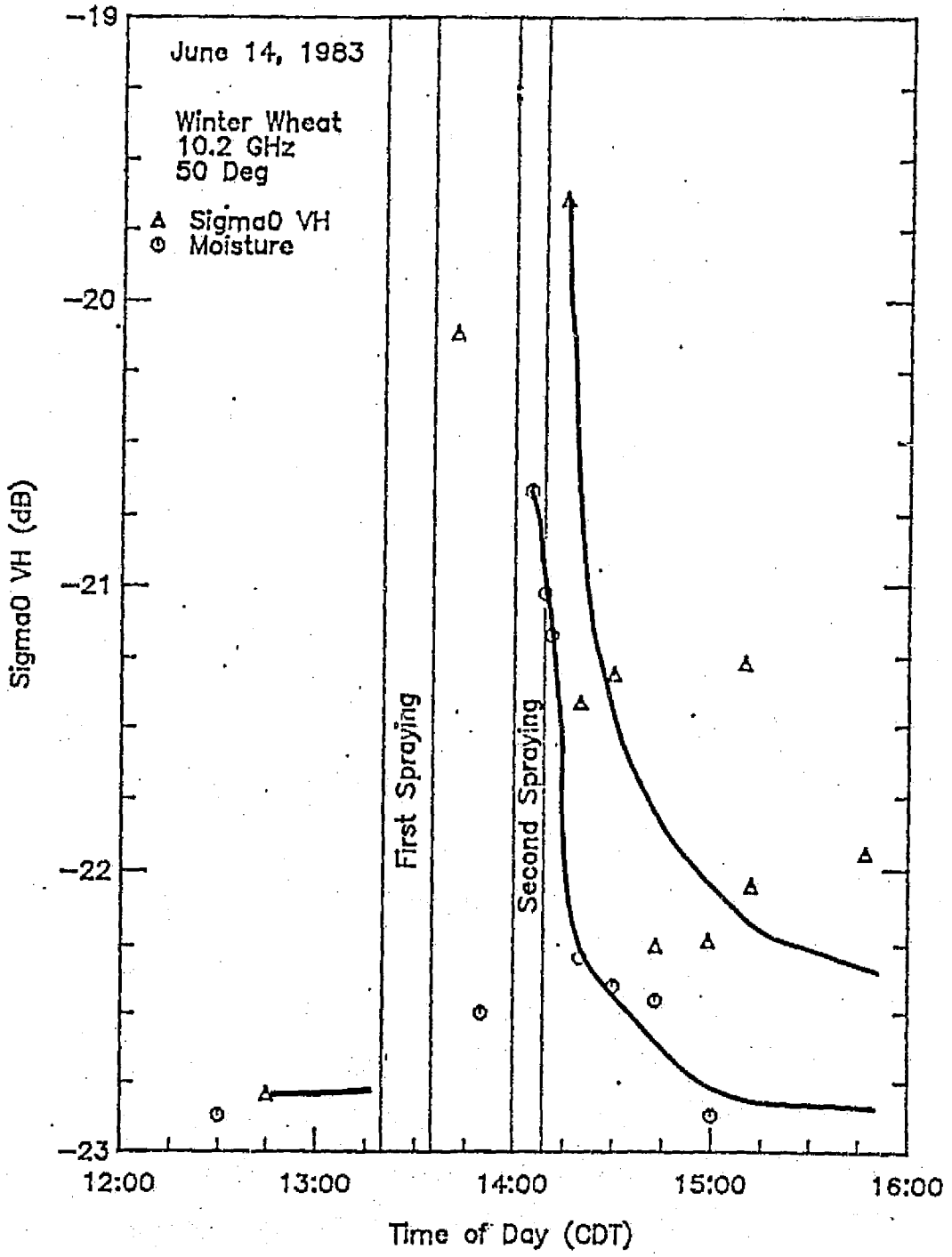

Figure 3.3 Effects on σ^{o}_{VH} of spraying water on a wheat canopy. Also shown is the response of a moisture sensor.

3.3.2 Soybeans

Plots of σ^o_{VV} and σ^o_{VH} versus time acquired on August 1, 1983 for soybeans are shown in Figures 3.4 and 3.5. Also indicated are the spraying event and moisture-sensor data. The measured resistance of the moisture sensor varies from > 20 MΩ when dry to about 30 kΩ when moist.

In the case of σ^o_{VV}, a trend is discernible similar to the one seen in wheat. Overall, an increase of about 3 dB is seen in the σ^o_{VV} of the dry canopy.

In the case of σ^o_{VH}, an overall increase of about 3 dB is again apparent. A large amount of scattering in the data obscures any definite trend beyond a general decrease.

In both cases the level of σ^o at the end of the experiment was higher than the level before spraying. The moisture sensor indicates that the canopy is nearly dry by 1100 hours, which may indicate the influence of the change in soil moisture upon σ^o.

3.3.3 Corn

Figures 3.6 and 3.7 are plots of σ^o_{VV} and σ^o_{VH} versus time acquired on August 1, 1983 for corn, with the spraying event and moisture sensor data indicated also. The measured resistance of the moisture sensor varied from > 20 MΩ when dry to about 30 kΩ when moist. Equipment problems limited the number of sensor measurements.

In the case of σ^o_{VV}, a single point acquired immediately after spraying is the only anomaly in an otherwise flat temporal

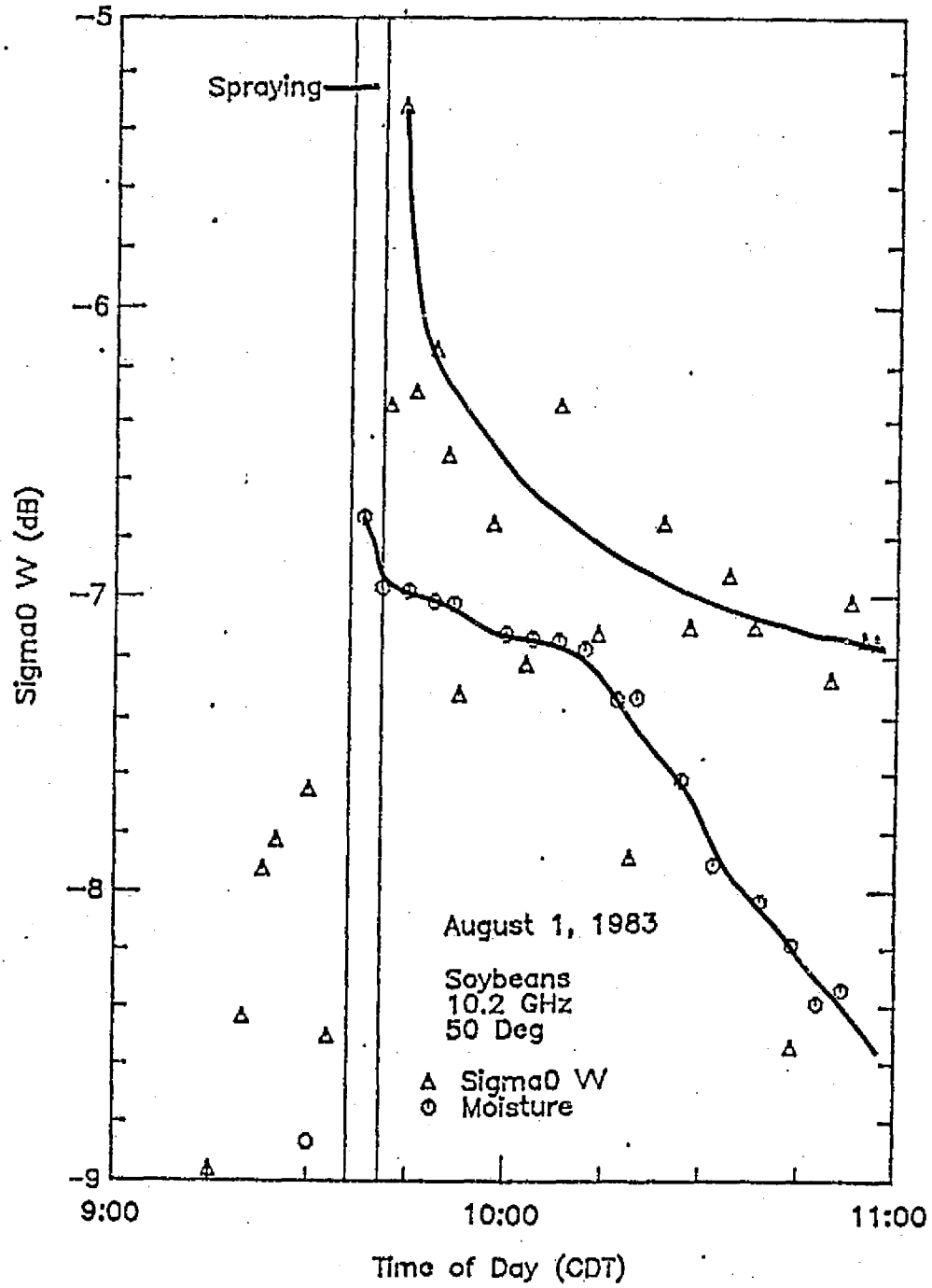

Figure 3.4 Effects on σ^{o}_{VV} of spraying water on a soybean canopy. Also shown is the response of a moisture sensor.

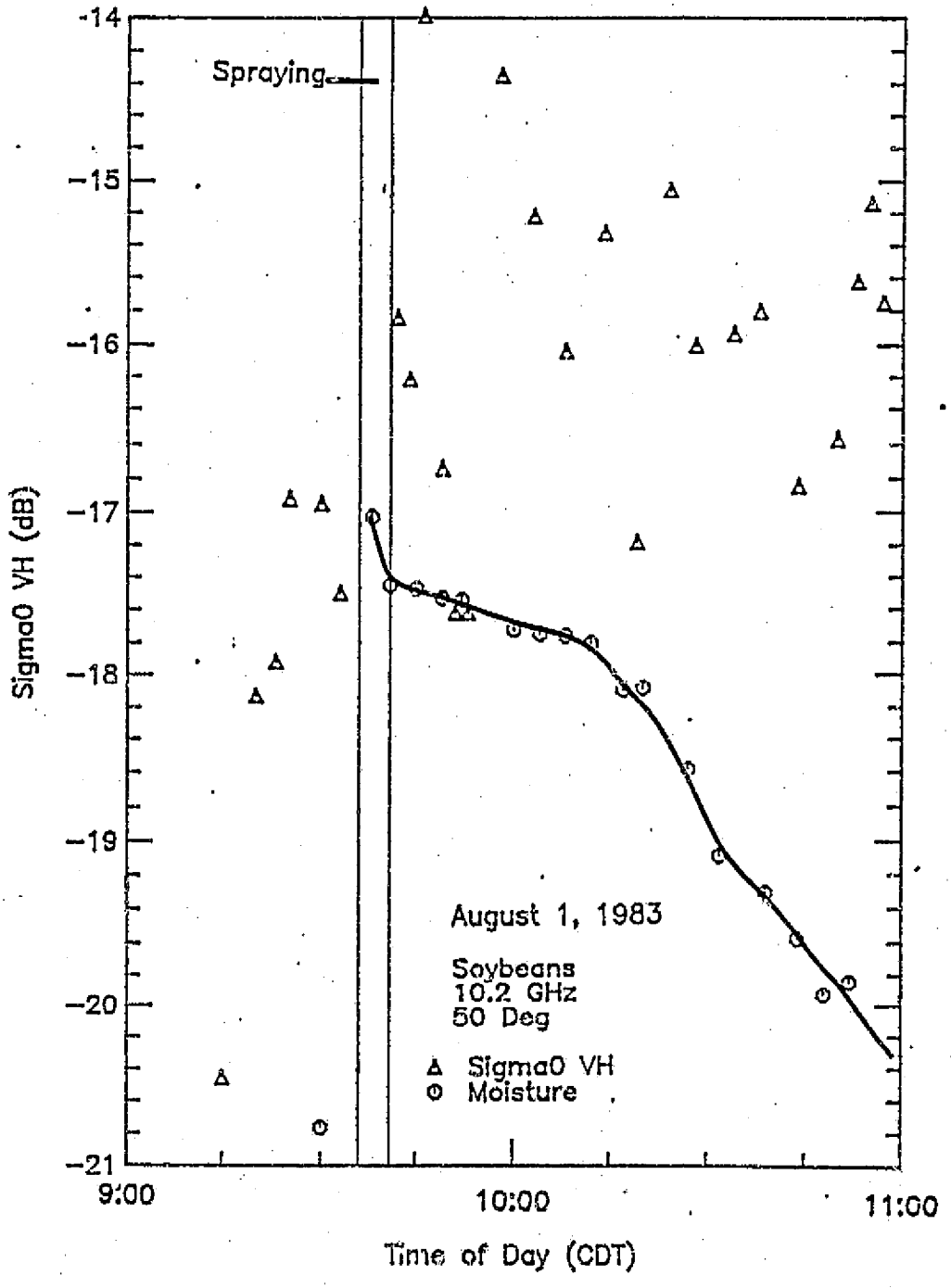

Figure 3.5 Effects on σ^o_{VH} of spraying water on a soybean canopy. Also shown is the response of a moisture sensor.

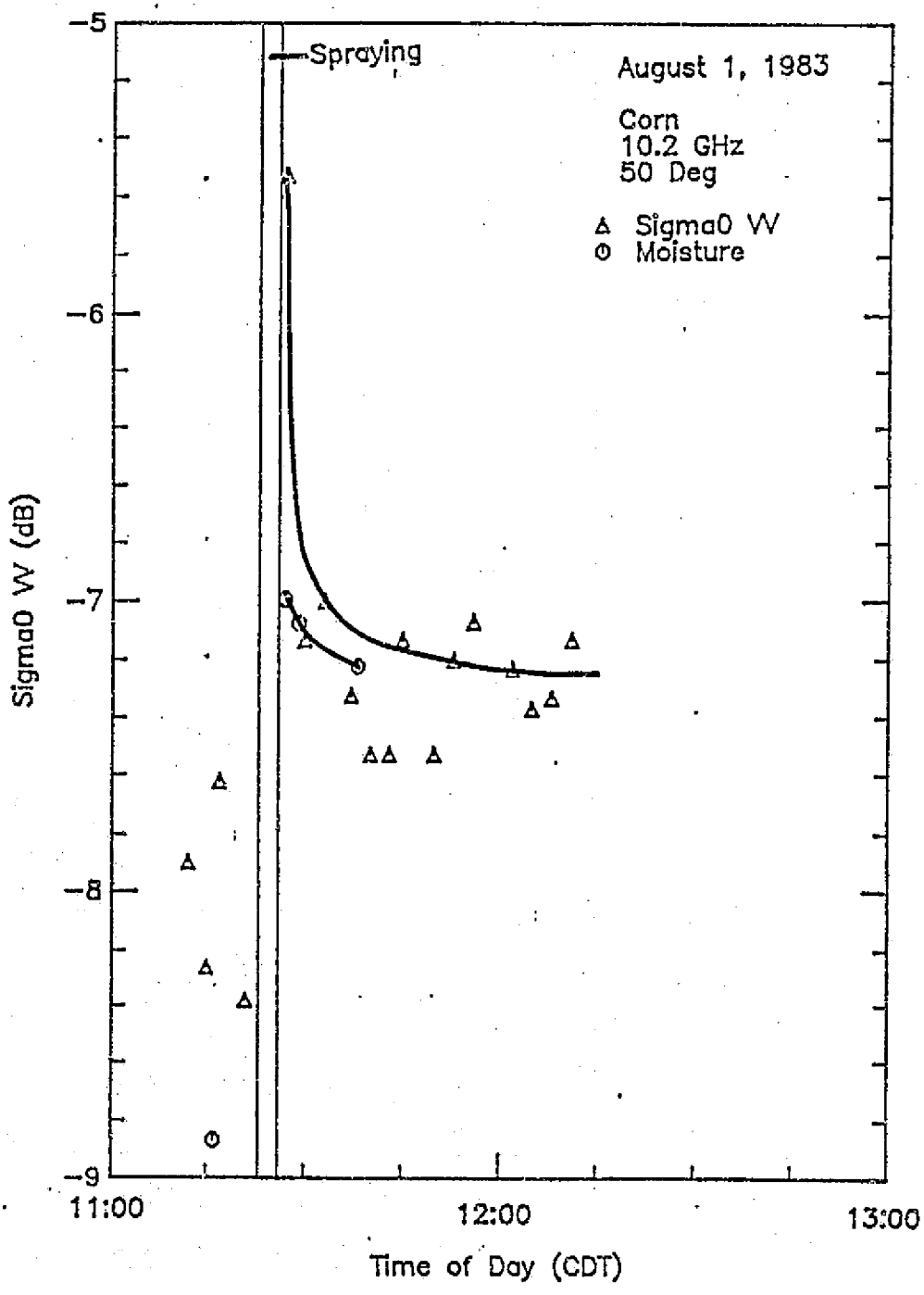

Figure 3.6 Effects on σ^o_{VV} of spraying water on a corn canopy. Also shown is the response of a moisture sensor.

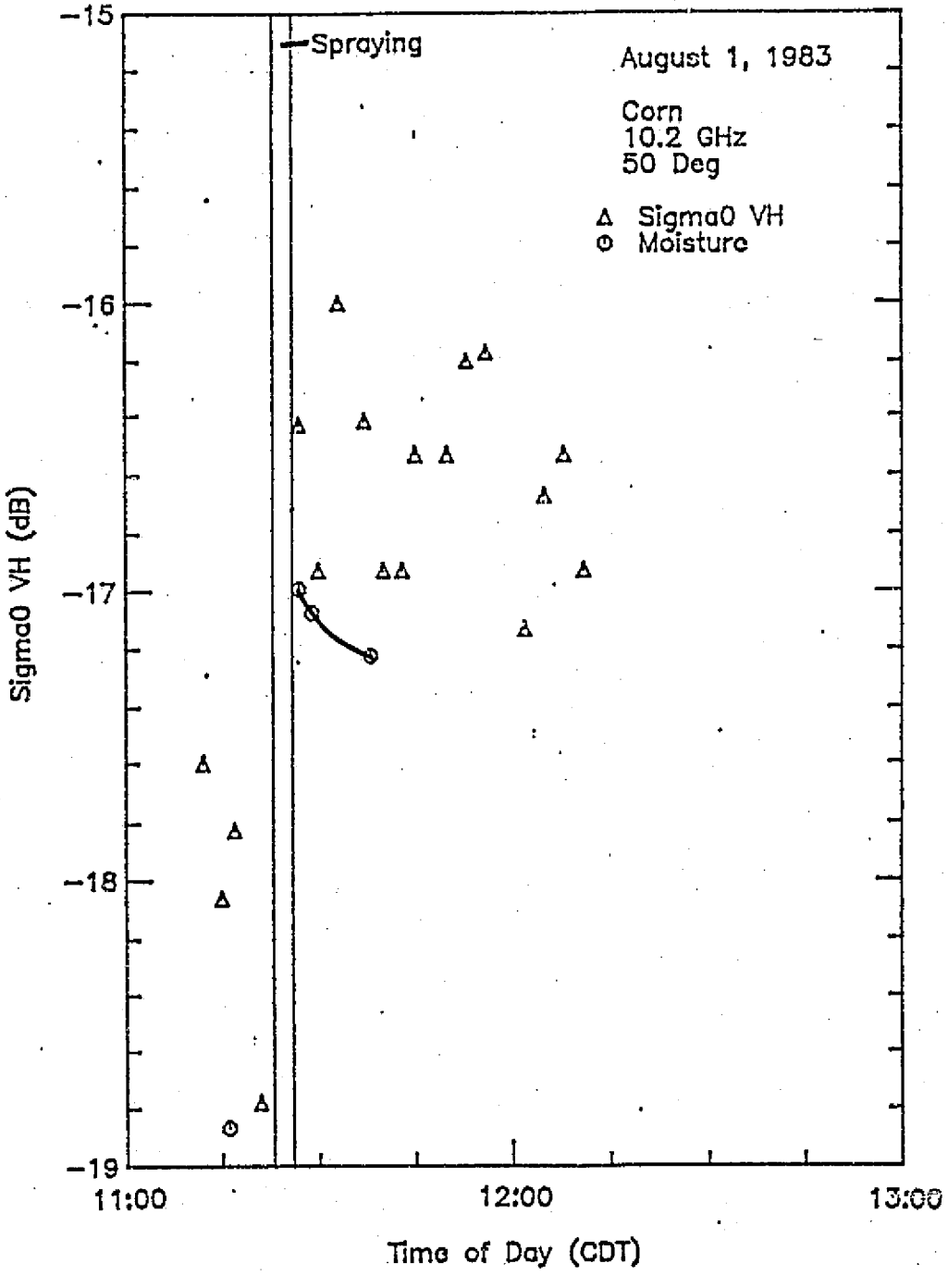

Figure 3.7 Effects on σ^{o}_{VH} of spraying water on a corn canopy. Also shown is the response of a moisture sensor.

response. In the case of σ^o_{VH}, an overall increase of about 1.5 dB is all that separates the conditions before and after spraying.

Again, as in the case of soybeans, this overall increase may be attributed to an increase in the soil term due to an increase in soil moisture. Although no soil-moisture measurement was made after spraying, it is expected to be similar to the case of soybeans, since the soil type is almost identical and comparable amounts of water were applied.

3.4 Conclusions

For all three crops observed (wheat, soybeans, and corn), the presence of free water in the canopy results in about a 3-dB increase in σ^o_{VV} over the case in which no free water is present. For corn and soybeans this value may be only 2 dB, as the soil may contribute an additional 1 dB due to the increased soil moisture.

For σ^o_{VH}, an overall increase is seen in all three crops; however, trends indicating dry-down are difficult to discern because of an increase in the amount of data scatter.

4.0 MODELS FOR THE PREDICTION OF σ^0

The use of radar as a remote-sensing tool in the field of agriculture has been explored with promising results by investigators throughout the world (van Kastern and Smit, 1977; Ulaby et al., 1984; Peiyu et al., 1983). By selecting the proper frequency, polarization, incidence angle, revisit interval, and resolution cell size, information such as crop type, areal extent, and in some cases stage of growth (Brisco et al., 1982; Ulaby et al., 1984) can be acquired.

In order to use radar data effectively, an understanding of the microwave interaction process is necessary. By knowing which target elements produce dominant backscattering, an understanding of the way a target might appear at another frequency, polarization, or incidence angle, as well as some knowledge of its temporal behavior, may be gained. Such an understanding is made possible by the use of mathematical models of the target.

These models incorporate such factors as the target's geometric and dielectric properties as well as variations in both its spatial and temporal scope. In order to test such models once conceived, reliable radar data collected concurrently with necessary information about the target's parameters (ground truth) must be available. The understanding gained by such a process can help to pinpoint which target parameters are and which are not significant as well as which new target parameters should be sampled as a result of their potentially significant influence on radar data. The modeling-testing process provides feedback to the data-acquisition effort, thus forming a closed loop.

4.1 Modeling

The first step in the modeling process draws upon prior knowledge based on both theory and previous observations. The fundamentals of microwave behavior are based upon Maxwell's equations, from which, given sufficient knowledge about the target, exact deterministic solutions are theoretically possible. Due to the complex and probabilistic nature of all but the simplest remote sensing targets, however, this approach is not widely used. Nevertheless, basic elements do lend themselves to this effort in a general fashion. For example, in the case of a vegetation canopy, the basic geometry consists of a layer of vegetation separating semiinfinite spaces of air and soil.

Vegetation may be thought of as a collection of lossy scatterers uniformly distributed horizontally, with a known but changing vertical distribution. Such a description leads to a mathematical model of the form of Eq. (2.1). Each term in (2.1) depends on frequency, polarization, and incidence angle. Therefore, depending on the application, a certain set of radar parameters is indicated as being preferable. When monitoring soil condition, namely, soil moisture, it is preferable to minimize the influence of the vegetation by selecting the proper frequency, incidence angle, and polarization. Investigations (Ulaby et al., 1977) have shown that the use of low frequencies (C-band), low incidence angles (around 10° from nadir), and horizontal polarization is optimum for this application.

When monitoring vegetation, the proper choice of radar parameters can minimize the soil component with respect to the

vegetation term. Investigations (e.g., Ulaby et al., 1984) with this aim indicate the use of the higher frequencies (X-band and higher) at incidence angles around 50° (from nadir).

4.2 The "Cloud Model"

A conceptually simple model developed by Attema and Ulaby (1978) treats the vegetation layer as a "water cloud" composed of a uniform distribution of identical water particles. Based on this assumption, the following elements of (2.1) were derived:

$$\sigma^0_{veg}(\theta) = \frac{\sigma_v \cos\theta}{2\, k_e} \left(1 - L^{-2}(\theta)\right) \tag{4.1a}$$

$$L(\theta) = \exp(k_e\, h \sec\theta) \,, \tag{4.1b}$$

where k_e is the extinction coefficient of the vegetation medium (Np m^{-1}), h is the height of the vegetation canopy, and σ_v is the volume backscattering coefficient ($m^2\ m^{-3}$). Relating σ_v amd k_e to the physical p[illegible]nt parameters, Eqs. (4.1a) and (b) reduce, by virtue of the simple model, to

$$\frac{\sigma_v}{2\, k_e} = B \tag{4.2a}$$

$$k_e = A \cdot m_v \,, \tag{4.2b}$$

where m_v is the volumetric water content of the canopy (kg m^{-3}), and A and B are constants depending on frequency, polarization, and canopy geometry (or crop type).

An expression for the contribution of the soil was determined empirically from measurements made on bare soil (Ulaby et al., 1984) and takes the form

$$\sigma_s^o = C \exp(D \cdot m_s) \quad , \tag{4.3}$$

where C accounts for soil roughness, and D is a constant representing the sensitivity of σ_s^o to the soil moisture content m_s, both of which are functions of frequency, polarization, and incidence angle.

Inserting (4.1) through (4.3) into (2.1) leads to

$$\sigma_{can}^o(\theta) = B \cos\theta\left(1 - \frac{1}{L^2}\right) + \frac{C}{L^2} \exp(D \cdot m_s) \tag{4.4}$$

with

$$L = \exp(A \cdot m_v \cdot h \cdot \sec\theta) \; . \tag{4.5}$$

This model met with significant success when applied to a number of crops, namely, alfalfa, corn, milo, and wheat, at incidence angles ranging from 0 to 70°, frequencies from 8.6 to 17.0 GHz, and HH and VV polarizations.

4.3 The "Two-Layer Model"

In 1979, further measurements by Dutch investigators concerning the backscattering coefficient from vegetation substantiated the effectiveness of the cloud model for predicting σ^o_{can} for other plant types as well (beets, potatoes, and peas) based on the knowledge of only a few plant parameters (Hoekman et al., 1982). Difficulties arose, however, when attempts were made to predict σ^o_{can} for certain crop types that produce small grains, such as wheat, barley, and oats. This was attributed by the investigators to the fact that in the course of development, the geometry of these plants changes significantly, as when the grain head appears. To account for this phenomenon, a two-layer cloud model was adopted. The upper layer consists of the grain heads, whereas the lower layer is composed of the stalk and leaf material. The upper layer contributes its own backscattering, while attenuating that emanating from below. As in the original cloud model, the same is true for the lower layer. This model has the form

$$\sigma^o_{can}(\theta) = C_2(\theta)\{1 - \exp(D_2 \cdot m_v \cdot h_2 \cdot \sec\theta)\}$$

$$+ C_1(\theta)\{1 - \exp(D_1 \cdot m_v \cdot h_1 \cdot \sec\theta)\}$$

$$\cdot \exp(D_2 \cdot h_2 \cdot m_v \cdot \sec\theta)$$

$$+ G(\theta) \cdot \exp(k \cdot m_v)$$

$$\cdot \exp\{(D_1 \cdot h_v \cdot m_v + D_2 \cdot h_2 \cdot m_v) \cdot \sec\theta\} \,. \qquad (4.6)$$

This two-layer model, which proved more suitable for predicting σ^{o}_{can} using the indicated plant and soil parameters as inputs was tested at 10 GHz for HH and VV polarizations at incidence angles ranging from 20° to 75° from nadir.

4.4 Multiconstituent Canopy Model

On a different tack, investigators from the University of Kansas in 1979 and 1980 (Ulaby et al., 1983) made measurements of σ^{o}_{can} and supporting ground truth with the aim of refining the cloud model to include backscattering terms for individual plant parts. The crops observed were corn, sorghum, and wheat. Again, it was necessary to treat wheat differently than corn or sorghum because of its changing geometry, as mentioned above. The available ground-truth information included soil moisture, fresh and dry plant biomass by plant part, and plant density, height, and green leaf area index (LAI).

Analysis of all three sets of crop data indicated that the variation of σ^{o}_{can} with respect to LAI was much the same as that

observed using m_v, the volumetric canopy water content. Replacing m_v with LAI improved σ^o_{can} prediction accuracy, given the necessary ground-truth parameters. The explanation for this is attributed to the fact that green leaves contain mostly water and are thus strong scatterers of microwave energy. Although the the stalks contain significant amounts of water, they do not contribute much in the way of backscattered energy, especially in the case of wheat, because of their geometry. Hence the LAI term includes much of the same information as m_v; nevertheless, it also includes some information not previously available, i.e., the areal coverage of the leaf material. This ability to relate LAI to σ^o_{can} is significant in that LAI is an important element in the yield-prediction algorithm (Coelho and Dale, 1980).

The wheat model that evolved includes a backscattering contribution by the heads, by the leaves as attenuated by the heads, and by the soil as attenuated by both the leaves and the heads. Thus, this model for wheat takes the form

$$\sigma^o_{can} = \sigma^o_{leaf} + \sigma^o_{head} + \sigma^o_{soil}$$

$$\sigma^o_{can} = A \cdot LAI\{1 - \exp(-E \cdot LAI)\} \cdot \exp(-D \cdot DWT)$$

$$+ B \cdot DWT + C \cdot m_s \cdot \exp(-E \cdot LAI - D \cdot DWT) , \quad (4.7)$$

where DWT is the dry head biomass per square meter (kg m^{-2}), m_s is the volumetric soil moisture (g cm^{-3}), and A, B, C, D, and E are all constants determined for each frequency and polarization.

This model is different from those presented above in three significant ways. First, there is the appearance of the LAI term multiplying the [1. - exp( )] term. Secondly, there is a different form for σ^o_{head}. Thirdly, there is a linear rather than an exponential dependence of σ^o_{soil} on soil moisture. As for the first difference, in the original derivation of the cloud model it was assumed that there is a uniform distribution of identical water particles. If these water particles are not in fact identical but are distributed in much the same way that water is distributed in an atmospheric water cloud, the dependence of σ^o_{can} will have an m_v term included in the σ^o_{leaf} term. Hence, in keeping with the utilization of LAI in place of m_v, LAI appears as a multiplying factor in Eq. (4.7) because this form is superior to the one that does not include this factor, and there is a rationale behind it.

As for the second difference, a linear dependence on dry head biomass was found to work best for σ^o and therefore was adopted.

The third difference is the result of a simplification in the model treating σ^o_{soil} as a linear function of m_s rather than as an exponential. Indeed, there is but little difference over narrow ranges of m_s.

This model provided good agreement between observed and predicted σ^o_{can}, thus providing insight into the factors determining what the radar is "seeing." The model was tested at four frequencies (8.6, 13, 17, and 35.6 GHz), two polarizations (VV and HH), and one incidence angle (50°).

When applied to the corn and sorghum data, the model is similar in its use of LAI rather than m_v, and in the linear rather than exponential dependence of σ^o_{soil} on m_s.

One point of difference, however, is that the σ^o_{leaf} term includes LAI in the exponential only. This choice was made because the model gave results in better agreement with measurements. Since the distribution of water particles is unknown, this criterion is reasonable.

A second difference is that a new term, σ^o_{stalk}, replaces the σ^o_{head} term.

The full model takes the form

$$\sigma^o_{can} = \sigma^o_{leaf} + \sigma^o_{stalk} + \sigma^o_{soil}$$

$$\sigma^o_{can} = A'_{leaf} \cdot \{1 - \exp(-B'_{leaf} \cdot LAI)\}$$

$$+ A'_{stalk} \cdot m_v \cdot h_2 \cdot \exp(-B'_{leaf} \cdot LAI)$$

$$+ C_{soil} \cdot m_s \cdot \exp(-B'_{leaf} \cdot LAI \cdot -B'_{stalk}\, m_v \cdot h_2) \cdot \qquad (4.8)$$

The stalk term is attenuated by the leaves, based on the assumption that backscattering by leaves occurs in the top portion of the canopy, whereas backscattering from the stalk must first pass through the leaves. The dependence of σ^o_{stalk} on $m_v \cdot h_2$ is reminiscent of the cloud model in that m_v represents the

volumetric water content of the stalks, and h_2 is the effective stalk height, which in this case is set to be the physical canopy height. The soil term is attenuated by both leaves and stalks, but in the course of obtaining coefficients it was revealed that when $B'_{stalk} = 0$, the model behaves best; hence, apparently, no significant stalk attenuation exists.

This model proved to be superior to the cloud model in its predictive capacity for σ^o_{can} at all four frequencies, i.e., 8.6, 13, 17, and 35.6 GHz, for both VV and HH polarizations, at an incidence angle of 50°. In addition, it worked slightly better for sorghum than for corn.

4.5 1981 Vegetation Experiment

During the 1981 growing season, extensive radar backscattering measurements were made as well as supporting ground-truth data (Brisco and Allen, 1982). Ten fields each of winter wheat, corn, and soybeans were observed repeatedly throughout the growing season. These fields are located in the floodplain north of Lawrence, Kansas, and are indicated in Figure 4.1.

The radar data consist of σ^o values for 10.2 GHz at two polarizations (VV and VH), at an angle of incidence of 50°. On occasion, three fields of each crop type were observed at incidence angles of 30°, 40°, 50°, 60°, and 70°. Two-hundred and six complete radar data sets were acquired on the ten wheat fields, 318 on the ten corn fields, and 348 on the ten soybean fields, giving a total of 869 data sets consisting of σ^o_{VV} and σ^o_{VH}

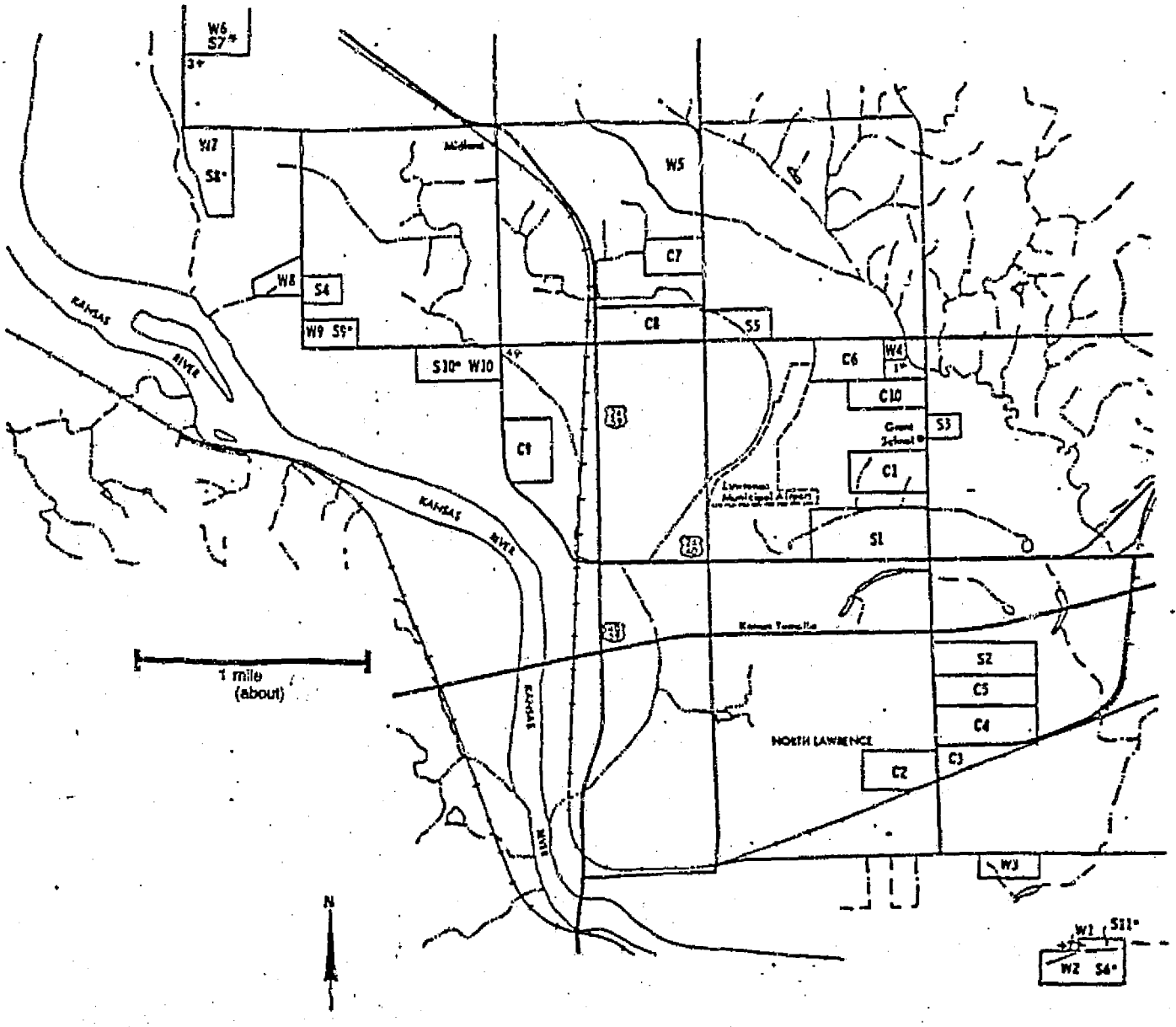

Figure 4.1 Location of the target fields in the North Lawrence study area.
* indicates a wheat field double-cropped with soybeans
+ indicates rain gauges.

C2

at a 50° incidence angle and 10.2 GHz. Among these, 70 data sets include incidence angles of 30°, 40°, 50°, 60°, and 70°. This volume of data was made possible by using for the first time the Mobile Agricultural Radar Sensor (MARS 10.2 GHz), which acquires data while aboard a truck being driven alongside a field, all the while integrating the received signal strength. This greatly reduced the time required to acquire a single radar data set.

The supporting ground truth consisted of 0 - 5-cm soil-moisture content, plant height, planting density, and fresh and dry plant biomass. For wheat plants, plant biomass data were broken down into two parts: head material and leaves with stalks. For corn plants, plant biomass data were broken down into three parts: leaves, stalks, and fruit or cobs. For soybean plants, the plant biomasses were for the entire soybean plant. Soil type and bulk-density measurements were also made for each field. Weather data consisting of daily high and low temperatures, humidity, wind speed and direction, and rainfall amounts, were provided by the University of Kansas Weather Station. Additional rainfall information was made possible by monitoring four rain gauges distributed throughout the north-Lawrence test area. Farm operators cooperated by providing such information as planting date, tillage history, harvest date, seed variety, fertilizer used, herbicide used, field-preparation method yield, and bushel weight. Growth stage was also recorded periodically for each field, as was any crop damage due to insects, weather, etc.

Due to the ambitious size of the experiment and to limited facilities, only small, inadequate samples of variables having large within-field variances (Brisco et al., 1981) such as plant biomasses were acquired. This became noticeably severe during the data-processing sequence, when it was decided that a smoothing of the variables in question was necessary. This was accomplished by fitting the raw data to a best-fit third- or fourth-order polynomial, depending on the shape required. Once this was accomplished, a manual check was made to ensure that the overall trend and absolute level of the data were intact. This sequence was followed for all plant variables (biomass data and heights) but not for soil moisture. The rationale behind the smoothing is that the parameters in question, though changing, follow a predictable, even pattern. Figure 4.2 shows the temporal behavior of σ^{o}_{VV} and σ^{o}_{VH} and the associated ground truth after smoothing of plant biomasses and height for Wheat Field No. 8.

One reason for choosing such a large number of fields on such a frequent revisit basis was to look at the statistical side of modeling. All previous modeling attempts, with the exception of the 1979-1980 Kansas experiments, were restricted to examining one or possibly two fields of a single crop type. (The 1979-1980 data represent an exception because of their scope). The 1979 experiment examined two fields of wheat, six of corn, and six of sorghum. At most, ten data sets were acquired for each field in 1979. In 1980, three fields each of corn and sorghum were

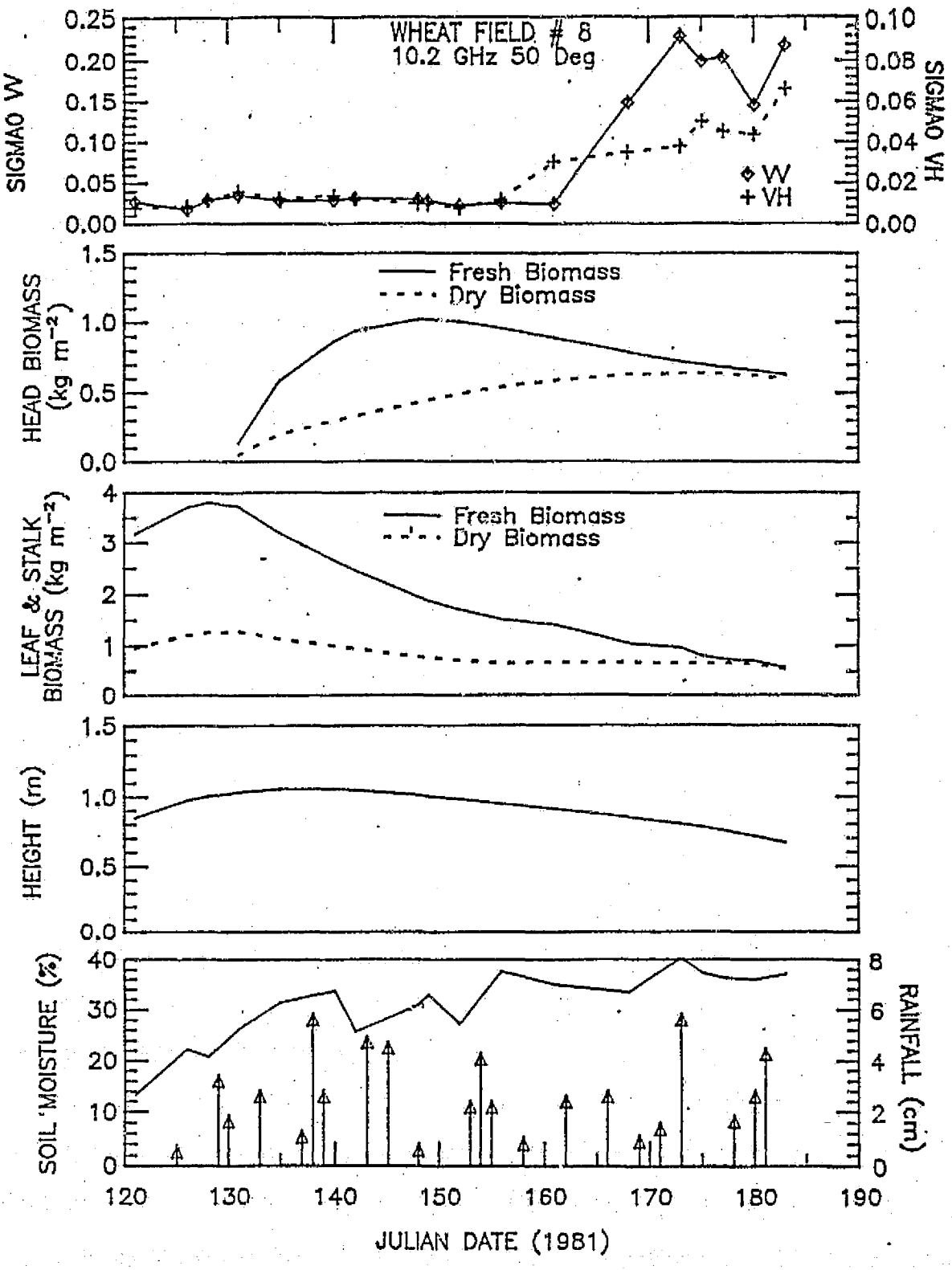

Figure 4.2 Temporal histories of the radar data (σ^o) and the ground-truth parameters (after smoothing) along with the measured rainfall events, for a given wheat field (No. 8).

observed approximately 22 times per field throughout the growing season. In addition, this experiment examined actual agricultural fields, as opposed to small, uniform test plots.

4.6 1981 Wheat Data

As mentioned above, 206 data sets were acquired for the ten wheat fields used in the 1981 experiment. Twenty-two of these data sets were acquired after harvest. Of the remaining 184 data sets, another 41 were omitted from modeling due to abnormal σ^o behavior, which occurred apparently as a result of a weather event within the previous two days. The exact influence of these weather events (wind damage, hail damage, heavy rain, or strong wind during data acquisition) is not well understood and therefore would have complicated the modeling effort. Thus, of the original 206 data sets for wheat, 143, or about 14 per field, are available for modeling purposes. Figure 4.3 shows Wheat Field No. 8, with the weather-affected points and post-harvest data as examples.

By restricting the experiment to only one frequency and one incidence angle, the modeling process had only to deal with changes in plant geometry, dielectric (via water content), and soil-moisture changes throughout the growing season.

Figure 4.4 shows a plot of the temporal changes in σ^o for each field in real ($m^2\ m^{-2}$) units. Both σ^o_{VV} and σ^o_{VH} are shown with the σ^o_{VH} using the right-hand scale (which is 2.5 times larger than the left hand-scale). This was done to enhance the similarity between the like (VV) and cross (VH) polarizations. The same overall trend is seen in plots of both. At the time

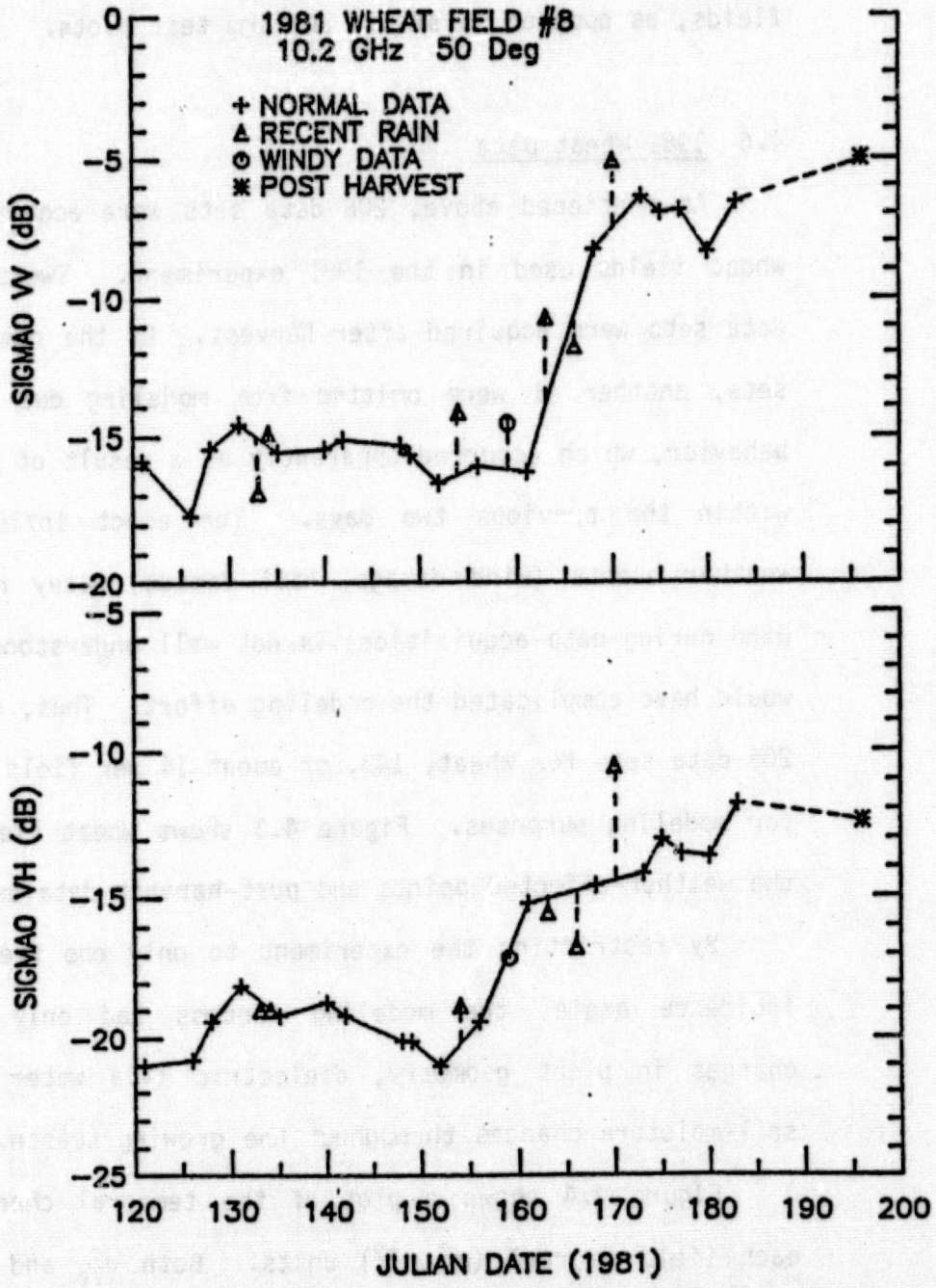

Figure 4.3 Temporal history of the measured σ^{o} from wheat field No. 8. Included are all weather-affected points as well as post-harvest points.

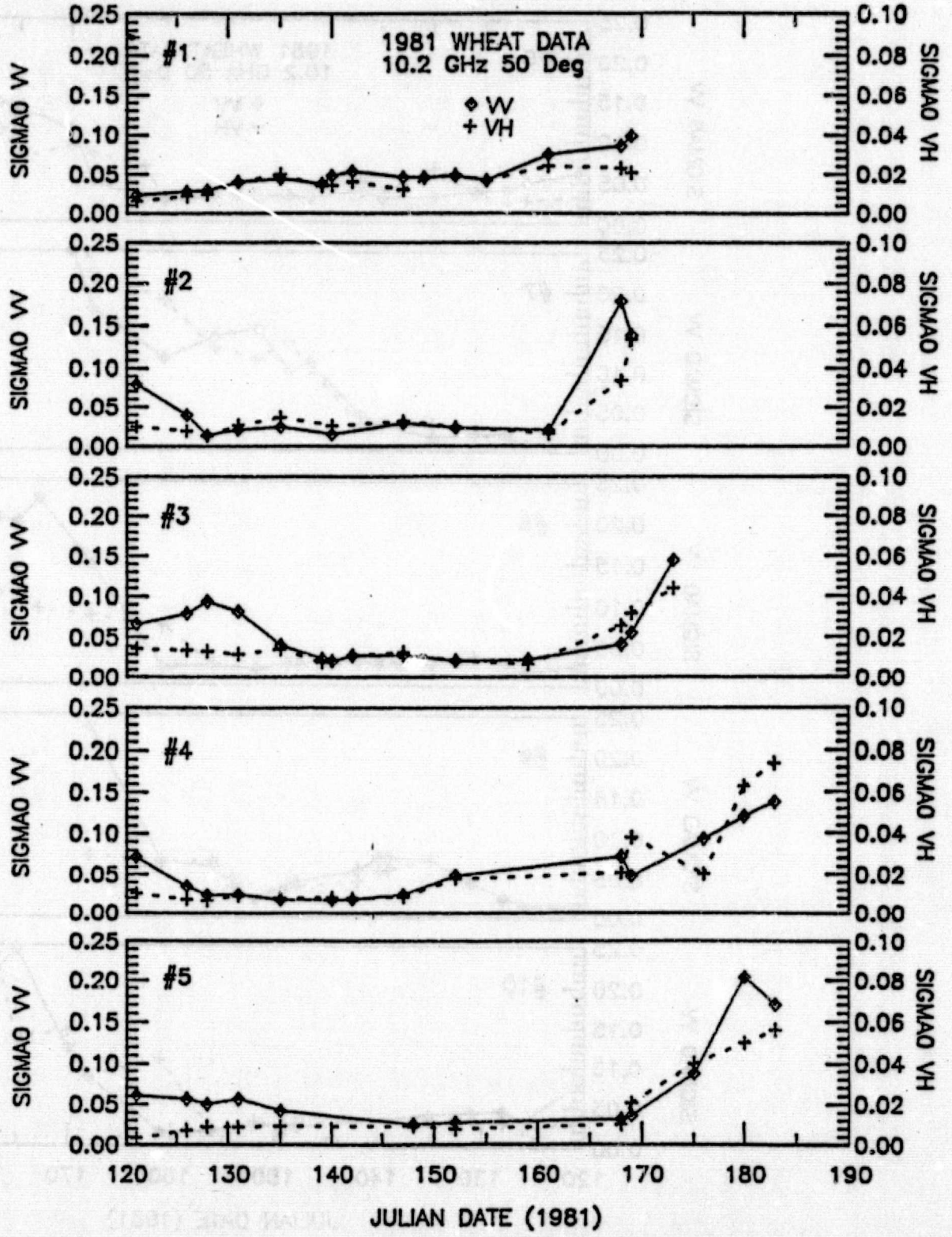

Figure 4.4 Temporal histories of the measured σ^{o} (VV and VH) from all ten wheat fields.

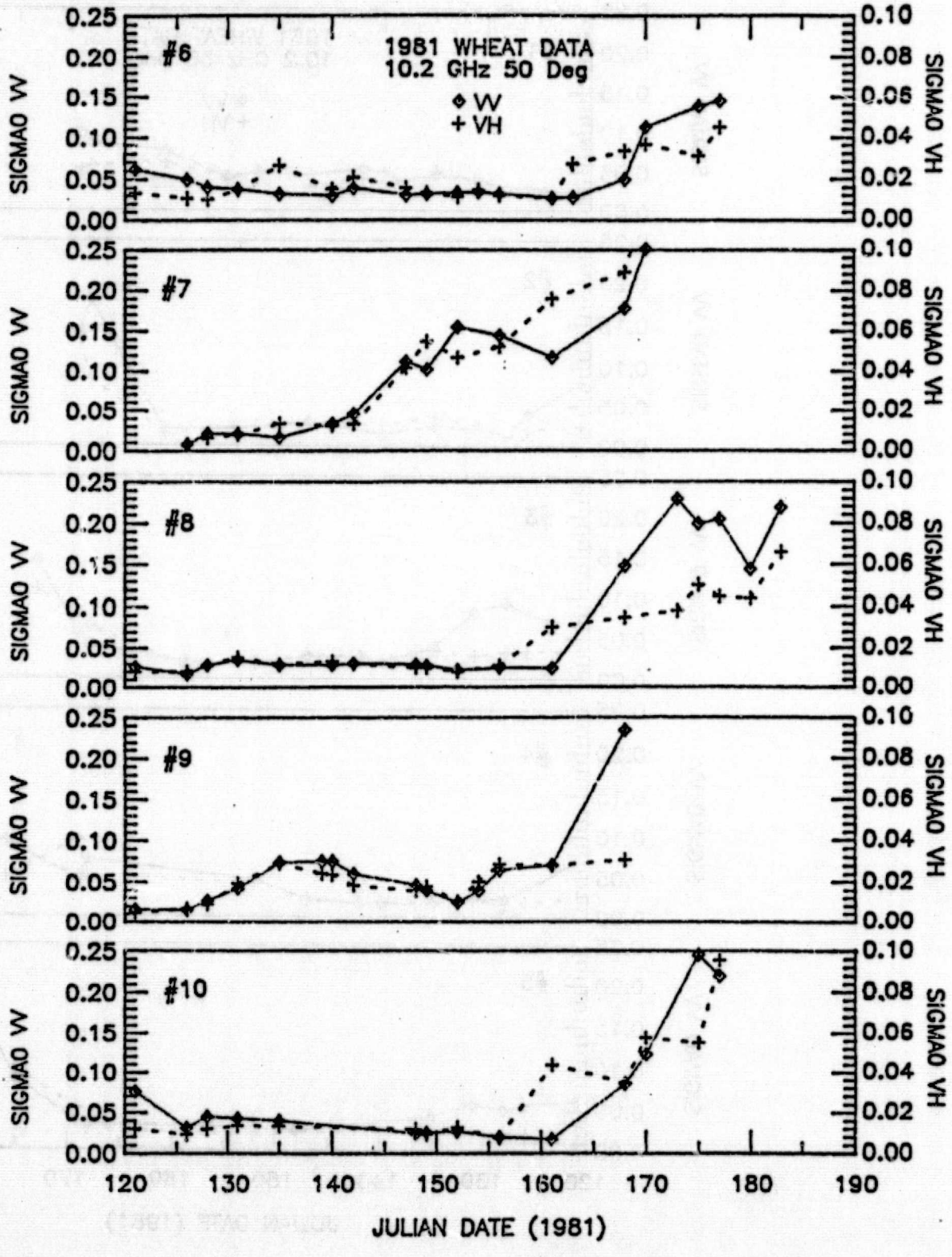

Figure 4.4 (Continued)

observation was begun (Day 121, May 1, 1981), there were few dynamics appearing in σ^o. This continued for most of the fields until a point on or after Day 160 (June 9, 1981), after which a dramatic increase occurred. Soon after, harvest occurred. The fact that this was repeated in most of the fields and that it has been seen in the past (Bush and Ulaby, 1975) indicates that this is a genuine phenomenon, characteristic of wheat. Additionally, the fact that the final weeks before harvest were accompanied by a dramatic increase in σ^o may in fact be useful in predicting the harvest and following its progress, as mentioned by Bush and Ulaby (1975). The lack of an early peak in σ^o prior to the seemingly uneventful period before the pre-harvest increase as seen by Ulaby et al. (1983) may be due to the late start in data-acquisition, differing rates of development at the two locations, and differing weather factors.

Figure 4.5 shows a superposition of temporal plots of σ^o for all ten fields shifted in time to coincide at approximately the same peaking time. The upper plot shows σ^o_{VV} versus time, and the lower one shows a plot of σ^o_{VH} versus time using the time shifts determined for the σ^o_{VV} case. The fact that all ten overlap nicely reinforces the supposition that this behavior is characteristic of wheat and is not an anomaly. The required time-shifts varied from no shift for two reference fields to as many as 29 days for another field. This is the result of different growth rates due to slightly different environmental conditions, such as available

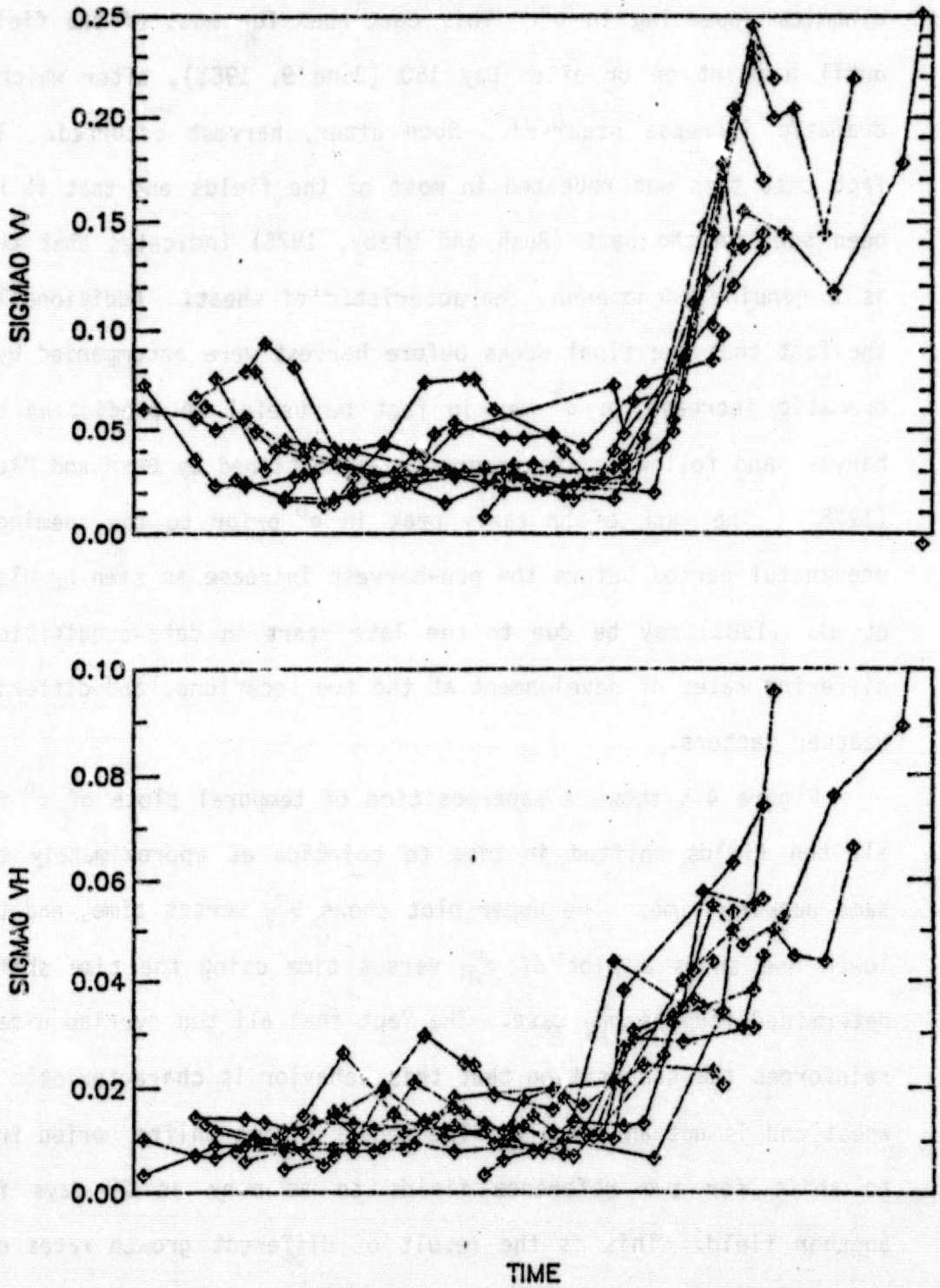

Figure 4.5 A superposition of all ten wheat fields' σ^{o} values presented versus time with some shifts along the time axis so as to make the peaks late in the season coincide.

water and nutrients. Such differences in developmental stage were not, however, seen in the periodic stage-of-growth observations made by ground-truth personnel.

4.6.1 Initial Analysis

As a first step in the analysis of the wheat data, linear correlation coefficients between measured σ^o values expressed in dB and ground-truth parameters were computed. Tables 4.1 and 4.2 show the results. For VV polarization, high correlations were revealed relating σ^o_{VV}(dB) to the percentage of moisture in the plant (expressed on a fresh-weight basis). Also of significance is the fact that these high correlations (0.68 to 0.77) were all negative, indicating that as the percentage of moisture decreased σ^o_{VV}(dB) increased. This agrees almost exactly with what Bush and Ulaby observed in 1974 at all frequencies (8.6 to 17 GHz); incidence angles of 30°, 50°, and 70°; and HH and VV polarizations. Their conclusion was that as plant moisture decreased, penetration into the canopy increased, resulting in a larger σ^o value. This implies that the σ^o of a wheat canopy alone, at the frequencies and angles specified, is less than that of the underlying soil and that the attenuation of the canopy layer is sufficient to reduce the soil's contribution significantly. This hypothesis provides one possible explanation of what is seen in the 1981 wheat data. In terms of changes in σ^o, the period of time several weeks prior to harvest is observed to be relatively flat. This occurs when the canopy is still lush and quite moist; thus, what is being observed is the σ^o of the

TABLE 4.1

1981 Wheat Statistics

	Mean	Std. Dev.	Maximum	Minimum	Units
Volumetric Soil Moisture	27.3	10.4	54.0	3.8	$cm^3/cm^3 \times 100$
Fresh Leaf and Stalk Biomass	2.06	1.23	4.81	0.27	kg/m^2
Dry Leaf and Stalk Biomass	0.79	0.33	1.80	0.16	kg/m^2
Height	0.83	0.14	1.06	0.29	m
Fresh Head Biomass	0.57	0.40	1.53	0	kg/m^2
Dry Head Biomass	0.31	0.24	0.89	0	kg/m^2
σ^o_{VV}	-13.3	3.3	-6.0	-20.8	dB
σ^o_{VH}	-17.8	3.2	-9.1	-24.8	dB
Leaf and Stalk Water Content	1.28	0.95	3.85	0.03	kg/m^2
Head Water Content	0.26	0.23	0.75	0	kg/m^2

TABLE 4.2

Linear Correlation Analysis (r)
1981 Wheat Data

Correlation Coefficient r	1	2	3	4	5	6	7	8	9	10	11	12
1. Volumetric Soil Moisture	1											
2. Leaf and Stalk Fresh Biomass	-0.07	1										
3. Leaf and Stalk Dry Biomass	0.14	0.88	1									
4. Leaf and Stalk Water Content	-0.13	0.97	0.79	1								
5. Leaf and Stalk Percent Moisture (Fresh Basis)	-0.43	0.69	0.41	0.74	1							
6. Head Fresh Biomass	0.29	-0.00	0.14	-0.06	0.07	1						
7. Head Dry Biomass	0.50	-0.41	-0.18	-0.48	-0.45	0.74	1					
8. Head Water Content	-0.04	0.39	0.38	0.37	0.54	0.77	0.15	1				
9. Head Percent Moisture (Fresh Biomass)	-0.45	0.68	0.51	0.72	0.89	0.00	-0.63	0.60	1			
10. Height	0.28	0.64	0.68	0.59	0.34	0.14	-0.25	0.44	0.56	1		
11. σ^{o}_{VV}(dB)	0.31	-0.40	-0.31	-0.41	-0.68	0.00	0.45	-0.44	-0.42	-0.35	1	
12. σ^{o}_{VV}(dB)	0.47	-0.54	-0.34	-0.58	-0.76	0.06	0.49	-0.38	-0.19	-0.23	0.81	1

N = 143 in all cases except cases involving head ground truth information, then N = 116.

wheat canopy plus an attenuated background σ^o term due to the soil.

A positive correlation of 0.31 between σ^o_{VV}(dB) and volumetric soil moisture content is consistent with this hypothesis, since observations of bare soils yield higher positive correlations (Batlivala and Ulaby, 1977). Other correlation coefficients that support this hypothesis are seen in the dry head biomass, the water content of the leaves and stalks between σ^o_{VV}, and the water content of the heads. A positive correlation between σ^o_{VV} and dry head biomass indicates that the heads may also be a source of significant backscattering. Again, negative correlations with the water content of plant parts support the attenuation hypothesis.

Similar results were seen in the linear correlation analysis between σ^o_{VH}(dB) and plant moisture, soil moisture, dry head biomass, and plant water content. This would indicate that a similar mechanism drives both σ^o_{VH} and σ^o_{VV}.

To further examine the relationship between σ^o and plant moisture, plots were made of σ^o (in real units, $m^2\ m^{-2}$) versus plant-part moistures. These are shown in Figures 4.6 and 4.7. The choice to express σ^o in real units rather than decibels was made to enhance small changes in σ^o. A linear dependence of σ^o(dB) on some parameter corresponds to an exponential dependence of σ^o (in real units) on the same parameter. Previous models have shown that attenuation takes on an exponential form; thus, it is linear when expressed in dB.

Figures 4.6 and 4.7 show similar results. In both cases, when the percentage of moisture is at a maximum (around 70%), very

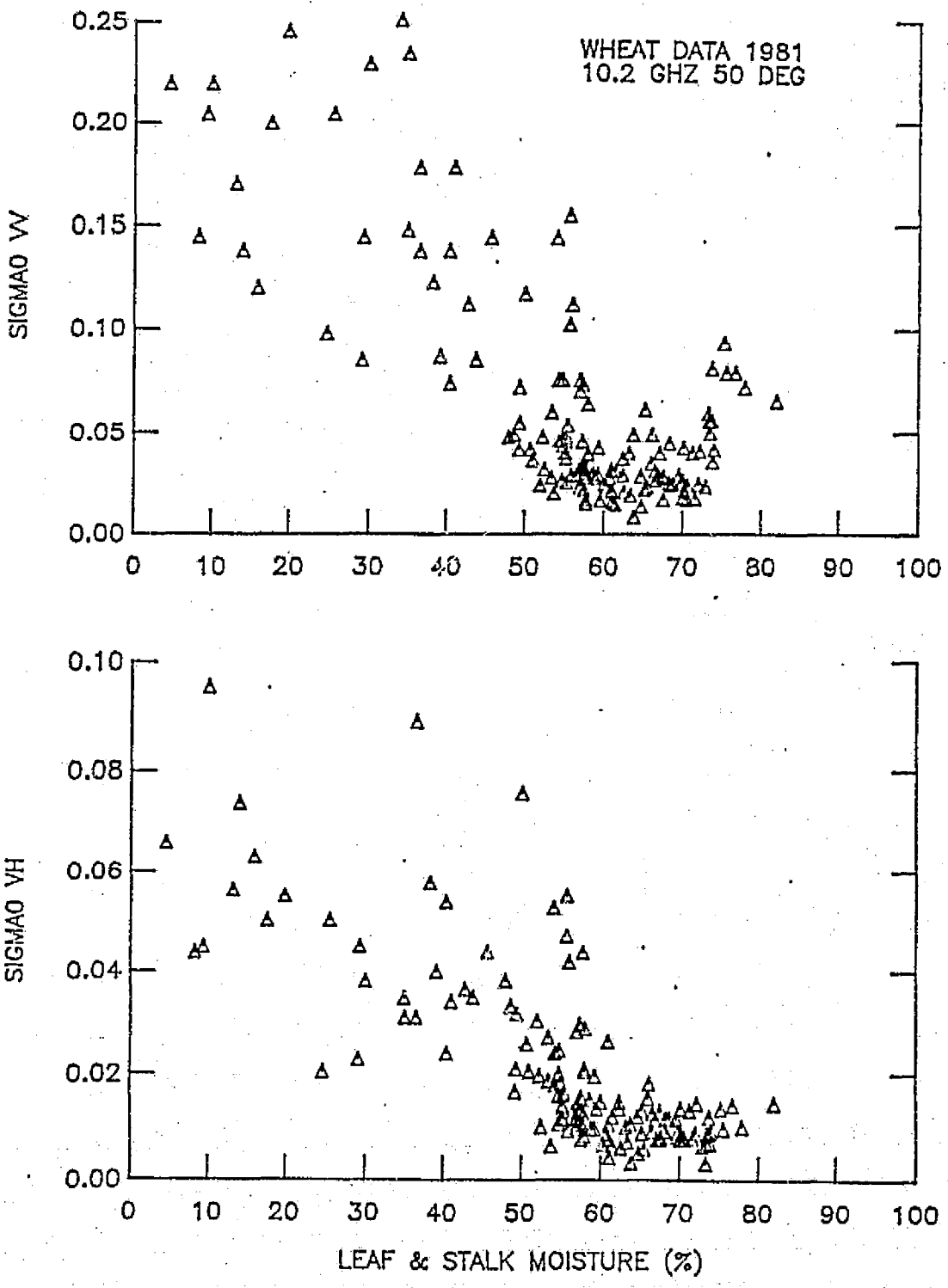

Figure 4.6 The effect of leaf and stalk moisture on the level of σ^{o}.

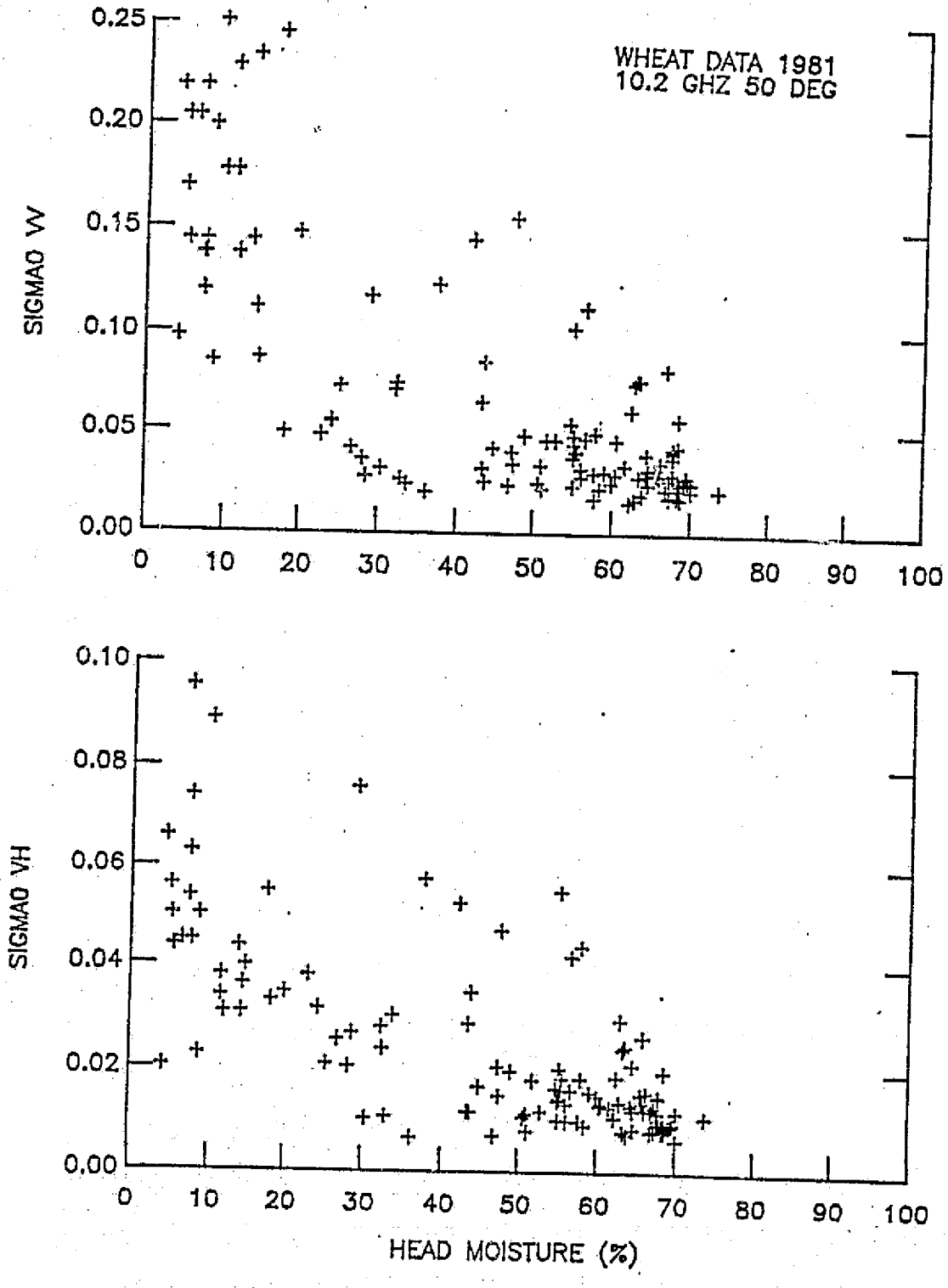

Figure 4.7 The effect of head moisture on the level of σ^o.

little scattering in σ^o is observed. As the percentage of moisture decreases, increased scattering is observed and higher overall σ^o values are seen. This is true in both the VV and the VH cases. The scattering in σ^o for low moisture contents may be due to varying soil moistures as well as to varying contributions to σ^o_{can} from the canopy itself.

To further investigate the relationship between σ^o and plant moisture, a plot was made of σ^o versus volumetric soil moisture content, as shown in Figure 4.8. To elucidate the effects of canopy moisture, the data were broken into two sets: one with leaf- and stalk-moisture percentages exceeding 50% (indicated by asterisks), and the other with leaf- and stalk-moisture percentages of less than 50% (indicated by circles). In general, with only a few exceptions, the data denoted by asterisks maintain an almost constant level for all of the soil-moisture values available. The data marked by circles, on the other hand, show considerable scattering. A weak yet observable trend is detected in the relationship between σ^o and increasing soil moisture, which agrees with previous models that predict σ^o given soil moisture (Ulaby et al., 1983). This result serves as further evidence that some form of attenuation of soil backscattering by the wheat canopy is occurring, along with significantly smaller backscattering due to the canopy itself. Finally, a multiple correlation coefficient r^2 of 0.65 was found between σ^o_{VV}(dB) and σ^o_{VH}(dB), indicating that the same or similar mechanisms are driving both. A plot of σ^o_{VV}(dB) versus σ^o_{VH}(dB) is shown in Figure 4.9 for all wheat data unaffected by weather or harvest.

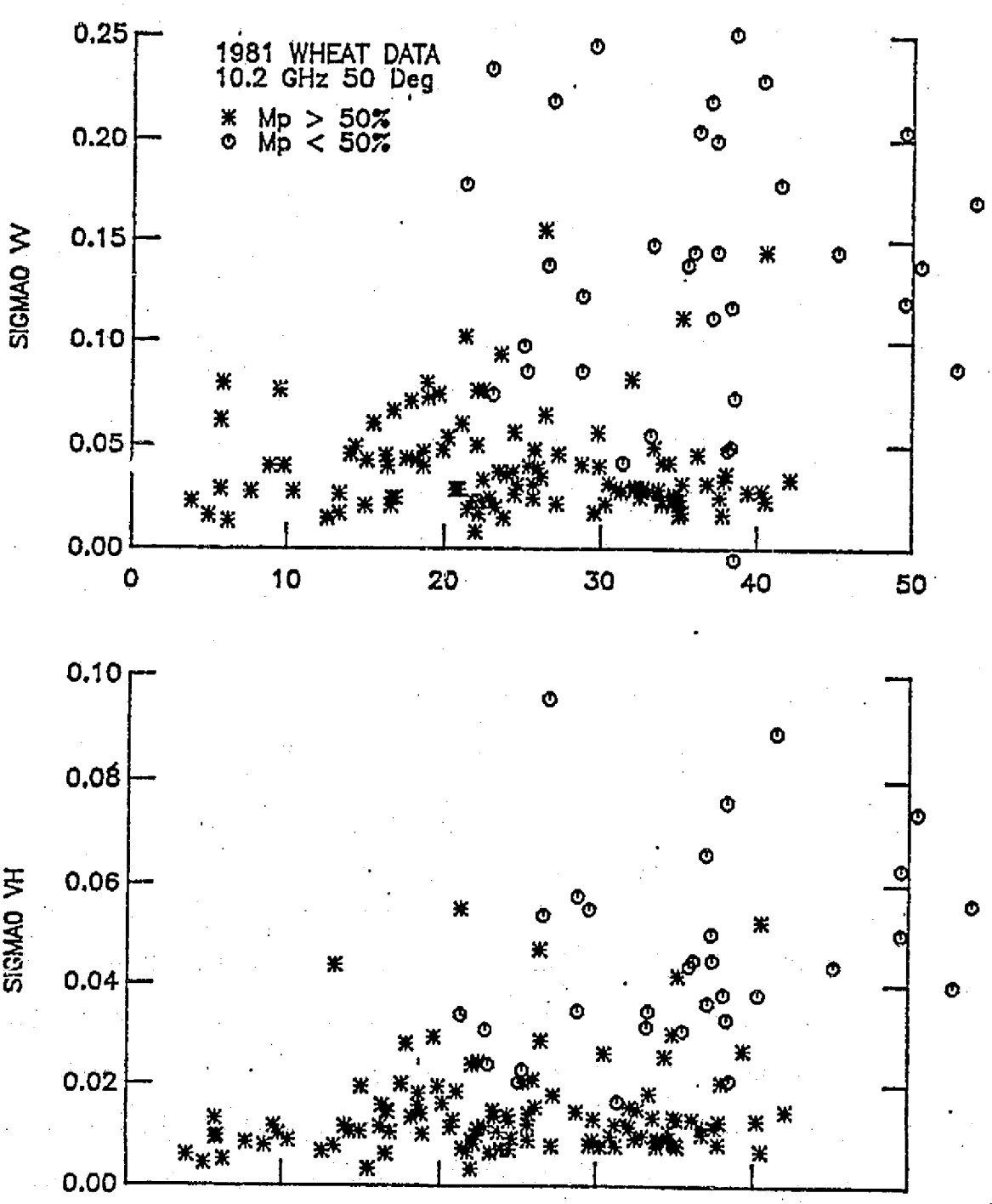

Figure 4.8 The effect of soil moisture on the level of σ^o under two conditions: plant moisture over 50% and plant moisture under 50%.

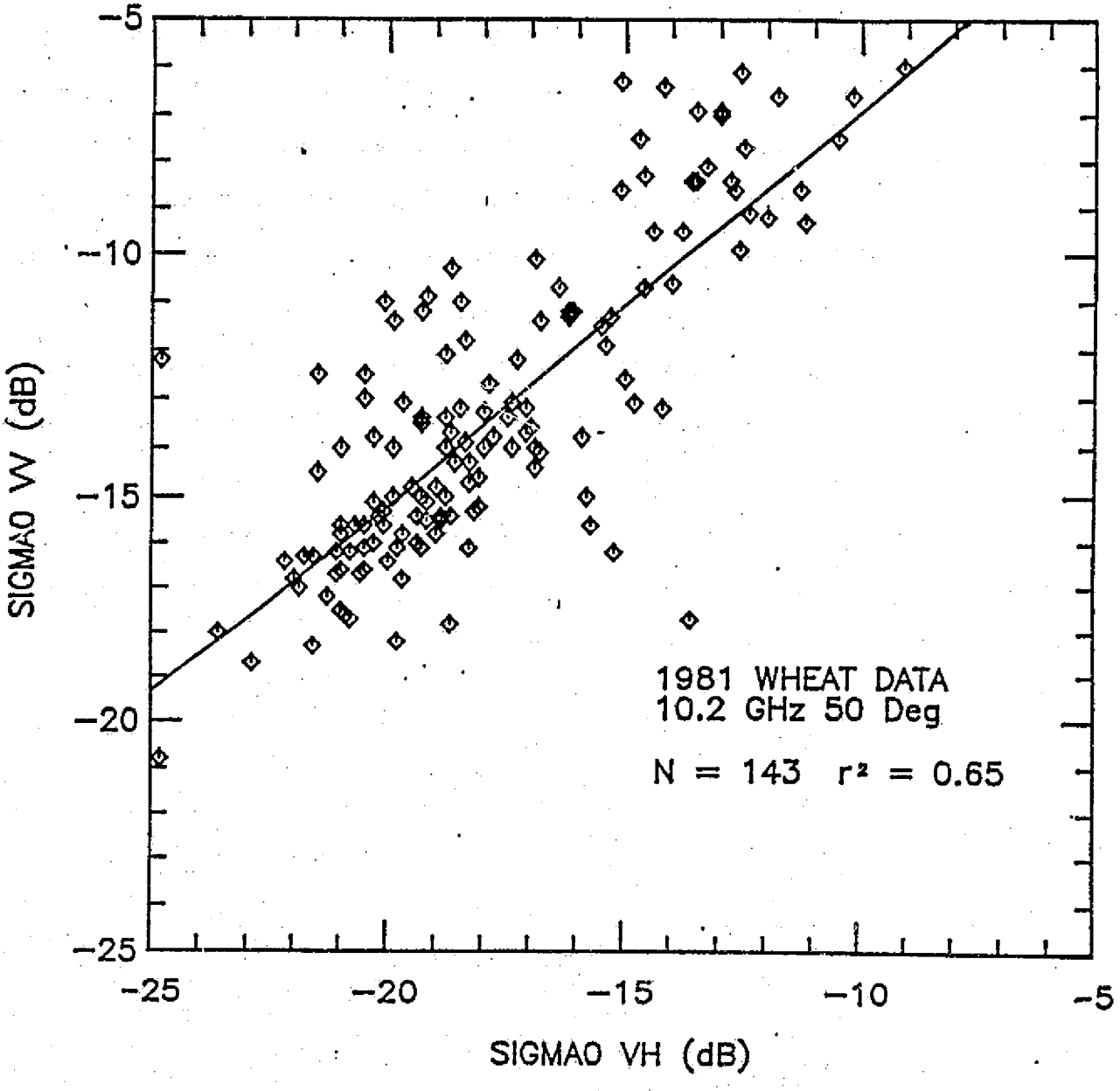

Figure 4.9 The way in which σ^{o}_{VV} changes with respect to σ^{o}_{VH} from the wheat data.

4.6.2 Modeling of the 1981 Wheat Data

For two reasons, the availability of the 1981 wheat data provides a heretofore impossible opportunity to test and develop canopy models. First, this data set includes ten actual agricultural fields grown using current and widely used farming techniques, and a variety of seed types, fertilizers, and soil textures. All fields were observed frequently, using the same calibrated system, thus removing any possible calibration problems that might have been encountered when data sets from different systems and/or different years were combined.

Secondly, because of the design of the radar system, reliable cross polarization (VH) is now available throughout the growing season of a wheat crop. In previous years, due to system limitations mainly in the antenna area, the ability to measure VH data was degraded. However, by restricting the design of the MARS system so that it would deal with only one frequency, and by employing two distinct antennas, sufficient isolation was achieved to make reliable cross-polarization measurements possible.

With this in mind, attempts to model the 1981 wheat data were begun by testing the models previously presented. The criterion for judging the ability of a model to predict σ^o_{can} given the necessary canopy parameters was based on three major factors. First, a high correlation coefficient between measured and predicted σ^o_{can} was desired. Similarly desirable was a small RMS difference error expressed in dB (RMS dB), defined here as

$$\text{RMS error (dB)} = \left[\frac{\sum_{1}^{n} [\sigma^{o}_{meas}(dB) - \sigma^{o}_{pred}(dB)]^2}{N} \right]^{1/2}, \quad (dB) \tag{4.9}$$

representing the average deviation of the predicted value of σ^{o}_{can} from that measured, expressed in dB. The third factor determining the effectiveness of a model for predicting σ^{o}_{can} is the number of model parameters or constants that are necessary. Logically, as the number of model parameters increases, so too will the correlation coefficient that measures the model's effectiveness. However, this also increases the complexity of the model; therefore, a tradeoff is made between model complexity (the number of parameters required), the correlation coefficient, and the RMS error (dB).

Models that require the determination of parameter values for optimization may show a superior fit per field when new constants are determined for each field. However, in order to test the effectiveness of a model for predicting σ^{o}_{can} for a given crop type rather than for a specific field, it should be able to predict, on the basis of the ground-truth information available, σ^{o}_{can} for all fields from a set of constants determined on the basis of all available data for that crop type. Therefore, each model will be tested on the basis of the entire data set.

The first model tested was the cloud model developed by Attema and Ulaby (1976). It has the form

$$\sigma^0 = A \cdot [1 - \exp(-B \cdot w \cdot h)] + C \cdot \exp(D \cdot m_s - B \cdot w \cdot h) , \quad (4.10)$$

where w is the volumetric water content of the canopy, h is the physical height of the canopy, and m_s is the volumetric soil-moisture content. This model requires only four parameters (A,B,C,D) and provides a correlation coefficient (r^2) of 0.50 with an RMS error of 2.30 dB when applied to the VV data, and 0.55 and 2.12 dB for the VH data. All four parameters were determined to yield an optimum model in each case (VV and VH) when a nonlinear regression package program on a digital computer was used. The values determined were different from those published by Attema and Ulaby but not significantly different in the VV case. When a comparison of the predicted σ^0_{VV}, based upon their model and using their constants, was made with the measured 1981 data, a correlation coefficient (r^2) of 0.09 and an RMS error of 3.79 dB resulted. They did not attempt VH optimization.

The second model tested was the two-layer model presented by Hoekman et al. (1982). It takes the form

$$\begin{aligned} \sigma^0 = {} & C_2[1 - \exp(-D_2 \cdot w \cdot h_2)] \\ & + C_1[1 - \exp(-D_1 \cdot w \cdot h_1)] \exp(-D_2 \cdot w \cdot h_2) \\ & + G \cdot \exp[k \cdot m_s - (D_2 \cdot w \cdot h_w + D_1 \cdot w \cdot h_1)] \cdot \end{aligned} \quad (4.11)$$

After its six parameters (C_1, C_2, D_1, D_2, G, k) were optimized for each case (VV and VH), the following correlation coefficients (r^2) and RMS errors were determined: VV had 0.51 and 2.29 dB, whereas VH had 0.60 and 2.00 dB, respectively. Again, the parameters found were not significantly different from those published.

When a comparison was made between the predicted and measured 1981 data using their model and constants, a correlation coefficient (r^2) of 0.07 and an RMS error of 5.52 dB resulted. The fact that their correlation coefficient exceeded 0.9, whereas their RMS error remained below 0.9 dB, may be due to the fact that (a) they dealt with multiple angles giving a wide dynamic range for σ^o and determined eight additional parameters to handle the angular variation, and (b) they dealt with only two limited test plots of winter wheat, which had an artificially high uniformity not normally found in ordinary agricultural fields.

A third model tested was the plant-part model presented by Ulaby et al. (1983). This model requires five parameters and takes the form

$$\sigma^o = A \cdot LAI \{1 - \exp(-E \cdot LAI)\} \exp(-D \cdot DWT)$$

$$+ B \cdot DWT + C \cdot m_s \cdot \exp(-E \cdot LAI - D \cdot DWT) . \quad (4.12)$$

Here DWT is the dry head biomass per square meter, and LAI is the green leaf area index. The 1981 experiment did not include LAI as a ground-truth parameter; thus, in order to test this model, a substitute parameter was required. A previous investigation into

the relationship between LAI and fresh leaf biomass for corn and soybeans (Brisco et al., 1983) indicates a strong correlation between LAI and fresh leaf biomass. Therefore, assuming that this relationship is true for wheat as well, and further assuming that the ground-truth parameter measuring fresh leaf and stalk biomass is highly correlated to fresh leaf biomass alone, a substitution of fresh leaf and stalk biomass was made for LAI. The result was a correlation coefficient (r^2) of 0.45 with an associated RMS error of 2.42 dB for VV, and 0.57 and 2.06 dB for VH. It should be mentioned that part of the driving force behind using LAI as a model input had been the early season peak, which was attributed to the leaf material. However, as mentioned previously, no such peak was detected in the 1981 data due in part to the late start in data acquisition. Again, most of the model parameters determined for the VV case did not differ significantly from those published; however, two did vary, dramatically. The C and D constants, which determine the magnitude of the soil backscattering and head attenuation, were orders of magnitude smaller than those reported. In the case of the total soil contribution to σ^o_{can}, these changes offset one another, resulting in an appropriate overall level. The need for such a large value for D might have arisen in the early peak period, which again is missing from the current data.

Based upon these results it was determined that a new model should be developed, employing different aspects of the three models mentioned previously This semiempirical model should provide for head backscattering as well as attenuation, leaf and

stalk backscattering and attenuation, and soil backscattering.

The basic form adopted for this new model is

$$\sigma^o = \sigma^o_{\substack{\text{head} \\ \text{leaf} \\ \text{stalk}}} + \sigma^o_{\text{soil}} , \tag{4.13}$$

where

$$\sigma^o_h = B \cdot f_1(\text{head}) \tag{4.14a}$$

$$\sigma^o_{l+s} = A\{1 - \exp[-F \cdot f_2(l + s)]\} \{1 - \exp[-E \cdot f_3(l + s)]\} \cdot \exp[-D \cdot f_4(\text{head})] \tag{14.14b}$$

$$\sigma^o_s = C \cdot (\Gamma_{VV} + G \cdot \Gamma_{HH}) \cdot \exp[-D \cdot f_4(\text{head}) - E \cdot f_3(l + s)] , \tag{14.14c}$$

where $f_1(\text{head})$ and $f_2(l + s)$ relate the measured ground-truth quantities to the backscattering by heads, leaves, and stalks, respectively, and $f_3(l + s)$ and $f_4(\text{head})$ relate the measured ground-truth quantities to attenuation by the leaves, stalks, and heads, respectively. The exact nature of the functions ($f_i(\ )$) is left as an unknown at this point. In keeping with the objectives of this study, however, the dependence will be of the form of a simple relationship involving measured ground-truth quantities.

The form adopted for σ_s^o includes two new expressions: Γ_{VV} and Γ_{HH}. These represent the Fresnel reflection coefficients ($|R_{VV}|^2 = \Gamma_{VV}$). In Chapter 12 of their book, Ulaby et al. (1982) have shown that for a "rough" surface such as soil, the backscattering is proportional to Γ_{pp}, where pp indicates polarization. Subsequent to the 1981 experiment, soil samples from various fields representing all textures encountered in 1981 were characterized by dielectric measurements at various moisture contents and various frequencies, including X-band (Hallikainen et al., 1983). From this data, Γ_{pp} can be calculated at each moisture and entered into the model. In Appendix A, the 10-GHz dielectric data and Γ_{pp} plots are presented. They are neither truly linear nor exponential in shape; hence, this substitution should yield superior results.

For VV polarization, the factor G is set equal to zero, indicating that no HH backscattering is expected for a vertically polarized incident wave. For VH polarization, it is assumed that negligible depolarization occurs at the soil surface, compared to that from volume scattering in the canopy. It is also assumed that this polarization is as likely to occur when the wave is traveling downwards towards the soil as when it is traveling towards the antenna. One further assumption is that the attenuation through the vegetation canopy is polarization-independent. Although this last assumption seems weak, it is a necessary one in keeping with the goal of developing a simple model. Based on these assumptions, for VH polarization the G term is set equal to one.

Several simple, physically reasonable forms of the unknown $f_i(\quad)$ functions relating backscattering and attenuation to available ground-truth data were tried. Prior knowledge indicates that the amount of water present is a strong factor in determining attenuation, whereas its role in conjunction with the vegetative matter in backscattering is less understood. After a trial-and-error process, optimum choices for the $f_i(\quad)$'s for both polarizations were found to be

$$f_1(\text{head}) = \text{FWT}, \qquad f_2(1 + s) = \text{SH2O/HT} \tag{4.15a}$$

$$f_3(1 + s) = \text{SH2O}, \qquad f_4(\text{head}) = \text{FH2O}\ , \tag{4.15b}$$

where FWT represents the fresh fruit (or head) biomass (kg m^{-2}), SH2O represents the water contained in the leaves and stalks (kg m^{-2}), HT is the height of the full canopy, and FH2O is the water contained in the fruit (or head) layer (kg m^{-2}).

Incorporating these functions into Eq. (4.13) resulted in correlation coefficients (r^2) of 0.61 and 0.64 and RMS errors of 2.04 dB and 1.90 dB for VV and VH, respectively. Table 4.3 lists the coefficients determined and the resulting correlation coefficients (r^2) and RMS errors (dB) for all fields, both combined and individually. Figure 4.10 shows a plot of σ^o_{pred} versus σ^o_{meas} in dB for VV, whereas Figure 4.11 shows the same for VH. In both cases a linear regression indicates a slope of less than one and an intercept less than 0 dB.

TABLE 4.3

Model Coefficients and Resulting Statistics - Wheat

Pol.	A	B	C	D	E	F	G
VV	0.153	0.036	1.148	4.271	2.446	0.112	0
VH	0.025	0.013	0.073	2.377	1.440	0.125	1

Field (N)	r^2/RMS Error (dB) VV	r^2/RMS Error (dB) VH
All (143)	0.61/2.04	0.64/1.90
1 (15)	0.85/1.26	0.71/1.21
2 (11)	0.62/2.27	0.62/1.93
3 (14)	0.65/1.75	0.46/1.64
4 (13)	0.76/2.06	0.93/1.08
5 (12)	0.85/1.20	0.88/1.59
6 (18)	0.58/1.64	0.52/1.71
7 (13)	0.56/3.46	0.88/3.34
8 (18)	0.86/1.81	0.78/1.54
9 (15)	0.47/2.64	0.50/1.92
10 (14)	0.83/1.57	0.62/2.32

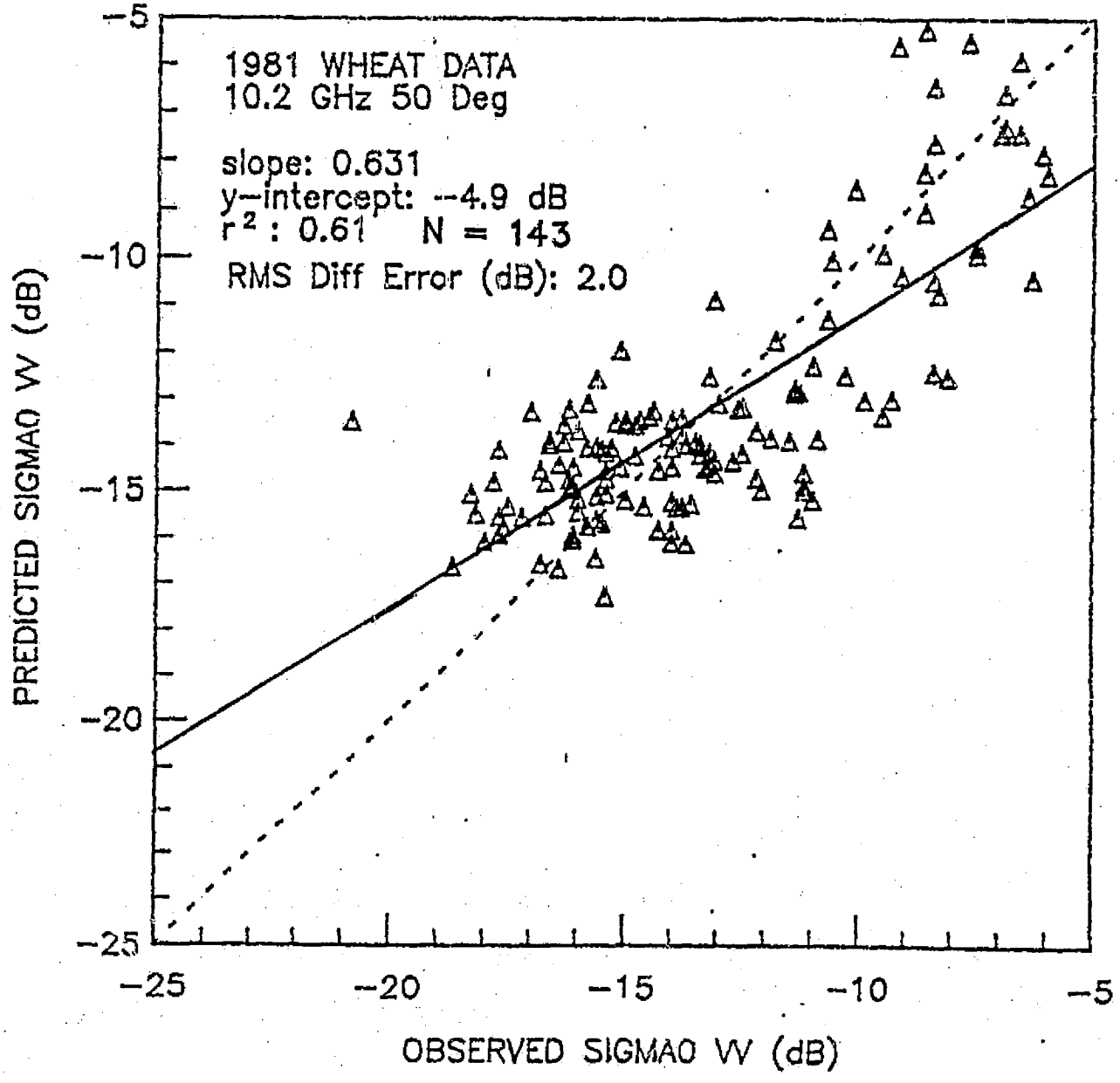

Figure 4.10 Predicted versus observed (measured) σ^o_{VV}, with predicted σ^o from Eq. (4.14).

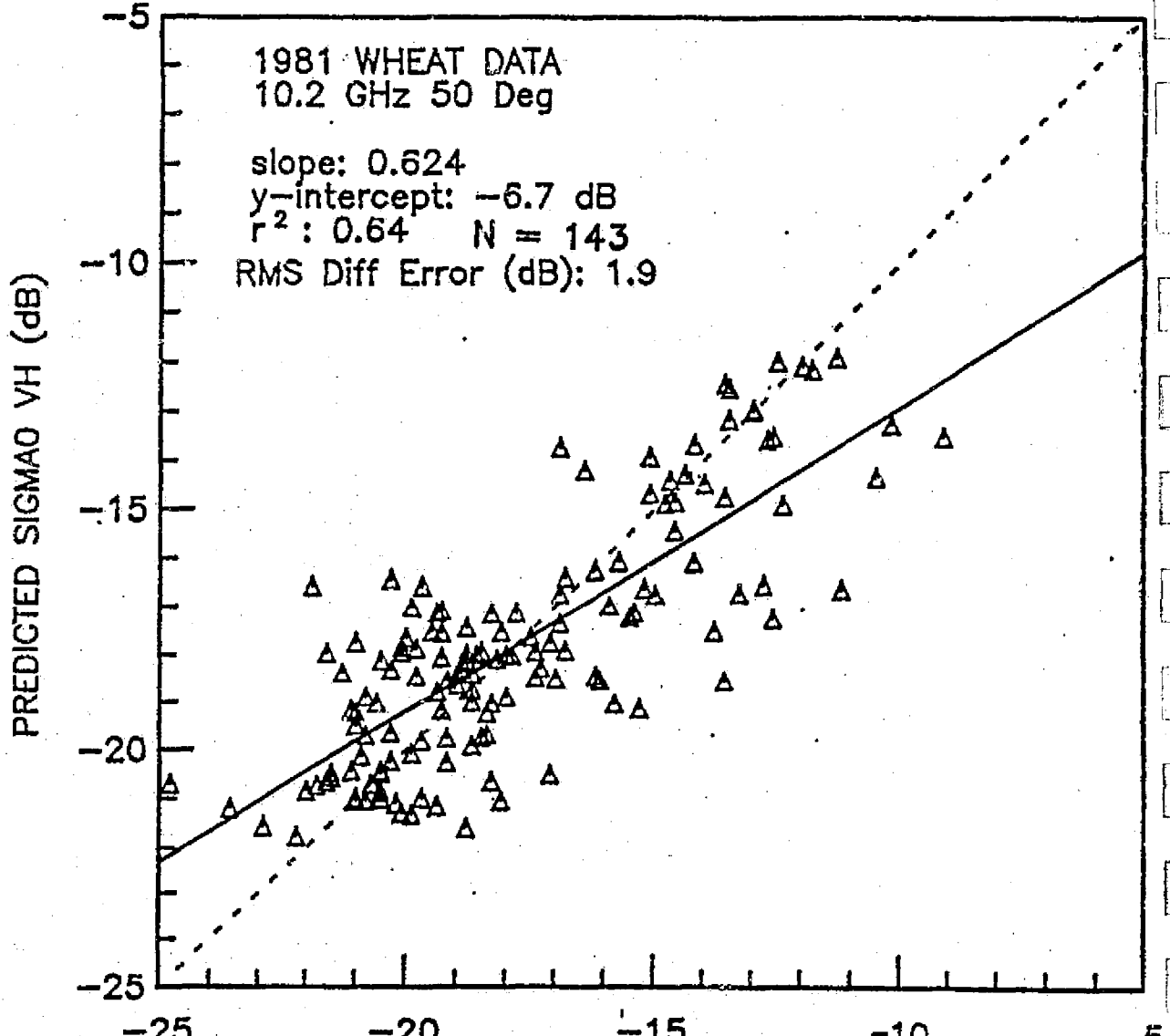

Figure 4.11 Predicted versus observed (measured) σ^{o}_{VH}, with predicted σ^{o} from Eq. (4.14).

Figure 4.12 shows a plot of the errors (defined here as $\sigma^o_{meas}(dB) - \sigma^o_{pred}(dB)$) for VV polarization versus VH polarization. As the statistics given previously indicate, there is a tighter grouping in the VH errors than in the VV errors--again implying that the VH model is superior.

Figures 4.13 and 4.14 show a plot of σ^o in real units ($m^2\ m^{-2}$) versus time for a given field (No. 8) showing measured, predicted, and individual components of σ^o due to plant parts and soil for both polarizations, VV and VH, respectively. As proposed earlier, the model indicates that the increases in σ^o late in the season are due, in both polarizations, primarily to soil. The magnitude of the head, leaf, and stalk attenuation agrees with measurements made during the summer of 1983 on a winter wheat canopy (as shown in Chapter 2). In all cases, the attenuations in the VH model are smaller than the attenuations in the VV model, indicating that our assumption that attenuation is polarization-independent is not a very good one.

Figures 4.15 and 4.16 show temporal plots of predicted and observed σ^o for all fields at both polarizations. In all cases, both models do a good job of predicting σ^o while the canopy is still moist, i.e., prior to Julian date 150 to 160. After this time the models do fairly well, yet large discrepancies are obvious, e.g., Field No. 4, VV pol.; Field No. 7, VV pol.; Field No. 7, VH pol.; and Field No. 10, VH polarization. The cause is not clear; however, as the canopy dries and the soil contribution becomes important, surface roughness may be the culprit, or head backscattering may be the cause. One way to deal with this

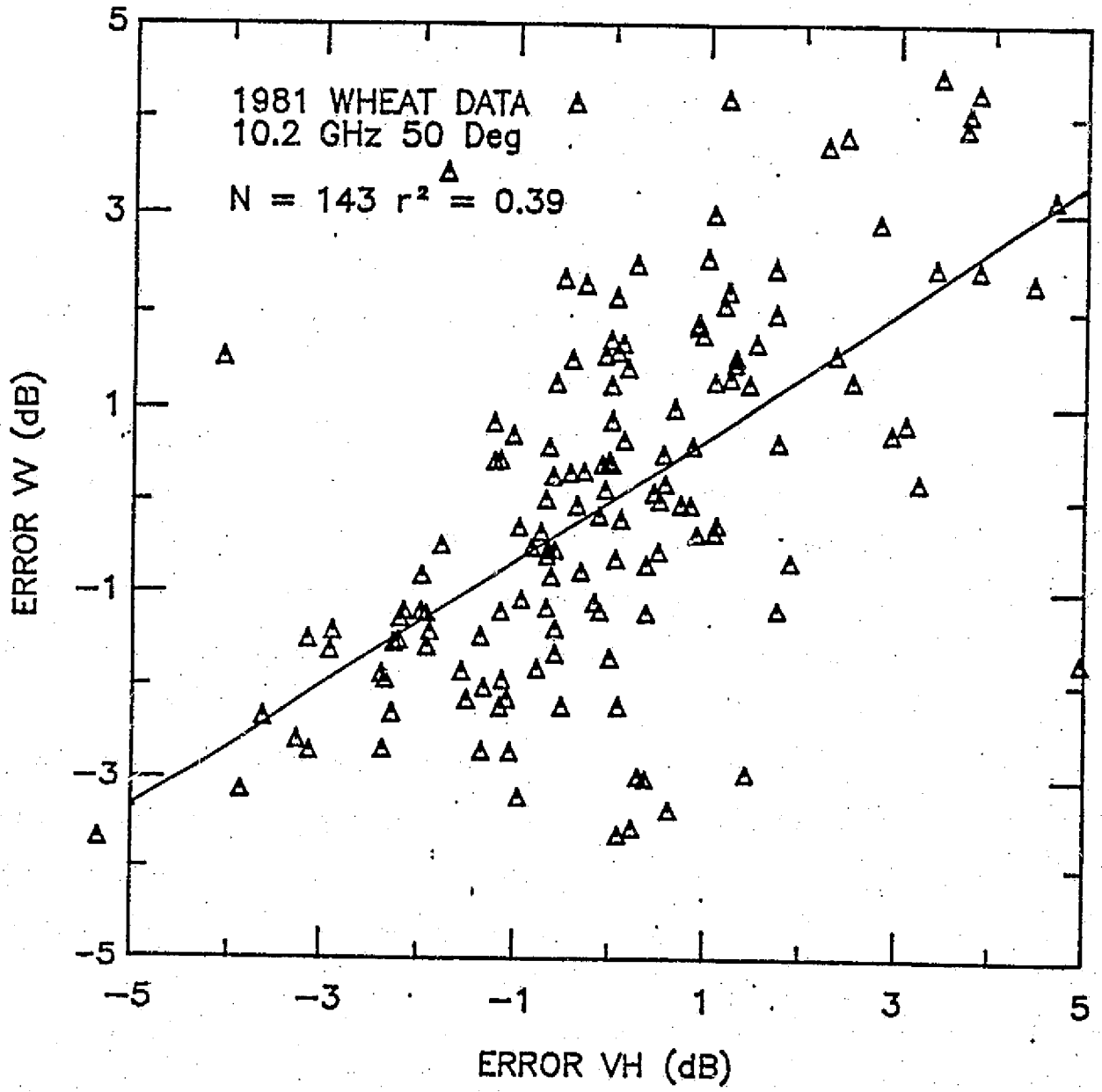

Figure 4.12 A comparison of the ways in which errors in predicting σ°_{VV} relate to errors in predicting σ°_{VH}.

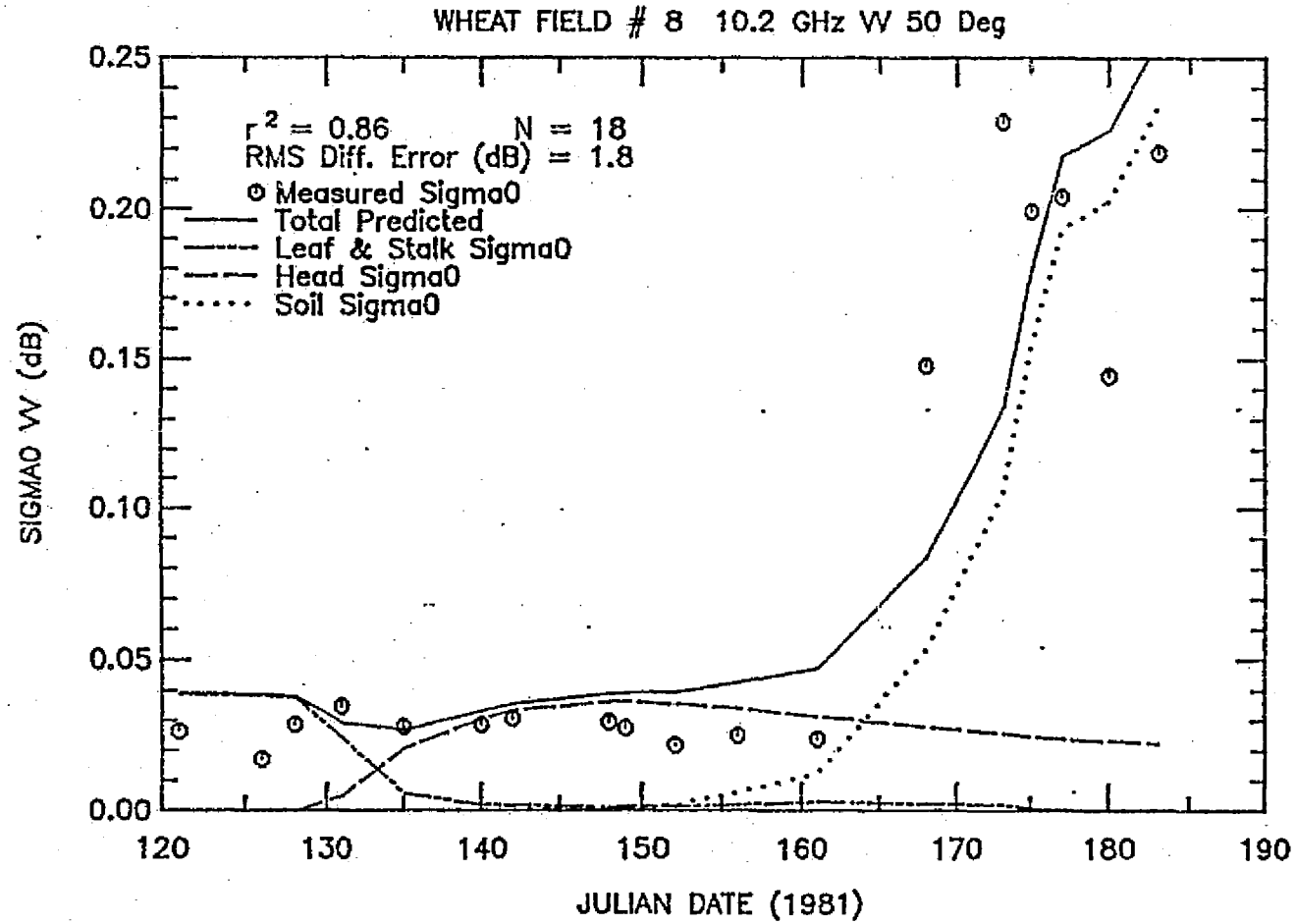

Figure 4.13 The measured σ^o_{VV} along with the predicted σ^o_{VV} from wheat field No. 8. The predicted value is the sum of three components, also shown here.

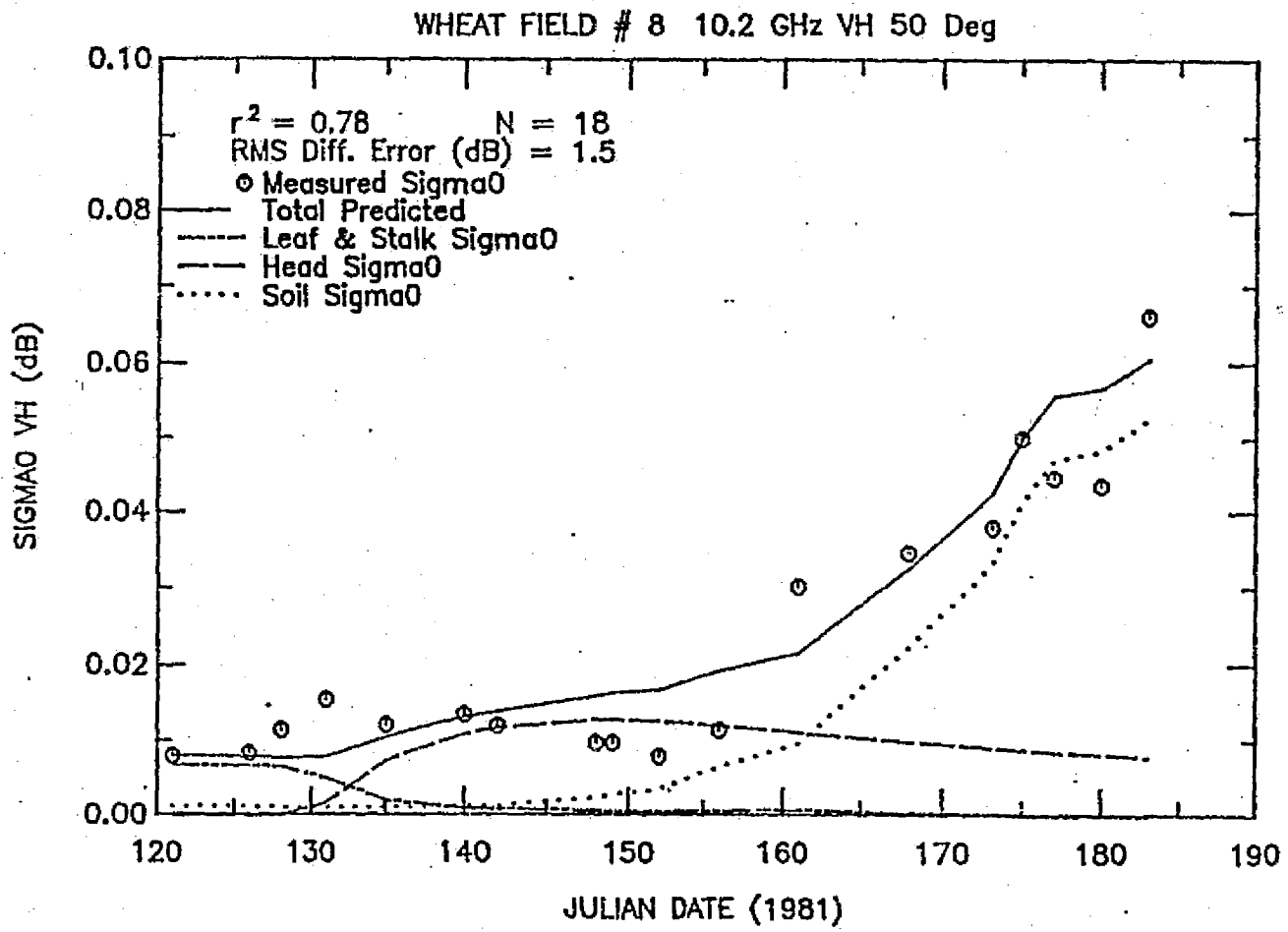

Figure 4.14 The measured σ^o_{VH} along with the predicted σ^o_{VH} from wheat field No. 8. The predicted value is the sum of three components, also shown here.

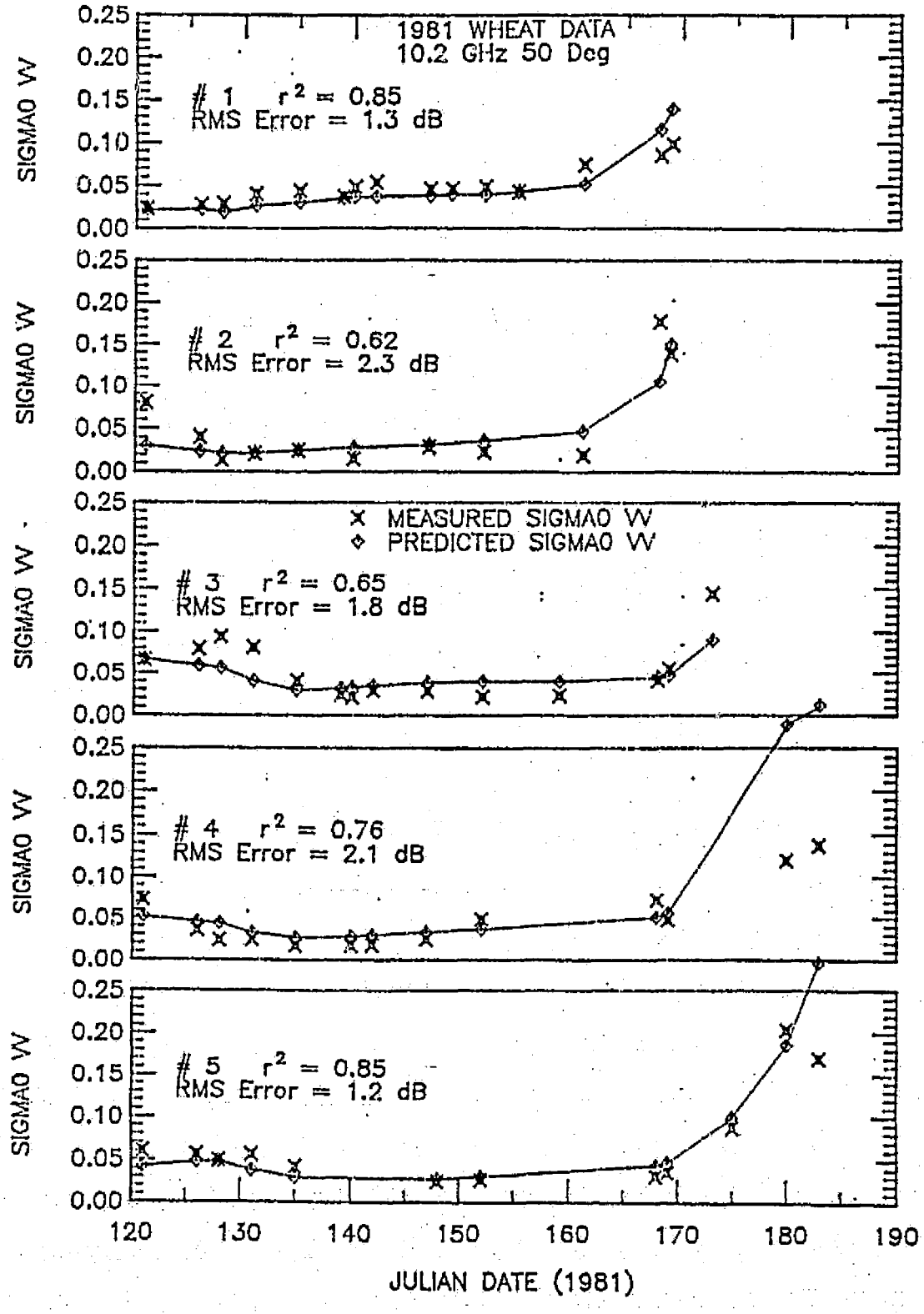

Figure 4.15 A comparison of measured and predicted σ^{o}_{VV} over time presented on a per-field basis.

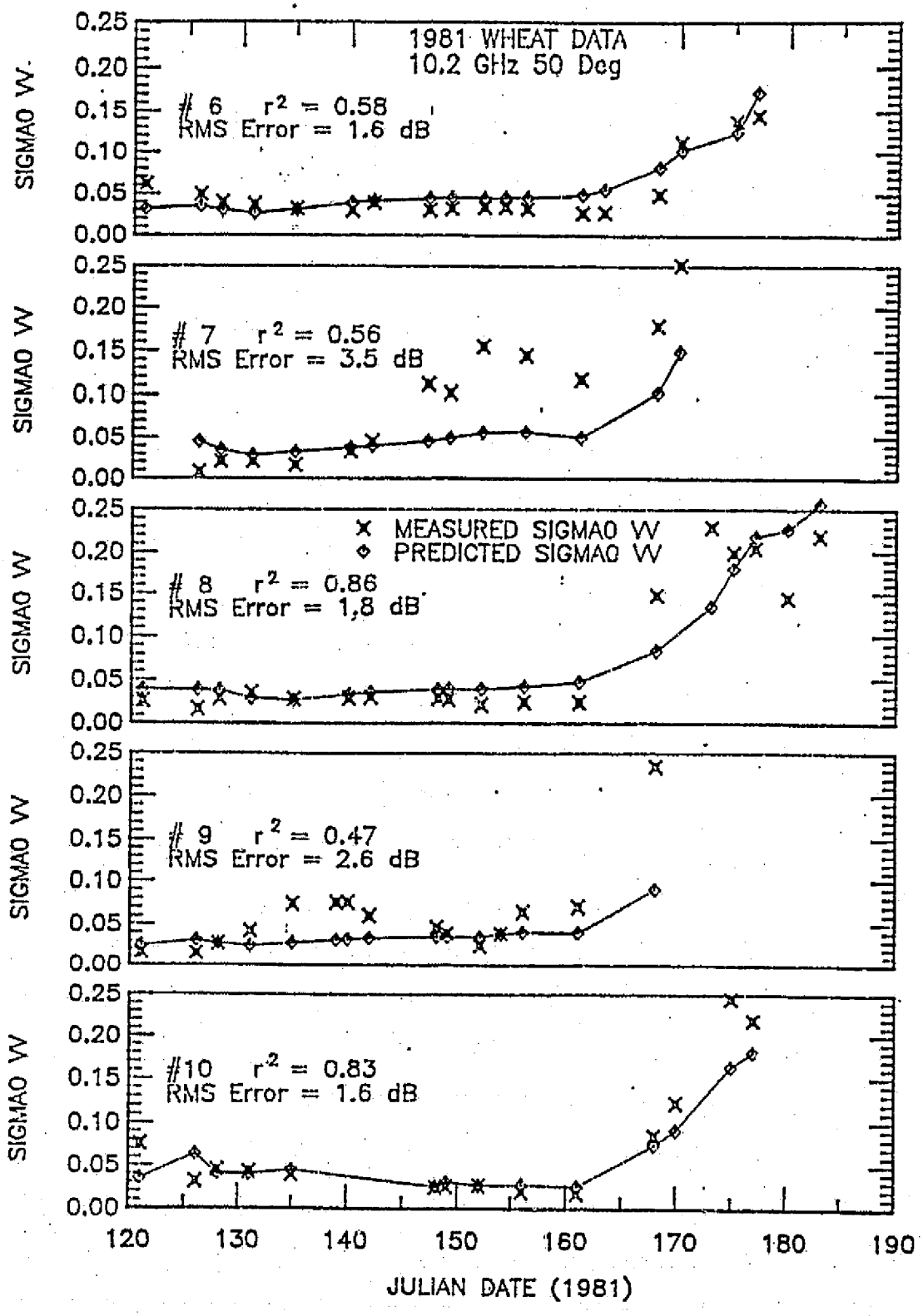

Figure 4.15 (Continued)

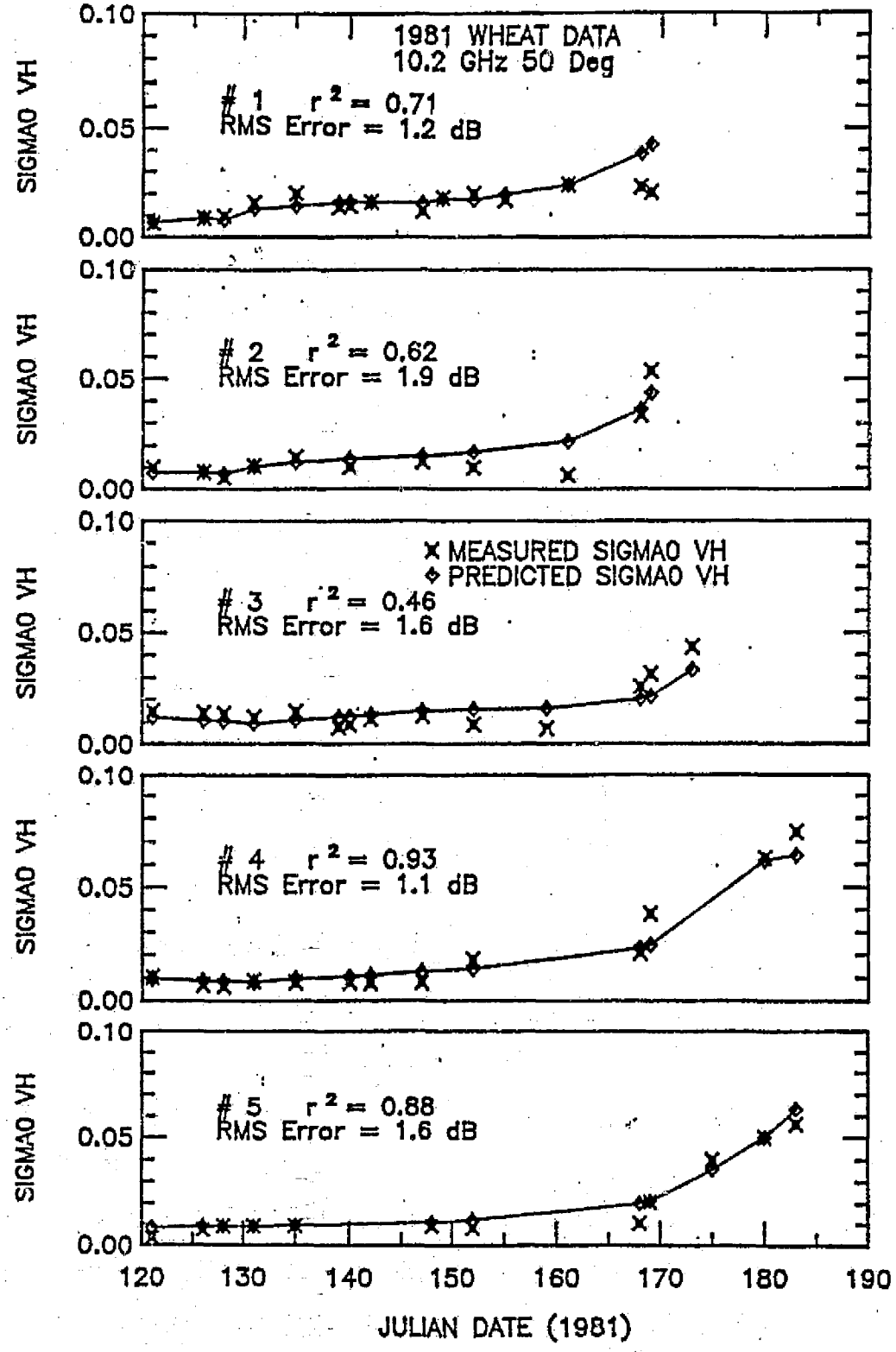

Figure 4.16 A comparison of measured and predicted σ^{o}_{VH} over time presented on a per-field basis.

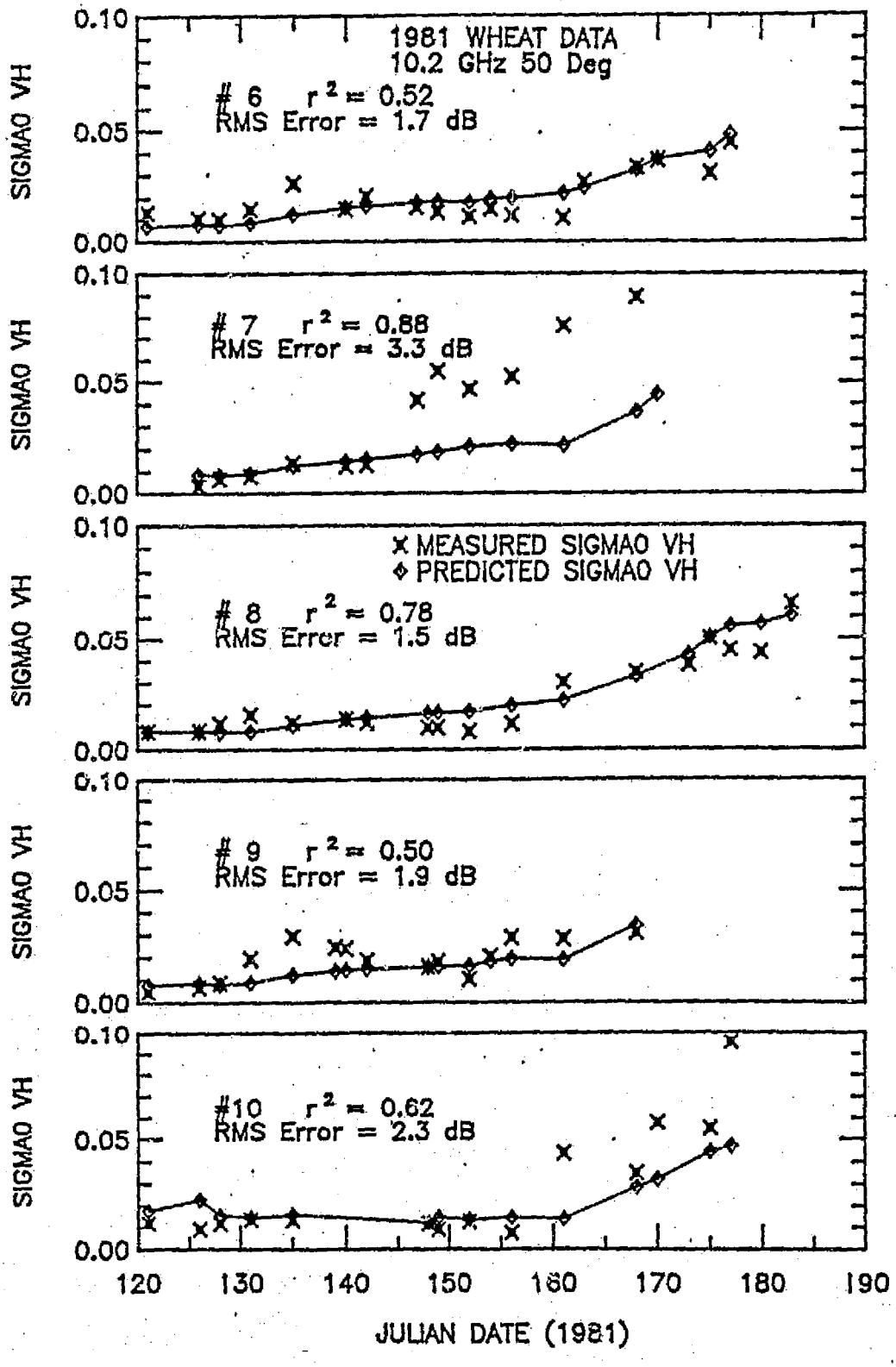

Figure 4.16 (Continued)

complication is to optimize the model for each field individually. This was done with the results shown in Table 4.5. As expected, the r^2 values for each field exceeded the previous values obtained using the coefficients in Table 4.3, indicating there are between field differences for which the model does not account.

4.6.3 Error Analysis

In deriving and testing a mathematical model based on experimental data, the quality of the data determines, to a degree, the quality of the model. Errors exist in both parts of the data involved, i.e., in the independent data (ground truth) and in the dependent data (radar measurements). Errors on both sides of the equation tend to degrade the model's performance, i.e.,

$$\sigma^o_{meas} \pm \varepsilon_{meas} = \sigma^o_{pred}(\text{ground truth}) \pm \varepsilon_{pred}.$$

In order to evaluate the significance of these errors, the following approach was taken: First, choosing the model considered to be best in terms of "goodness of fit" and number of parameters, we assume that it is ideal, i.e, that it represents exactly the relationship between σ^o and the crop parameters. Secondly, by examining the statistics of the raw ground truth, variances for each parameter are estimated. Thirdly, by performing experiments and examining the temporal history of "constant" quantities such as σ_{lens} data, the variances associated

with the radar measurements can be estimated. Finally, the experiment is numerically simulated on a computer using a Gaussian random-number generator to simulate measurement errors to perturb the "true" ground truth. This data then are used in the model to determine a simulated σ^{o}_{calc}. Similarly, the measurement of radar data is simulated by first assuming that the original ground-truth information is perfect. These data predict the measured radar data, which are assumed to be ideal. This ideal σ^{o} is then perturbed by the estimated variance again using the Gaussian random-number generator. Thus, for each data set of ground truth, a simulated σ^{o}_{calc} and a simulated σ^{o}_{meas} are determined. Thus, it can be seen that even a perfect model relating σ^{o} to ground-truth data will not yield a correlation of 1.00.

The errors in the ground-truth data are from two sources: one is true within-field variability, and the other is measurement error. Both contribute to the total error and are represented in the associated variance. Analysis of these ground-truth data indicates that the standard-deviation-to-mean ratio is much more constant than the standard deviation by itself, which implies that the magnitude of the error is dependent on the magnitude of the quantity being measured. The estimated values for the standard deviation associated with the ground-truth parameters involved are listed in Table 4.4.

There are three sources of error in the radar data: the first is fading, which may be minimized by acquiring large numbers of independent samples for each data point; the second is within-field variability (both factors are reduced by the method of data

TABLE 4.4

Error Simulation Results - Wheat

Parameter	Leaf and Stalk Wet Biomass	Leaf and Stalk Dry Biomass	Height	Head Wet Biomass	Head Dry Biomass	Soil Moisture
Standard Dev.	0.21μ	0.20μ	0.09μ	0.23μ	0.23μ	0.20μ

μ represents the mean of the measured value

σ^o_{VV} has a standard deviation of 0.8 dB
σ^o_{VH} has a standard deviation of 2.0 dB

VV results: $r^2 = 0.64$ RMS error: 1.85 dB
VH results: $r^2 = 0.69$ RMS error: 1.56 dB

acquisition, namely determining a field average by integrating the received power over a portion of the field), and the third is calibration. The system is externally calibrated periodically, yet changes that are not corrected via calibration still occur. Experiments (Brisco and Allen, 1982) have shown that an additive standard deviation of 0.8 dB should be used in simulating σ^{o}_{VV} measurements, and that an additive standard deviation of 1 dB should be used in simulating σ^{o}_{VH} measurements, since the determination of $\sigma^{o}_{VH}(dB)$ depends in a linear fashion on $\sigma^{o}_{VV}(dB)$.

Results

Based upon the assumptions stated, it was shown that given data with the types of errors discussed, the "best" that could be done in modeling the data would result in a correlation coefficient (r^2) of about 0.64 for VV data and about 0.69 for VH data, using the model, which is indeed exact. Therefore, the correlations reported in the modeling section should be regarded as statistically respectable.

4.6.4 Analysis of Weather Effects

As mentioned previously, of the original volume of data acquired in 1981, a part was set aside for future analysis after the modeling effort was completed. In the case of wheat, 206 data sets were obtained originally. Of these, 22 represent data sets acquired after harvest, and 41 correspond to data sets that might have been influenced by weather events. To illustrate, Figure 4.3 shows the temporal behavior of σ^{o}_{VV} and σ^{o}_{VH} for Wheat Field No. 8,

including data that apparently had been influenced by weather. To investigate the significance, if any, of weather influence, the model developed previously will be employed to predict a value for σ^o based on ground-truth parameters. This predicted value will then be compared to the measured value. The magnitude and distribution of the errors found using the weather-influenced data will be compared to the magnitude and distribution of the errors found using the "unaffected" data.

In order to increase the reliability of the model (or to reduce the RMS difference error) the model was optimized for each field, i.e., new constants were determined for each field. These coefficients are shown in Table 4.5, with the associated r^2 and RMS difference errors.

The types of weather influence observed include recent rain (affecting 18 data sets), strong winds during data acquisition (affecting 11 data sets), and blown-down vegetation (affecting 10 data sets). Two additional data sets were deleted from the analysis for other reasons.

The results of the comparison using a T-test are shown in Table 4.6. In each case the errors found using "affected" data are statistically compared to those "unaffected" data on which the model was optimized. For the case of blown-down canopy regions, significant differences in the nature of the errors are shown. For the case of strong wind during data acquisition, the nature of the errors is shown to be quite similar, indicating few, if any, weather effects. In the case of a recent rain, the nature of the

Table 4.5
(a)
Model Coefficients and Resulting Statistics
Optimized on a Per Field Basis - Wheat

Crop: 1981 Wheat Polarization: VV

Field No.	A	B	C	D	E	F	G	r^2	RMS Difference Error(dB)	N
1	0.086	0.029	0.827	0.826	2.954	0.288	0	0.88	0.59	15
2	2.132	0.026	1.500	5.144	3.880	0.011	0	0.78	1.74	11
3	0.221	0.007	1.500	1.786	2.237	0.108	0	0.91	0.77	14
4	0.800	0.030	0.490	5.440	0.906	0.014	0	0.83	1.28	13
5	0.110	0.001	0.856	1.233	2.243	0.223	0	0.94	0.65	12
6	0.134	0.012	1.500	0.977	4.711	0.199	0	0.88	0.82	18
7	0.045	0.030	1.500	0.003	1.509	0.064	0	0.86	1.71	13
8	0.075	0.010	1.150	0.117	3.408	0.167	0	0.89	1.34	18
9	0.098	0.047	1.500	0.144	4.251	0.128	0	0.65	1.77	15
10	0.133	0.000	1.500	1.362	4.008	0.182	0	0.91	1.13	14
All	0.153	0.036	1.148	4.271	2.446	0.112	0	0.61	2.04	143

TABLE 4.5(b)

Crop: 1981 Wheat Polarization: VH

Field No.	A	B	C	D	E	F	G	r^2	RMS Difference Error(dB)	N
1	0.001	0.006	0.033	1.175	0.037	0.082	1	0.82	0.71	15
2	0.136	0.009	0.079	4.330	1.403	0.022	1	0.72	1.52	11
3	0.145	0.001	0.203	0.018	2.284	0.023	1	0.82	0.94	14
4	0.040	0.008	0.081	1.586	1.135	0.053	1	0.94	0.87	13
5	0.031	0.006	0.087	0.004	2.267	0.070	1	0.91	1.12	12
6	0.046	0.005	0.103	0.010	3.337	0.148	1	0.66	1.17	18
7	0.018	0.010	0.303	0.006	1.714	0.056	1	0.93	1.31	13
8	0.001	0.007	0.067	3.100	0.492	0.007	1	0.87	1.09	18
9	0.000	0.012	0.032	0.668	0.217	0.001	1	0.71	1.34	15
10	0.051	0.022	0.135	0.000	4.916	0.119	1	0.75	1.74	14
All	0.025	0.013	0.073	2.377	1.440	0.125	1	0.64	1.90	143

TABLE 4.6

1981 Wheat - Weather Effects

Data Class	N	Mean Error (dB)	RMS Diff. Error (dB)	T-Test 2-Tail Probability
		VV Polarization		
Normal	143	0.04	1.24	
Blown-Down	10	1.62	3.95	0.002
Windy	11	0.31	2.21	0.530
Recent Rain	18	1.58	2.73	0.000
		VH Polarization		
Normal	143	0.00	1.21	
Blown-Down	10	1.14	3.62	0.019
Windy	11	0.56	2.11	0.167
Recent Rain	18	1.96	2.68	0.000

errors is shown to differ significantly, thus indicating that the rain effects probably were a genuine source of error.

In order to visualize the nature of the errors caused by weather effects as compared to residual errors in the model, examine Figures 4.17 and 4.18, which are histograms of these errors, separated by class (blown-down canopy, wind during data acquisition, recent heavy rain, and "normal" data). For both polarizations (VV and VH), the "normal" errors are centered on zero and decrease gradually in both directions. For both "blown down" errors and rain errors, the distribution is much wider and uniform in level. The wind-influenced errors are more like those found in the "normal" data. Hence, the T-test indicates that the rain and blown-down canopy errors are from a distribution unlike that for the "normal" data errors, whereas the wind-influenced errors are from a distribution similar to that of the "normal" data errors.

Finally, a plot of the errors (in dB) for VV polarization versus those (in dB) for VH polarization is given (Figure 4.19). Small correlations are shown between the VV and VH errors for both "normal" data and "rain" data, indicating that the mechanism causing the errors is either random or it behaves independently as a function of polarization. For blown-down-canopy data and wind-influenced errors, relatively high correlations are shown, which indicates the converse.

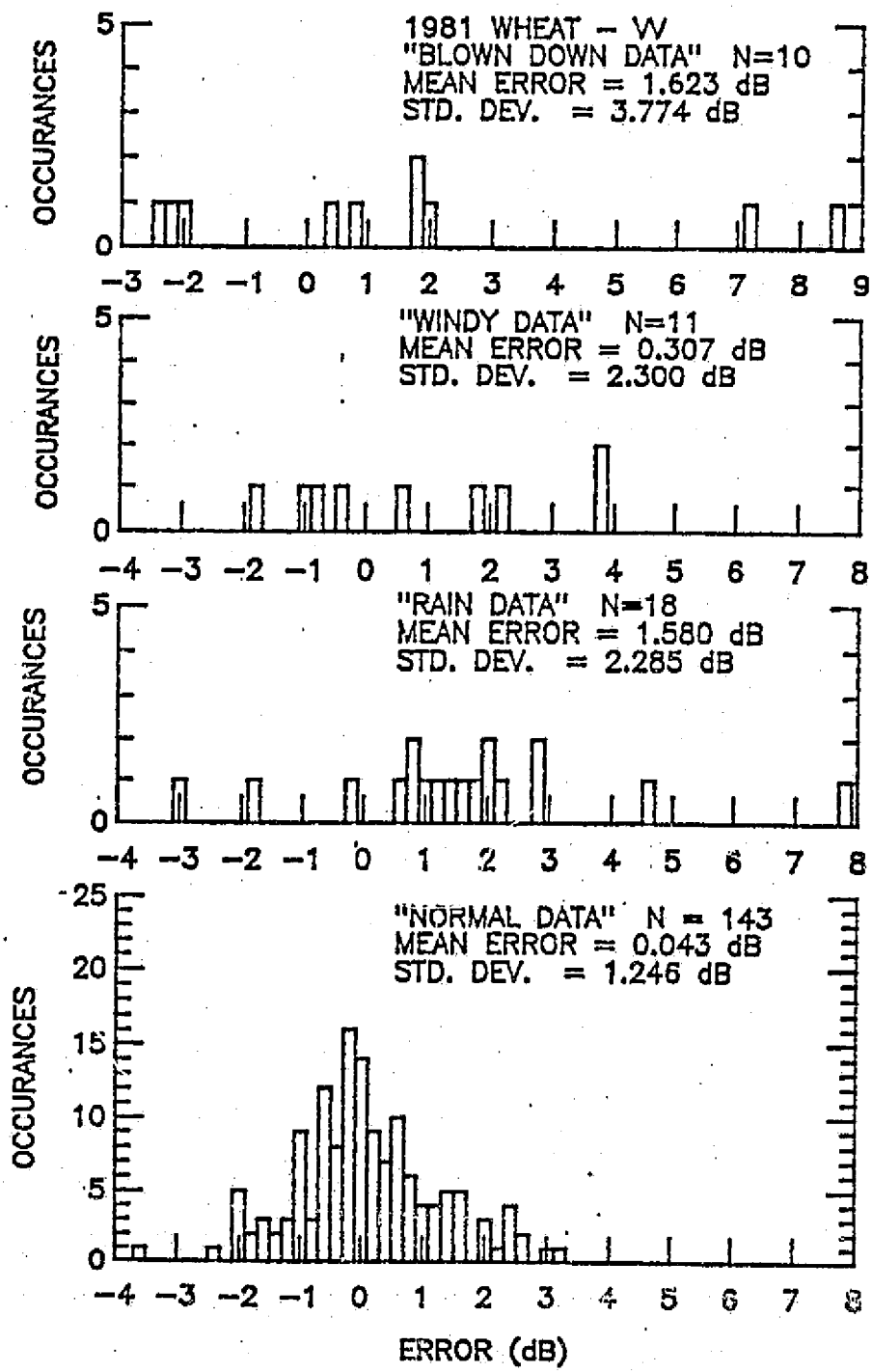

Figure 4.17 Histograms of the errors between predicted and measured σ^{o}_{VV} for various types of weather-affected data.

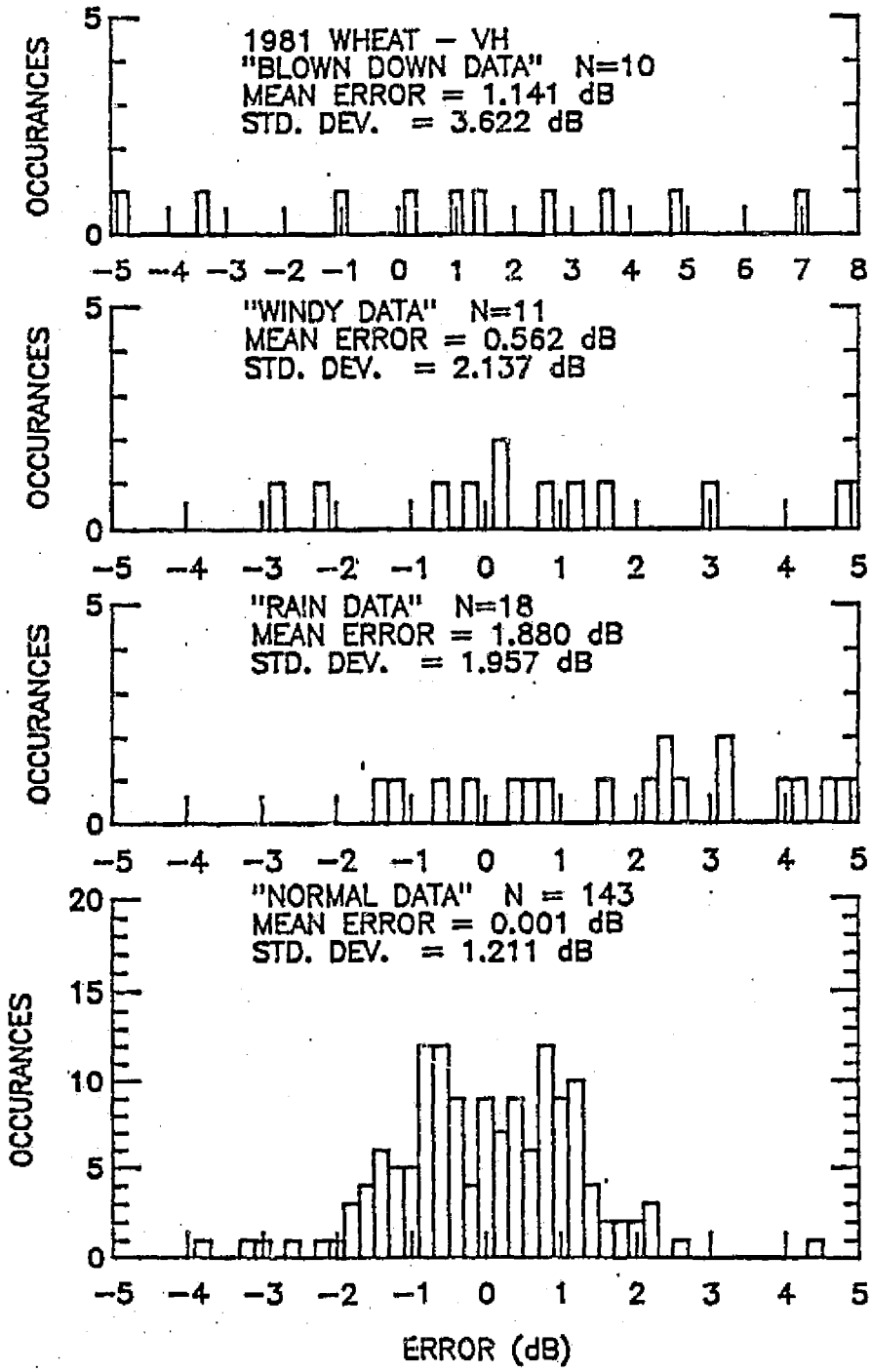

Figure 4.18 Histograms of the errors between predicted and measured σ^o_{VH} for various types of weather-affected data.

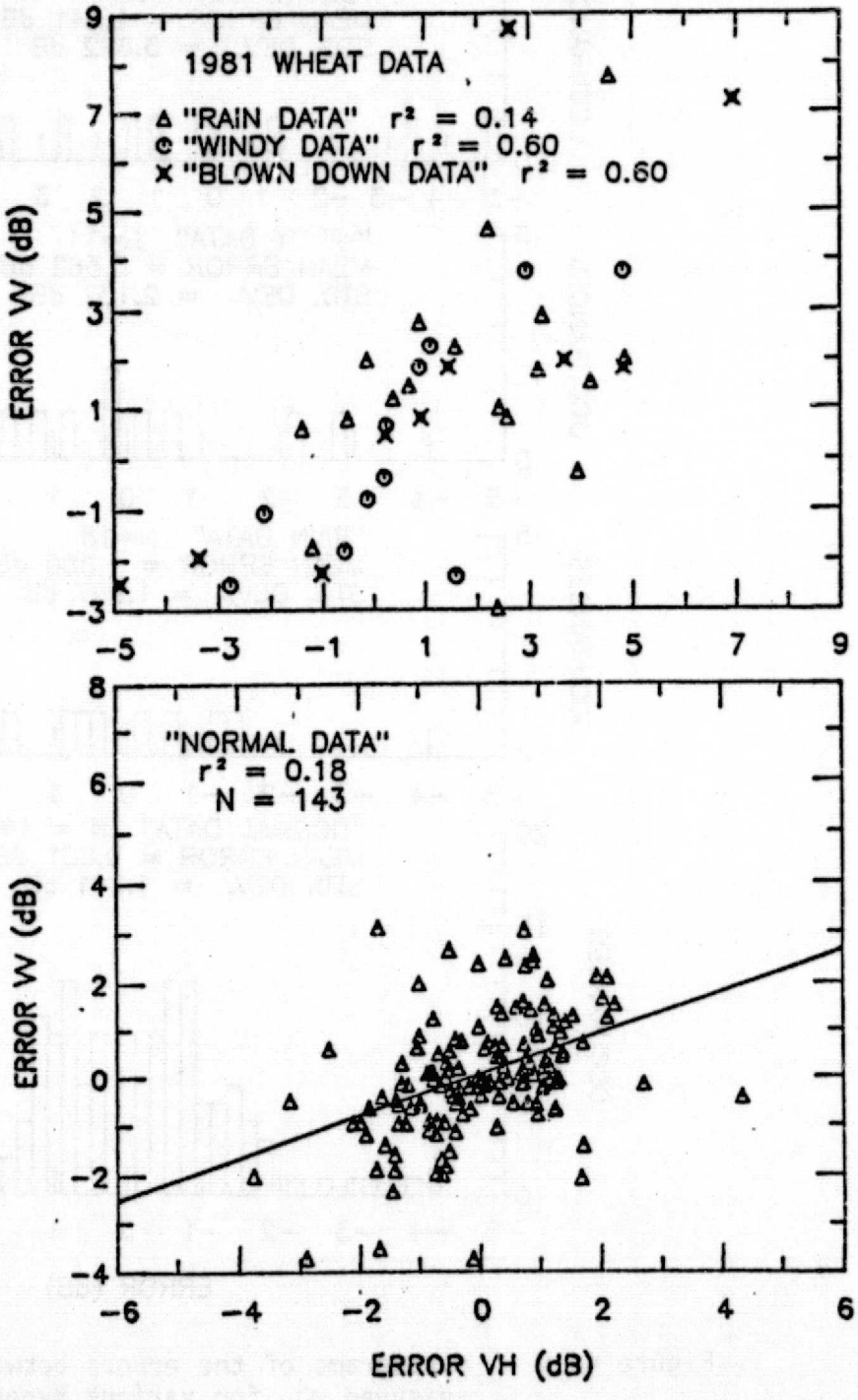

Figure 4.19 A comparison of the ways in which the errors between predicted and measured σ^o vary with polarization and weather influence.

Conclusion

A statistical investigation into the nature of the errors introduced by weather events as compared to sources of error that are not weather-related demonstrated that a recent rain or a blown-down canopy introduced significant error that was unlike any observed previously in the analysis; however, the presence of wind during data acquisition had no significant influence.

These results reaffirm the belief that microwave interaction depends upon the dielectric and geometric properties of the target. Following a rain event, the dielectric property may be influenced by the presence of free water in the canopy, whereas for blown-down areas of canopy, geometric changes drive the varied response. In the presence of wind during data acquisition, neither the dielectric nor the geometric changes are significant. In fact, the presence of wind may improve the estimate of σ^{o} by providing more independent samples, which in turn reduces fading.

4.7 1981 Corn Data

Of the 318 data sets obtained from the ten corn fields during the summer of 1981, 130 were omitted from modeling due to the fact that they might have been affected by rain (within two days of data collection); another 10 points were acquired after the fields were harvested, and thus do not represent a normal corn canopy; 12 were omitted due to either missing data (soil moisture) or incorrect σ^o values; and the remaining 166, or about 17 per field, were used in the following analysis and modeling. The accompanying ground truth consisted of fresh and dry biomass per unit area for three plant parts (stalks, fruit or cobs, and leaves), canopy height, and soil moisture. A smoothing of the plant variables, as described earlier, completes the data clean-up. A sample data-set is shown in Figure 4.20. Note the similarity between σ^o_{VV}, σ^o_{VH}, fresh leaf biomass, and fresh stalk biomass. A temporal plot of fresh and dry fruit biomass is not included because previous experiments have shown that the fruit is not important at this frequency (X-band) and incidence angle (50°) [Ulaby (1982)]; subsequent analysis has reaffirmed this finding.

Figure 4.21 shows temporal plots of both σ^o_{VV} and σ^o_{VH} (in real units, $m^2\ m^{-2}$) for all ten fields. Although there is no clear overall pattern as there was for the wheat fields, a subtle behavioral trend is present in the form of a relatively small σ^o early and late in the growing period, with the middle part showing a gentle increase and then a decrease. This behavior is seen in most of the fields observed, although anomalies were present late in Fields Nos. 1 and 7, and early in Fields Nos. 4 and 10. The

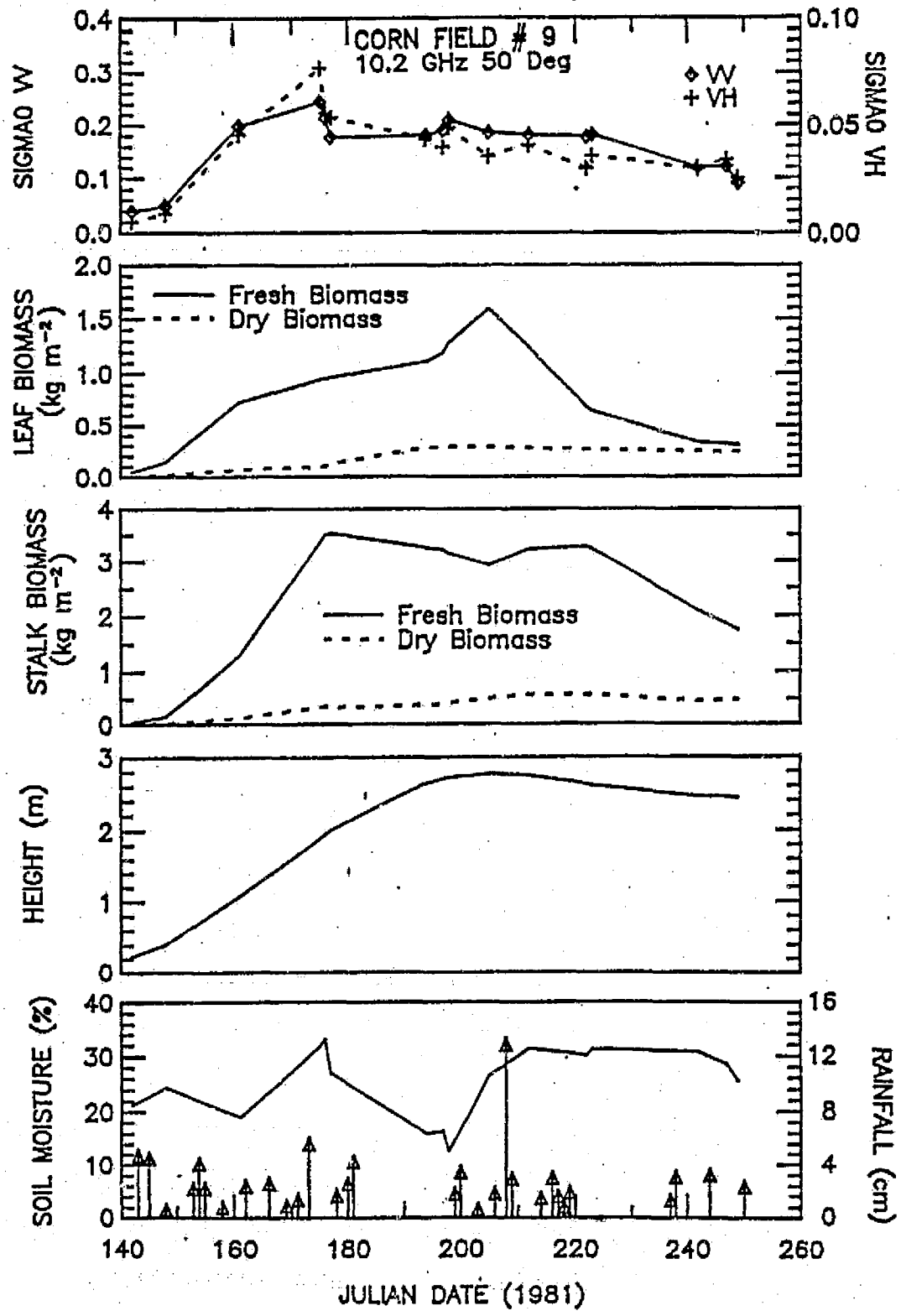

Figure 4.20 Temporal histories of the radar data (σ^o) and the ground-truth parameters (after smoothing) along with the measured rainfall events for a given corn field (No. 9).

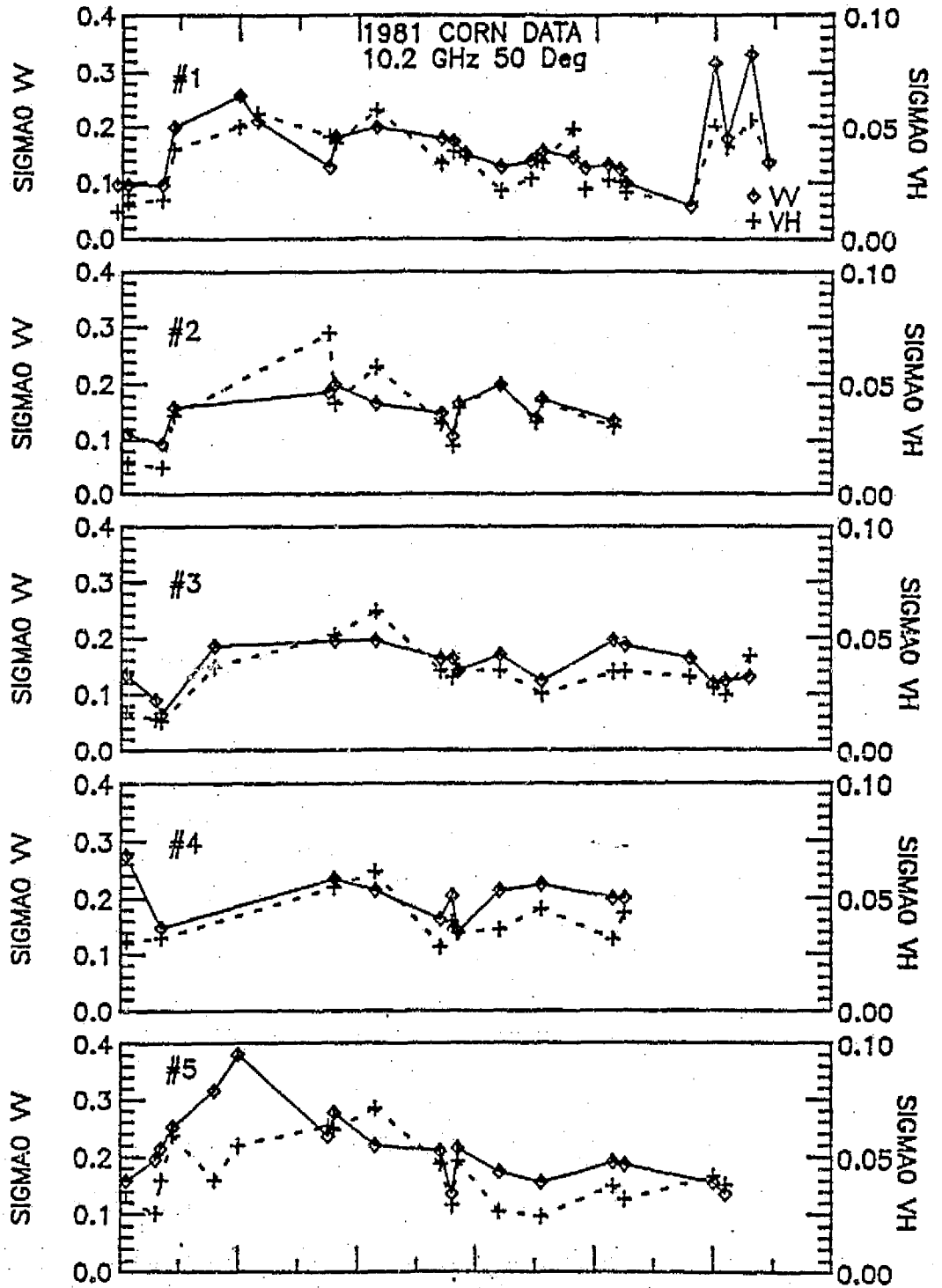

Figure 4.21 Temporal behavior of σ^{o}_{VV} and σ^{o}_{VH} from all ten corn fields.

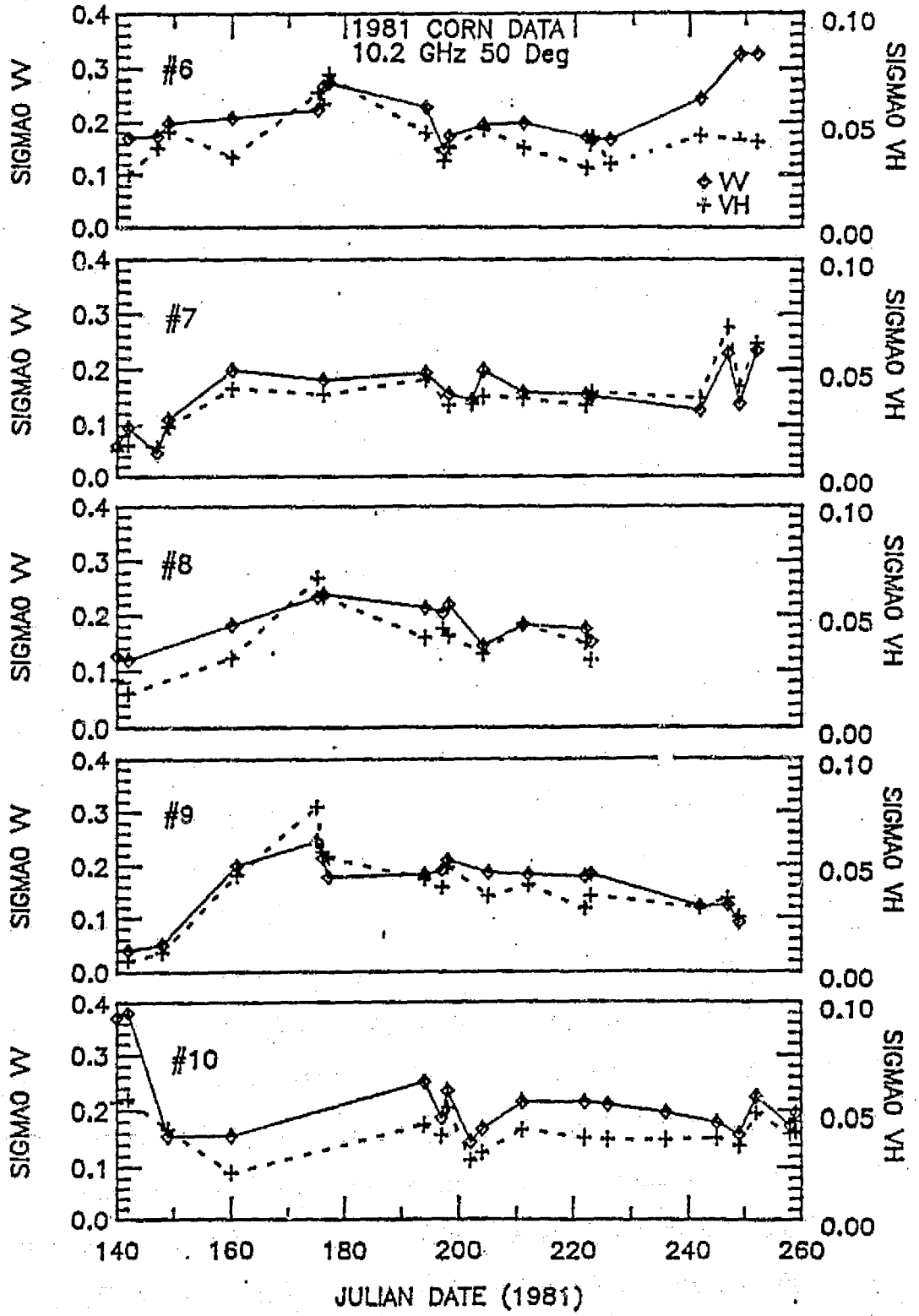

Figure 4.21 (Continued)

characteristics of Fields Nos. 5 and 9 are reminiscent of the overall behavior seen by Ulaby et al. (1983), i.e., early in the growing cycle there is an obvious peak, which then levels off for the remainder of the cycle and falls off again towards the end to reach a level comparable to that seen at the beginning.

Also apparent from these ten plots is the similarity between σ^o_{VV} and σ^o_{VH}. Figure 4.22 shows a plot of σ^o_{VV}(dB) versus σ^o_{VH}(dB) for this corn data. It is readily apparent that there is a fairly high correlation between the two, which indicates that either the same or a similar mechanism is driving both of them.

4.7.1 Initial Analysis

As a first step in the analysis of the corn data, statistics and linear correlation coefficients between measured σ^o values expressed in dB and ground truth-parameters were computed and are shown in Tables 4.7 and 4.8. From the statistics we have seen that the dynamic range of σ^o_{VV} is almost 10 dB, and for σ^o_{VH} it is just over 11 dB. This means that the value of the backscattering coefficient varies by about a factor of 10 (in real units of $m^2\ m^{-2}$). Therefore, subsequent analysis may be presented in real units ($m^2\ m^{-2}$) and the finer details may become more apparent than when the data are compressed into the decibel scale. However, when the models are tested, the decibel scale will be retained to ensure that errors remain proportional to the values they are trying to estimate.

An examination of Table 4.8 shows that σ^o_{VV} and σ^o_{VH} do not correlate well with any of the ground-truth parameters. In the

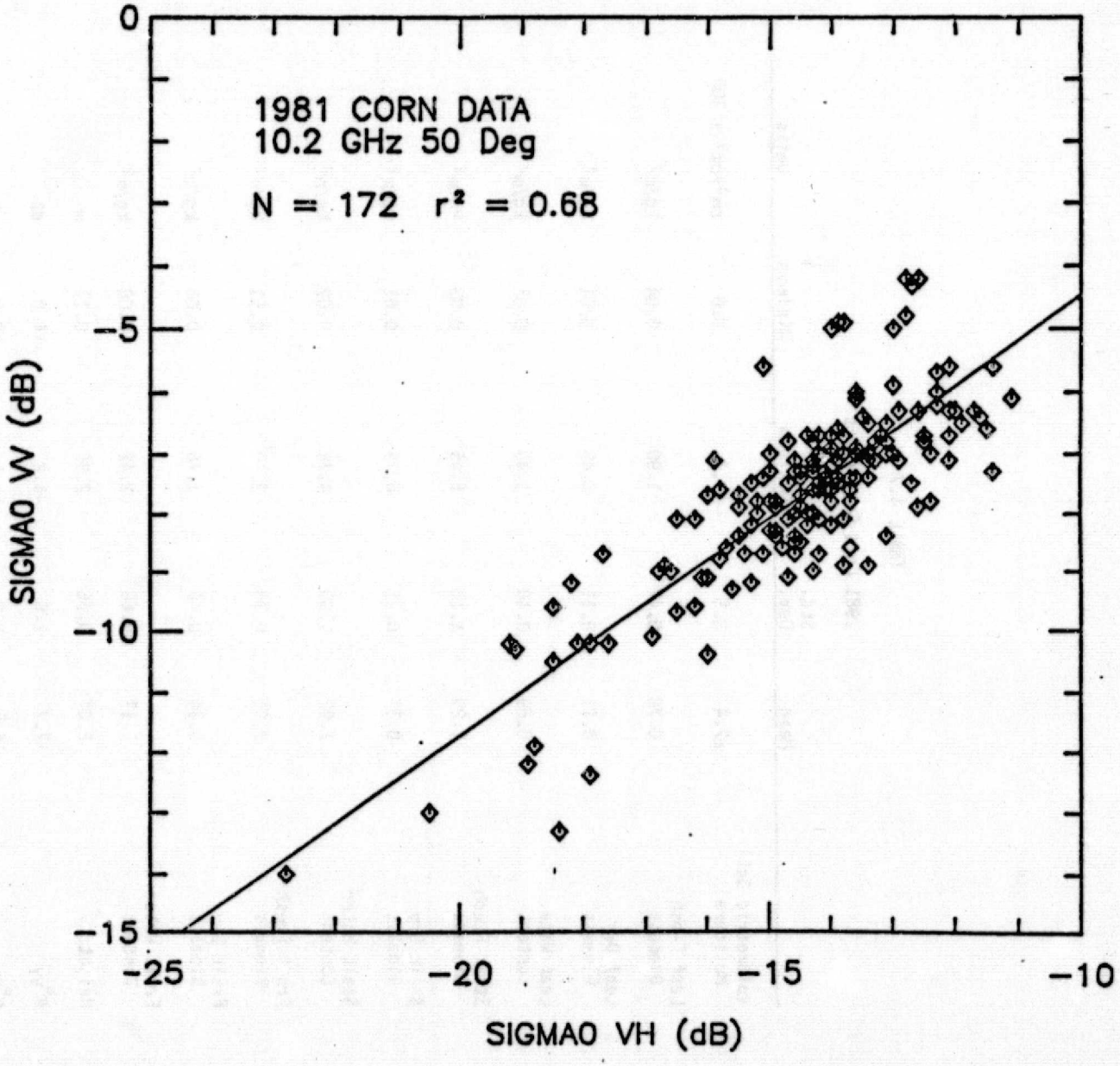

Figure 4.22 The way in which σ^{o}_{VV} varies with σ^{o}_{VH} from the corn data.

TABLE 4.7

1981 Corn Statistics

	Mean	Std. Dev.	Maximum	Minimum	Units
Volumetric Soil Moisture	27.4	8.5	47.3	6.0	$cm^3/cm^3 \times 100$
Leaf Fresh Biomass	0.78	0.47	1.90	0.04	kg/m^2
Leaf Dry Biomass	0.21	0.11	0.49	0.01	kg/m^2
Leaf Water Content	0.59	0.40	1.48	0.01	kg/m^2
Stalk Fresh Biomass	2.29	1.18	5.45	0.03	kg/m^2
Stalk Dry Biomass	0.37	0.21	0.79	0.01	kg/m^2
Stalk Water Content	1.92	1.00	4.78	0.02	kg/m^2
Fruit Fresh Biomass	2.01	0.73	3.10	0.11	kg/m^2
Fruit Dry Biomass	0.84	0.46	1.76	0.03	kg/m^2
Fruit Water Content	1.17	0.66	2.42	0.08	kg/m^2
Height	2.07	0.86	2.95	0.17	m
σ^o_{VV}	-7.7	1.6	-4.2	-14.0	dB
σ^o_{VH}	-14.5	1.8	-11.1	-22.8	dB

TABLE 4.8

Linear Correlation Analysis
1981 Corn Data

Correlation Coefficient r	1	2	3	4	5	6	7	8	9	10	11	12
1. Volumetric Soil Moisture	1											
2. Leaf Fresh Biomass	-0.22	1										
3. Leaf Dry Biomass	-0.21	0.65	1									
4. Leaf Water Content	-0.20	0.98	0.50	1								
5. Stalk Fresh Biomass	-0.12	0.70	0.84	0.61	1							
6. Stalk Dry Biomass	-0.09	0.51	0.88	0.37	0.66	1						
7. Stalk Water Content	-0.13	0.71	0.80	0.64	0.99	0.80	1					
8. Fruit Fresh Biomass	-0.25	0.23	0.62	0.13	-0.11	0.40	-0.20	1				
9. Fruit Dry Biomass	0.21	-0.60	0.22	-0.66	-0.25	0.41	-0.36	-0.45	1			
10. Height	-0.17	0.60	0.92	0.47	0.89	0.90	0.85	0.71	0.31	1		
11. σ^{o}_{VV}(dB)	0.12	0.30	0.20	0.29	0.28	0.16	0.30	-0.16	-0.22	0.25	1	
12. σ^{o}_{VV}(dB)	0.11	0.40	0.33	0.37	0.47	0.[illegible]	0.50	-0.43	-0.40	0.41	0.82	1

N = 172 for all cases except cases involving leaf or fruit biomass, then N = 130.
for all cases involving soil moisture, N is smaller by 6.

case of the fruit biomass data (fresh and dry) the correlations are negative, which is contrary to expectations if we assume that the fruit contributes significant backscattering. As mentioned earlier, the backscattering from the fruit is believed to be insignificant compared to the backscattering from the other components and will therefore be omitted from subsequent modeling attempts.

Ulaby et al. (1984) showed that leaves are the dominant source of backscattering (at a 50° incidence angle in the X-, Ku-, and Ka-band frequencies) over the bulk of the growing season. The linear correlation between leaf biomass and σ^o is not too impressive, due mainly to the fact that the relationship is nonlinear. Figure 4.23 shows plots of σ^o versus fresh-leaf biomass that are similar to those presented by Ulaby et al. (1984). The fact that Ulaby et al. characterized the leaves by using the leaf-area-index (LAI) parameter, whereas here we use the fresh-leaf biomass quantity, is not a serious inconsistency, since LAI and fresh-leaf biomass are highly correlated, as was shown by Brisco et al. (1983). The overall trend is the same. For low values of leaf matter, σ^o shows more scattering and is in general lower than σ^o for higher values of leaf matter. The scattering at the low leaf-biomass end may be explained by variations in soil moisture and other contributing factors, while for higher values of leaf biomass, the reduced scattering supports the theory that the leaves dominate backscattering while attenuating other sources.

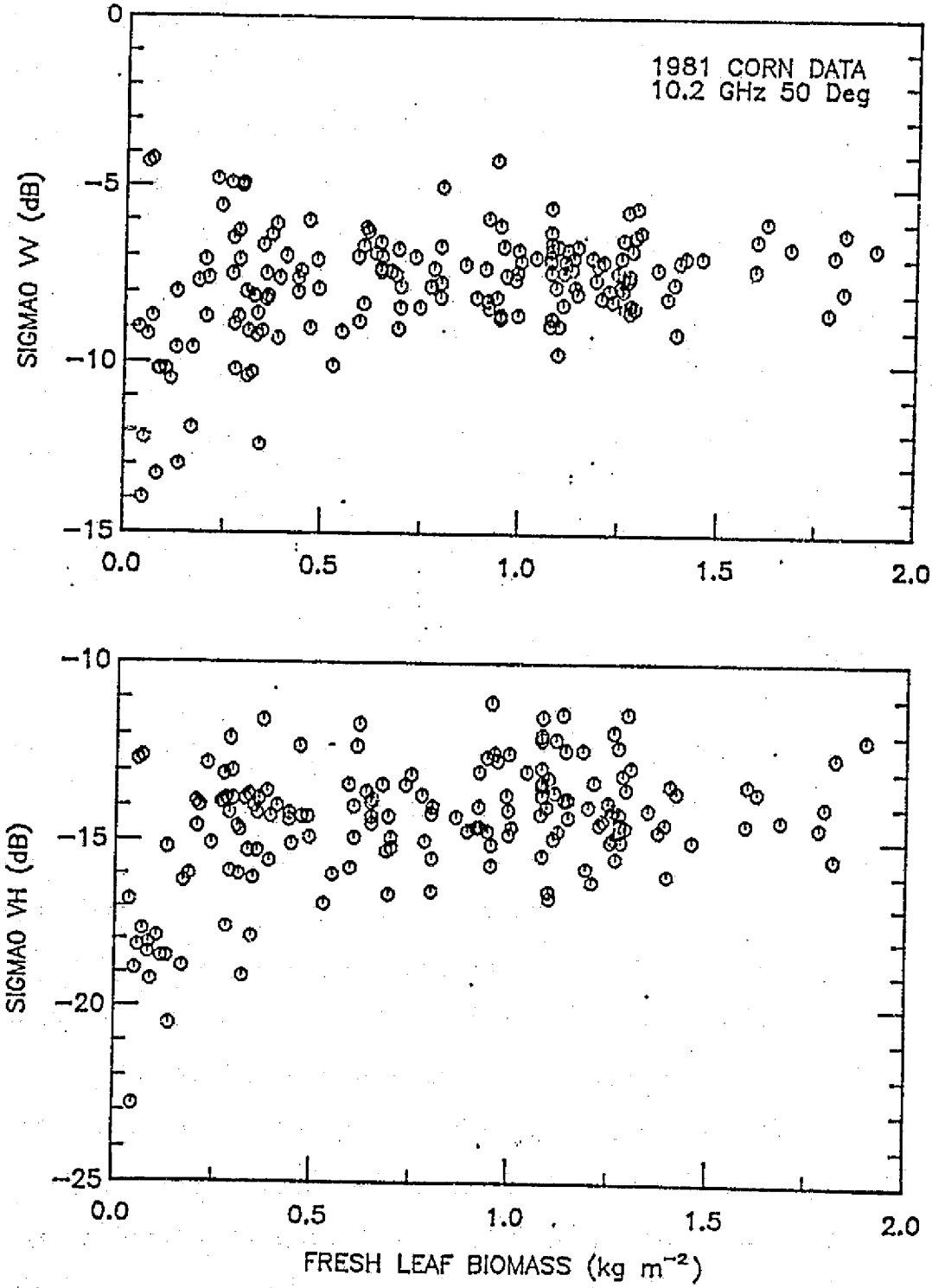

Figure 4.23 Effects of fresh leaf biomass on the level of σ^{o}.

4.7.2 Modeling of the 1981 Corn Data

The same criterion used in evaluating the models used previously for the wheat data will also apply here. Again, appropriate models presented in the literature will be evaluated, and then any variations on them will be evaluated in order to find the "best" model for predicting measured σ^o with the highest correlation coefficient, the lowest RMS difference error (in dB), and the fewest model parameters. In order to evaluate the ability of a particular model to predict the backscattering from a given canopy type (and underlying soil), data from all ten corn fields will be pooled in the evaluation, i.e., the coefficients determined will be optimum for the combination of all ten fields.

The first model tested was the cloud model developed by Attema and Ulaby (1976) and given earlier by (4.10),

$$\sigma^o = A[1 - \exp(-B \cdot w \cdot h)] + C \exp(D \cdot m_s - B \cdot w \cdot h) , \tag{4.16}$$

where w is the volumetric water content of the canopy, h is the physical height of the canopy, and m_s is the volumetric soil-moisture content. This model requires only four parameters (A,B,C,D) and provides a correlation coefficient (r^2) of 0.29 with an RMS error of 1.34 dB when applied to the VV data, and $r^2 = 0.43$ and RMS error of 1.39 dB for the VH data. The model coefficients determined via a nonlinear regression computer program that minimizes the squared errors were different from those presented by Attema and Ulaby for VV polarization, although not

significantly. They did not treat the case of VH polarization.

The next model tested was the plant-part model presented by Ulaby et al. (1983). This model requires five parameters and takes the form

$$\sigma^o = A(1 - e^{-E \cdot LAI}) + B \cdot W \cdot H\,(1 - e^{-E \cdot LAI}) + C \cdot m_s \cdot e^{-D \cdot W \cdot H}\, e^{-E \cdot LAI}. \quad (4.17)$$

Here, LAI is the green leaf area index, H is the height of the canopy, and W is the volumetric water content of the stalks. Again, the 1981 summer experiment did not include LAI as a ground-truth parameter; therefore, a substitution of fresh leaf biomass was used. As a result, correlation coefficients (r^2) were determined to be 0.25 and 0.42 for VV and VH polarization, respectively, and RMS errors were 1.37 dB and 1.40 dB for VV and VH polarization, respectively. The coefficients that were determined to optimize the model for the 1981 corn data, which generated the above correlation coefficients and RMS errors, are not identical to those given by Ulaby et al.; however, they are similar in magnitude, except for the stalk attenuation term, which Ulaby finds to be insignificant but which appears to be significant in the 1981 data.

From these results, it was determined that a new model or models should be developed. The experimental data described in Chapter 2 is also available as a further improvement, giving

typical values for canopy attenuation at X-band, 50° incidence angle, and VV polarization.

The basic form adopted for this new model for corn backscattering is

$$\sigma^o = \sigma^o_{leaf} + \sigma^o_{stalk} + \sigma^o_{soil} \tag{4.18}$$

where

$$\sigma^o_{leaf} = \sigma^o_{\ell} = A\{1 - \exp[-F \cdot f_2(leaf)]\}$$

$$\{1 - \exp[-E \cdot f_3(leaf)]\} \tag{4.19a}$$

$$\sigma^o_{stalk} = \sigma^o_{st} = B \cdot f_1(stalk) \exp[-E \cdot f_3(leaf)] \tag{4.19b}$$

$$\sigma^o_{soil} = \sigma^o_{s} = C(\Gamma_{VV} + G\Gamma_{HH}) \exp[-D \cdot f_4(stalk) - E \cdot f_3(leaf)] , \tag{4.19c}$$

where $f_1(stalk)$ and $f_2(leaf)$ relate the measured ground-truth quantities to backscattering by the stalks and leaves, respectively, and $f_3(leaf)$ and $f_4(stalk)$ relate the measured ground-truth quantities to attenuation by the leaves and stalks, respectively. The exact nature of these functions ($f_i(\ )$) are unknowns at this point. In keeping with the objectives of this study, this dependence will be represented by a simple relationship involving measured ground-truth quantities. The form

of the soil backscattering component is the same as that used in the wheat model and is explained there.

Several models were tried using various combinations of available ground-truth data. As with the development of the wheat model, an emphasis on variables related to water content, e.g., fresh leaf biomass and leaf water content, is appropriate because water has been shown to be a significant factor at microwave frequencies. After a trial-and-error process, the optimum combination of ground-truth parameters for the $f_i(\ )$'s was found to be

$$f_1(\text{stalk}) = \text{SH2O}, \tag{4.20a}$$

$$f_2(\text{leaf}) = \text{LWT/HT} \tag{4.20b}$$

$$f_3(\text{leaf}) = \text{LWT} . \tag{4.20c}$$

Also in the course of the model evaluation, the attenuation due to the stalks was found to be insignificant, i.e., the model coefficient D = 0. Thus, f_4(stalks) is not necessary. Here SH2O represents the stalk water content (kg m^{-2}), LWT represents the fresh leaf biomass (kg m^{-2}), and HT is the canopy height (m).

Incorporation of these functions into Eq. (4.19) resulted in a correlation coefficient (r^2) of 0.35 and 0.44 for VV and VH polarization, respectively, with associated RMS difference errors of 1.28 dB and 1.37 dB. Table 4.9 lists the seven model coefficients determined, and the r^2 and RMS errors for each field

TABLE 4.9

Model Coefficients and Resulting Statistics
1981 Corn, 10.2 GHz, 50° Incidence Angle

Pol.	A	B	C	D	E	F	G
VV	0.298	0.080	0.546	0	2.030	1.836	0
VH	0.079	0.018	0.023	0	1.340	1.263	1

Field (N)	r^2/RMS Error (dB) VV	r^2/RMS Error (dB) VH
All (166)	0.35/1.28	0.44/1.37
1 (26)	0.44/1.37	0.53/1.40
2 (13)	0.48/1.00	0.67/1.51
3 (17)	0.43/1.18	0.73/1.17
4 (11)	0.16/1.05	0.30/0.97
5 (18)	0.40/1.20	0.22/1.39
6 (18)	0.21/1.18	0.38/1.00
7 (17)	0.67/1.19	0.70/1.11
8 (12)	0.36/1.10	0.71/1.36
9 (16)	0.93/1.30	0.93/1.59
10 (18)	0.34/1.81	0.20/1.84

for both VV and VH polarization. Figures 4.24 and 4.25 present plots of predicted versus observed or measured σ^o for all fields combined. In both cases, a linear regression indicates a slope of less than one and an intercept of less than 0 dB.

Figure 4.26 shows a plot of the errors (defined here as $\sigma^o_{meas}(dB) - \sigma^o_{pred}(dB)$) for VV polarization versus VH polarization. As the statistics indicate, the quality of fit is comparable for both models.

Figures 4.27 and 4.28 show plots of σ^o_{meas} and σ^o_{pred} as a function of time, as well as of the constituent parts (σ^o_ℓ, σ^o_{st}, and σ^o_s) for Corn Field No. 9. In both cases, the soil is the dominant backscattering source early in the season, whereas in mid-season, when the canopy is the most lush, the leaves dominate. Towards the end of the season, as the leaves dry out, the stalks begin to dominate, although the soil component is nearly as significant.

Figures 4.29 and 4.30 show a comparison of σ^o_{meas} and σ^o_{pred} for all ten fields over time. In general, it is apparent that while the correlation coefficients are not too impressive, a better measure in this case is the RMS difference error value. With a few exceptions, the agreement between σ^o_{meas} and σ^o_{pred} is quite good. An explanation of why this is not reflected in the correlation coefficients goes back to the limited dynamic range in the data. Referring back to Figures 4.24 and 4.25, it is clearly evident that most of the data lie in a cluster 3 or 4 dB in extent. Unfortunately, the way the correlation coefficient is computed introduces a factor that is dependent on slope, and the

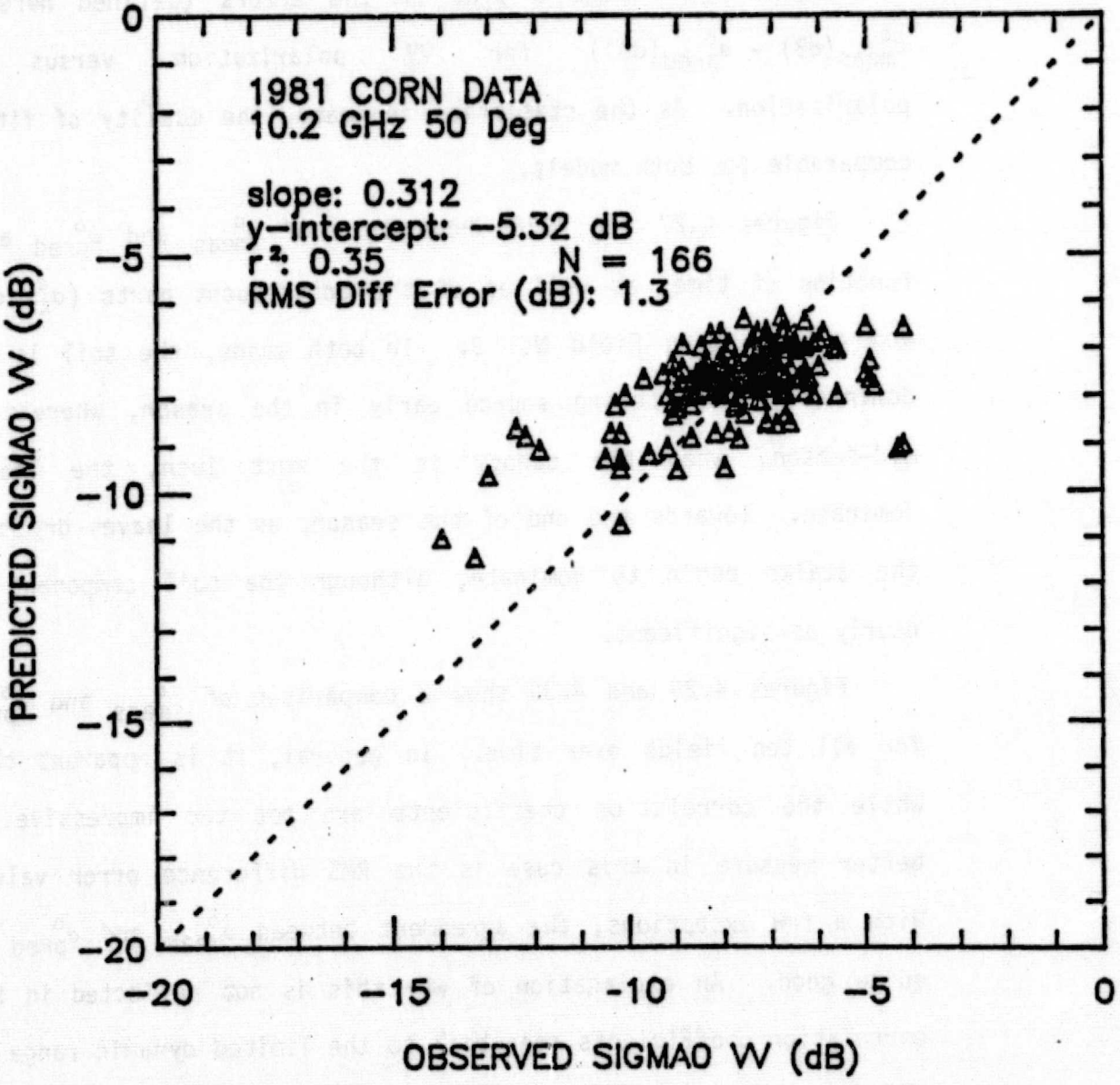

Figure 4.24 A comparison of observed (measured) σ^o_{VV} with predicted σ^o_{VV}, using Eq. (4.18).

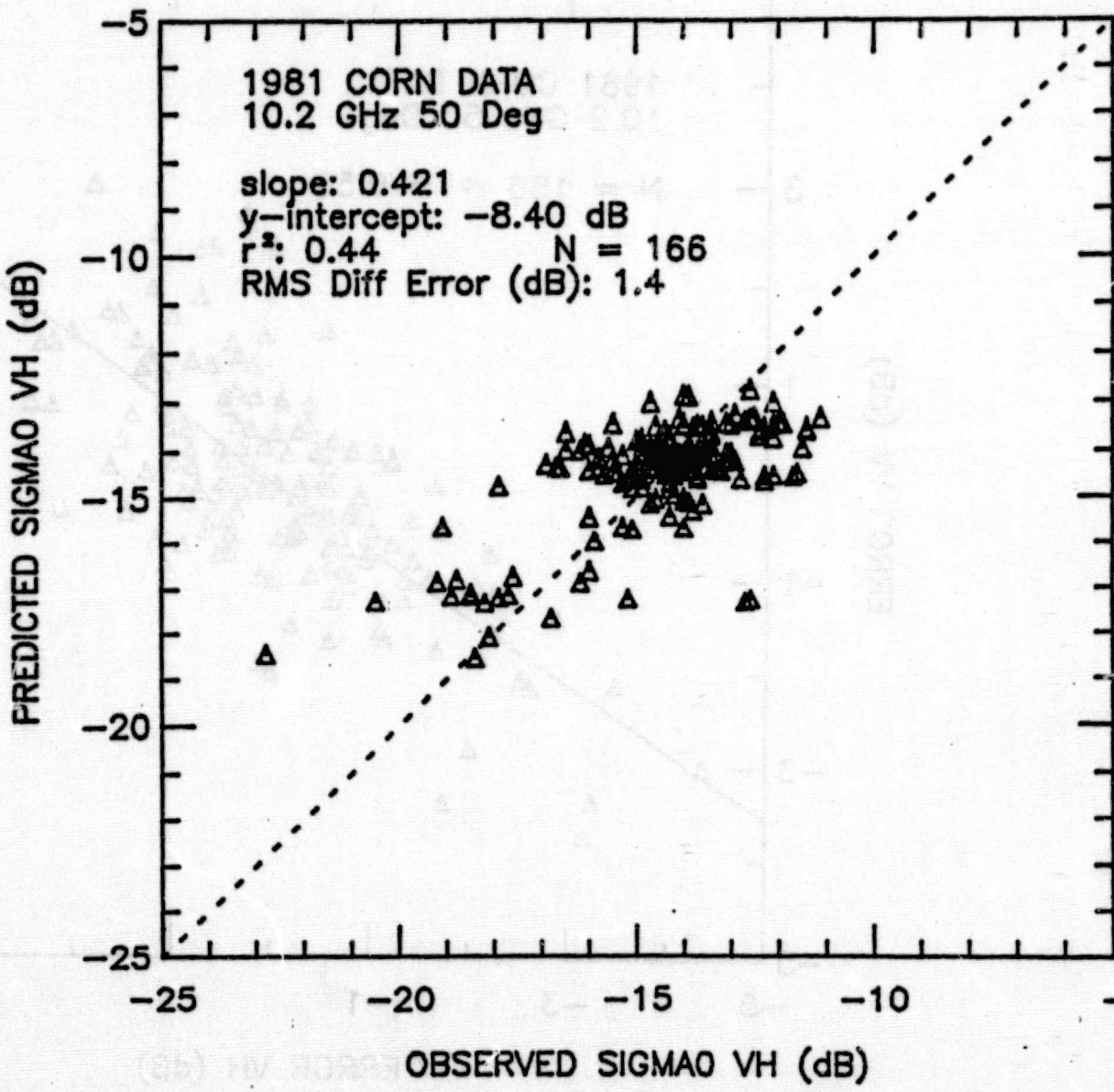

Figure 4.25 A comparison of observed (measured) σ^o_{VH} with predicted σ^o_{VH}, using Eq. (4.18).

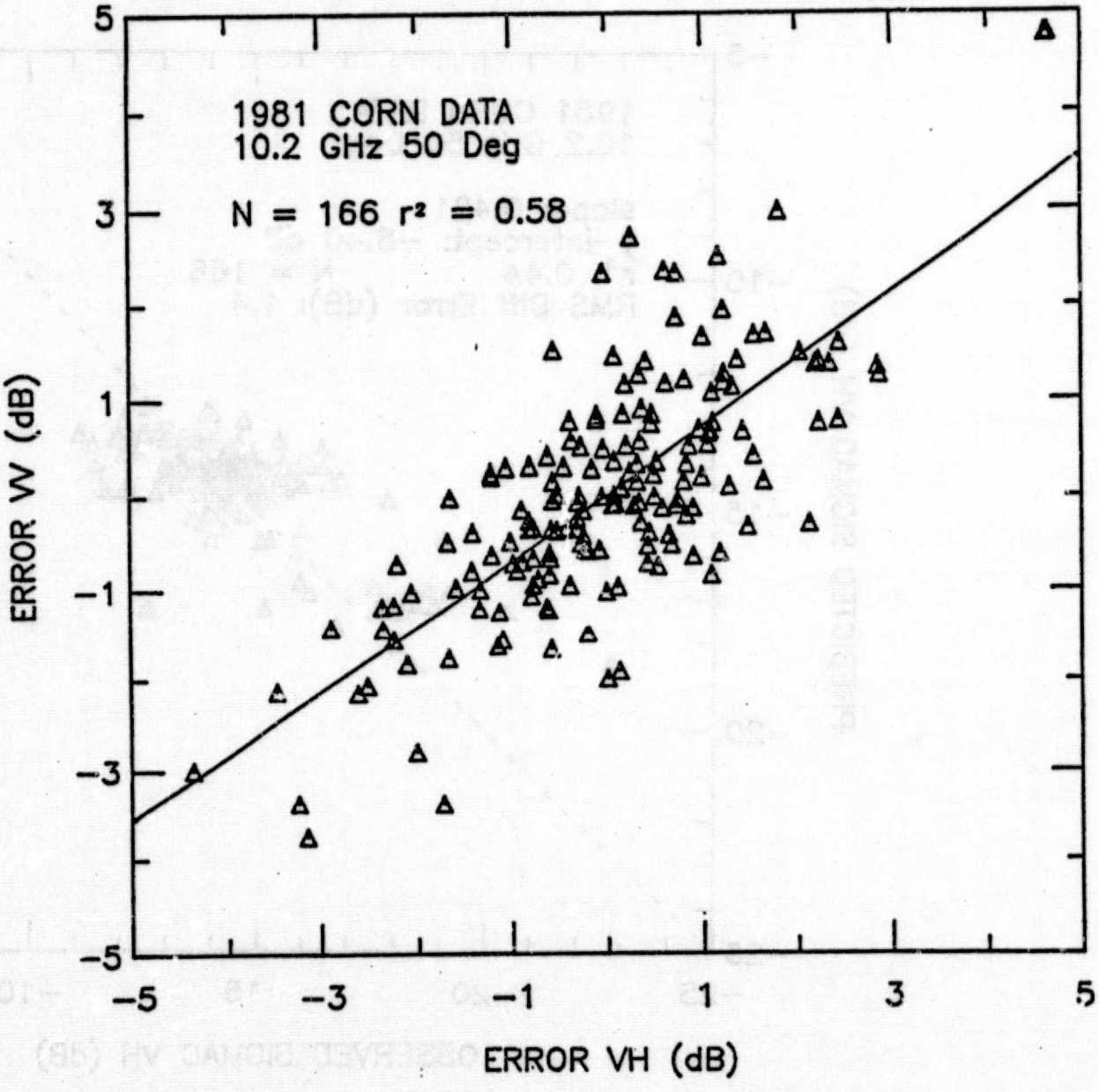

Figure 4.26 A comparison of the errors in predicting σ^{o}_{VV} with the errors in predicting σ^{o}_{VH}.

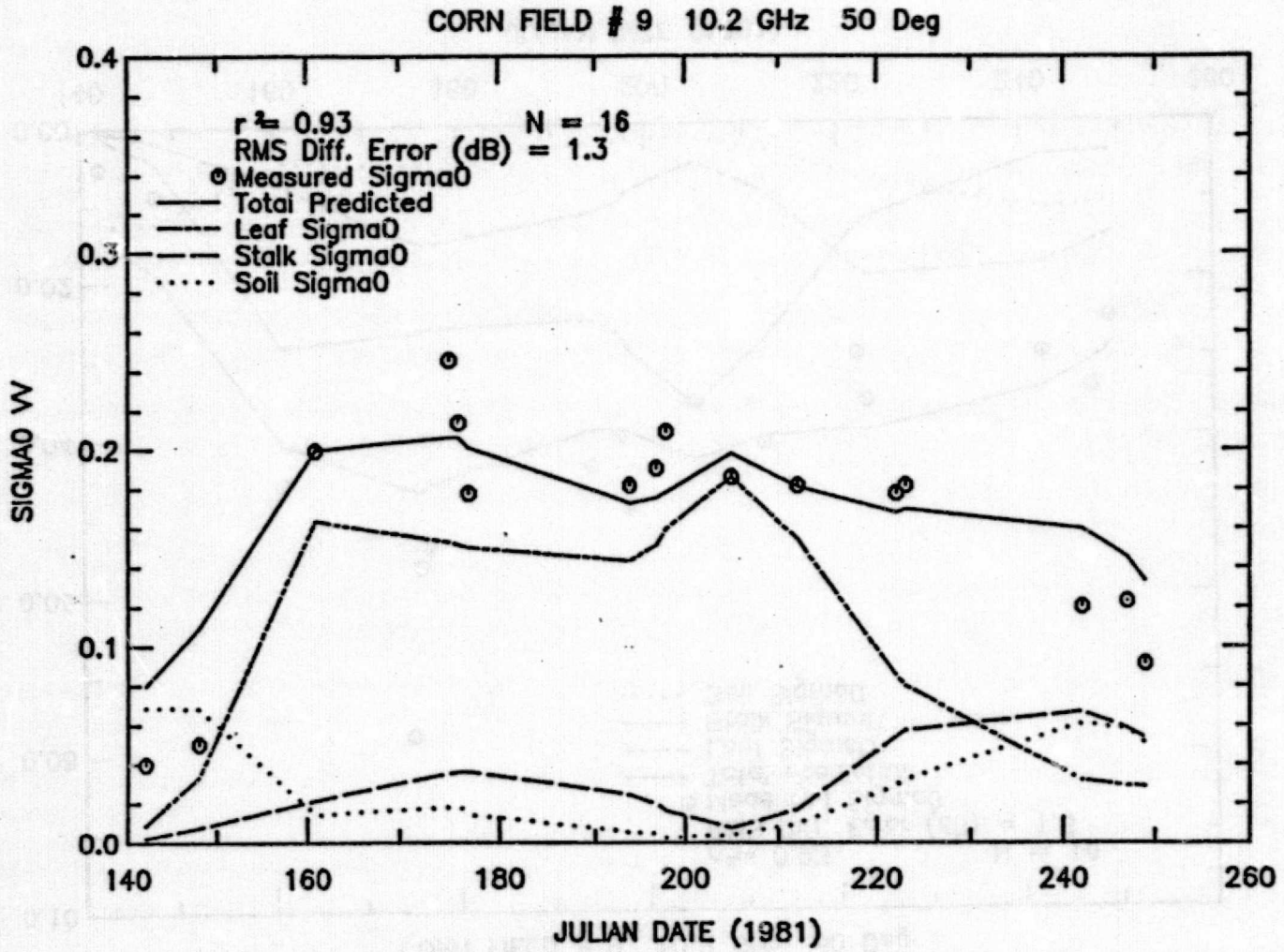

Figure 4.27 A comparison of measured and predicted σ^o_{VV} over time for corn field No. 9. The predicted value is the sum of three components, also shown here.

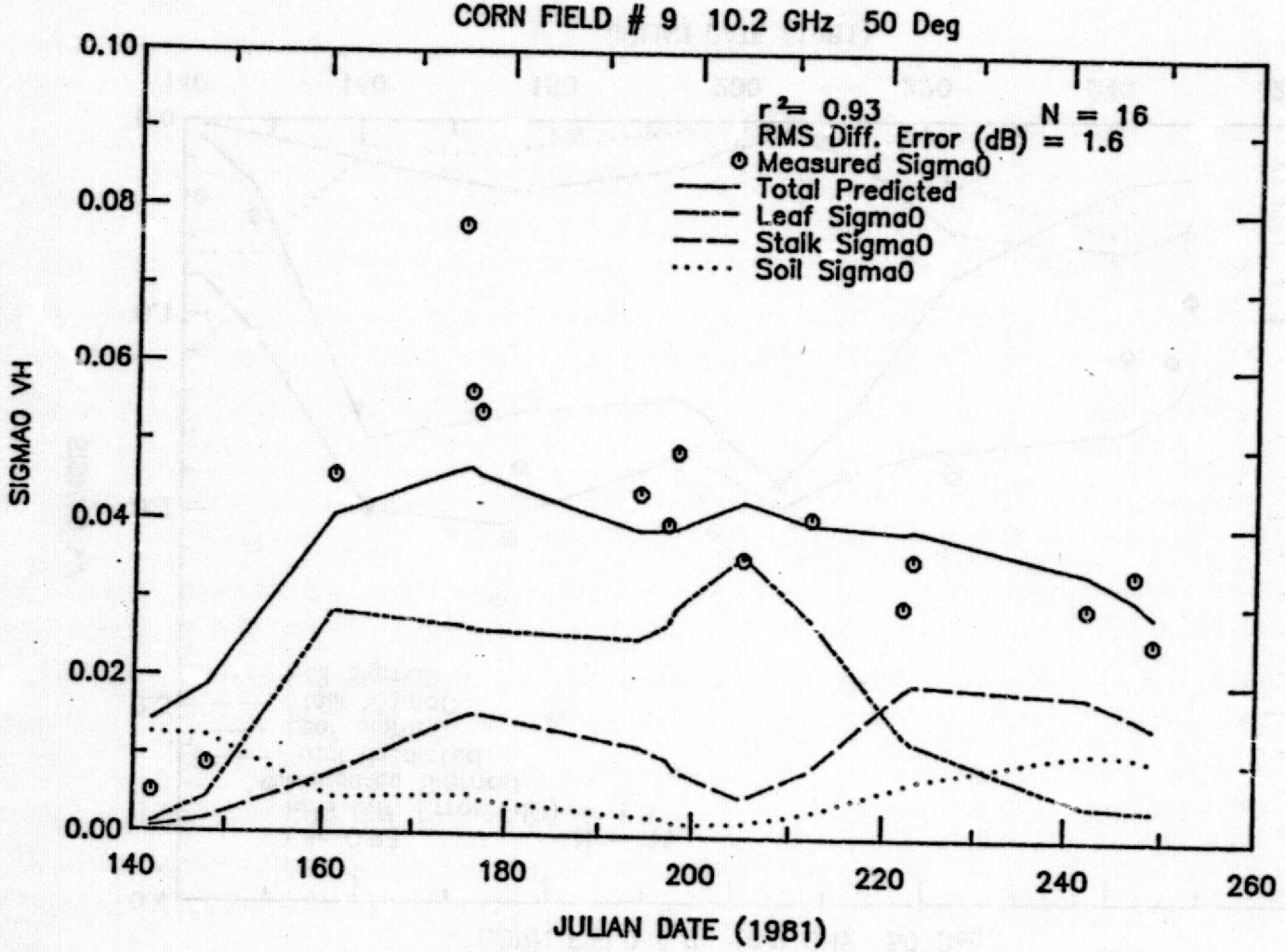

Figure 4.28 A comparison of measured and predicted σ^o_{VH} over time for corn field No. 9. The predicted value is the sum of three components, also shown here.

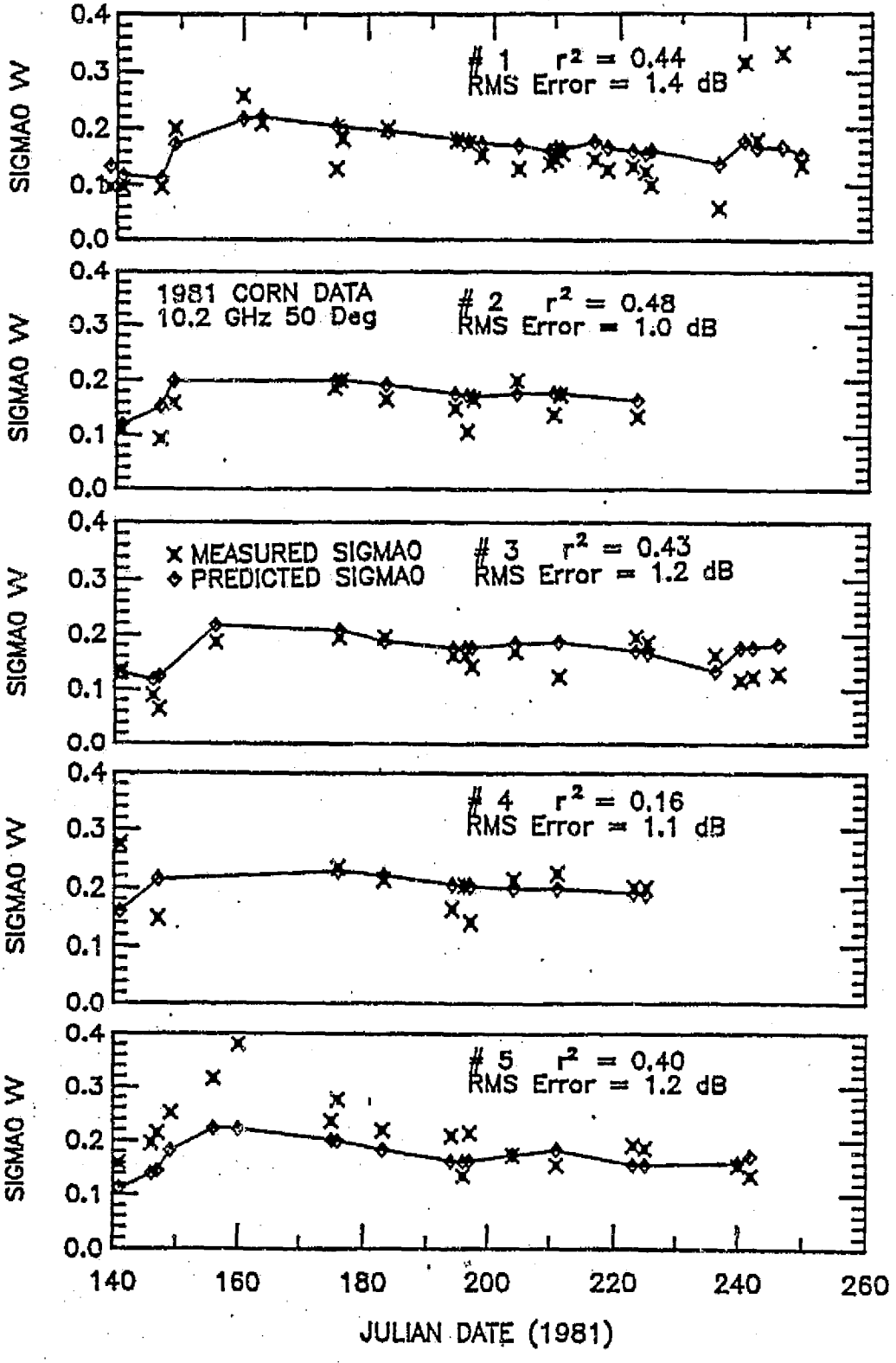

Figure 4.29 A comparison of measured and predicted σ^{o}_{VV} over time is presented on a per-field basis.

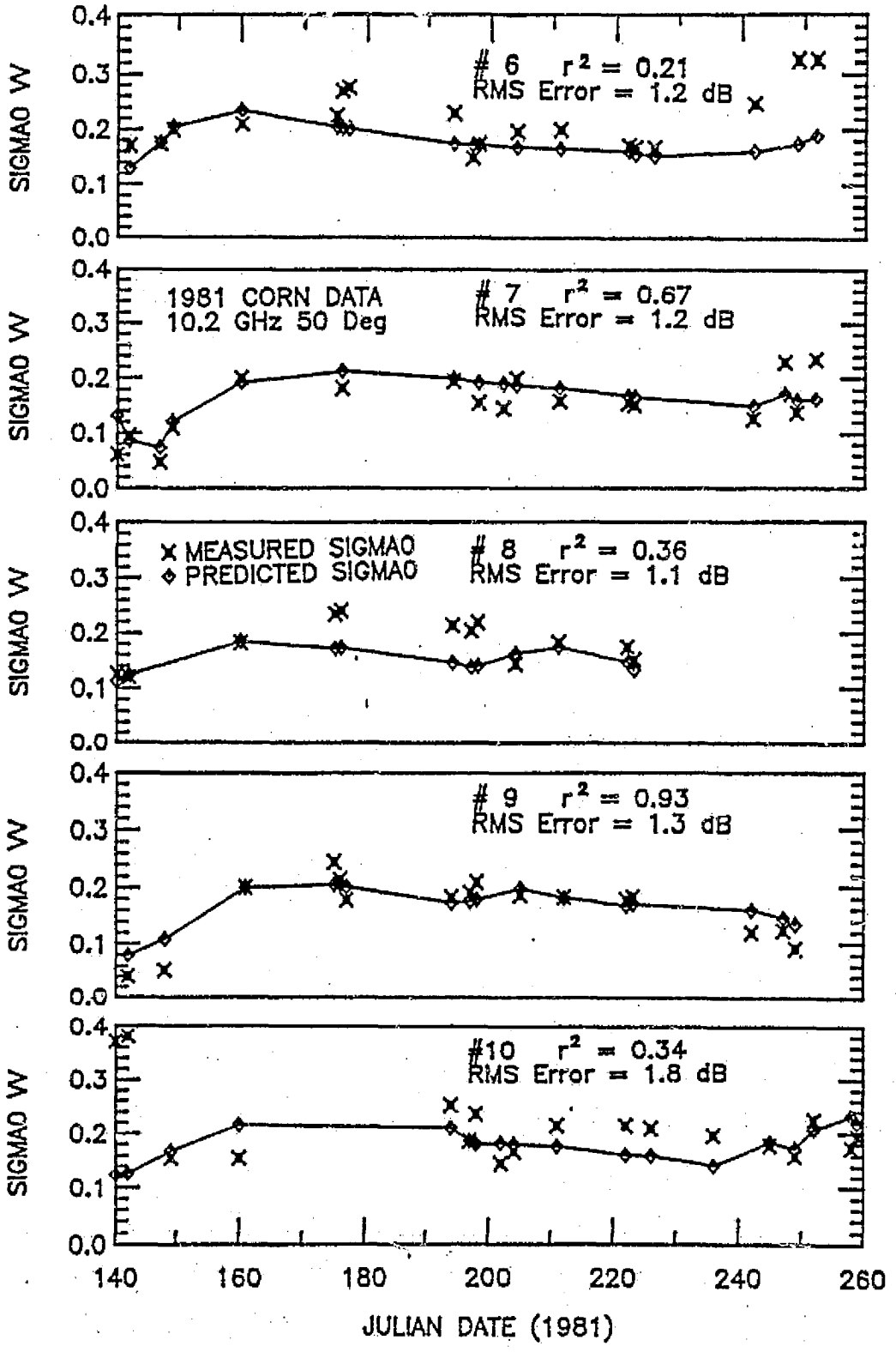

Figure 4.29 (Continued)

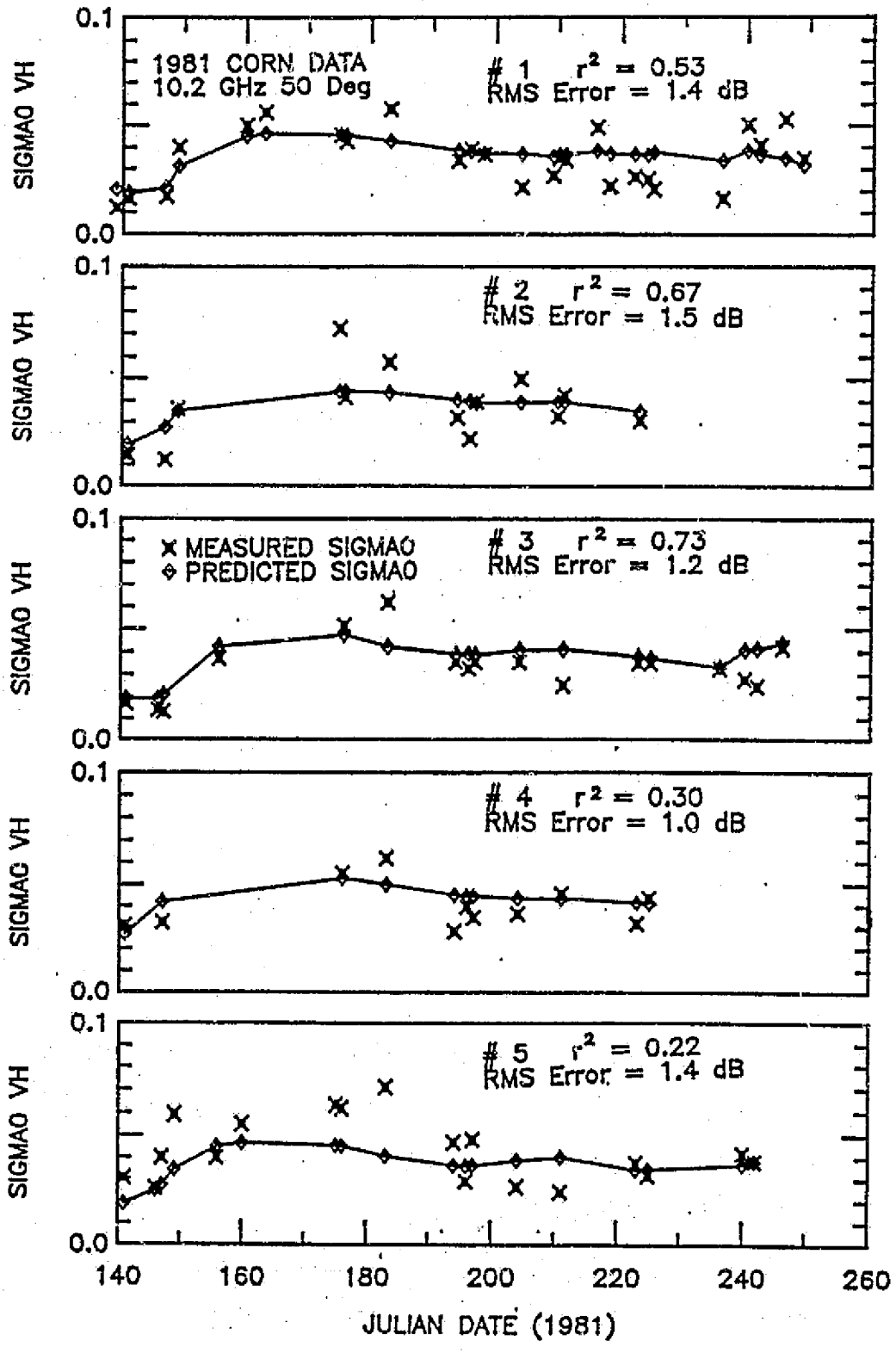

Figure 4.30 A comparison of measured and predicted σ^{o}_{VH} over time is presented on a per-field basis.

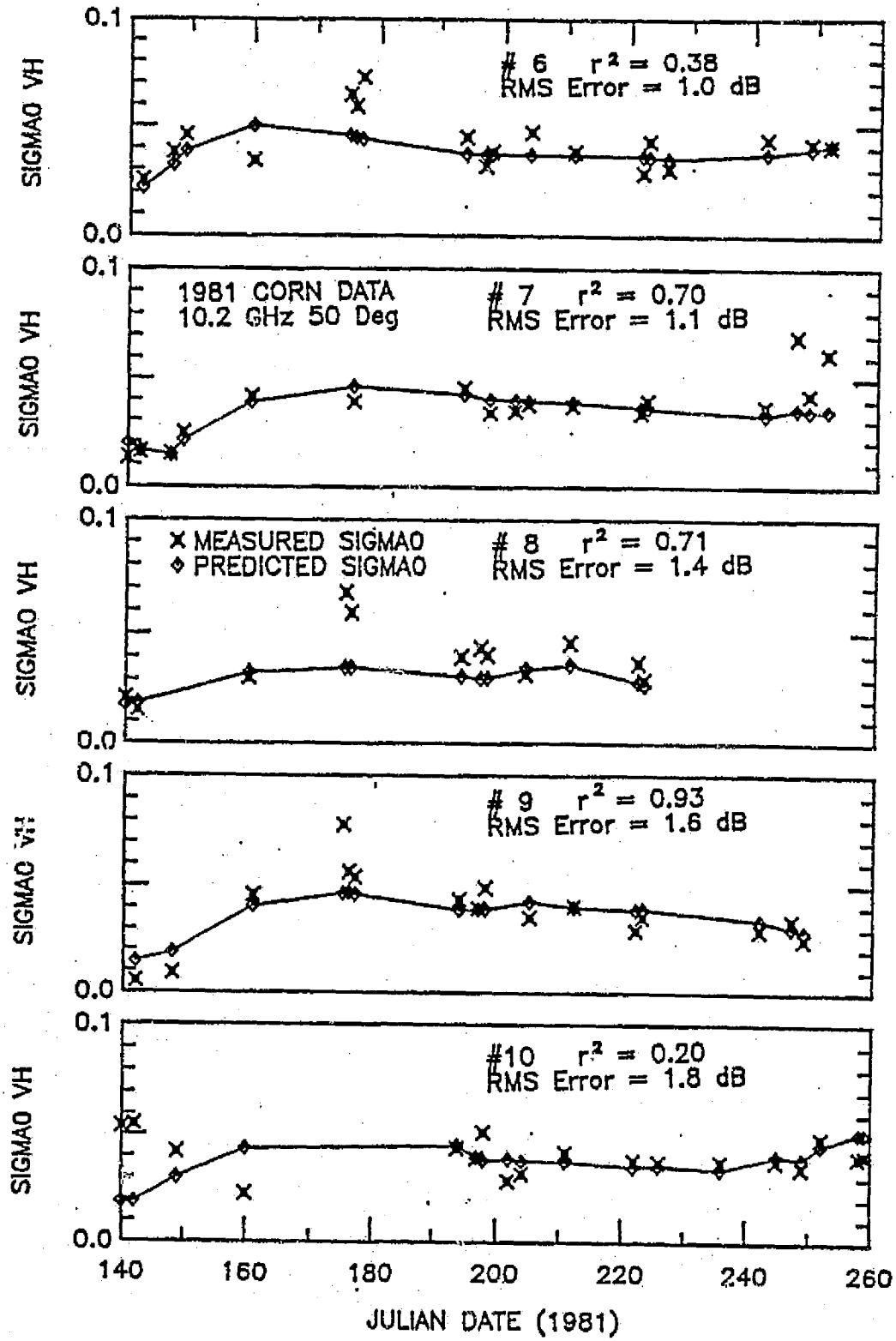

Figure 4.30 (Continued)

estimated slope of such a tight cluster is open to error. Hence the correlation coefficient is not entirely indicative of the quality of the fit, and here the RMS difference error becomes useful.

One final observation is in order before we move on to the error-analysis phase. In August of 1981, one of the corn fields used in this experiment (No. 6) was the subject of another experiment. In this special one-day experiment, a plot of about 7 x 7 meters of this field was defoliated, i.e., the leaves, fruit, and stalks were removed sequentially, and radar observations were made between each defoliation step. These data, reported by Ulaby (1982), provided a unique chance to test the corn model one component at a time.

Table 4.10 lists the measured ground truth on the day of the experiment (Day 224) as well as the measured σ^o throughout the experiment. At the bottom of Table 4.10 is a listing of the measured σ^o of each component along with that predicted by this new model. The measured σ^o for the stalks is obtained by subtracting (in real units of $m^2\ m^{-2}$) the soil term from the $\sigma^o_{soil} + \sigma^o_{stalk}$ measurement. This is also true for the leaf term, although the attenuation predicted by the model is also taken into account. For stalk and soil backscattering, the model does quite well, although for the leaf term the agreement is not quite so good. One reason may be that for the leaf term the attenuation estimate is used twice: once in reducing the measured σ^o to σ^o_{leaf}, and again to obtain the predicted σ^o_{leaf}.

TABLE 4.10

Corn Defoliation Experiment
Day 224 Corn Field No. 6

Stalk Water Content: 2.357 kg m^{-2}
Fresh Leaf Biomass: 0.772 kg m^{-2}
Height: 2.779 m
Soil Moisture: 29% + (Γ_{VV} = 0.1906, Γ_{HH} = 0.5059)

θ = 50°	Full Canopy	Leaves Removed	Leaves and Fruit Removed	Bare Soil
σ^o_{VV}(dB)	- 6.79	- 5.77	- 5.78	-10.05
σ^o_{VH}(dB)	-12.74	-13.42	-13.43	-18.30

		Measured σ^o	Predicted σ^o	% Error
σ^o_{soil}	VV	0.099	0.104	+ 5
	VH	0.015	0.016	+ 7
σ^o_{stalk}	VV	0.165	0.189	+15
	VH	0.031	0.042	+35
σ^o_{leaf}	VV	0.154*	0.094	-39
	VH	0.037*	0.015	-59

*The leaf values assume an attenuation of 6.8 dB and 4.5 dB (2-way) for VV and VH, respectively, as predicted by the model.

Overall, the test increases the credibility of the models for corn.

4.7.3 Error Analysis

Because a model is only as good as the data from which it is derived, an evaluation of the errors (on both sides if the equation) may permit some insight into the impact such errors have. As originally described in the evaluation of the wheat model, measurement errors tend to degrade the model's ability to represent nature,

$$\sigma^o_{meas} + \varepsilon_{meas} = \sigma^o_{pred}(\text{ground truth}) + \varepsilon_{pred} .$$

In this evaluation, a numerical simulation of these errors is performed and a correlation coefficient of σ^o_{meas} with σ^o_{pred} is computed. Thus, given that we assume that this model describes nature exactly, these errors degrade it to some degree, solely because of these data errors.

The sources of error are described in the evaluation of the wheat model. To summarize, an estimate of all measurement errors, both for ground truth and radar values, is necessary. When this has been done, the simulation will provide the desired data. The values of variance in the ground-truth and radar quantities are listed in Table 4.11. These values were arrived at by examining the variance in the raw data.

The results of the simulation indicate that given these sources of error, an exact model of nature could, at best, have a

TABLE 4.11

Error Simulation Results, 1981 Corn Data

	Stalk		Fruit		Leaf			
Parameter	Fresh Biomass	Dry Biomass	Fresh Biomass	Dry Biomass	Fresh Biomass	Dry Biomass	Height	Soil
Std. Dev.	0.21μ	0.20μ	0.23μ	0.23μ	0.21μ	0.22μ	0.09μ	0.20μ

μ represents the mean of the measured value

σ^o_{VV} has a std. dev. of 0.8 dB

σ^o_{VH} has a std. dev. of 1 dB

N = 166

VV results: $r^2 = 0.35$ RMS Diff. Error = 1.10 dB
VH results: $r^2 = 0.48$ RMS Diff. Error = 1.09 dB

correlation coefficient (r^2) of 0.35 and 0.48 and RMS errors of 1.10 dB and 1.09 dB for VV and VH polarization, respectively. That is not to say that this simple model is an exact mathematical description of nature, only that given the sources of error, which may or may not be as modeled, a large number of the errors in predicting σ^o may be attributed to uncertainties in both ground truth parameters and in measured values of σ^o.

4.7.4 Analysis of Weather Effects

Of the 318 original data sets, 130 were omitted from the model development set due to the fact that they might have been affected by a recent rain (within two days). In this section, those 130 data sets are examined to determine, what, if any, effect the rain might have had on σ^o. This is possible because a model describing the behavior of σ^o as a function of ground-truth parameters is now available. Since the effect may be small, a more accurate model is desirable. Hence, the form of the previously described model will be optimized for each field individually. These new model coefficients are presented in Table 4.12. Given these models, optimized on a per field basis, a determination of errors in the "normal" data used to determine the model coefficients, and the errors in the "rain-affected" data is made. A statistical comparison of these errors is performed to determine if the nature of the errors is similar, (i.e., no rain effect) or dissimilar (some rain effect).

The results are shown in Table 4.13. Significant differences are apparent in the two classes of errors for both VV and VH

Table 4.12
(a)
Model Coefficients and Resulting Statistics
Optimized on a per-Field Basis - Corn

Crop: Corn Polarization: VV

Field No.	A	B	C	D	E	F	G	r^2	RMS Difference Error(dB)	N
1	1.288	0.083	0.556	0	2.178	1.833	0	0.51	1.24	26
2	0.283	0.035	0.507	0	0.949	0.257	0	0.67	0.59	13
3	0.177	0.028	0.386	0	1.503	1.357	0	0.58	0.83	17
4	0.185	0.074	1.175	0	0.779	12.643	0	0.58	0.54	11
5	0.997	0.062	0.792	0	2.773	5.412	0	0.71	0.63	18
6	0.232	0.500	0.236	0	5.268	4.013	0	0.64	0.60	18
7	0.274	0.381	0.144	0	4.927	1.838	0	0.87	0.68	17
8	0.212	0.022	0.518	0	5.400	9.085	0	0.61	0.61	12
9	0.533	0.066	0.224	0	1.034	0.793	0	0.96	0.44	16
10	0.190	0.035	1.911	0	7.0	14.840	0	0.62	0.71	18
All	0.283	0.080	0.546	0	2.029	1.833	0	0.35	1.28	166

TABLE 4.12(b)

Crop: Corn Polarization: VH

Field No.	A	B	C	D	E	F	G	r^2	RMS Difference Error(dB)	N
1	0.244	0.034	0.009	0	2.927	0.257	1	0.57	1.24	26
2	0.406	0.003	0.016	0	0.175	1.357	1	0.71	1.19	13
3	0.253	0.012	0.018	0	0.301	12.643	1	0.75	0.87	17
4	0.308	0.003	0.039	0	0.399	5.412	1	0.70	0.60	11
5	0.117	0.020	0.037	0	0.833	0.511	1	0.27	1.21	18
6	0.069	0.021	0.022	0	1.952	4.013	1	0.41	0.90	18
7	0.042	0.078	0.010	0	3.734	1.838	1	0.93	0.52	17
8	0.126	0.019	0.022	0	1.256	9.085	1	0.72	0.91	12
9	0.208	0.023	0.006	0	0.427	0.793	1	0.93	0.76	16
10	0.037	0.011	0.076	0	9.764	14.840	1	0.31	0.78	18
All	0.079	0.018	0.023	0	1.338	1.253	1	0.44	1.37	166

TABLE 4.13

1981 Corn - Weather Effects Analysis

Data Class	N	Mean Error (dB)	RMS Diff. Error (dB)	T-Test 2-Tail Probability
		VV Polarization		
Normal	166	0.0009	0.77	
Recent Rain	130	0.7880	1.54	0.000
		VH Polarization		
Normal	166	0.0069	0.95	
Recent Rain	130	0.5459	1.51	0.000

polarizations; thus, there is a high probability that the errors come from two different distributions. To illustrate this difference, histograms of the two types of errors are presented in Figures 4.31 and 4.32. In both VV and VH polarizations, the "normal" data has errors that appear to have a Gaussian distribution with a mean error of 0 dB. The "rain" data shows a much wider distribution, with errors of over 4 dB that do not occur in the "normal" data and a mean clearly larger than 0 dB. Hence, the effect of the rain seems to be to increase σ^o over that of the "normal" canopy.

Finally, Figure 4.33 compares the relationship between VV errors and VH errors for the two classes. Scattering is much greater for the "rain" data; it also has a higher correlation coefficient. This may indicate that recent rain affects σ^o_{VV} in much the same way as it does σ^o_{VH}; hence, the errors are correlated.

4.8 1981 Soybean Data

During the 1981 summer experiment, 11 soybean fields were monitored with the truck-mounted radar system, and a total of 348 data sets were acquired. Shortly after beginning the observation phase, Field No. 7 had to be dropped from the experiment because of farm-operator problems; therefore, the five data sets acquired on that field have been omitted from the analysis because of size limitations. Another six data sets were omitted from analysis because they were gathered after the field was harvested. A recent rain (within two days) might have influenced another 64

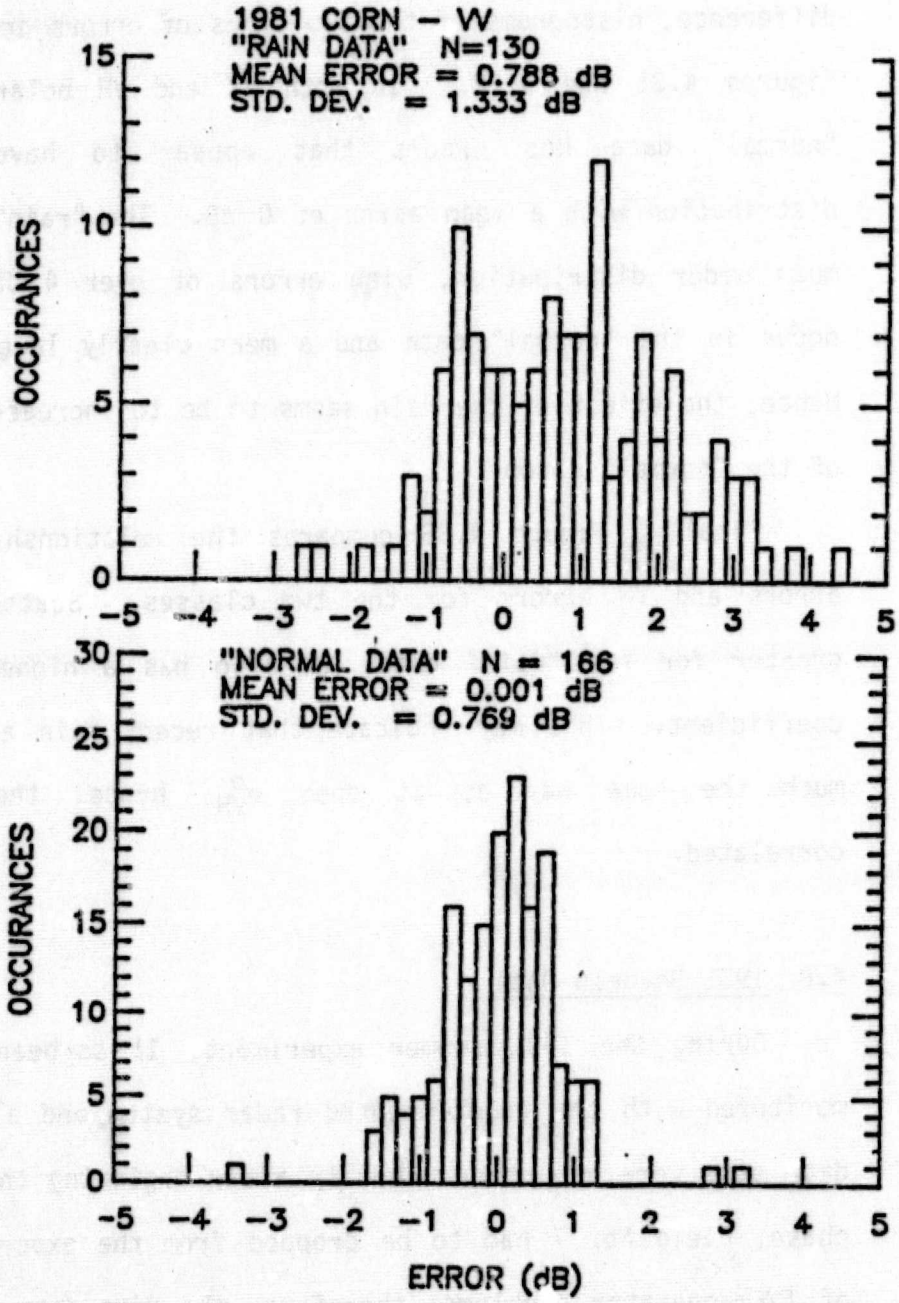

Figure 4.31 Histogram of the errors between predicted and measured σ^{o}_{VV} for the two sets of corn data: normal and rain-affected.

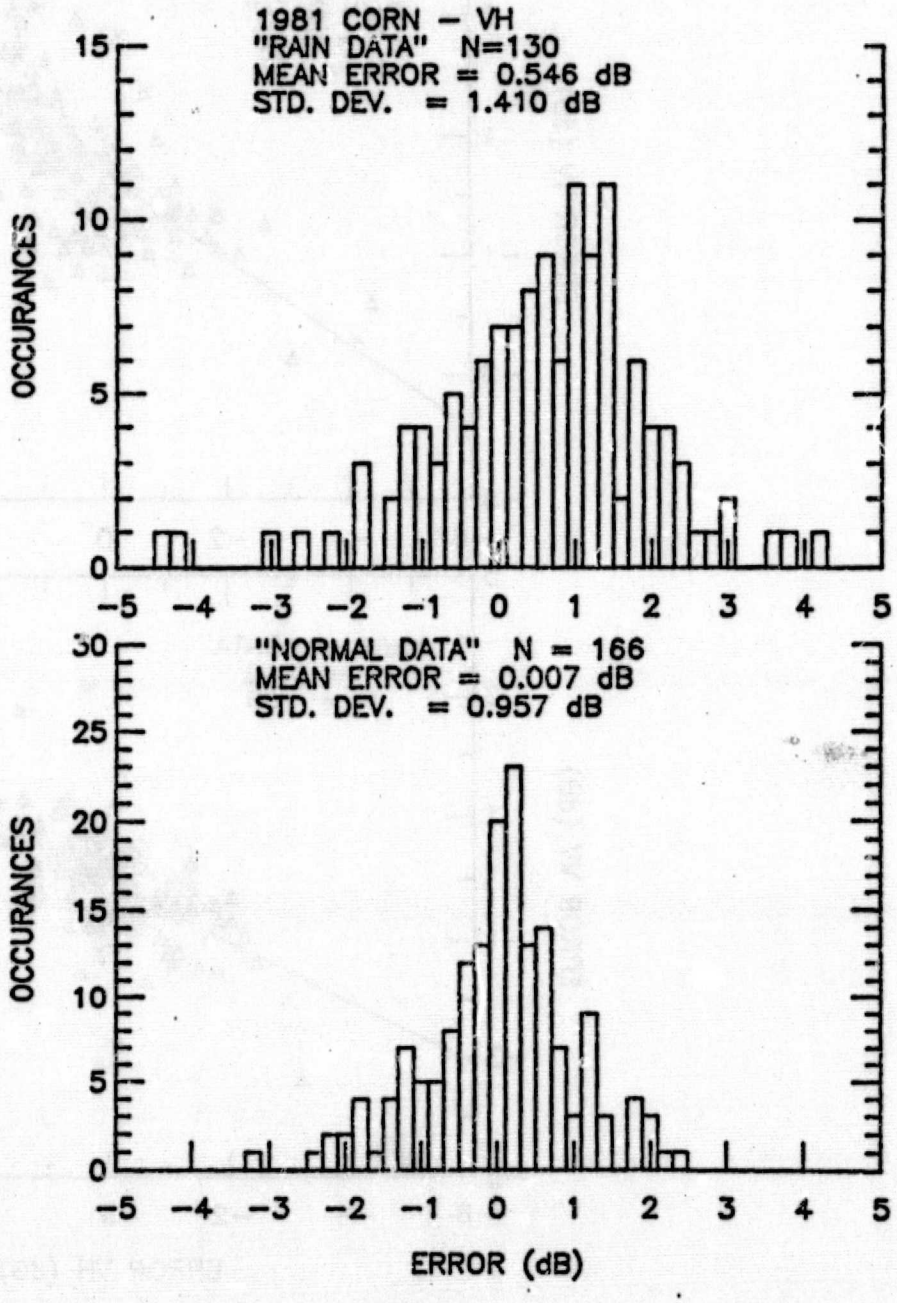

Figure 4.32 Histogram of the errors between predicted and measured σ°_{VH} for the two sets of corn data, normal and rain-affected.

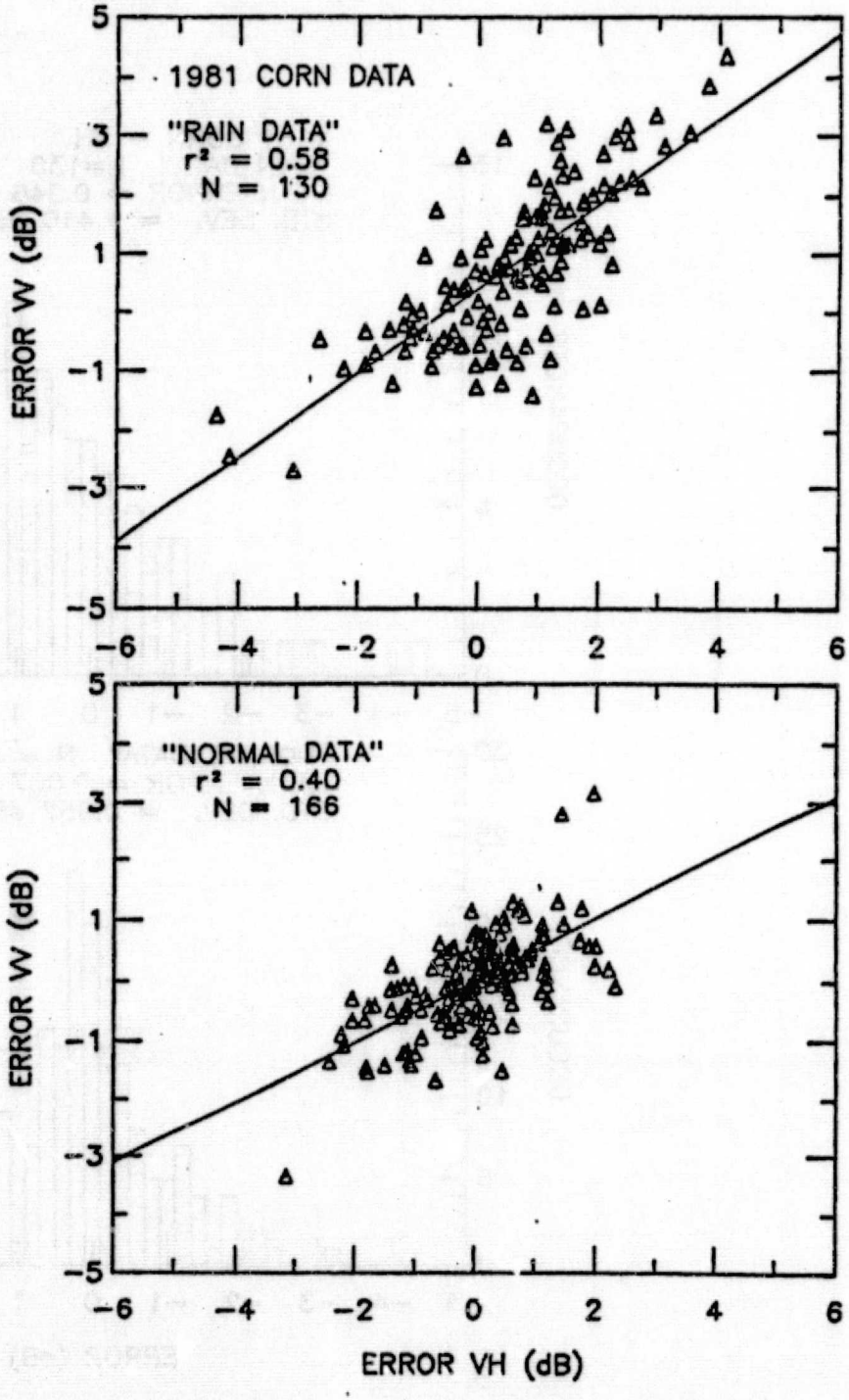

Figure 4.33 A comparison of how the errors between predicted and measured σ° vary with polarization and weather influence.

data sets, so these data sets are excluded from initial analysis and modeling. Another 18 data sets lacked soil moisture data and had to be omitted. Thus, of the original 348 data sets, only 255 will be analyzed and modeled. The smoothing of the plant variables (ground truth) completes the clean up. (Smoothing is performed on all data excluding post-harvest and Field No. 7). Due to the structure of the canopy, no differentiation among plant parts was made while obtaining biomass data. A sample data set is shown in Figure 4.34. Note the similarity between σ^o and soil moisture prior to Julian date 210 - 220 when plant fresh biomass values surge.

Figure 4.35 shows the temporal behavior of σ^o for all ten fields. Note the differing time scales in Figure 4.35a and b. This is because Fields No. 1 through 5 were all planted in early-to-mid May, whereas Fields No. 6 through 11 were double-cropped, i.e., they were planted in fields previously planted with winter wheat, and thus were not planted until late June or early July. Due to the late start, these plants did not in general develop as large a biomass, and correspondingly, did not produce as good a yield as the first five. The overall temporal behavior of all ten fields is somewhat similar in that most begin with smaller σ^o values, which increase as time progresses, fluctuate, and in a few cases decline to the values seen in the beginning. Also note the similarity between σ^o_{VV} and σ^o_{VH} for all ten fields. Figure 4.36 compares σ^o_{VV} with σ^o_{VH} directly. A correlation coefficient (r^2) of 0.75 indicates that similar mechanisms may be driving both σ^o_{VV} and σ^o_{VH}.

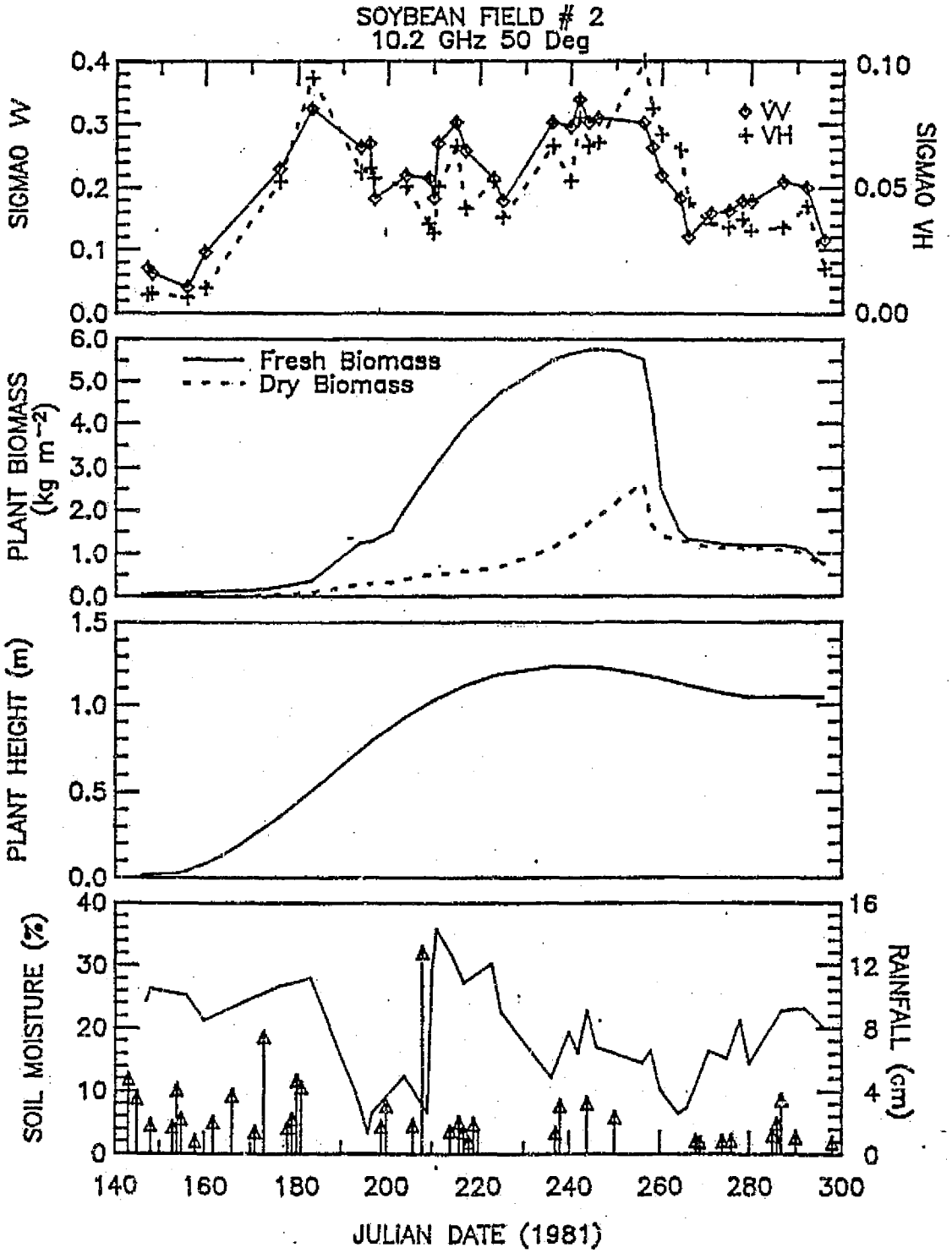

Figure 4.34 Temporal histories of the radar data (σ^{o}) and the ground-truth parameters (after smoothing) along with the measured rainfall events for a given soybean field (No. 2).

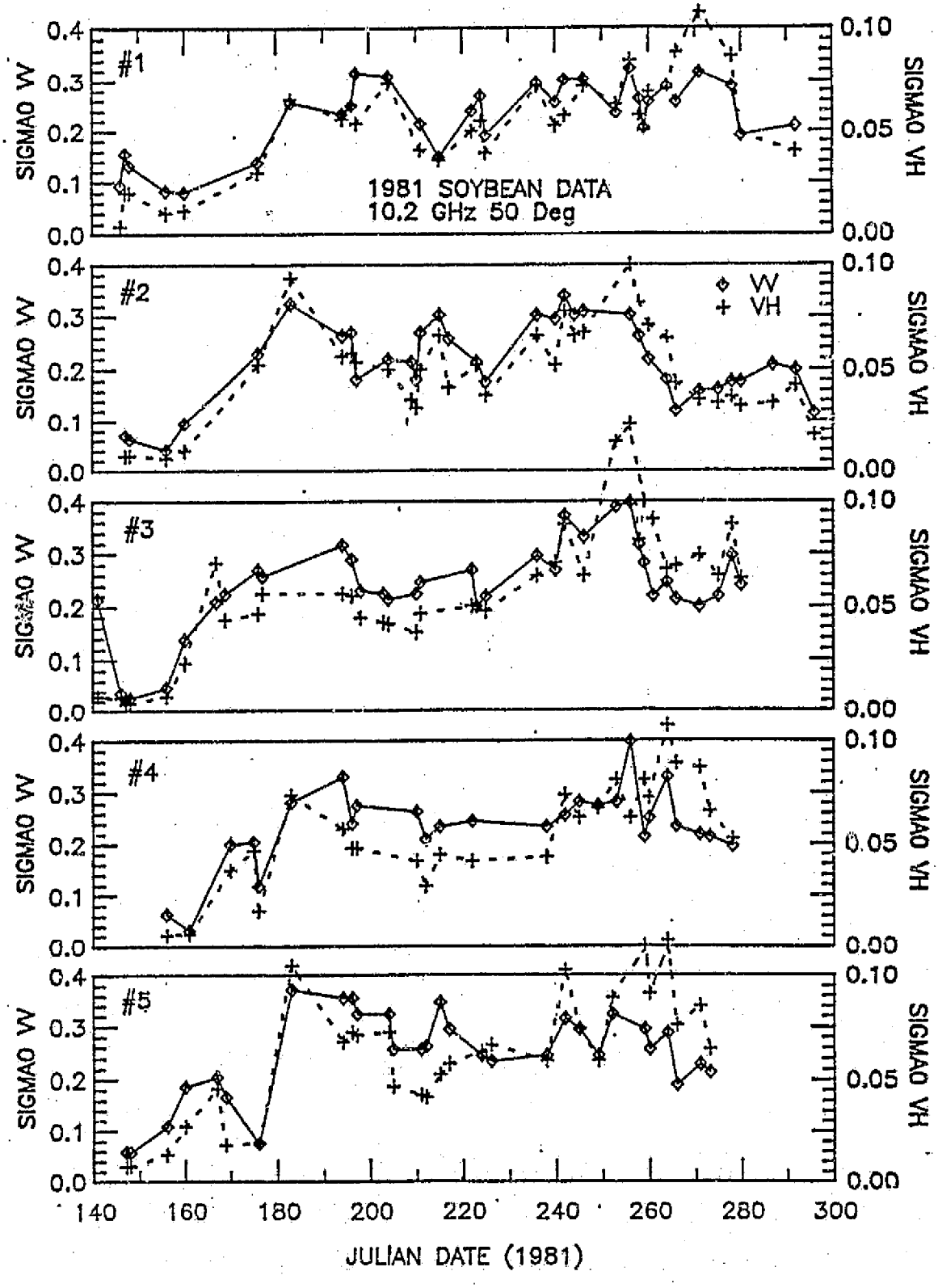

Figure 4.35 Temporal behavior of σ^{o}_{VV} and σ^{o}_{VH} from all ten soybean fields.

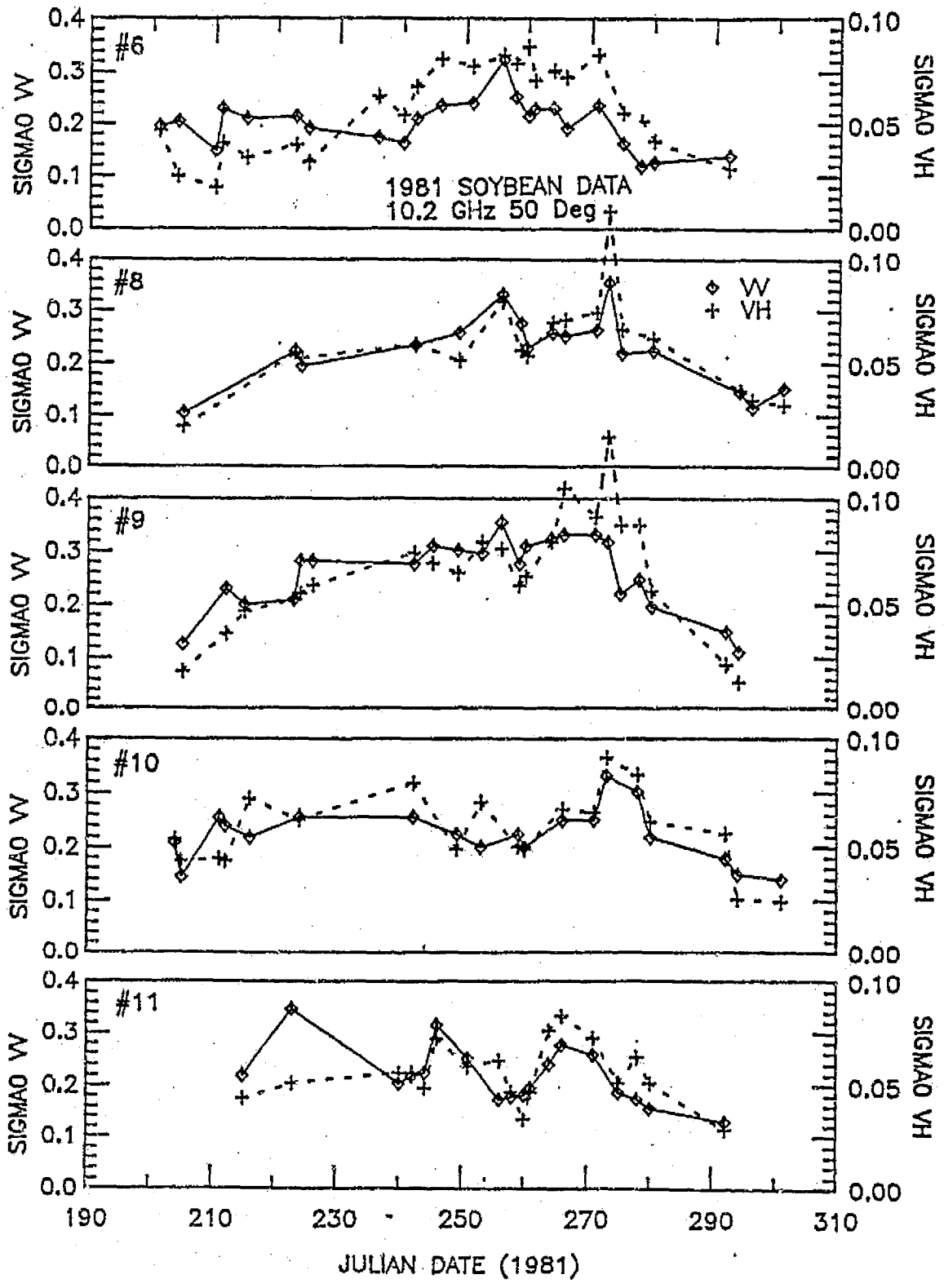

Figure 4.35 (Continued)

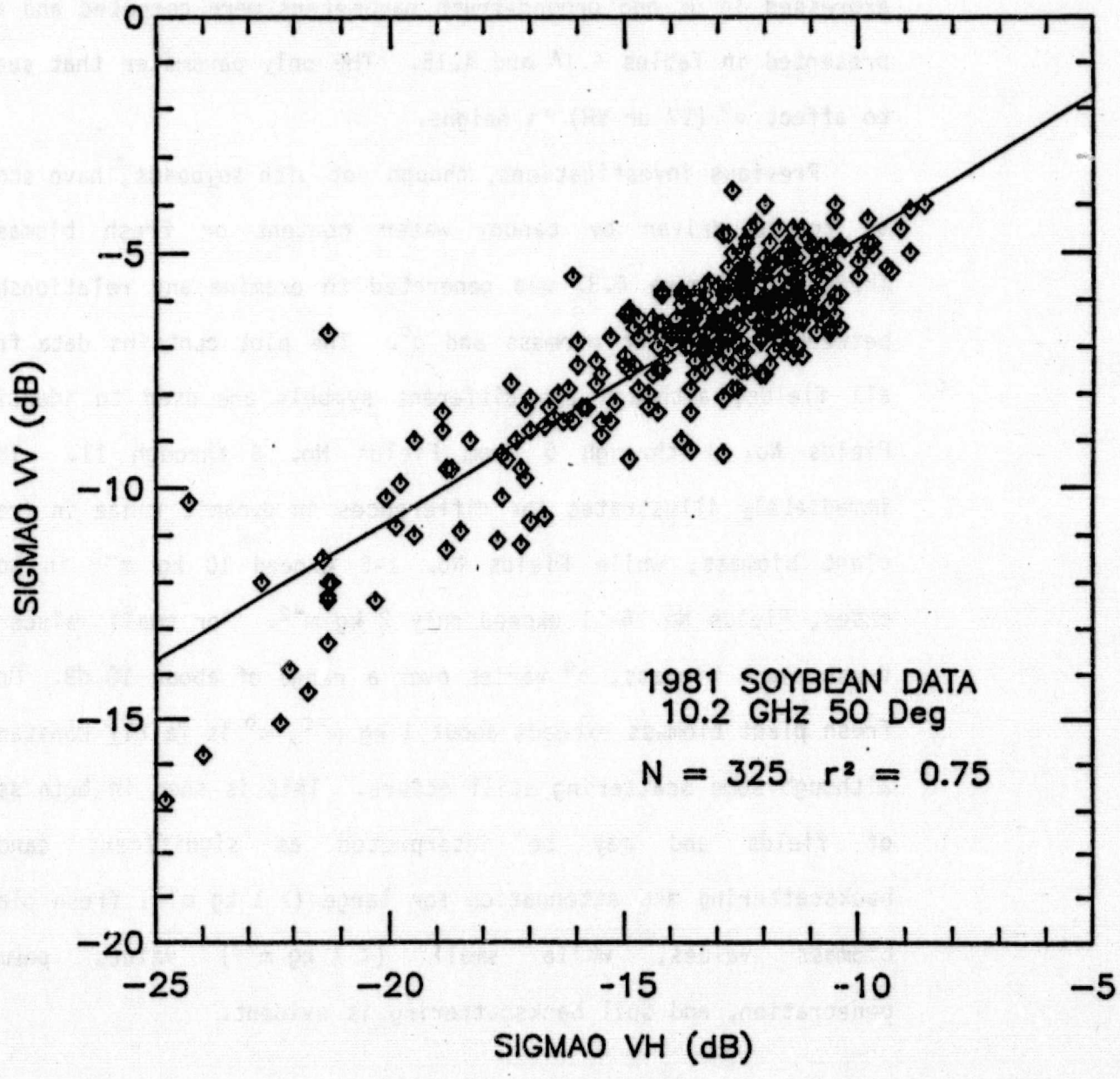

Figure 4.36 The way in which σ^o_{VV} varies with σ^o_{VH} from the soybean data.

4.8.1 Initial Analysis

As a first step in the analysis of the soybean data, statistics and linear correlation coefficients between σ^o values expressed in dB and ground-truth parameters were computed and are presented in Tables 4.14 and 4.15. The only parameter that seems to affect σ^o (VV or VH) is height.

Previous investigations, though not with soybeans, have shown σ^o to be driven by canopy water content or fresh biomass. Therefore, Figure 4.37 was generated to examine any relationship between fresh plant biomass and σ^o. The plot contains data from all fields, although two different symbols are used to identify Fields No. 1 through 5 from Fields No. 6 through 11. This immediately illustrates the differences in dynamic range in fresh plant biomass; while Fields No. 1-5 exceed 10 kg m^{-2} in some cases, Fields No. 6-11 exceed only 2 kg m^{-2}. For small values of fresh plant biomass, σ^o varies over a range of about 10 dB. Once fresh plant biomass exceeds about 1 kg m^{-2}, σ^o is fairly constant, although some scattering still occurs. This is seen in both sets of fields and may be interpreted as significant canopy backscattering and attenuation for large (> 1 kg m^{-2}) fresh plant biomass values, while small (< 1 kg m^{-2}) values permit penetration, and soil backscattering is evident.

4.8.2 Modeling of the 1981 Soybean Data

In this section, various models are evaluated for their ability to predict σ^o. The criteria will be the same as those used previously in evaluating both the wheat and the corn models,

TABLE 4.14

1981 Soybean Statistics

	Mean	Std. Dev.	Maximum	Minimum	Units
Volumetric Soil Moisture	22.4	9.9	51.1	3.4	$cm^3/cm^3 \times 100$
Plant Fresh Biomass	2.30	2.55	10.21	0.02	kg/m^2
Plant Dry Biomass	0.71	0.78	3.61	0.01	kg/m^2
Plant Water Content	1.60	1.96	8.43	0.00	kg/m^2
Height	0.80	0.32	1.23	0.02	m
σ^o_{VV}	- 6.8	2.0	-4.0	-16.8	dB
σ^o_{VH}	-13.2	2.9	-8.6	-24.8	dB

TABLE 4.15

Linear Correlation Analysis
1981 Soybean Data

Correlation Coefficient r	1	2	3	4	5	6	7
1. Volumetric Soil Moisture	1						
2. Fresh Plant Biomass	0.08	1					
3. Dry Plant Biomass	0.00	0.82	1				
4. Plant Water Content	0.10	0.97	0.66	1			
5. Canopy Height	-0.18	0.53	0.54	0.47	1		
6. σ^{o}_{VV}(dB)	-0.10	0.38	0.34	0.36	0.57	1	
7. σ^{o}_{VH}(dB)	-0.18	0.34	0.41	0.28	0.67	0.87	1

For all cases, N = 255

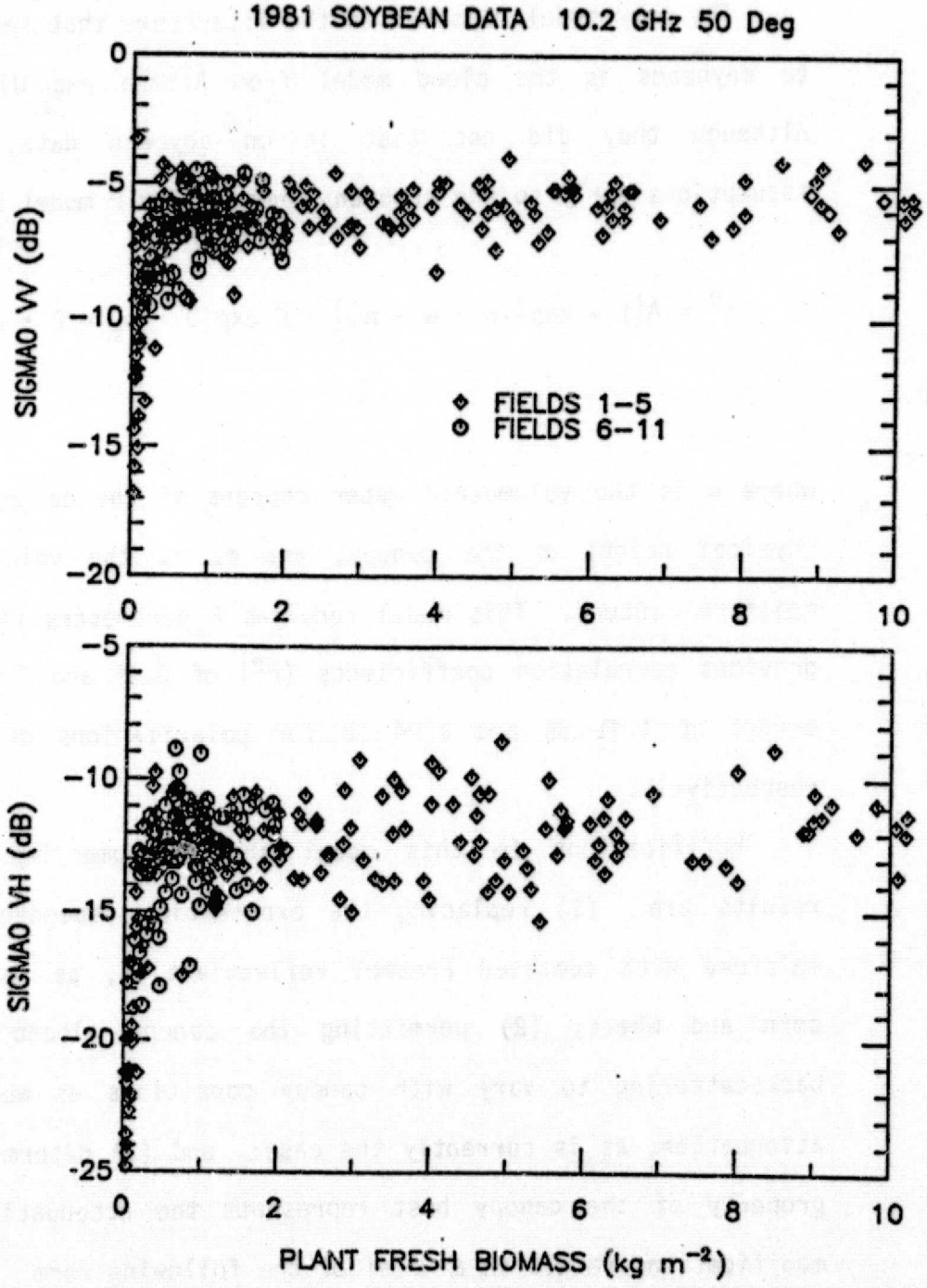

Figure 4.37 Effect of fresh plant biomass on the level of σ^{o} are shown for the ten fields divided into two groups of five.

i.e., correlation coefficient, RMS difference error (in dB), and number of model parameters or constants.

The only model reported in the literature that seems to apply to soybeans is the cloud model from Attema and Ulaby (1976). Although they did not test it on soybean data, the model assumptions apply to the soybean canopy. Their model has the form

$$\sigma^o = A[1 - \exp(-B \cdot w \cdot h)] + C \exp(D \cdot m_s - B \cdot w \cdot h) , \tag{4.21}$$

where w is the volumetric water content of the canopy, h is the physical height of the canopy, and m_s is the volumetric soil moisture content. This model requires 4 parameters (A,B,C,D) and provides correlation coefficients (r^2) of 0.49 and 0.50 with RMS errors of 1.41 dB and 2.04 dB for polarizations of VV and VH respectively.

Modifications to this model showing some improvement in results are (1) replacing the exponential dependence on soil moisture with computed Fresnel reflectivities, as was done for corn and wheat; (2) permitting the canopy albedo and hence backscattering to vary with canopy conditions as well as with attenuation, as is currently the case; and (3) determining which property of the canopy best represents the attenuation. These modifications result in a model of the following form

$$\sigma^o = \sigma^o_{canopy} + \sigma^o_{soil} \tag{4.22}$$

C-3

where

$$\sigma^{o}_{canopy} = A\{1 - \exp[-B \cdot f_2(plant)]\}\{1 - \exp[-D \cdot f_1(plant)]\} \tag{4.23a}$$

$$\sigma^{o}_{soil} = C(\Gamma_{VV} + G\Gamma_{HH}) \exp[-D \cdot f_1(plant)] , \tag{4.23b}$$

where $f_1(plant)$ is a function of plant ground truth that is proportional to canopy attenuation, and $f_2(plant)$ is a function of plant ground truth that varies in a manner similar to that of the backscattering of the canopy. In keeping with the objectives of this study, only simple relationships will be investigated. After trying various combinations of available ground-truth data through a process of trial and error, the optimum combination of ground-truth parameters was found to be

$$f_1(plant) = WET \quad , f_2(plant) = WET , \tag{4.24}$$

where WET is the fresh plant biomass. This results in correlation coefficients (r^2) of 0.58 and 0.67 with RMS errors of 1.28 dB and 1.65 dB for VV and VH polarizations. Table 4.16 lists the five model coefficients determined, and the r^2 and RMS errors for each field for both VV and VH polarization. Figures 4.38 and 4.39 present plots of predicted versus measured σ^o for all fields combined. In both cases, a linear regression indicates a slope of less than one and an intercept of less than 0 dB. Also, both

TABLE 4.16

1981 Soybean - 10.2 GHz, 50° Incidence Angle

Model Coefficients and Resulting Statistics

Pol.	A	B	C	D	G
VV	0.245	6.739	0.297	6.80	0
VH	0.061	5.263	0.005	5.77	1

Field (N)	r /RMS Error (dB) VV	r /RMS Error (dB) VH
All (255)	0.58/1.28	0.67/1.65
1 (31)	0.62/1.31	0.71/1.70
2 (34)	0.61/1.37	0.68/1.89
3 (35)	0.77/1.66	0.82/1.71
4 (26)	0.69/1.28	0.68/1.78
5 (30)	0.71/1.24	0.77/1.60
6 (23)	0.05/1.32	0.15/1.80
7 (17)	0.47/1.11	0.59/1.18
8 (22)	0.66/0.95	0.66/1.65
9 (19)	0.41/0.92	0.44/1.47
10 (18)	0.44/0.98	0.14/1.11

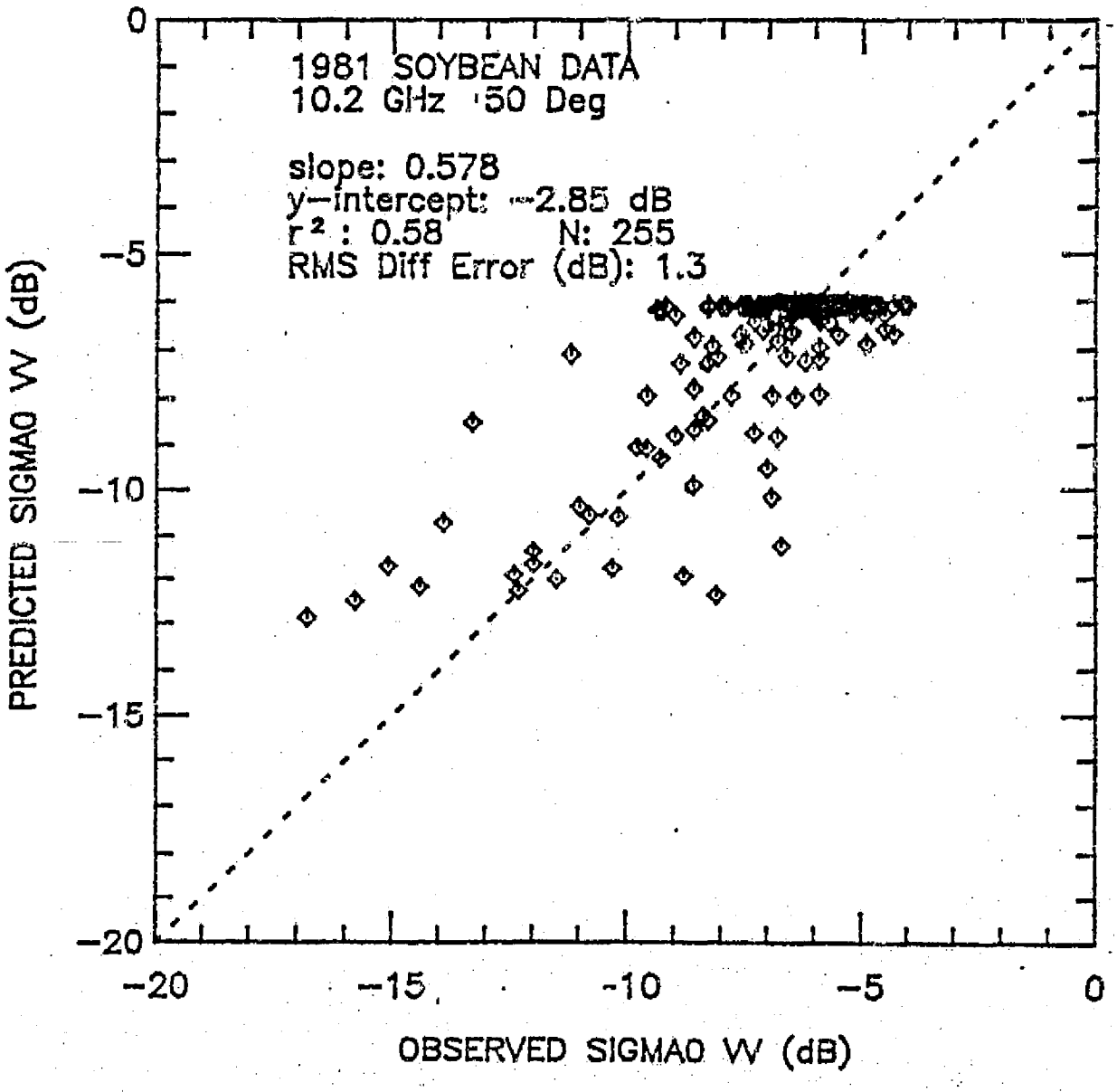

Figure 4.38 A comparison of observed (measured) σ^o_{VV} with predicted σ^o_{VV}, using Eq. (4.22).

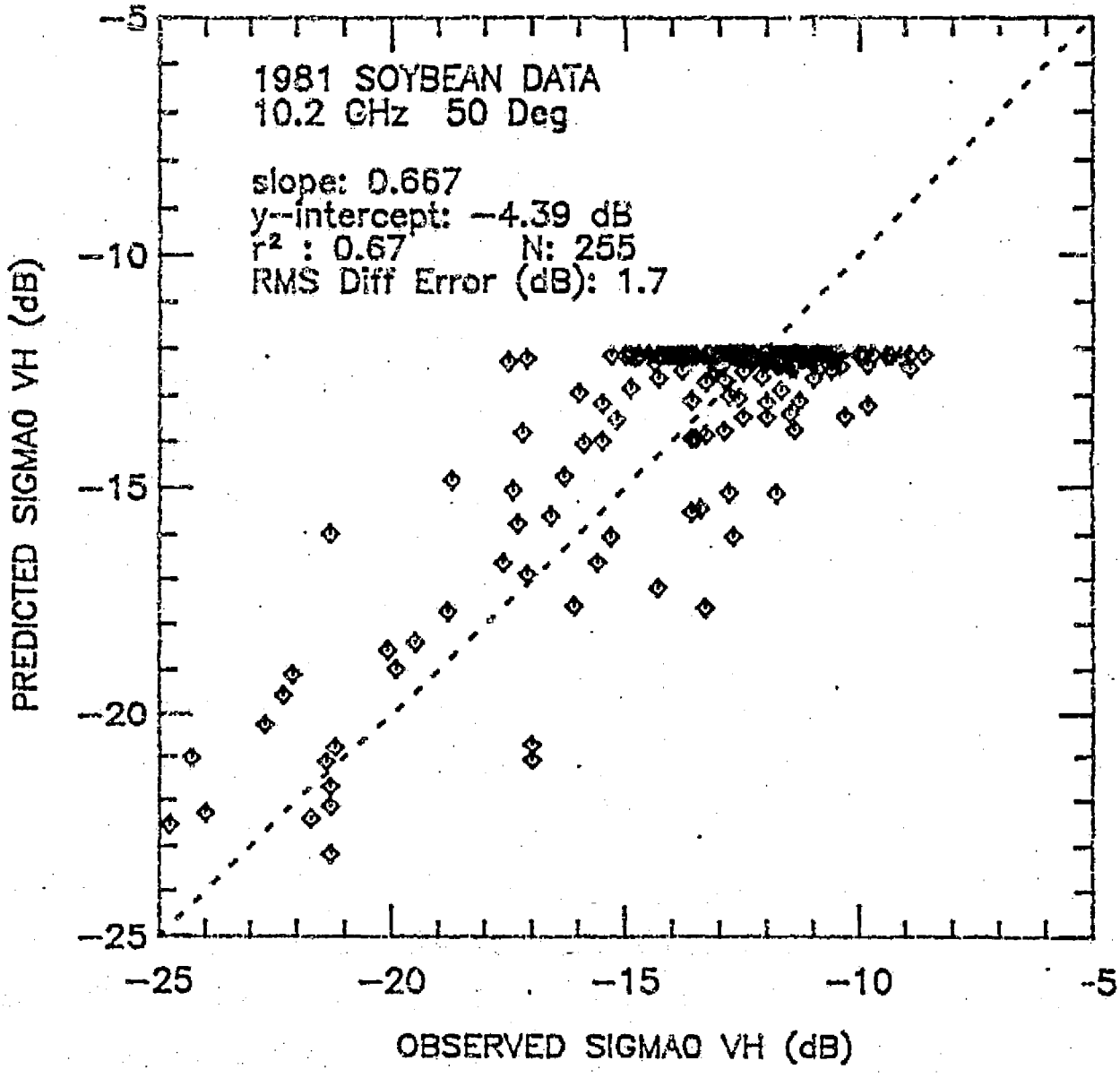

Figure 4.39 A comparison of observed (measured) σ^o_{VH} with predicted σ^o_{VH}, using Eq. (4.22).

plots show saturation along σ^o_{pred}. This is the model's attempt to follow the behavior shown in Figure 4.37, which shows σ^o becoming saturated soon after the fresh plant biomass exceeds 1 kg m^{-2}. The model is unable to explain the scattering in σ^o beyond biomass values greater than 1 kg m^{-2}.

Figure 4.40 shows a plot of the errors (defined here as $\sigma^o_{meas}(dB) - \sigma^o_{pred}(dB)$) for VV versus VH polarization. There is slightly less scattering along the VV axis than along the VH axis, which explains the fact that the RMS error for VV is less than VH.

Figures 4.41 and 4.42 present temporal comparisons of measured and predicted σ^o for a given field (No. 2). The predicted σ^o is broken into its components, which shows the reason it behaves the way it does. Again in both cases after about Julian date 200 the predicted σ^o, composed almost entirely of plant backscattering, becomes saturated. This level of saturation is the optimum for all the fields, since all the fields were used in determining the model coefficients.

Similar comparisons of measured and predicted σ^o on a temporal basis for each of the ten fields are presented in Figures 4.43 and 4.44. In most cases, the model predicts the early behavior of σ^o with a fair degree of accuracy. For the bulk of the season, the plant biomass is so great that the model becomes saturated in its prediction of σ^o and is unable to explain minor fluctuations given the available ground truth.

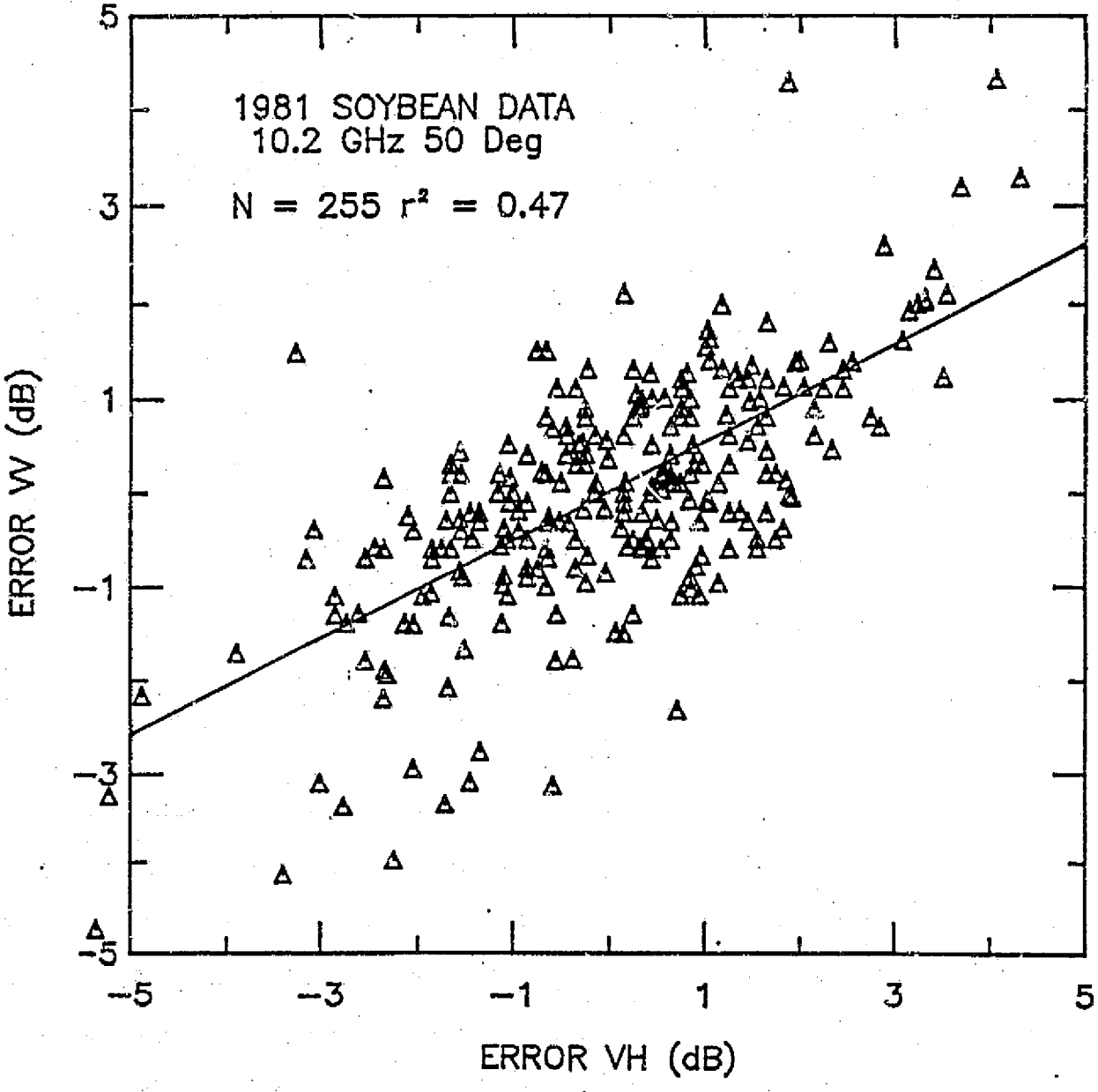

Figure 4.40 A comparison of the errors in predicting σ^o_{VV} with the errors in predicting σ^o_{VH}.

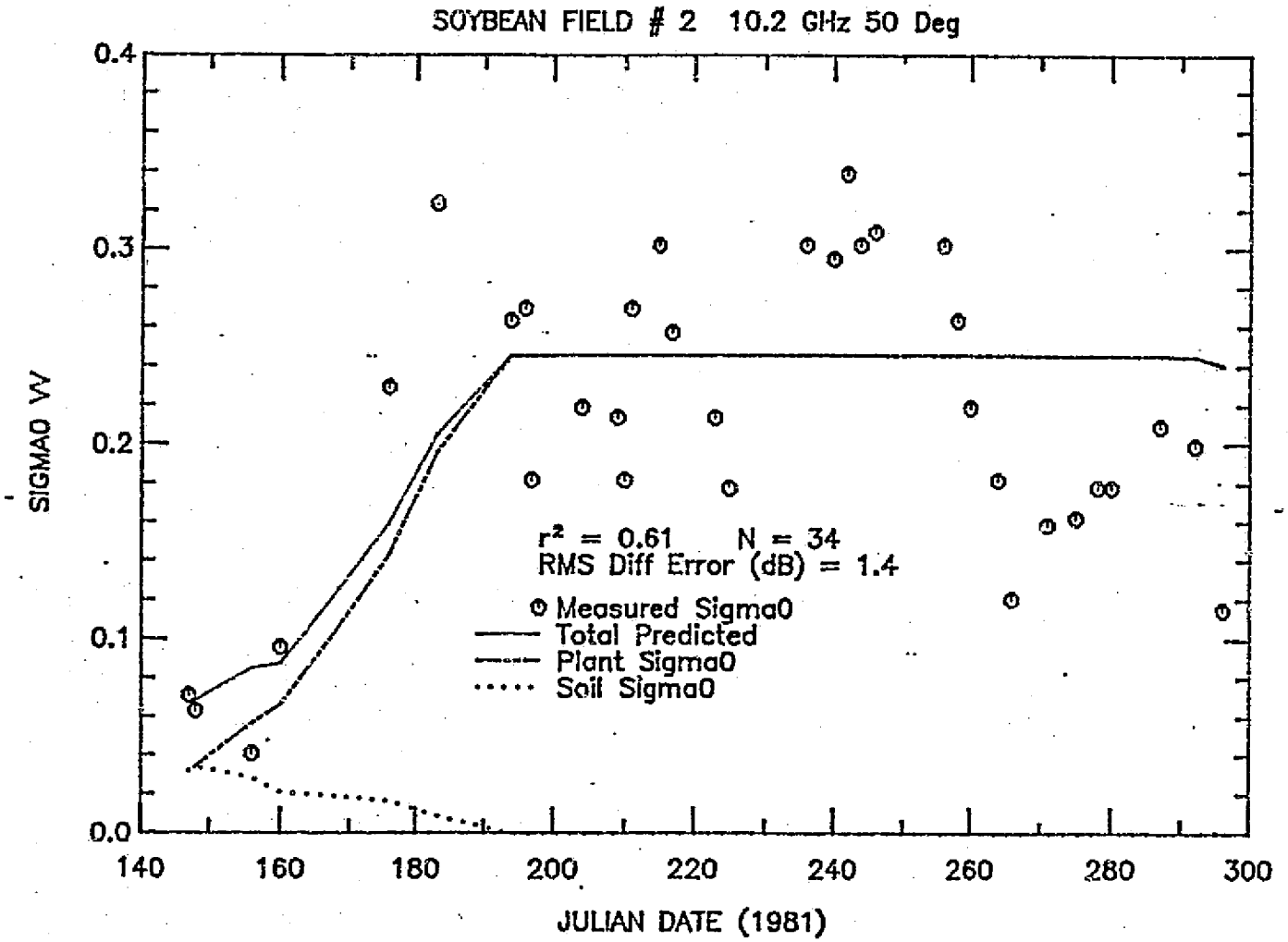

Figure 4.41 A comparison of measured and predicted σ^{o}_{VV} over time for soybean field No. 2. The predicted value is the sum of three components, also shown here.

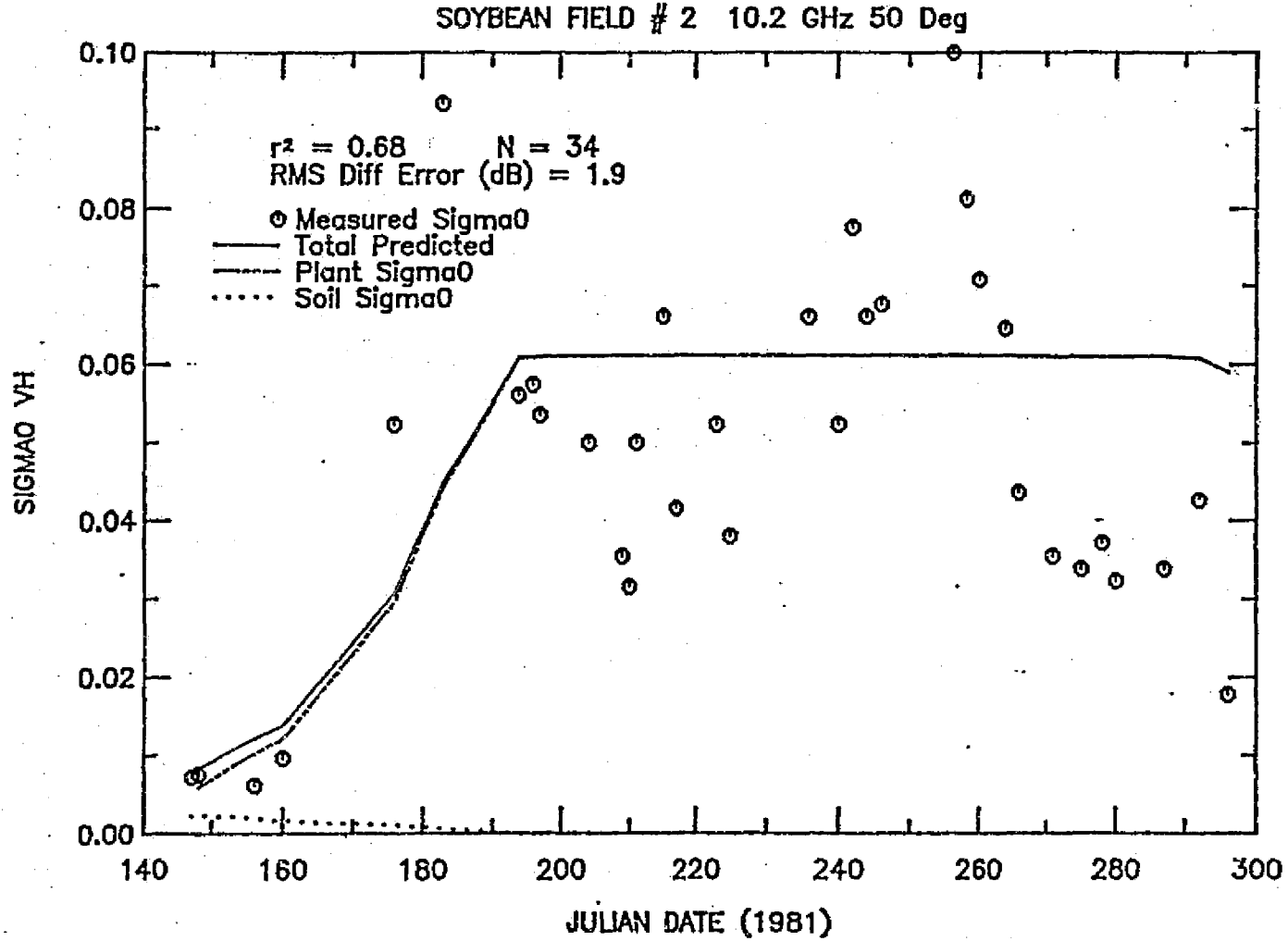

Figure 4.42 A comparison of measured and predicted σ^o_{VH} over time for soybean field No. 2. The predicted value is the sum of three components, also shown here.

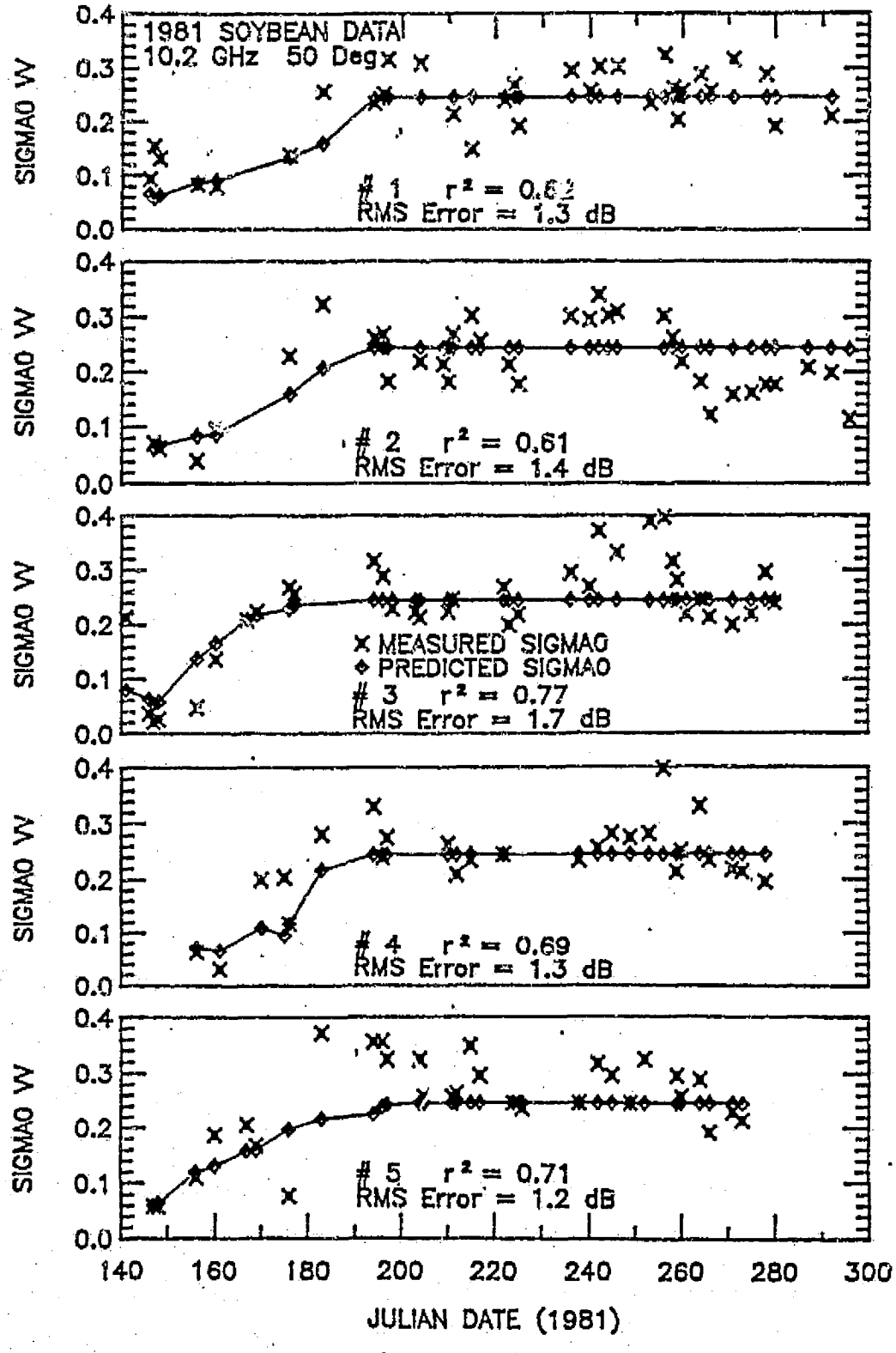

Figure 4.43 A comparison of measured and predicted σ^o_{VV} over time on a per-field basis.

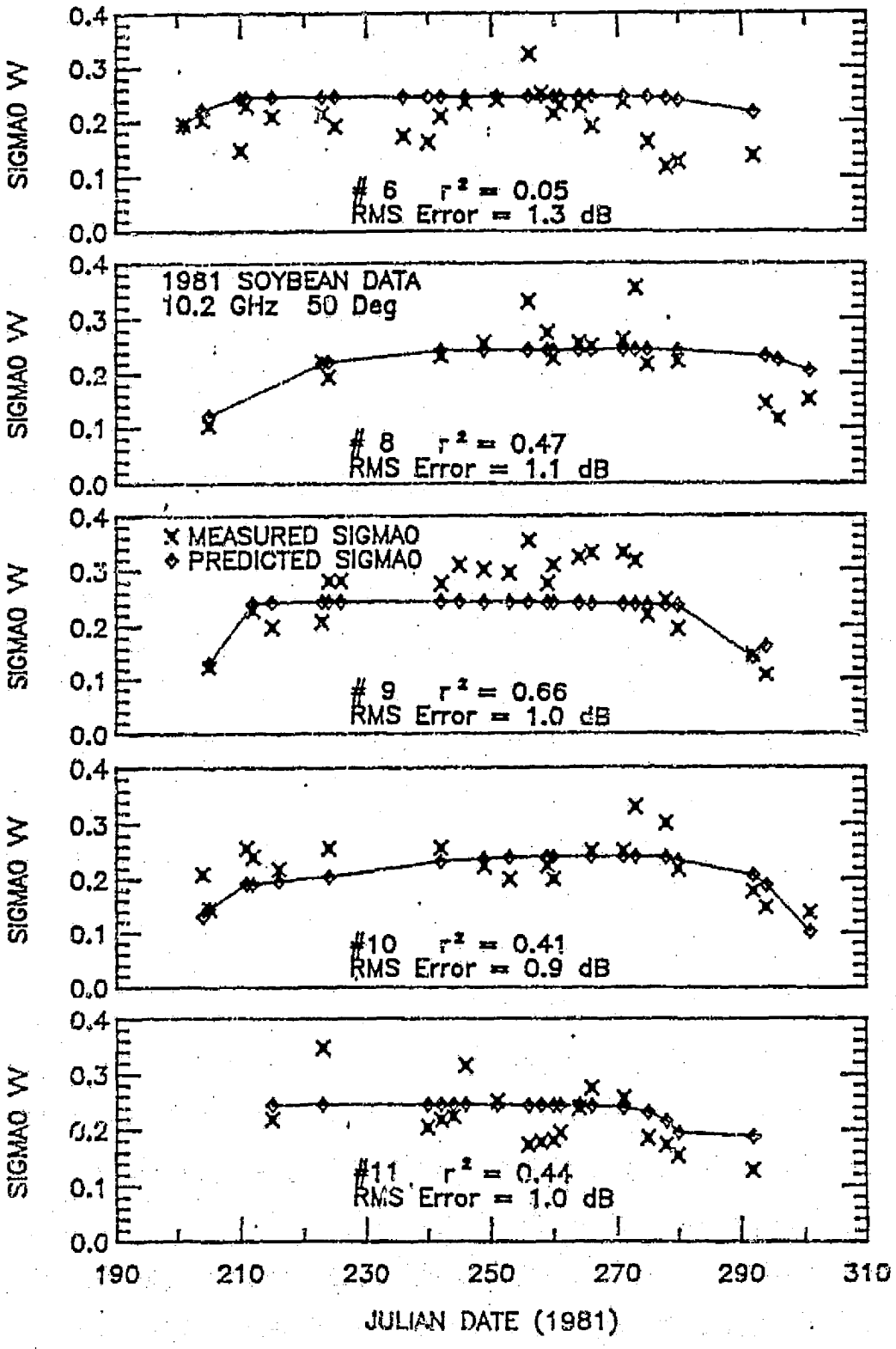

Figure 4.43 (Continued)

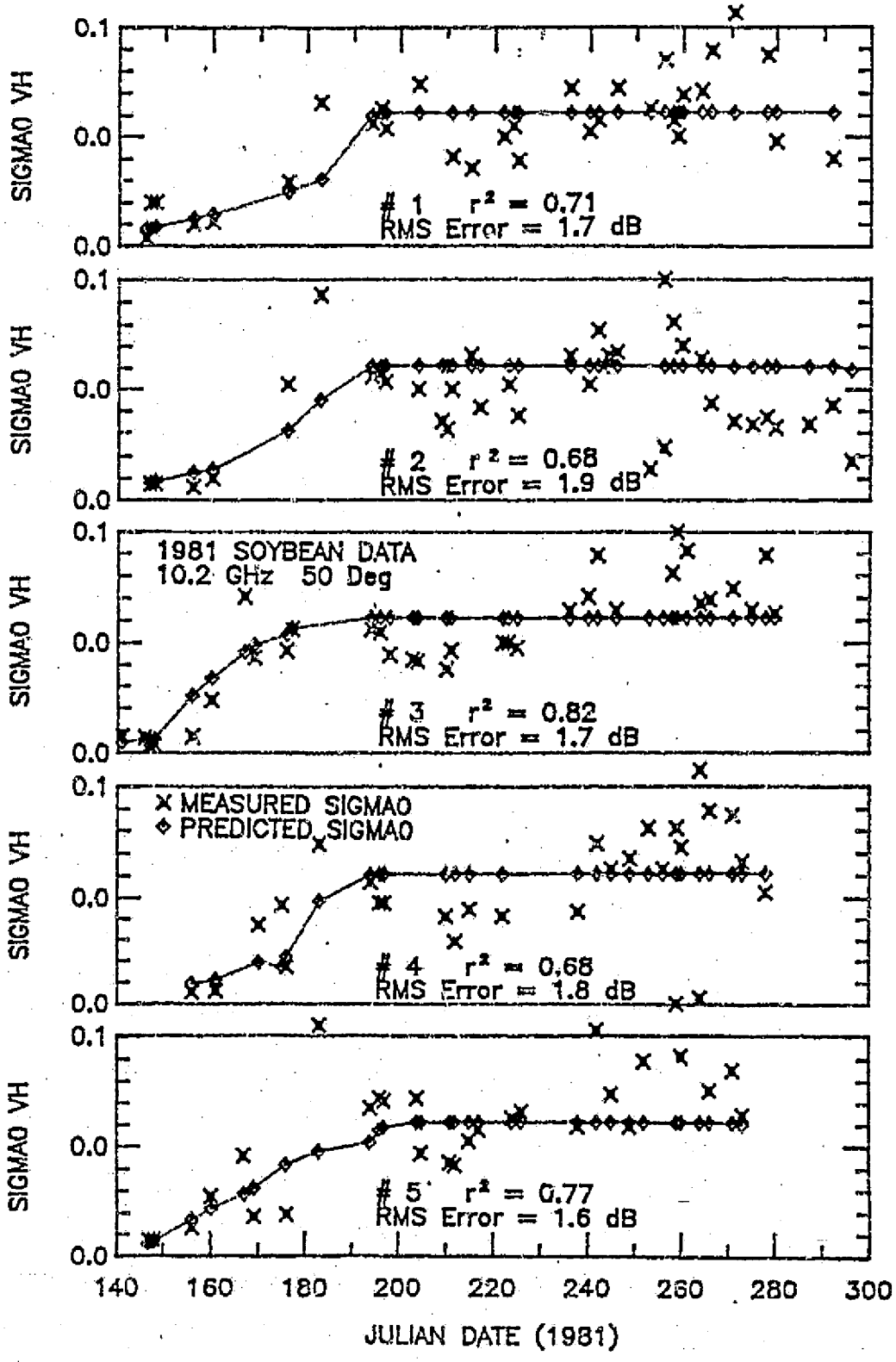

Figure 4.44 A comparison of measured and predicted σ^{o}_{VH} over time on a per-field basis.

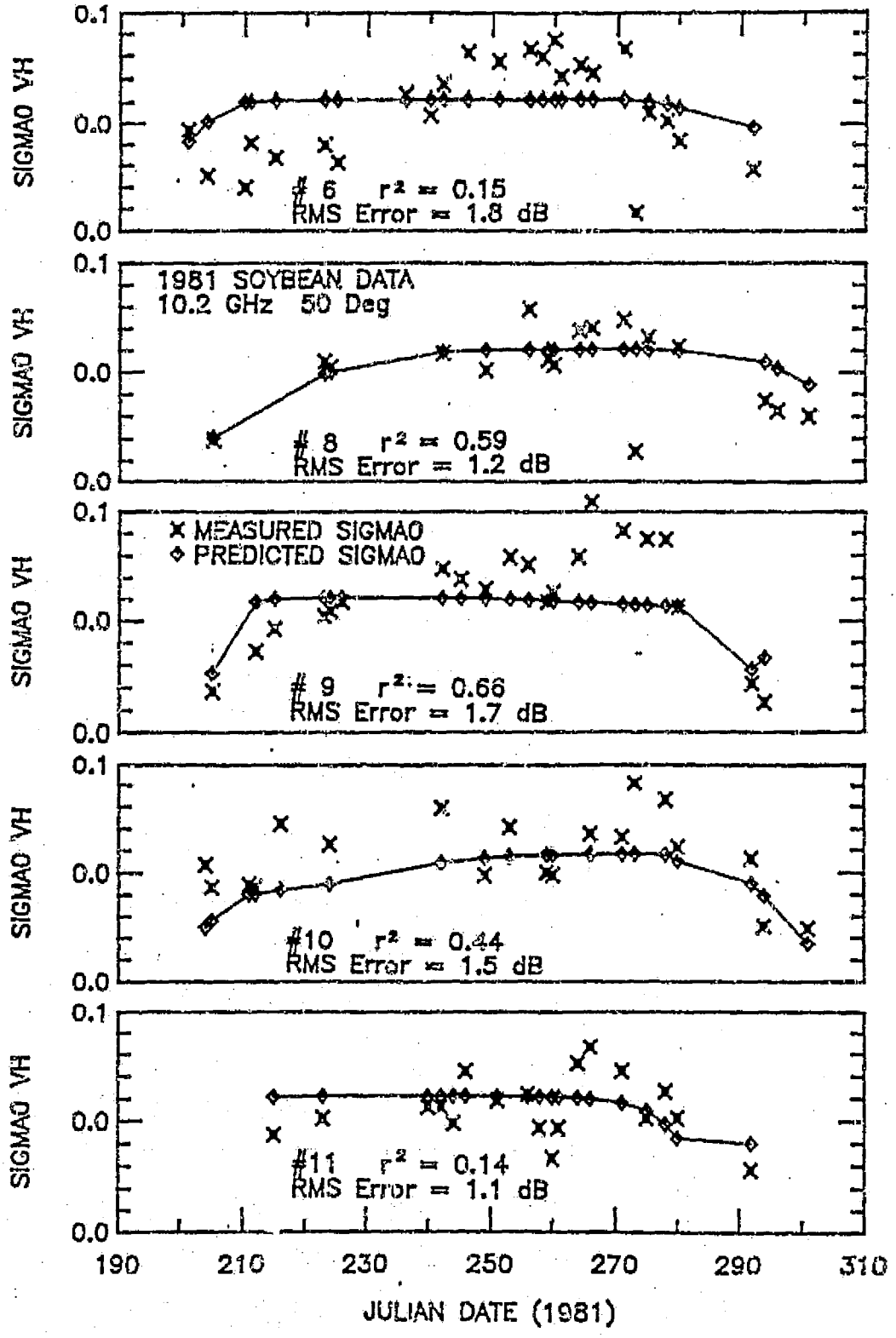

Figure 4.44 (Continued)

4.8.3 Error Analysis

As in the cases of the wheat and corn models developed earlier, an evaluation of the significance of data errors in the model's ability to predict measured σ^o was performed. The sources of errors and the method of simulation are identical to the previous two and hence further explanation would be redundant.

The values of variance in ground truth and radar quantities are listed in Table 4.17. These values were obtained through examination of variances in the raw data.

The results of the simulation indicate that the types and magnitudes of errors introduced in the data would permit an exact model to have correlation coefficients (r^2) of 0.62 and 0.79 and RMS difference errors of 1.10 dB and 1.14 dB for the VV and VH models, respectively. This would seem to enhance the credibility of the models.

4.8.4 Analysis of Weather Effects

Of the original 348 data sets acquired, 64 were omitted from analysis and modeling because the data might have been affected by a recent rain (within two days). An investigation as to what effect if any these rain events had on the data is now possible. Using the models previously optimized for the original 255 unaffected data sets, a comparison of the distribution of errors is possible. To make the analysis more sensitive to small changes, the models will be optimized on a per-field basis first. The results of this optimization, i.e., the new sets of

TABLE 4.17

1981 Soybeans- Error Simulation Results

Parameter	Fresh Biomass	Dry Biomass	Height	Soil
Std. Dev.	0.21μ	0.20μ	0.09μ	0.20μ

μ represents the mean of the measured value

σ^o_{VV} has a std. dev. of 0.8 dB

σ^o_{VH} has a std. dev. of 1.0 dB

VV results: $r^2 = 0.62$ RMS Diff. Error = 1.10 dB
VH results: $r^2 = 0.79$ RMS Diff. Error = 1.14 dB

model coefficients for each field along with the accompaning r^2 and RMS errors, are presented in Table 4.18.

Given these specialized models, errors between predicted and measured σ^o for the two cases ("normal" and rain-affected) may becompared. A statistical comparison of these errors was performed and the results are presented in Table 4.19. In the case of VV polarization, the test concludes that the errors are from different distributions, i.e., the errors introduced in the rain-affected data are unlike those seen in the "normal" data. In the case of VH polarization, the test concludes that there is only a 5% chance that the errors are from the same or similar distributions; hence there is a 95% chance that they are not. More insight as to the differing nature of the distribution of the errors may be gained by a visual inspection; therefore, Figures 4.45 and 4.46 are presented, which are histograms of the errors. In both cases (VV and VH polarization) the errors associated with the "normal" data display a distribution similar to a Gaussian distribution with a mean of 0 dB. The errors associated with the rain-affected data have much broader distributions, and they have values extending beyond those seen in the case of the "normal" data.

Finally, Figure 4.47 compares the relationship between errors as a function of polarization for the two cases, rain-affected and "normal." The correlation coefficients indicate higher correlations in the rain data, which may indicate that the effect of the recent rain may be similar for both polarizations.

Table 4.18
(a)
Model Coefficients and Resulting Statistics
Optimized on a Per-Field Basis - Soybeans
Crop: Soybeans Polarization: VV

Field No.	A	B	C	D	G	r^2	RMS Difference Error(dB)	N
1	0.253	5.669	0.759	6.80	0	0.62	1.04	31
2	0.224	9.620	0.173	6.80	0	0.62	1.31	34
3	0.268	2.934	0.248	5.83	0	0.79	1.43	35
4	0.260	9.766	0.021	6.80	0	0.71	1.21	26
5	0.274	6.770	0.254	6.70	0	0.71	1.16	30
6	0.209	38.15	0.189	3.22	0	0.13	0.95	23
8	0.334	1.669	0.619	3.375	0	0.68	0.81	17
9	0.284	4.849	0.227	5.595	0	0.66	0.79	22
10	0.244	24.771	0.033	6.80	0	0.42	0.76	19
11	0.235	3.679	0.226	6.80	0	0.44	0.79	18
All	0.245	6.738	0.297	6.80	0	0.58	1.28	255

TABLE 4.

Crop: Soybeans Polarization: VH

Field No.	A	B	C	D	G	r^2	RMS Difference Error(dB)	N
1	0.060	7.698	0.001	6.80	1	0.72	1.64	31
2	0.050	6.412	10^{-4}	6.80	1	0.69	1.70	34
3	0.066	3.139	0.006	3.61	1	0.85	1.53	35
4	0.062	5.485	10^{-4}	6.80	1	0.70	1.73	26
5	0.071	4.625	0.007	4.595	1	0.77	1.51	30
6	0.091	0.737	0.298	6.80	1	0.37	1.47	23
8	0.089	1.470	0.031	6.80	1	0.69	1.00	17
9	0.075	3.392	10^{-4}	4.162	1	0.63	1.46	22
10	0.065	8.915	0.001	6.80	1	0.43	1.12	19
11	0.057	6.185	0.004	6.80	1	0.16	1.07	18
All	0.061	5.256	0.005	5.781	1	0.67	1.65	255

TABLE 4.19

1981 Soybeans - Weather Effects Analysis

Data Class	N	Mean Error (dB)	RMS Diff. Error (dB)	T-Test 2-Tail Probability
		VV Polarization		
Normal	255	-0.0018	1.10	
Recent Rain	64	0.6606	1.76	0.000
		VH Polarization		
Normal	255	-0.0055	1.49	
Recent Rain	64	0.4472	2.20	0.051

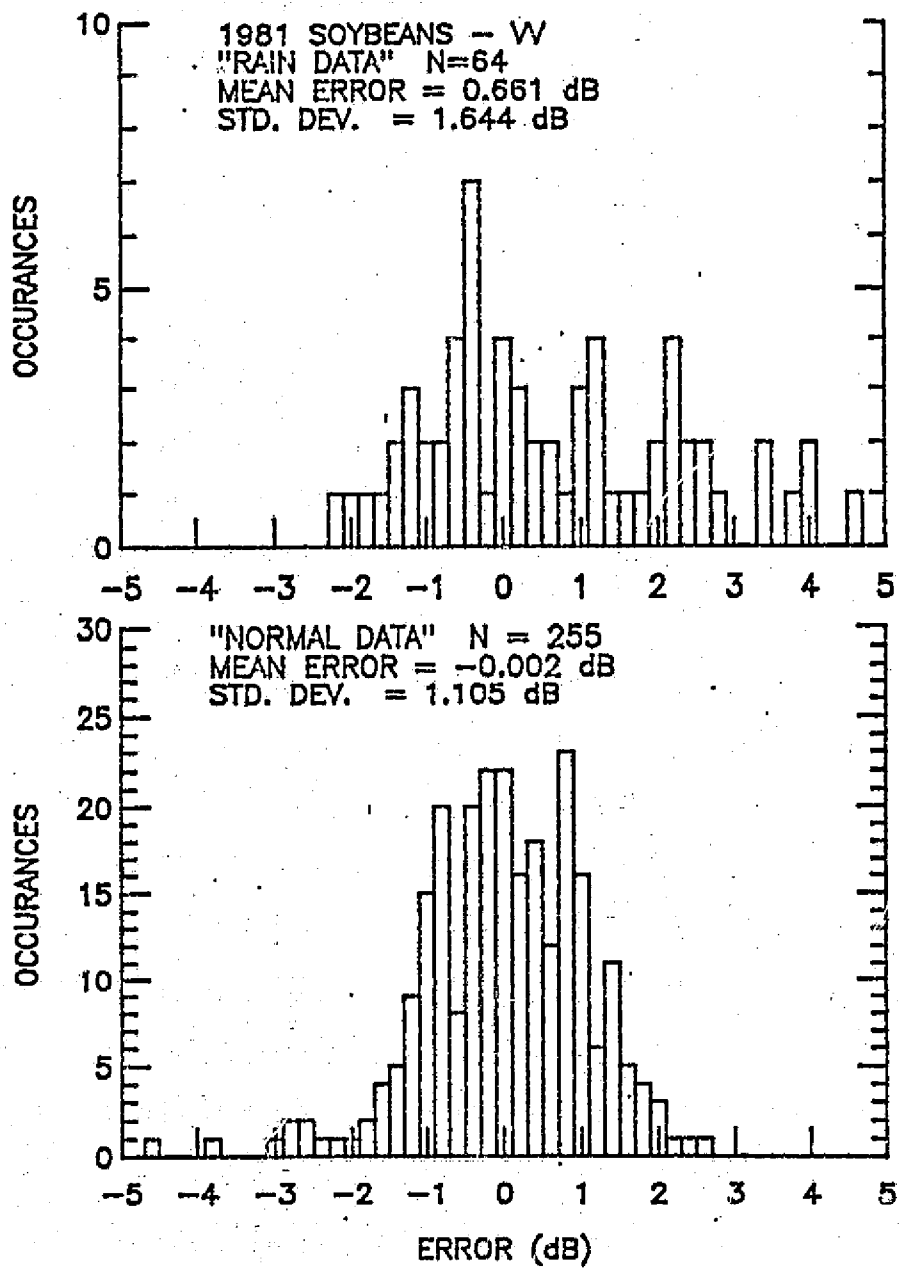

Figure 4.45 Histogram of the errors between measured and predicted σ^{o}_{VV} for the two sets of soybean data: normal and rain-affected.

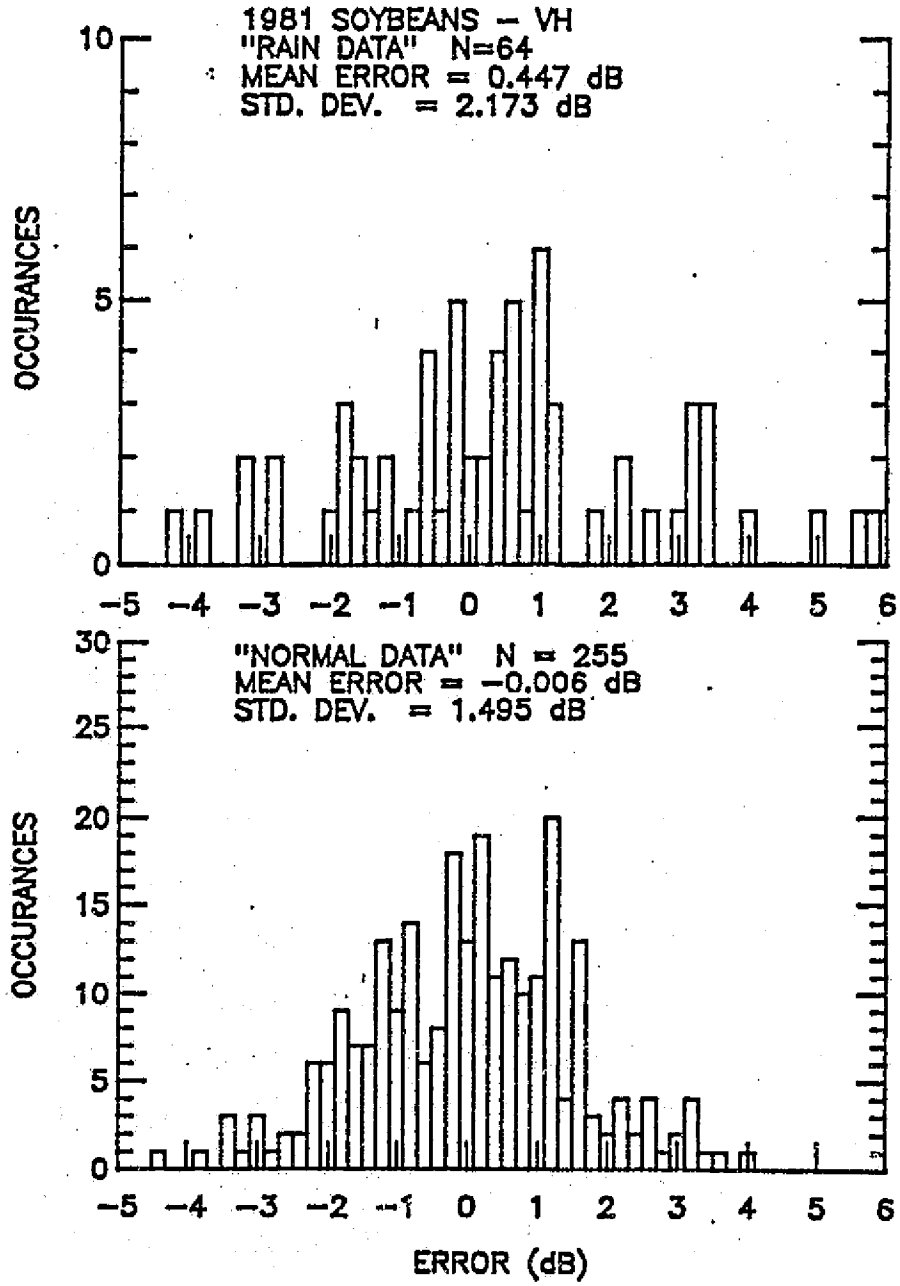

Figure 4.46 Histogram of the errors between measured and predicted σ^{o}_{VH} for the two sets of soybean data: normal and rain-affected.

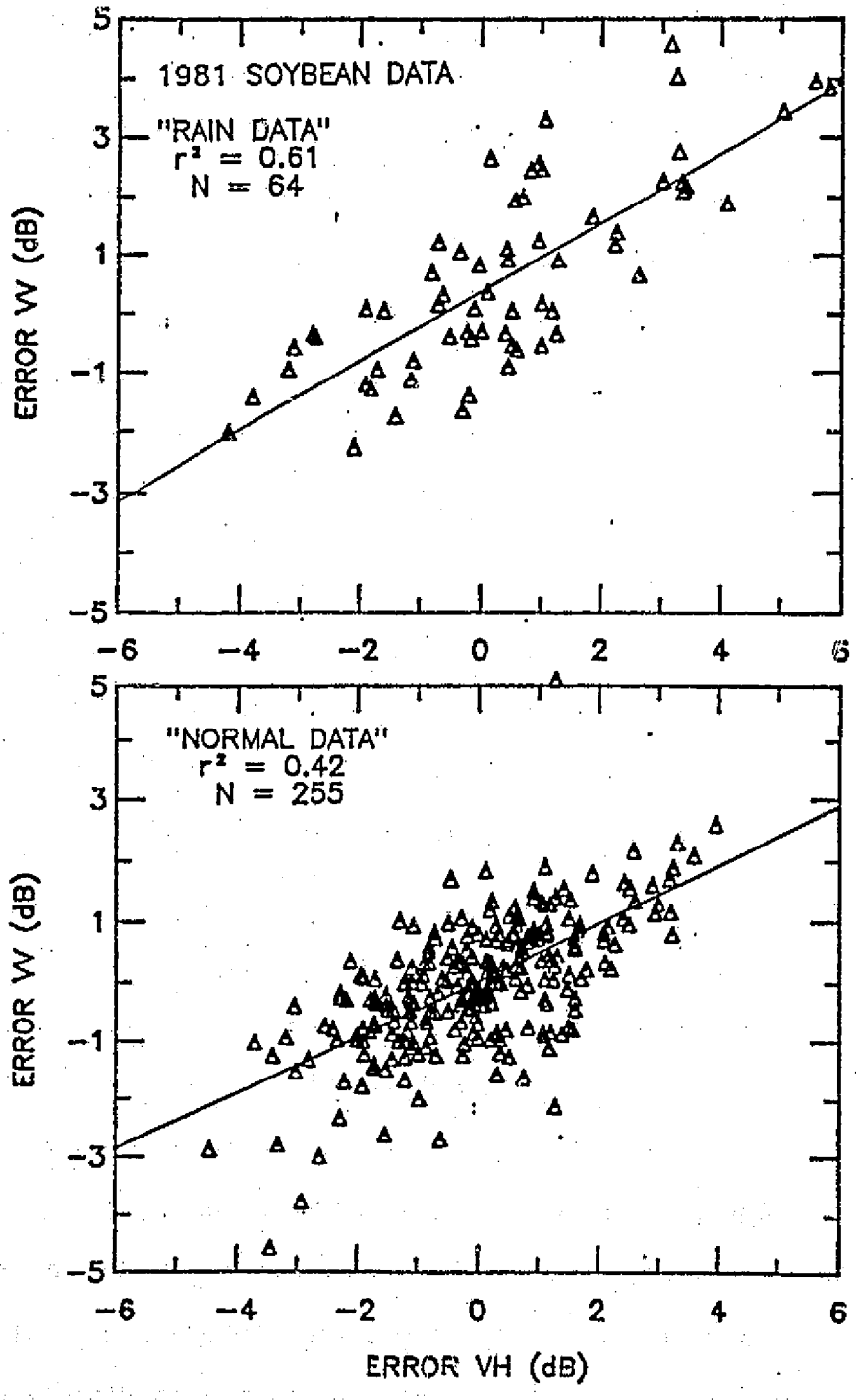

Figure 4.47 A comparison of the ways in which the errors between predicted and measured σ^o vary with polarization and weather influence.

4.9 Summary and Conclusions

An experiment conducted in the summer of 1981 by the University of Kansas Remote Sensing Laboratory measured the backscattering at X-band (10.2 GHz), at a 50° incidence angle, with polarizations of VV and VH using a truck-mounted FM-CW scatterometer. Coincident ground truth, consisting of plant biomass and height, soil moisture and texture, and the harvested yield, was also collected. The data set collected is unique in at least two ways. First, the data collected from typical agricultural fields incorporating commercial techniques, which are unlike special, prepared plots, consisted of ten fields of each crop type (corn, wheat, and soybeans). Each field was visited at least twenty times during its growing season, providing an enormous data set that will permit many new investigations. Secondly, due to the scatterometer's design, reliable VH data are available for the first time for agricultural data of this magnitude.

Initial examination showed that the temporal behavior of the ten fields of each crop type is similar but by no means identical. Wheat showed the greatest similarity of behavior, while corn and soybeans showed more variability. In all cases, high correlations were observed between σ^{o}_{VV} and σ^{o}_{VH}.

Models were developed for each crop type and polarization, and these proved to be superior to any previously reported in the literature. Although the same principles were applied in developing these models, an added feature was the introduction of a function representing an albedo dependent on crop parameters

(previous models had assumed a constant albedo). A second factor simplifying the modeling of soil backscattering was the use of Fresnel reflectivity. This was possible for the following reasons: (1) dielectric measurements at X-band of soils having the same or similar textures were made in conjunction with the 1981 summer experiment, and (2) theoretical models explaining rough surface backscattering indicate a factor of Fresnel reflectivity representing the dielectric dependence of the backscattering.

Table 4.20 lists the models developed, along with model coefficients, correlation coefficients, and RMS difference errors for each crop and polarization. In determining the model coefficients via a nonlinear regression computer program seeking to minimize the RMS error, the magnitude of the attenuation was kept within the limits of values reported from measurements. A comparison of the reported values and those predicted by the models are presented in Table 4.21. Clearly, the values do not match exactly, however for the most part they are not in great disagreement, with the exception of soybeans. In that case, the model would have selected an even higher value for attenuation had not limits been imposed to keep the values "reasonable." The exact influence of this high attenuation on the model's ability to predict σ^o is not clearly understood, so this trend for higher attenuation may be a numerical artifact, i.e., only slight (insignificant) improvements in r^2 and the RMS errors are achieved by increasing the attenuation. The modeled values may, therefore, not be indicative of the true attenuation, in the case of soybeans. Also, none of the attenuation measurements was made in

TABLE 4.20

Model Summary

Wheat:

$$\sigma^o = A(1 - e^{-F \cdot SH2O/Ht})(1 - e^{-E \cdot SH2O})\, e^{-D \cdot FH2O} + B \cdot FWT + C(\tau_{VV} + G\,\tau_{HH})\, e^{-D \cdot FH2O - E \cdot SH2O}$$

	A	B	C	D	E	F	G
VV	0.153	0.036	1.148	4.272	2.445	0.112	0
VH	0.025	0.013	0.073	2.382	1.440	0.125	1

N = 143 VV → r^2 = 0.61 RMS Error = 2.04 dB
VH → r^2 = 0.64 RMS Error = 1.90 dB

Corn:

$$\sigma^o = A(1 - e^{-F \cdot LWT/Ht})(1 - e^{-E \cdot LWT}) + B \cdot SH2O \cdot e^{-E \cdot LWT} + C(\tau_{VV} + G \cdot \tau_{HH})\, e^{-E \cdot LWT}$$

	A	B	C	E	F	G
VV	0.298	0.080	0.546	2.030	1.836	0
VH	0.079	0.018	0.023	1.340	1.263	1

N = 166 VV → r^2 = 0.35 RMS Error = 1.28 dB
VH → r^2 = 0.44 RMS Error = 1.37 dB

TABLE 4.20 (Continued)

Soybeans:

$$\sigma^o = A(1 - e^{-B \cdot WET})(1 - e^{-D \cdot WET}) + C(\Gamma_{VV} + G\,\Gamma_{HH})\, e^{-D \cdot WET}$$

	A	B	C	D	G
VV	0.245	6.739	0.297	6.80	0
VH	0.061	5.263	0.005	5.77	1

N = 255 VV + r^2 = 0.58 RMS Error = 1.28 dB
VH + r^2 = 0.67 RMS Error = 1.65 dB

GROUND-TRUTH VARIABLE IDENTIFICATION

SH2O = stalk water content (kg m^{-2})
(for wheat this includes leaf water content)

Ht = canopy height (m)

FH2O = fruit (grain head) water content (kg m^{-2})

FWT = fruit fresh biomass (kg m^{-2})

LWT = leaf fresh biomass (kg m^{-2})

WET = plant fresh biomass (kg m^{-2})

Γ_{pp} = Fresnel reflectivity $|R_{pp}|^2$ for polarization pp

TABLE 4.21

Attenuation Analysis (2-Way) 50° 10.2 GHz

Atten. Coeff.	Wheat Leaf	Wheat Head	Corn	Soybeans
VV	2.445	4.272	2.03	6.8
VH	1.44	2.382	1.34	5.77
GT Factor	**LH2O**	**FH2O**	**LWT**	**Wet**
Mean	1.276	0.256	0.782	2.249
Std. Dev.	0.954	0.231	0.467	2.530
Maximum	3.852	0.746	1.898	10.211
		VV Polarization		
Atten. (dB)				
Mean	13.5	4.7	6.9	66.4
± Std. Dev.	10.1	4.3	4.1	74.7
Maximum	40.9	13.8	16.7	301.3
		VH Polarization		
Atten. (dB)				
Mean	8.0	2.6	4.5	56.3
± Std. Dev.	6.0	2.4	2.7	63.4
Maximum	24.1	7.7	11.0	255.7
Reported Attenuation (VV) 50°, X-Band (dB)	30.4 ±12.3	9.9 ±2	20-30	32-44

1981; therefore, various climatic effects might have played a role in crop development and hence could have modified the canopy's attenuation.

Another check of the quality of these models was made in the form of an error analysis in which the various errors were accounted for in a simulation of the measurement process. The results indicated that a significant discrepancy between the measured and predicted σ^o could be explained in this way.

These models, in combination with the large, continuous data set, permitted an investigation into the effects (other than soil-moisture variations) of weather events on σ^o. The results indicate that the presence of wind during data acquisition does not alter σ^o significantly as long as it does not alter the canopy geometry significantly. However, these effects were only investigated for wheat canopies, as were the effects of blown-down areas of canopy, which showed a great deal of difference from normal canopy conditions. Rain effects were present in all three crop types and significantly altered the measured σ^o from the model-predicted values. In all cases, the average error was greater than 0 dB, indicating that rain events tend to increase σ^o. This agrees with the observations presented in Chapter 3, which experimentally determined the effects of free water in the canopy.

4.10 Yield Estimation from Remotely Sensed Data

As stated previously, the ultimate application of remote sensing with regard to agriculture is to estimate total crop

production in a timely and efficient manner. To arrive at total crop-production estimates, it is necessary to identify crop types, estimate the areal extent of each field, and finally, to estimate yield.

Other investigations have dealt with the first two objectives by utilizing various remote-sensing data; however, this investigation will restrict itself to an examination of yield estimation only.

The yield produced by a given crop at a given location is a function of many variables. The plants must have available to them certain nutrients, including water and nitrogen. They must also receive large amounts of solar radiation and their temperature should remain within certain limits to ensure vigorous growth. Biologists and agronomists have studied the effects of these factors on plant vigor, and models can now be developed that take these factors into consideration in order to estimate yield.

One such model was developed by Coelho and Dale (1980). It is called the Energy Crop Growth (ECG) model and is used for estimating corn (maize) yield. This model takes the form

$$ECG = \sum_{i=t_1}^{t_1} (SR/600)_i \, (SRI)_i \, (WF)_i \, (FT)_i \, , \qquad (4.25)$$

where SR is the daily solar radiation available to the canopy, WF is the ratio of daily evapotranspiration to potential evapotranspiration (a measure of water stress), and FT is a daily temperature function that relates growth rate to soil temperature. The summation occurs over the growing season. For

best results, it was found that t_1 and t_2 should be 12 weeks apart, with silting occurring midway. The Solar Radiation Intercepted (SRI) is a function that estimates a canopy's ability to intercept and utilize solar energy. Of the four factors, SR, WF, and FT are directly weather-dependent factors, and the last two are also functions of soil condition. SRI is the only factor that depends entirely on the plant. In essence, the model says that given adequate water and proper temperature ranges, yield will be proportional to the canopy's ability to intercept and utilize solar energy. Linville et al. (1978) showed a relationship between the canopy's LAI (leaf area index) and SRI (solar radiation intercepted) of the form

$$SRI = 1 - e^{-0.79 \cdot LAI} \qquad (4.26)$$

Hence when LAI is zero, no energy is intercepted, and when LAI is about 2.9, 90% of the available energy is intercepted.

Therefore, it would appear that if remote-sensing data could provide an estimate of LAI, and assuming that no significant water- or temperature-stress occurs during the growing season, a yield estimate is obtainable, for corn at least. Shibles and Weber (1966) reported similar SRI-LAI behavior for soybeans, indicating that the ECG may be appropriate for soybeans as well. Osman (1971) showed a relationship between SRI and dry-matter production in wheat, which again indicates another possible crop appropriate for the ECG model.

Remote-sensing research in the optical region shows that a

combination of channels (Green, Red, Infrared) termed "Greenness" may be related to LAI for corn and soybeans (Daughtry et al., 1982) for use in estimating yield. Tucker et al. (1981) showed that plant vigor was related to red and infrared spectral data, and goes on to show a relationship to total dry-matter accumulation.

Little if any work of this kind has been done using radar as the remote-sensing tool. Based on the models for vegetation backscattering, radar shows some of the properties necessary for crop monitoring, namely, that radar backscattering is strongly dependent on LAI (for corn, wheat, and milo) (Ulaby et al., 1983) and that radar is sensitive to the amount of soil moisture present (Batlivala and Ulaby, 1977), and hence can monitor moisture stress. Brisco et al. (1983) showed a strong linear dependence between LAI and fresh leaf biomass in corn and soybeans, indicating that the models developed earlier can be converted into LAI dependence, for corn at least.

With this in mind, an analysis of the 1981 radar data was performed to determine if there is any correlation between σ^o and yield. The farm operators provided yield data for each field after harvest. These data are shown in Table 4.22. Of the 30 fields, three were not harvested for grain; hence no yield data were available. With the remaining nine fields of each crop type, a correlation between the yields and mean σ^o for the growing stage was computed. These results are shown in Table 4.23. For wheat, the radar data were broken into two periods: one with high attenuation (low σ^o), typically Julian dates 120 to 160, and the

TABLE 4.22

Crop Yield Summary

Field No.	Yield (Bushels/Acre) Wheat	Corn	Soybeans
1	54	141	43
2	56.5	---	49
3	42	152	52
4	44	149	47
5	55	161	38
6	58	144	44
7	50	137	30 (8)
8	48	75	37 (9)
9	48.3	141	-- (10)
10	---	144	44 (11)
Mean	50.6	138.2	42.7
Std. Dev.	5.6 (11%)	24.8 (18%)	6.7 (16%)
N	9	9	9

TABLE 4.23

Mean σ^o vs. Yield: Correlation Analysis
Correlation Coefficient (r)

	VV(real)	VV(dB)	VH(real)	VH(dB)
(N = 9) Wheat				
Days 120-160	-0.083	-0.062	+0.015	+0.019
Days 161-190	-0.130	-0.104	-0.231	-0.315
Difference	-0.112	-0.030	-0.272	-0.326
Ratio	-0.313	-0.173	-0.042	0.004
(N = 9) Corn				
Days 135-220	0.115	0.085	0.062	0.042
(N = 9) Soybeans				
Days 180-260 (1-5) and 230-280 (6-11)	-0.166	-0.159	-0.524	-0.522

other with low attenuation (higher σ^o) typically 161 to 190. For corn, this period was from 135 to 220, inclusive, and for soybeans it was from 180 to 260 for Fields 1 to 5, and 230 to 280 for Fields 6 to 11. In each case the mean σ^o was found in real numbers ($m^2\ m^{-2}$) and correlations were done with σ^o in both real units ($m^2\ m^{-2}$) and in dB. The "difference" label under wheat indicates a difference in the means for the two periods per field; "ratio" indicates the ratio of the two means. Clearly, in all cases, no significant correlation is shown. It is only for soybeans with VH polarization that a correlation exceeds even 0.5.

Following the hypothesis that σ^o is proportional to LAI, or simply that σ^o is proportional to plant vigor and productivity, an integration of σ^o (real, $m^2\ m^{-2}$) over the growing period was performed. Since the early portion of the growing season in wheat was "missed," which apparently included the peak seen by Ulaby et al. (1983), wheat was excluded from this type of analysis. The period chosen for corn was the same as that recommended by Dale (1976) i.e., date of silking (182) ± six weeks (42 days) or Julian dates 140 to 224. The period chosen for soybeans was that period during which σ^o might be attributed mainly to vegetation and not to soil, i.e., for Fields 1 to 5, Days 180 to 260 and for Fields 6 to 11, Days 230 to 280. In order to perform the integration, interpolation was necessary. The results are shown in Table 4.24. Again, no significant correlation was found for either crop or polarization.

One possible explanation for the absence of a strong correlation between σ^o and yield, other than that they are truly

TABLE 4.24

Integrated σ^0 vs. Yield: Correlation Analysis
Coorrelation Coefficient (r)

		VV	VH
(N = 9)	Corn (Days 150-220)	0.150	0.093
(N = 9)	Soybeans (1-5, days 180-160) (6-11, days 230-280)	0.426	0.359

uncorrelated, is that the number of fields involved was small (N=9 per crop), and the variance in yields among these nine fields was not great. Hence, in order to study this relationship properly, a much larger sample of fields and a wider distribution of yields is necessary.

5.0 A DETERMINISTIC APPROACH

In the previous chapter, experimental data were modeled using a semi-empirical/semi-theoretical approach. Although this approach is usually successful, questions concerning the model's physical interpretation may be left unanswered. Furthermore, constants obtained through the optimization of the model for one set of data may differ significantly when the same model is applied to another experimenter's results. Aside from the question of absolute calibration level, one may reason that although the measurements were made thousands of miles and perhaps years apart, the physics of the phenomenon is the same; hence, should not the models be quite similar? Perhaps as our understanding of the physical processes involved becomes clearer, our models will begin to depend more on theory and less on empiricism.

This is certainly true in the case of modeling the microwave backscattering properties of agricultural fields. The form of the canopy backscattering model,

$$\sigma^o_{can} = \sigma^o_{veg} + \sigma^o_{soil}\, L^{-2} \qquad (5.1)$$

is theoretical in origin, as is the form for σ^{o}_{veg}

$$\sigma^{o}_{veg} = 0.75\ \omega[1-L^{-2}]\ \cos\ \theta \qquad (5.2)$$

where $L^{-2} = \exp(-2\tau\ \sec\ \theta)$,

which assumes single scattering in a lossy volume having diffuse boundaries. Here ω is the volume albedo and τ is the optical thickness of the volume. Armed with these relationships, the analyst need only determine (empirically) values for ω and τ as well as σ^{o}_{soil}, as was done in Chapter 4. Reliance on theoretical models may be taken one step further, since accurate formulas already exist for scattering from rough dielectric surfaces, e.g., the Kirchhoff stationary phase approximation, the small-perturbation model, etc. Although these models are quite complex mathematically, they agree nicely with measurements when certain characteristics about the surface are known (e.g., dielectric constant, surface RMS height, and roughness statistics such as the shape of the autocorrelation function). Again, in order to yield good results, these are usually left as free parameters to be determined by the analyst.

Summaries of these surface-scattering models are presented in Appendix C along with examples of the ways in which various input parameters affect backscattering properties. In addition, an effort was made to increase the usefulness of these theoretical models by removing an obstacle for many would-be users, i.e., mathematical complexity. When appropriate, relatively simple empirical models were derived that agree closely with these

"exact" models, thus eliminating the need for elaborate computer programs. The same is true for a radiative-transfer solution to the volume scattering situation (Ulaby et al., 1982). The theoretical model, which requires complex integration and matrix inversion, was approximated by a relatively simple empirical model, which is in close agreement with the original over given regions of applicability. It should be noted here that the theoretical model for volume scattering treats the case of multiple scattering as well as the case of surface-volume interaction backscattering.

Given this level of understanding of the interaction process, the next step would be to develop theoretical models for canopy attenuation (L^2) and canopy albedo (ω). Electromagnetic theory tells us that one of the inputs into any such model will be the canopy's dielectric properties. Therefore, investigators at the University of Kansas Remote Sensing Laboratory (and others) have begun detailed investigations into this topic. Determination of the exact relationship between canopy properties and canopy attenuation and albedo, as yet unattained, will result in deterministic, rather than empirical, models that will not need to be "fitted" to a given crop type, frequency, incidence angle, polarization, etc. Given the necessary ground truth, the model will predict σ^o within an accuracy limited only by the uncertainties in the ground truth. Because the geometry of a vegetation canopy represents a random process, some flexibility will undoubtedly remain in the model.

5.1 A Deterministic Model for Canopy Attenuation

The experimental data coupled with dielectric measurements and dielectric mixing formulas presented in Chapter 2 have shown a deterministic relationship with a theoretical basis for attenuation by wheat stalks and heads. Thus, given information on the size-, spatial-, and angular-distributions of the stalks and/or heads, a good estimate of the attenuation (due to absorption) by these canopy components becomes available. Unfortunately, the lack of a sufficiently large, independent data-set prohibits such a test at this time, although future experiments will no doubt be conducted to test and improve upon these deterministic models.

The case of attenuation (resulting from absorption) due to leaves in a canopy has been examined by Ulaby et al. (1984). In their approach, leaves are considered to be thin layers of a lossy dielectric material, all of which for simplicity are assumed to be horizontally aligned. Two approaches are taken. The first is one in which the dimensions of the individual leaves are assumed to be much larger than a wavelength (in the leaf material), which is the case for a dielectric slab (for $\lambda \to 0$). Hence the coherent transmissivity (T_c) is computed for a wave passing through a leaf. To account for the number of leaves in the volume, multiple layers are superimposed (incoherently) and the result is an expression for leaf attenuation (due to both scattering and absorption) of the form

$$L_\ell = T_c^{-LAI}. \tag{5.3}$$

For the details of computing T_c, the interested reader is referred to Ulaby et al. (1982), Chapter 4.

The second approach treats leaves as being much smaller than a wavelength (in the leaf material). By treating the leaves as small, lossy, disc-shaped inclusions of finite thickness, the mixing formulas of Polder and Van Santen (1946) may be applied to obtain an effective dielectric constant of the volume. In order to obtain the volume fraction of the leaf inclusions, LAI is used, resulting in the following expression for leaf attenuation (due to absorption):

$$L_\ell = \exp\left(\frac{4\pi}{3\lambda_0}\,\varepsilon''_\ell\, t_\ell \sec\theta \cdot \mathrm{LAI}\right). \tag{5.4}$$

Here ε''_ℓ is the imaginary part of the dielectric constant of the leaf material, and t_ℓ is the thickness of the disc, taken here to be the thickness of a leaf. Both models require as inputs ε_ℓ and t_ℓ and although the assumptions concerning the relative sizes of leaves and wavelength are vastly different, the results of each approach do not differ drastically for electrically thin leaves.

As a result, another step towards a wholly deterministic canopy backscattering model has been made. Before these models can be applied with any confidence, however, tests verifying their applicability will need to be made. As mentioned previously, a data set of adequate extent does not exist at this time to test the validity of the wheat stalk and head absorption model.

However, because leaves dominate both backscattering and attenuation in the case of a corn canopy, and since leaf biomass data, soil-moisture data, and σ^o data are available, a test of the deterministic model of corn leaf attenuation is in order.

5.2 Test of the Corn Leaf Attenuation Model

In order to test the proposed deterministic model with the 1981 corn σ^o data, a direct replacement of L_ℓ as given in Eq. (5.4) will be made for the $\exp[-E \cdot f_3(\text{leaf})]$ in Eq. (4.19). The choice of Eq. (5.4) over (5.3) is a matter of simplicity, i.e., since both formulas give approximately the same value for L_ℓ, Eq. (5.4) is chosen because it is much easier to compute. This test cannot prove beyond doubt the accuracy of either (5.4) or (5.3), since the data are not measures of L_ℓ directly, rather they are measures of σ^o. Hence any number of formulas may work equally well. However, since this model has its foundation in theory, if it proves satisfactory it will add credibility to its utility. Thus, the equation for σ^o will be of the form

$$\sigma^o = \sigma^o_{\text{leaf}} + \sigma^o_{\text{stalk}} + \sigma^o_{\text{soil}} \tag{5.5}$$

where

$$\sigma^o_{\text{leaf}} \triangleq \sigma^o_\ell = A\{1 - L_\ell^{-2}\}\ \{1 - \exp(-D \cdot LAI/HT)\} \tag{5.6a}$$

$$\sigma^o_{\text{stalk}} \triangleq \sigma^o_{st} = B\ SH2O\ L_\ell^{-2} \tag{5.6b}$$

$$\sigma^o_{soil} \triangleq \sigma^o_s = C\Gamma_{VV}L_\ell^{-2} \qquad (5.6c)$$

where SH2O and Γ_{VV} are as defined in Section 4.5.2, and L_ℓ is from Eq. (5.4). The necessary inputs for L_ℓ include λ_o, ε''_ℓ, t_ℓ, θ, and LAI. Both λ_o and θ are system parameters and will be taken to be 3 cm and 50^o, respectively. The average leaf thickness will be taken to be 0.2 mm, since this was recommended by Ulaby in his presentation of Eq. (5.4). The imaginary part of the leaf dielectric constant (ε''_ℓ) was measured by Ulaby and Jedlicka (1983) at 1.5, 5.0 and 8 GHz, and an application of their 8 GHz data will be made. A polynomial fit of ε''_ℓ resulted in the following equation:

$$\varepsilon''_\ell = 9.847\ m_v + 15.462\ m_v^2 - 4.39\ m_v^3, \qquad (5.7)$$

with a correlation coefficient of 0.999 and an RMS error of 0.0397. The range of values for volumetric leaf moisture, m_v, is $0 \leq m_v \leq 0.8$. The final necessary input, LAI, is available in the form of an estimate based on the fresh leaf biomass value. Brisco et al. (1983) showed a correlation coefficient (r) between fresh leaf biomass and LAI of 0.94. The estimate is of the form

$$LAI = 3.63\ m_w,$$

where m_w is the fresh leaf biomass per unit area (kg m^{-2}).

Thus, all of the inputs necessary to evaluate the model are available. Because uncertainties are present in t_ℓ, and to

account for the fact that the leaves are not in fact all horizontal, a fitting factor E will be included in L_ℓ of the form

$$L_\ell = \exp\left[\frac{4\pi}{3\lambda_o}\,\varepsilon''_\ell\, t_\ell \sec\theta \cdot LAI \cdot E\right]. \qquad (5.8)$$

To maintain the deterministic nature of L_ℓ, the range of E will be from about 0.3 to 2.5, since these are the approximate limits of the uncertainties in the quantities involved.

With the model thus defined, a test using the 1981 corn data set (containing 166 observations) was conducted with the following results. The model was found to be optimum with the following values for the model constants: A = 0.350, B = 0.0374, C = 0.579, D = 0.710, E = 0.586. Such an assignment resulted in a correlation coefficient (r^2) of 0.34 and an RMS error of 1.29 dB. This is nearly identical to the results obtained in Section 4.5.2 using the empirical formula. Thus, by eliminating a degree of freedom in developing the empirical model through the introduction of a deterministic quantity, a comparable fit of the measured data was obtained.

Before proceeding to a discussion of some of the benefits of using such a deterministic model, a word or two should be said about how an r^2 of 0.34 is seen to be significant. It was shown in Section 4.5.3 that the bulk of the RMS error, as well as the seemingly poor r^2 result, may be attributed to measurement error. A simulation of the errors was made and the result showed statistics similar to those obtained above. The true cause of the low r^2 lies in the fact that the overall dynamic range of σ^o is

less than 10 dB, with a majority of the data varying by less than about 3 dB. Hence, the RMS error of just over 1 dB may be a better measure of the quality of the model than r^2, because r^2 is influenced by the slope of the relationship between the two variables being correlated.

The significance of the fact that σ^o has a 10-dB dynamic range over the entire season should not be lost in this statistical anomaly. The reason the values of σ^o are quoted in units of dB rather than in $m^2\ m^{-2}$ is that variations of several orders of magnitude in σ^o are a common occurrence. This is particularly true when σ^o is presented as a function of incidence angle. Still, a variation of no more than 10 dB over time, when canopy height and biomass quantities go from near zero to their maximum and then down again, is somewhat surprising. Errors of the order of 1 dB in σ^o measurement may reduce dramatically the apparent quality of a model (determined statistically).

5.3 Analysis Using the Deterministic Model

One advantage of a model having a definite physical interpretation is that it enables the analyst to perform simulations of the effects of changes in sensor specifications. In this case, the effects of changes in frequency and incidence angle as well as the effects of variations in target conditions are "built into" the formula for L_ℓ.

Using data reported by Ulaby and Jedlicka (1983), expressions for ϵ''_ℓ similar to Eq. (5.7) were obtained for frequencies of 1.5 GHz and 5 GHz. For 1.5 GHz, the form of ϵ''_ℓ is

$$\varepsilon''_{\ell} = 15.69\ m_v + 21.29\ m_v^2 - 9.489\ m_v^3, \tag{5.9}$$

and for 5 GHz, the form for ε''_{ℓ} is

$$\varepsilon''_{\ell} = 7.400\ m_v + 19.14\ m_v^2 - 7.797\ m_v^3. \tag{5.10}$$

In both cases, r^2 was found to be 0.9999 and the RMS error was 0.052. Ulaby and Jedlicka (1983) also present values for ε''_{ℓ} (as well as ε'_{ℓ}) for various frequencies (from 1 to over 8 GHz) for corn leaves having a volumetric moisture (m_v) of 60%. Using this data, values for L_{ℓ} were computed with Eq. (5.8) using a value for E of 0.586 as determined earlier. Figure 5.1 shows the behavior of L_{ℓ} as a function of frequency at three incidence angles. The parameters characterizing the canopy are a leaf area index (LAI) of 4, a leaf volumetric moisture (m_v) of 60%, and a leaf thickness (t_{ℓ}) of 0.2 mm. On the basis of this figure, the effect of increasing the frequency (decreasing λ_0) is clearly shown. As the incidence angle is increased, the attenuation increases, as expected. It is interesting to note that while values for ε''_{ℓ} decrease with increasing frequency up to about 2.5 GHz after which ε''_{ℓ} increases with frequency, this behavior is masked by the λ_0^{-1} factor. The dip around 2.5 GHz is attributed to the saline nature of the water in the leaf, measured by Ulaby and Jedlicka (1983) to be about 11 parts per thousand or 11 $^0/_{00}$. The influence of this dip in ε''_{ℓ} is apparent in the rate of increase in attenuation with frequency--between 5 and 10 GHz, a factor of two in frequency,

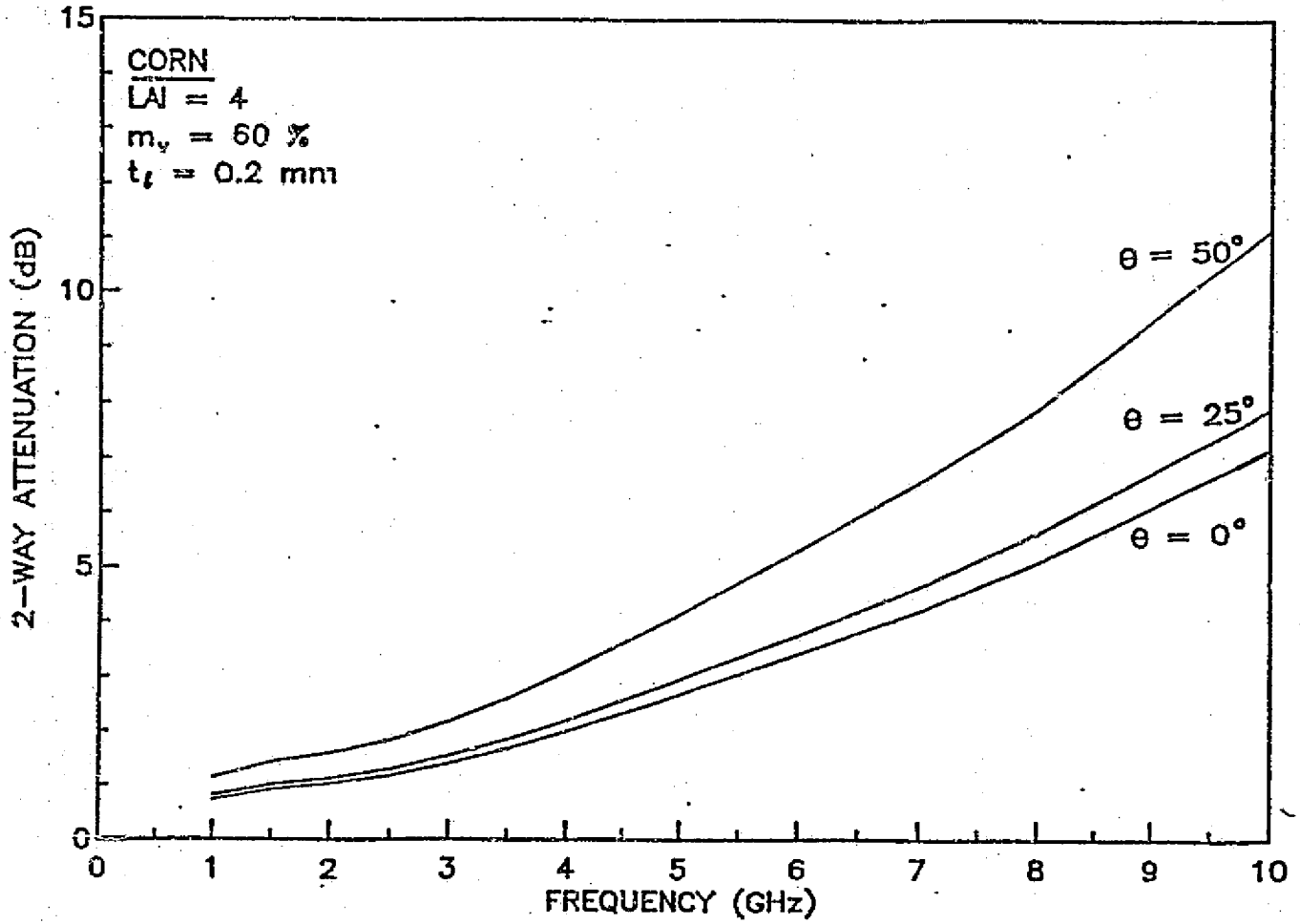

Figure 5.1 Computed two-way canopy attenuation as a function of frequency, using Eq. (5.7) with E = 0.586.

attenuation increases by about a factor of 3, yet between 1.5 and 3 GHz attenuation increses by only a factor less than 2.

As we now have models for both soil backscattering and leaf attenuation, σ^{o}_{can}, as defined in Eq. (5.1) using Eq. (5.2) to define σ^{o}_{veg}, can be calculated and studied. In adopting the form for σ^{o}_{veg} of Eq. (5.2), we are modeling the backscattering from the leaves only (neglecting any stalk contribution), which is acceptable only when leaves are dominant, i.e., when leaves are lush and fully developed. This assumption is based on observations at X-band, and since data on this subject are not available at lower frequencies, we will apply it to L- and C-band simulations as well.

One more assumption is needed before proceeding, and that is a choice of values for the canopy albedo, ω. To keep the analysis as simple as possible, the albedo will be modeled as being independent of LAI, i.e., a constant albedo will be used, its value depending on the wavelength and the dielectric properties of the leaves. As Rayleigh scattering has been used in obtaining Eq. (5.2), it is appropriate to adopt the Rayleigh approximation for albedo, ω, where ω takes the form

$$\omega = \xi_s/\xi_e \tag{5.11}$$

where ξ_s and ξ_e are the scattering and extinction efficiencies. In the Rayleigh approximation these efficiencies take the form (Ulaby et al., 1981)

$$\xi_s = \frac{8}{3} \chi^4 |K|^2 \quad (5.12a)$$

and

$$\xi_e = \frac{8}{3} \chi^4 |K|^2 + 4 \chi \, \mathrm{Im}\{-K\} \quad (5.12b)$$

where

$$\chi \triangleq \frac{2\pi r}{\lambda_o} \sqrt{\varepsilon_\ell'} \quad (5.13a)$$

and

$$K \triangleq \frac{\varepsilon_\ell - 1}{\varepsilon_\ell + 2} . \quad (5.13b)$$

Here r is the effective radius of the spherical scatterer.

From the values obtained in applying the deterministic leaf attenuation model to the 1981 corn σ^o data, an average albedo of about 0.45 was determined optimum. This value shall be adopted as the X-band albedo and by scaling, values for C- and L-bands will be obtained. From corn leaf dielectric measurements (Ulaby and Jedlicka, 1983) a value for ε_ℓ at a given volumetric moisture (45%) is available at all three bands. At X-band, $\varepsilon_\ell = 16.76 - j7.16$; at C-bands, $\varepsilon_\ell = 17.68 - j6.50$; at L-band, $\varepsilon_\ell = 26.57 - j10.51$, when $m_v = 45\%$. Thus by knowing ε_ℓ and ω at X-band ($\lambda_o = 3$ cm) the only unknown is r which when assigned the value of 0.57 mm gave the desired value for ω of 0.45. By using this same value for r at C-band an albedo of 0.15 was obtained.

At L-band the use of this value for r resulted in an albedo of 0.012. These values for albedo, 0.45, 0.15, and 0.012, shall be used at X-, C-, and L-bands, henceforth.

For the soil backscattering term, the Kirchhoff scalar-approximation model is chosen, and values for the RMS height (σ) and correlation length (L) of 0.8 cm and 10 cm were chosen. A volumetric soil moisture of 0.15 cm^3 cm^{-3} was assumed also. Using dielectric measurements of a given soil type (Soil Type No. 3) as discussed in Appendix A, the Fresnel reflection coefficients were computed as the final input into the model.

Figure 5.2 shows the angular behavior of σ^o(dB) computed using the model given above at L-, C-, and X-bands (1.5, 5.75, and 10 GHz). As expected, all three curves show a decrease in σ^o as incidence angle increases. As the attenuation due to leaves becomes sufficient, canopy backscattering begins to dominate at large angles.

To examine the significance of variations in σ^o_{soil} due to changes in soil moisture, a study of the sensitivity of σ^o to soil moisture was undertaken. Figure 5.3a shows the level of change in σ^o_{can} (dB) due to a 0.10 cm^3 cm^{-3} increase in soil moisture. As one might expect, L-band shows the highest sensitivity because it suffers the least attenuation and has the lowest canopy albedo. In addition, small incidence angles enhance sensitivity in most cases, again primarily because of reduced attenuation. The fact that C-band is considered optimum for soil-moisture sensing (Ulaby, 1977) rather than L-band is supported by the fact that C-band is less sensitive to surface-roughness changes, an aspect not

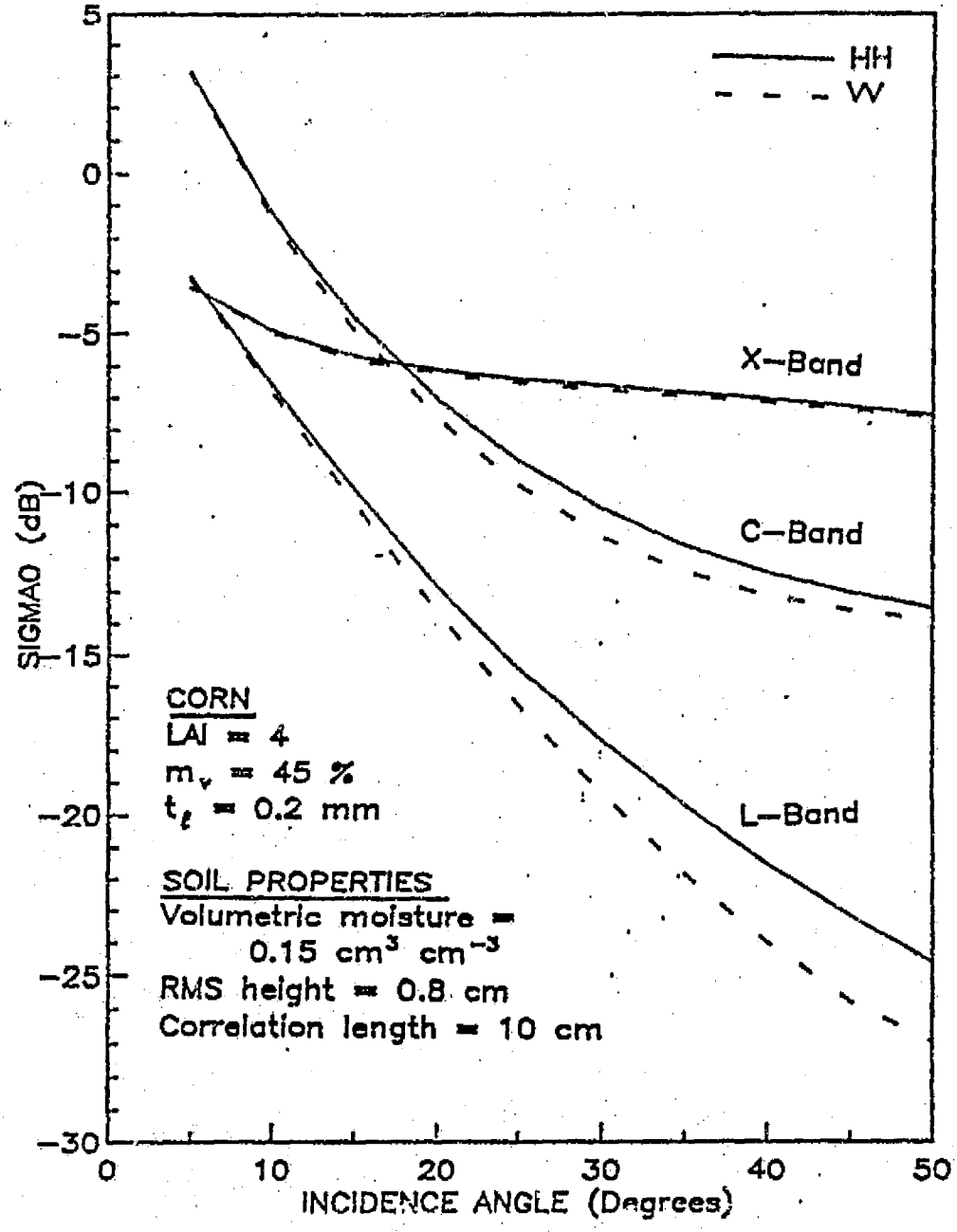

Figure 5.2 Computed σ^o as a function of incidence angle (θ).

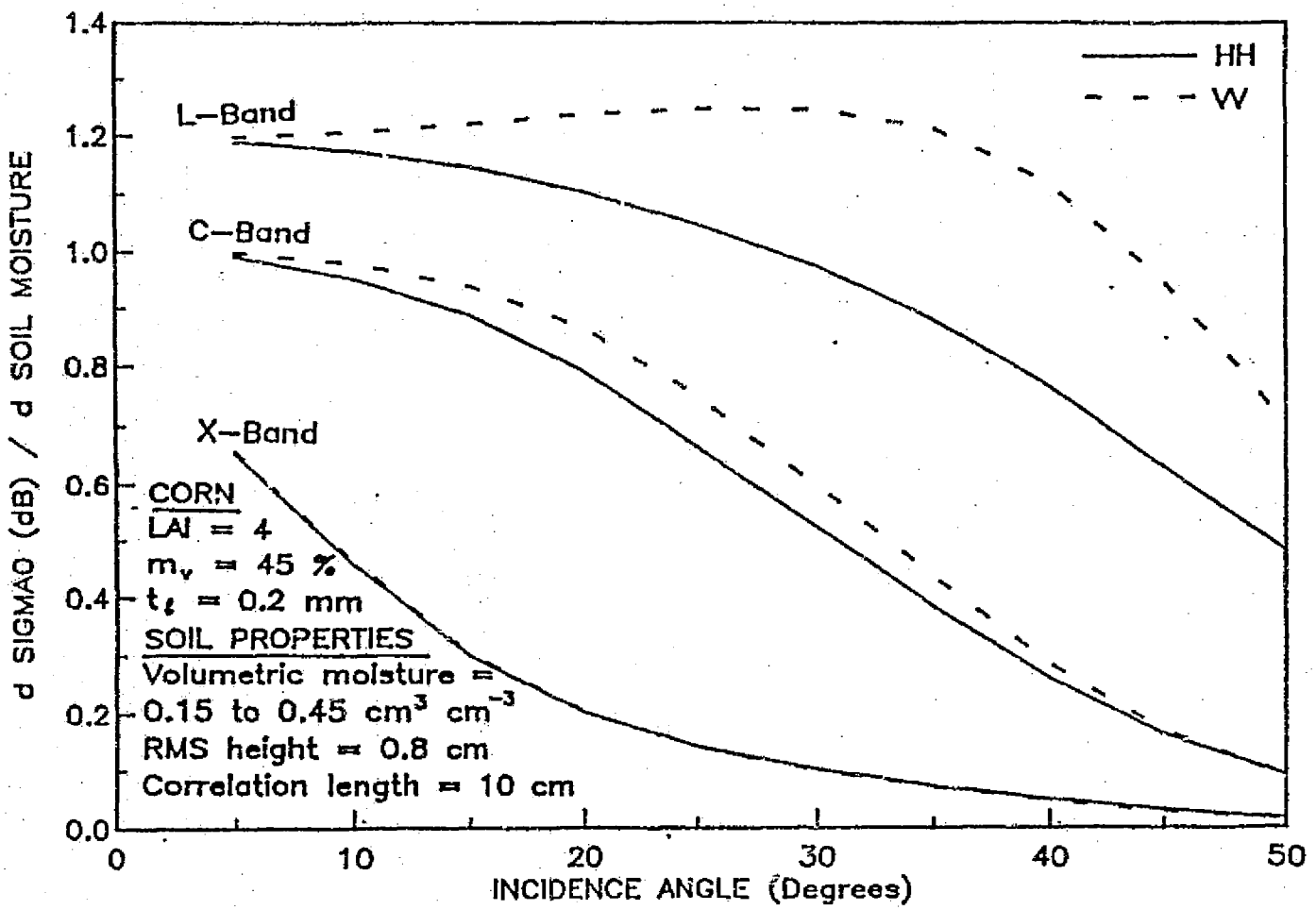

Figure 5.3 Computed difference in σ^0 as a result of changing soil moisture for (a) a corn canopy over soil, and (b) bare soil. Units are (dB/0.10 cm cm^{-3}).

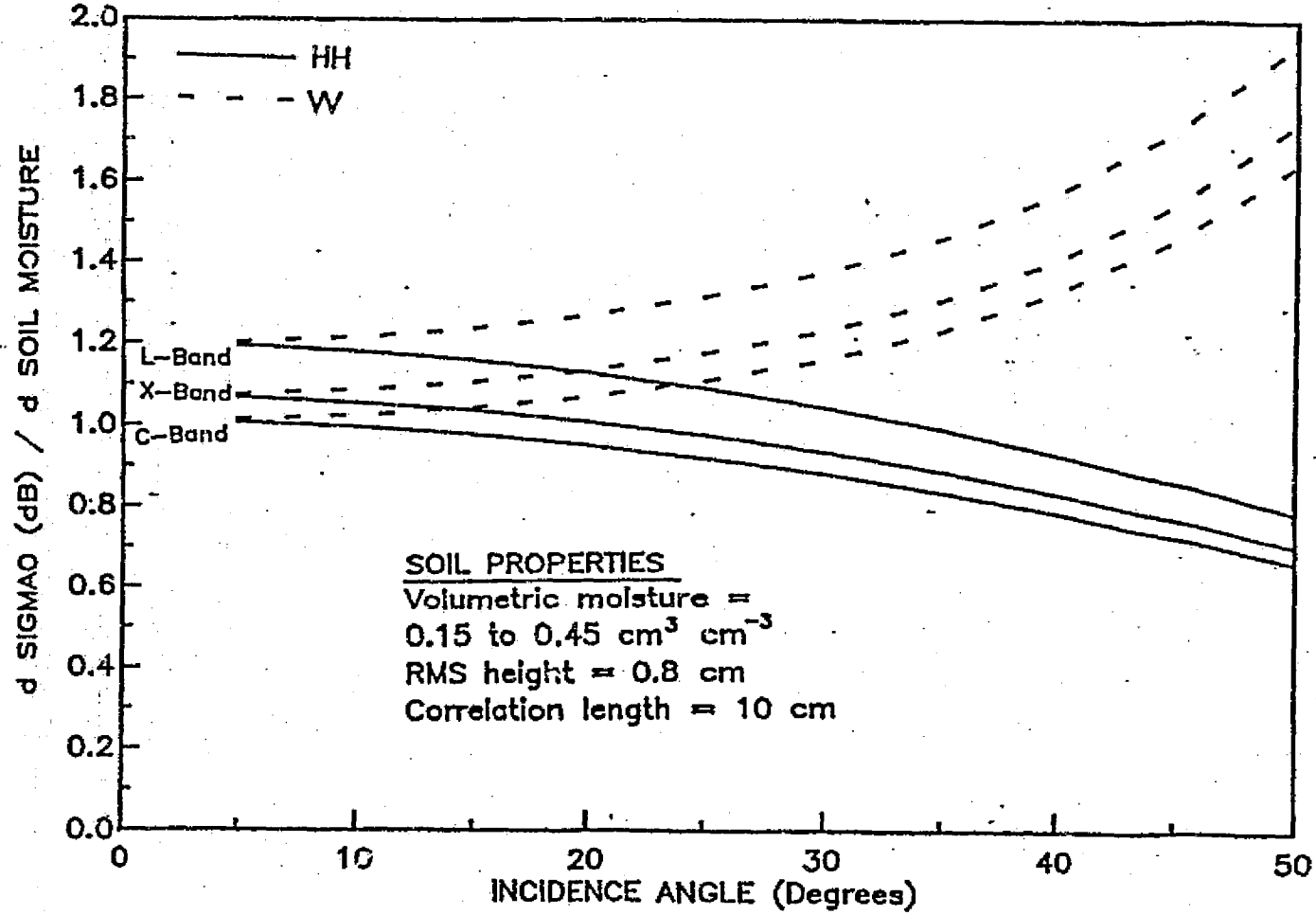
HH
W
L-Band
X-Band
C-Band
d SIGMAO (dB) / d SOIL MOISTURE
INCIDENCE ANGLE (Degrees)
SOIL PROPERTIES
Volumetric moisture =
0.15 to 0.45 cm³ cm⁻³
RMS height = 0.8 cm
Correlation length = 10 cm
2.0
1.8
1.6
1.4
1.2
1.0
0.8
0.6
0.4
0.2
0.0
0
10
20
30
40
50

Figure 5.3(b)

treated here. For comparison, Figure 5.3b shows a the level of change in σ^o_{soil}(dB) (bare soil) due to a 0.10 cm^3 cm^{-3} increase in soil moisture.

To investigate the sensitivity of σ^o to leaf area index (LAI), the model was again used to compute σ^o, this time with fixed soil moisture (0.15 cm^3 cm^{-3}) and varying LAI. Figures 5.4(a) through (c) show the results. For all three frequencies, it is apparent that the larger incidence angles are the most sensitive to LAI. It would seem that, given the behavior shown in these curves, C-band might serve as well as X-band for monitoring LAI. It should be kept in mind, however, that C-band is also more sensitive to soil-moisture changes, and hence measured σ^o values would contain two unknowns (soil moisture and LAI), each having a strong impact upon σ^o. An example of how variations in soil moisture might impact on the σ^o-LAI relationship is presented in Figure 5.5(a) through (c) for L-, C-, and X-bands, respectively, all at a 50° incidence angle and VV polarization. Here σ^o_{can} is computed for two conditions, one with a dry soil (0.05 cm^3 cm^{-3}) background and one with a wet soil (0.50 cm^3 cm^{-3}) background. Clearly X-band is the least sensitive to changes in soil moisture. For this reason, X-band is more suitable for monitoring LAI.

Finally, it is apparent from Figures 5.4(a) through (c) that as the incidence angle, as well as the frequency, is changed, the level of LAI at which σ^o becomes less sensitive also changes. To quantify this effect, we may define a new term: the LAI Sensitivity Range (LSR), which is expressed in the same units as LAI (m^2 m^{-2}). The definition of LSR is that level of LAI at which

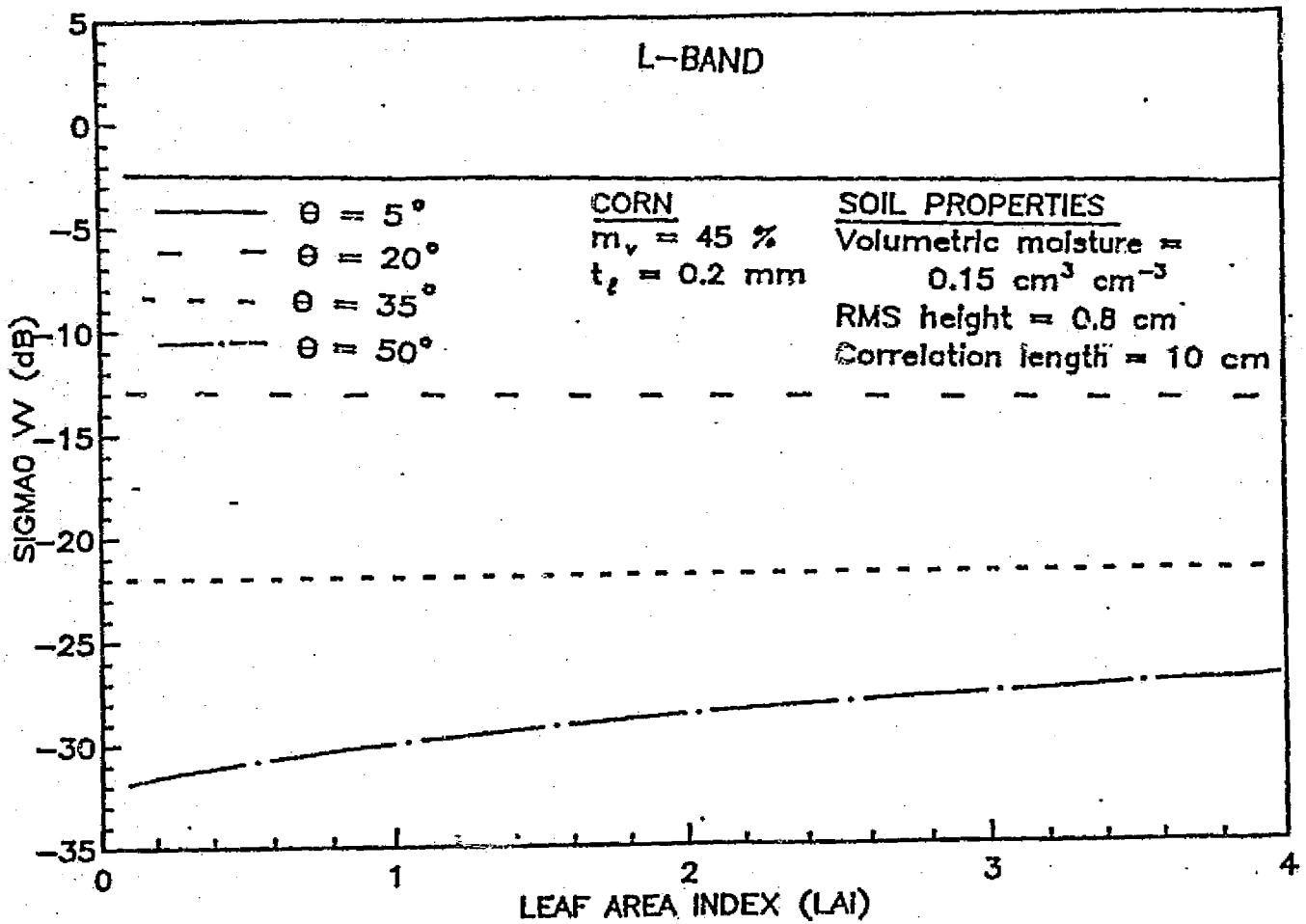

Figure 5.4 Computed variation in σ^o as a function of LAI, at (a) L-band, (b) C-band, and (c) X-band.

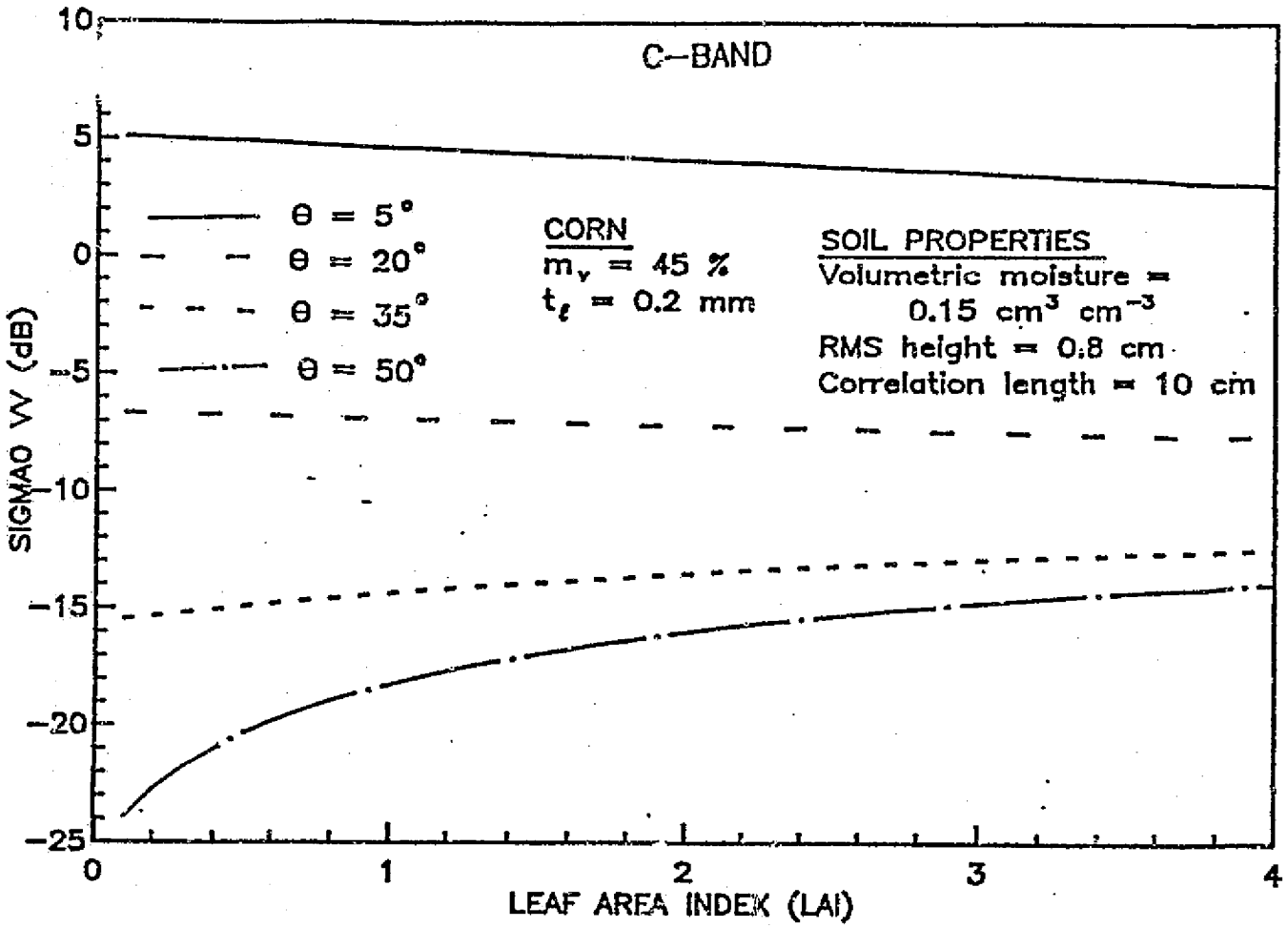
C-BAND
θ = 5°
θ = 20°
θ = 35°
θ = 50°
CORN
m_v = 45 %
t_ℓ = 0.2 mm
SOIL PROPERTIES
Volumetric moisture = 0.15 cm³ cm⁻³
RMS height = 0.8 cm
Correlation length = 10 cm
SIGMAO VV (dB)
LEAF AREA INDEX (LAI)
10
5
0
-5
-10
-15
-20
-25
0
1
2
3
4

Figure 5.4(b)

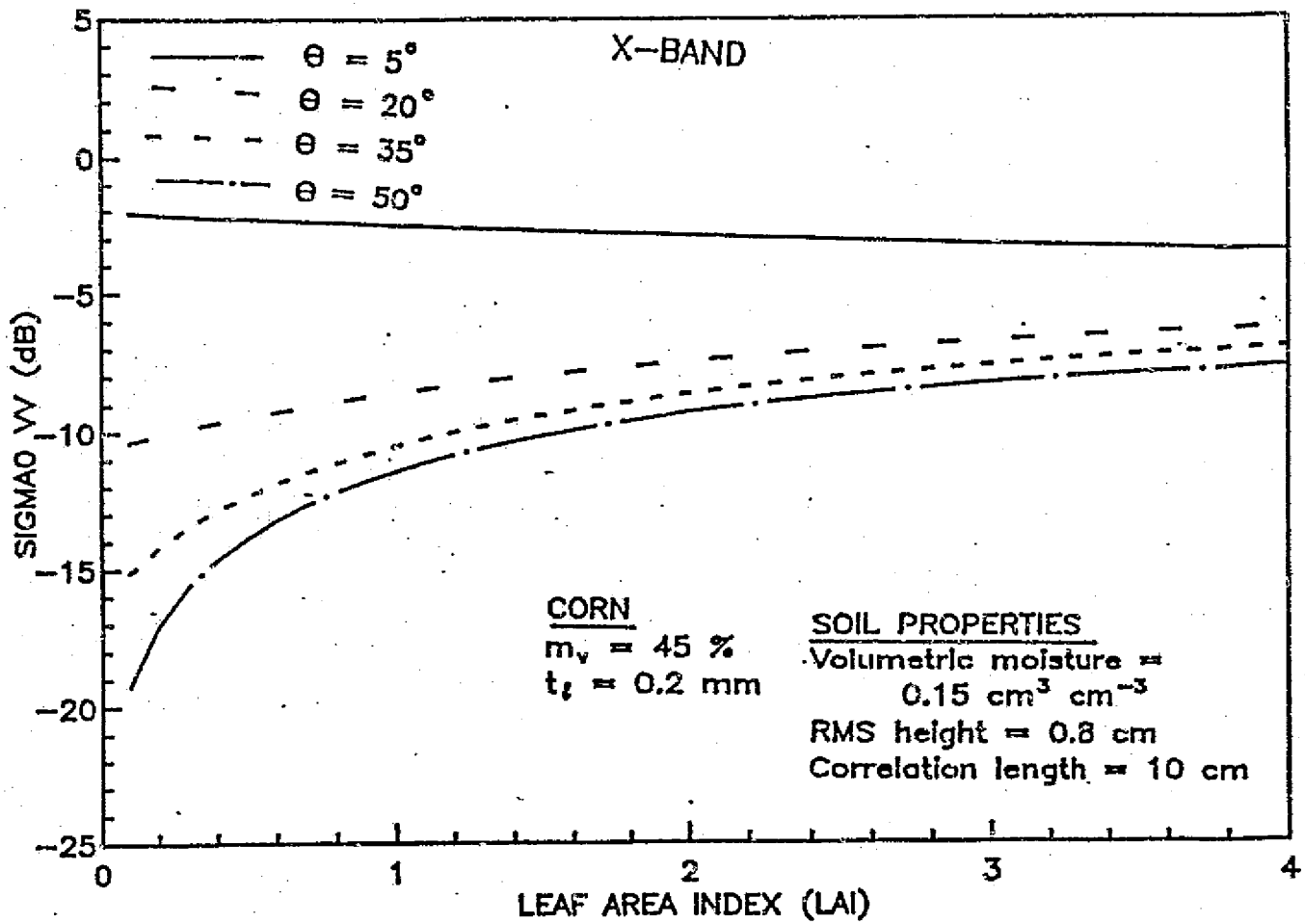
X-BAND
θ = 5°
θ = 20°
θ = 35°
θ = 50°
SIGMA0 VV (dB)
5
0
-5
-10
-15
-20
-25
0
1
2
3
4
LEAF AREA INDEX (LAI)
CORN
m_v = 45 %
t_l = 0.2 mm
SOIL PROPERTIES
Volumetric moisture = 0.15 cm^3 cm^{-3}
RMS height = 0.8 cm
Correlation length = 10 cm

Figure 5.4 (c)

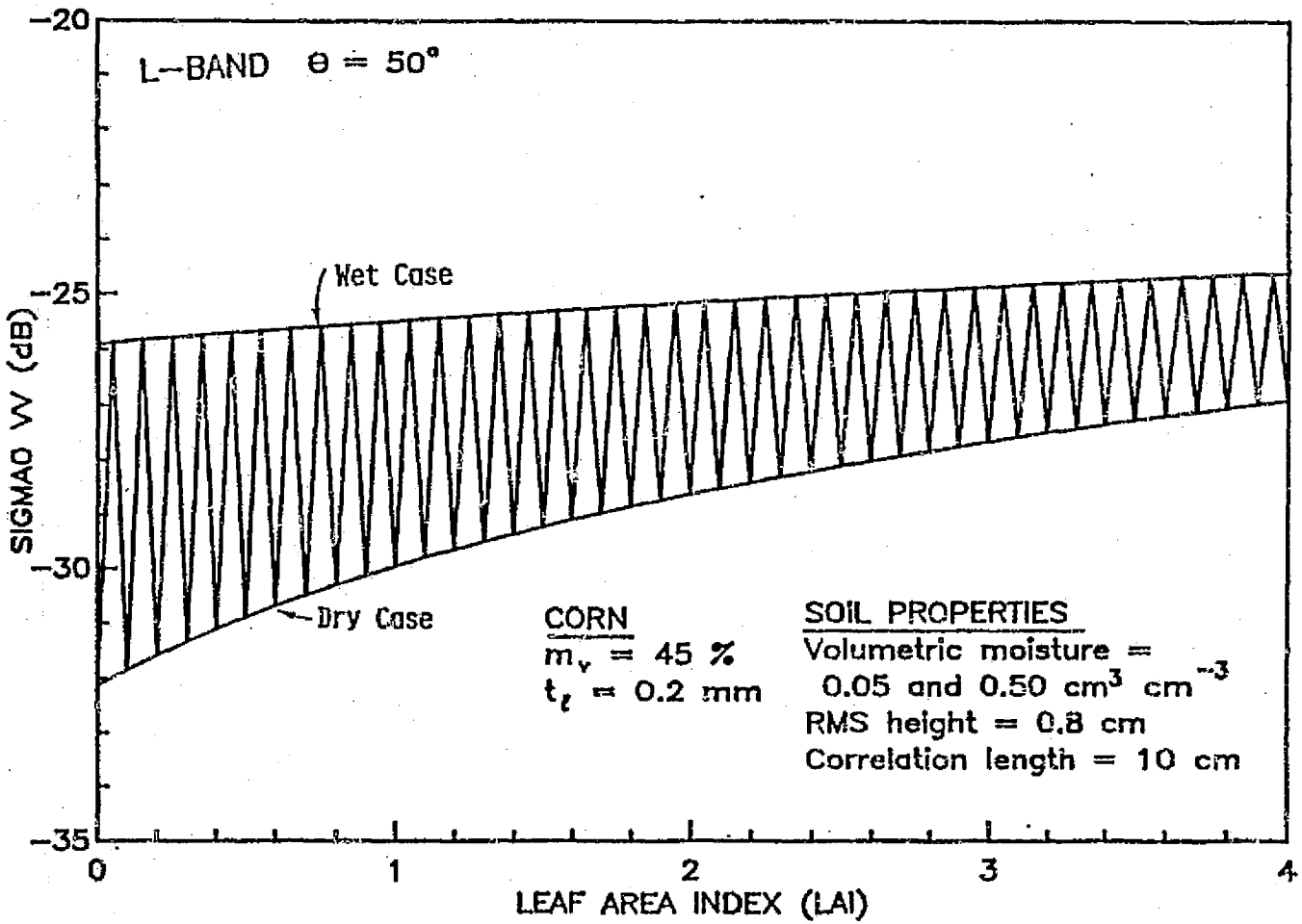

Figure 5.5 Computed variation in σ^0 due to changes in soil moisture as a function of LAI at (a) L-band, (b) C-band, and (c) X-band.

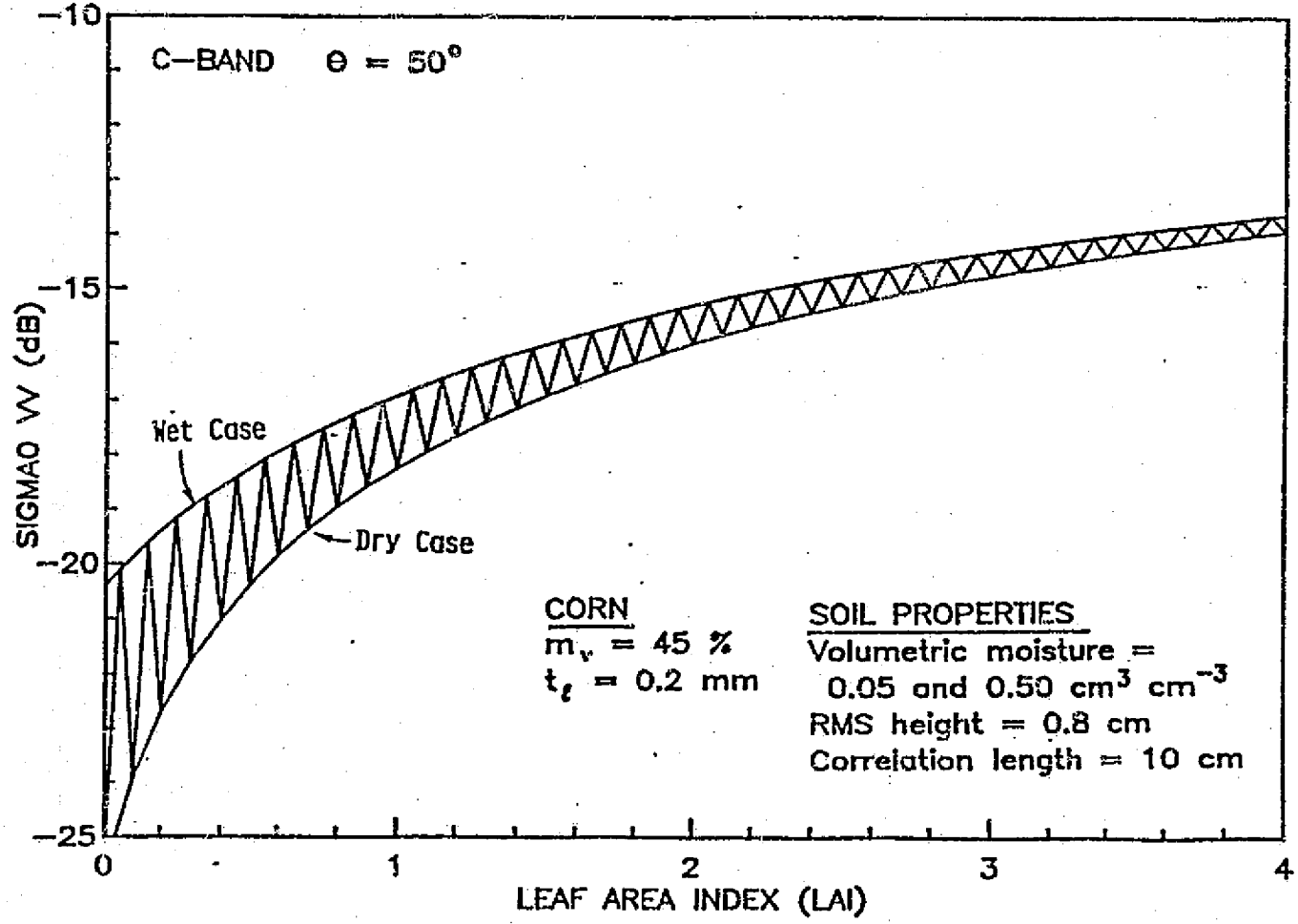
C—BAND θ = 50°
SIGMAO VV (dB)
−10
−15
−20
−25
Wet Case
Dry Case
CORN
m_v = 45 %
t_ℓ = 0.2 mm
SOIL PROPERTIES
Volumetric moisture =
0.05 and 0.50 cm^3 cm^{-3}
RMS height = 0.8 cm
Correlation length = 10 cm
0
1
2
3
4
LEAF AREA INDEX (LAI)

Figure 5.5(b)

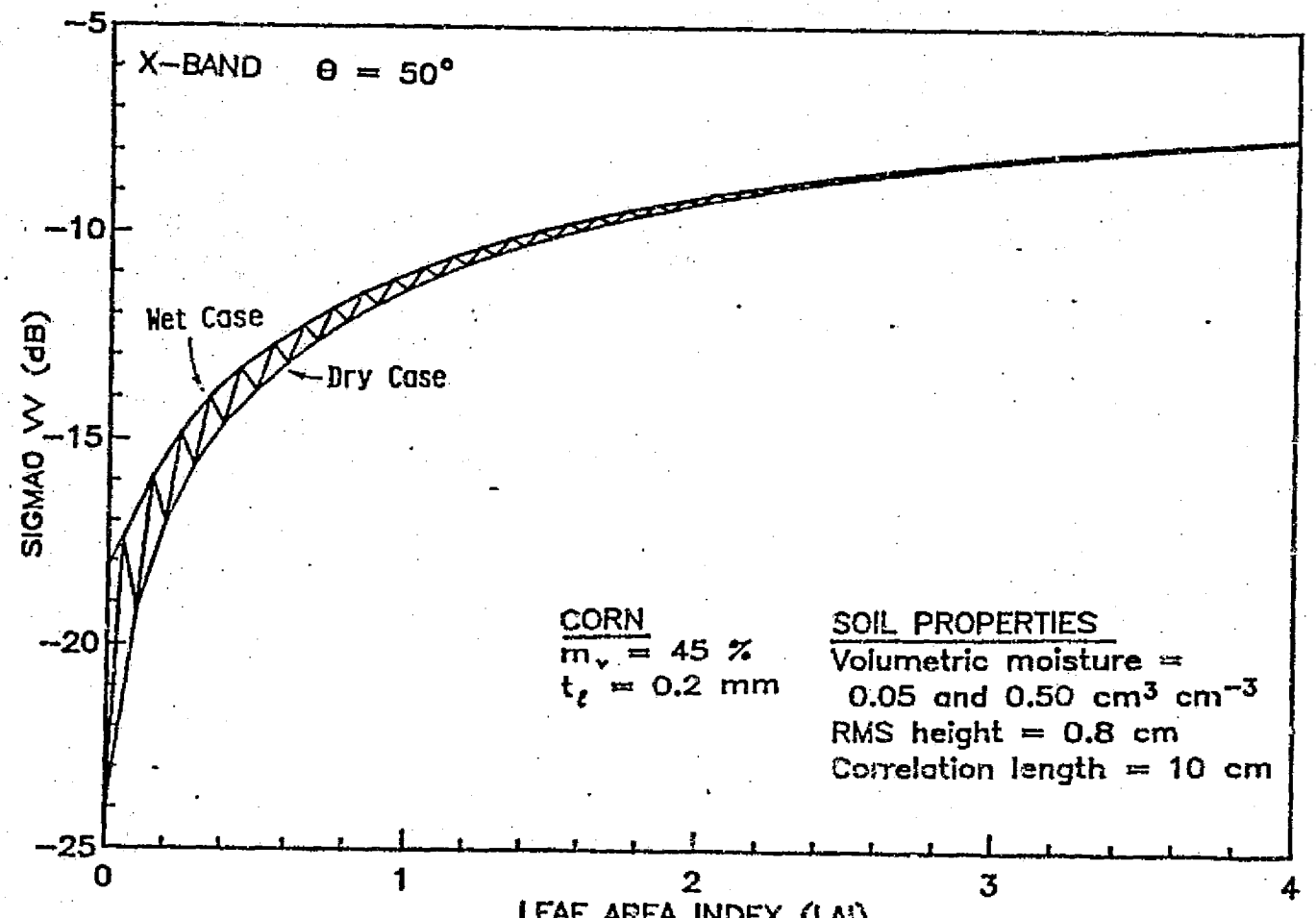
X–BAND θ = 50°
Wet Case
Dry Case
CORN
m_v = 45 %
t_ℓ = 0.2 mm
SOIL PROPERTIES
Volumetric moisture =
0.05 and 0.50 cm³ cm⁻³
RMS height = 0.8 cm
Correlation length = 10 cm
SIGMA0 VV (dB)
LEAF AREA INDEX (LAI)
-5
-10
-15
-20
-25
0
1
2
3
4

Figure 5.5(c)

the value $[1 - L_{\ell}^{-2}]$ is 0.80 or 80%. In the case in which σ^{o}_{soil} is less than $\sigma^{o}_{can}(LAI = \infty)$, the saturation value of σ^{o}, then when LAI reaches LSR, σ^{o}_{can} will be within 80% (or about 1 dB) of its saturated value. A further increase in LAI would result in a less than 1 dB increase in σ^{o}. Clearly, if $\sigma^{o}_{soil} > \sigma^{o}_{can}$ (LAI = ∞), then this is not necessarily true. Assuming $\sigma^{o}_{soil} = 0$, the LAI Sensitivity Range was computed at L-, C-, and X-bands, for a given canopy condition, as a function of incidence angle. This is shown in Figure 5.6. If we choose X-band as the frequency of our LAI monitor at an incidence angle of 50^{o}, then we can monitor LAI up to about 4 m^2 m^{-2} (neglecting the influence of soil backscattering). If, on the other hand, we accept the increased corruption of our measurement due to variations in soil moisture and choose a C-band monitor, we can monitor LAI up to about 9 m^2 m^{-2} at an incidence angle of 50^{o}. Clearly some trade-offs between decreased soil sensitivity and increased LAI sensitivity range will have to be made in defining a real system. One possible alternative is to use more than one frequency and incidence angle in the sensor configuration. Thus with two or more measures of two unknowns, an estimate of both soil moisture and LAI may be made.

5.4 Conclusion

The value of deterministic models over empirical models is clear. As more measurements of canopy scattering and attenuation are made and our understanding of the various phenomena is

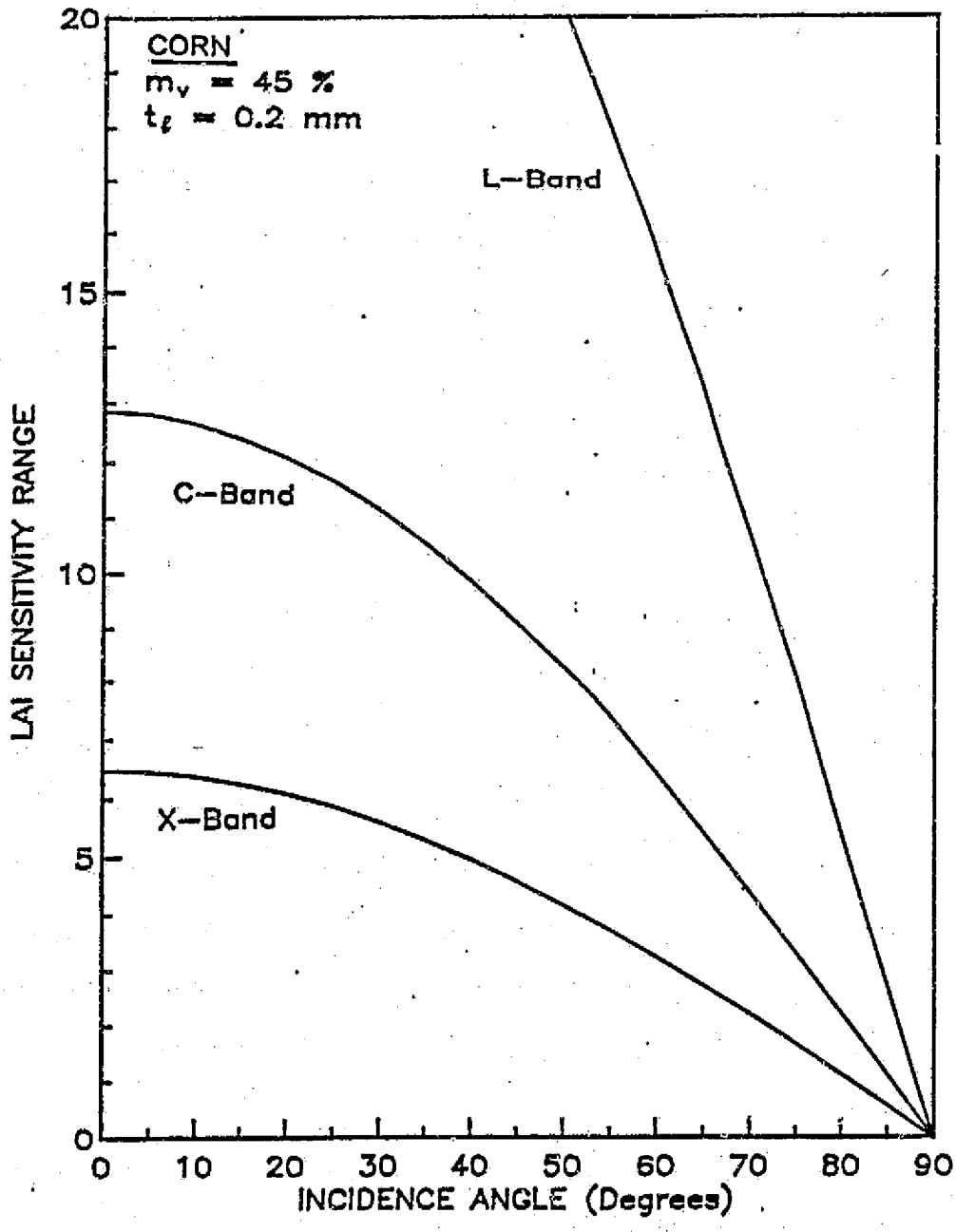

Figure 5.6 Variation of the LAI Sensitivity Range (LSR) as a function of incidence angle.

improved, our choice of parameters for system design will be optimized, and our ability to extract information from remotely sensed data will be maximized.

6.0 SUMMARY AND CONCLUSIONS

After having established the need for models and experiments to verify or refute the models presented in Chapter 1, a course of research was undertaken to further understanding of the ways in which microwave energy interacts with vegetation material.

In Chapter 2, descriptions of experiments designed to measure the attenuation of X-band microwave energy by wheat stalks and heads and soybean leaves (with stalks) were presented. Overall values of canopy attenuation, with an associated standard deviation, were a result that was used in Chapter 4 in setting realistic limits on these quantities. Further, theoretical models for attenuation caused by dielectric inclusions of varying geometries were shown to give similar values for attenuation. One interesting result was the effect of polarization on attenuation through wheat stalks, which was substantiated by data from Lopes (1983).

In Chapter 3, the effect of free water in the canopy on σ^o was investigated experimentally. The result from all three crop types was an increase in σ^o of the order of 2 to 3 dB, although some uncertainties remain in the case of the corn canopy, since changes in soil moisture also seem to be a factor. In the case of wheat, it was shown that the increase in σ^o over that of a "dry"

canopy tracks closely with the amount of free water present in the canopy. Establishing the need for careful treatment, in quantitative work, of data acquired from canopies containing free water as a result of dew or condensation, recent rainfall, or irrigation is one result of this investigation.

In Chapter 4, a review of past models for predicting σ^o from vegetation canopies was presented, followed by a description of the 1981 summer experiment involving multitemporal σ^o measurements of 30 agricultural fields. Various models for predicting σ^o (VV and VH) from each crop type (wheat, corn, and soybeans) were tried, including those reviewed earlier. Finally, a single model, yielding the best results among the models tested, was optimized for each crop-canopy type. The quality of fit was measured by correlation coefficient (r^2) and RMS error. The influence of experimental error (both in ground-truth data and in radar data) was investigated and found to be a probable source of low r^2 values (<70%) and RMS errors of the order of 1.2 dB. A comparison between data possibly affected by weather conditions (previously omitted from analysis) and "unaffected" data was also made using the newly developed models. The errors between the measured and predicted values showed the effect of recent rain upon σ^o values in most cases. The same was true of wheat data acquired following a wind storm in which the fields were blown down. Winds present during data acquisition produced no data significantly different from the "unaffected" or normal data. Finally, an attempt to relate the measured σ^o values to the reported yield values was made, without success. The probable cause for failure lies in the

limited number of data (9 yield values per crop type) and quite similar yields.

In Chapter 5, the need for additional deterministic models was justified, and an assessment of the progress of this line of research was given. A deterministic model for leaf attenuation was tested and shown to be adequate. The lack of quality data for testing the model did not provide strong evidence either to confirm or deny the usefulness of the model. An analysis using the model was performed to investigate the ability of radar as a monitor of LAI. The results confirmed previous reports indicating that L- or C-band is optimum to monitor soil moisture, using incidence angles near nadir. Some trade-offs are necessary between the LAI sensitivity range (LSR) and the necessity of minimizing the influence of soil.

Recommendations

Upon concluding this investigation, several areas for further investigation became apparent. To extend our current level of understanding of the ways in which microwave energy interacts with vegetation, additional detailed investigations of canopy attenuation should be made at various frequencies and polarizations. The backscattering models and experimental data presented here pertain to "normal" environmental and developmental crop conditions. Ordinarily, such models are based upon a certain set of assumptions about canopy geometry, which if violated will invalidate the model. The effects of abnormal environmental factors such as strong winds, heavy rain, hail (i.e., weather

events) upon σ^o of a vegetation canopy are difficult to incorporate into the design of a backscattering model. Hence, such effects may be regarded as deviations from normal behavior and should either be quantified or deleted from the data. In future experiments aimed at modeling canopy σ^o, ground truth should be acquired on a scale that will reduce uncertainty to reasonable limits. Also, the nature of σ^o_{soil} should be determined for each field used, so as to eliminate one area of uncertainty for which the models must account.

As the dynamic range of the temporal variation in σ^o is of the order of 10 dB, extra care should be taken to ensure the accuracy of the σ^o measurement. Because dynamic changes in canopy condition may result in a 1- or 2-dB variation in σ^o, the resolving power of the sensor should, if possible, be a fraction of a decibel.

Finally, as a result of the experiment described in this report, it is apparent that the temporal patterns of σ^o from agricultural fields of the same crop type are not identical. Although a model based on one set of observations from one or several fields may perform nicely, it may not represent the overall behavior of the entire population.

REFERENCES

Attema, E. P. W., and J. Van Kuilenburg, "Short Range Scatterometry," Proceedings of the URSI Commission II Specialist Meeting on Microwave Scattering and Emission from Earth, Berne, Switzerland, pp. 177-183, 1974.

Attema, E. P. W., and F. T. Ulaby, "Vegetation Modeled as a Water Cloud," Radio Science, Vol. 13, pp. 357-364, 1978.

Batlivala, P. P., and F. T. Ulaby, "Feasibility of Monitoring Soil Moisture Using Active Microwave Remote Sensing," Remote Sensing Laboratory Technical Report 264-12, University of Kansas Center for Research, Inc., Lawrence, KS, 1977.

Baier, W., "Crop Weather Models and Their Use in Yield Assessments," World Meteorological Organization Technical Report 151, Geneva, Switzerland, 1977.

Bauer, M. E., J. E. Cipra, P. E. Anuta, and J. B. Etheridge, "Identification and Area Estimation of Agricultural Crops by Computer Classification of LANDSAT MSS Data," Remote Sensing of Environment, Vol. 8, pp. 77-92, 1979.

Born, M., and E. Wolf, Principles of Optics, Pergamon Press, Oxford, England, 1965.

Bradley, G. A., "Remote Sensing of Ocean Winds Using a Radar Scatterometer," Remote Sensing Laboratory Technical Report 177-22, University of Kansas Center for Research, Inc., Lawrence, KS, 1971.

Brisco, B., and C. Allen, "Data Documentation for the 1981 Summer Vegetation Experiment," Remote Sensing Laboratory Technical Report 360-19, University of Kansas Center for Research, Inc., Lawrence, KS, 1982.

Brisco, B., C. Allen, C. Dobson, C. Martin, and N. McCarty, "Leaf Area, Biomass and Percent Moisture Measurements of Corn and Soybeans," Remote Sensing Laboratory Technical Memorandum 460-4, University of Kansas Center for Research, Inc., Lawrence, KS, 1983.

Brisco, B., and R. Protz, "Corn Field Identification Accuracy Using Airborne Radar Imagery," Can. J. Rem. Sens., Vol. 6, pp. 14-25, 1980.

Brisco, B., F. T. Ulaby, and M. C. Dobson, "Within-Field Variability of Plant and Soil Parameters," Remote Sensing Laboratory Technical Report 360-16, University of Kansas Center for Research, Inc., Lawrence, KS, 1981.

Brisco, B., F. T. Ulaby, and R. Protz, "Improving Crop Classification through Attention to the Timing of Airborne Radar Acquisitions," Photogram. Eng. and Remote Sensing, Vol. 50, No. 6, pp. 739-745, 1984.

Bush, T. F., and F. T. Ulaby, "Remotely Sensing Wheat Maturation with Radar," Remote Sensing Laboratory Technical Report 177-55, University of Kansas Center for Research, Inc., Lawrence, KS, 1975.

Bush, T., and F. T. Ulaby, "An Evaluation of Radar as a Crop Classifier," Rem. Sens. Environ., Vol. 7, pp. 15-36, 1978.

Carlson, N. L., "Dielectric Constant of Vegetation at 8.5 GHz," TR 1903-5, Electroscience Laboratory, Ohio State University, Columbus, Ohio, 1967.

Coelho, D. T., and R. F. Dale, "An Energy Crop Growth Variable and Temperature Function for Prediction Corn Growth and Development: Planting to Silking," Agronomy Journal, Vol. 72, pp. 503-510, 1980.

Daughtry, C. S. T., K. P. Gallo, and M. E. Bauer, "Estimation of Agronomic Variables Associated with Yields of Corn and Soybeans," AgRISTARS Final Report, Remote Sensing of Agricultural Crops and Soils, SR-P2-04266, pp. 31-42, 1982.

de Loor, G. P., "Dielectric Properties of Heterogeneous Mixtures Containing water," Journal of Microwave Power, Vol. 3, pp. 67-73, 1968.

Dobson, M. C., and F. T. Ulaby, "Soil Textural Effects on Radar Response to Soil Moisture," Remote Sensing Laboratory Technical Report 264-30, University of Kansas Center for Research, Inc., Lawrence, KS, 1979.

Eom, H. J., and A. K. Fung, "Scattering Coefficients of Kirchhoff Surfaces with Gaussian and Non-Gaussian Surface Statistics," Remote Sensing Laboratory Technical Report 4601-2, University of Kansas Center for Research, Inc., Lawrence, KS, 1982.

Fung, A. K., and H. J. Eom, "Coherent Scattering of a Spherical Wave from an Irregular Surface," IEEE Trans. Antennas and Propagation, Vol. AP-31, No. 1, pp. 68-72, 1983a.

Fung, A. K., and H. J. Eom, "Scattering from a Random Layer with Applications to Snow, Vegetation, and Sea Ice," IEEE Proceedings, Vol. 130, No. 7, 1983b.

Gabel, P. F., F. T. Ulaby, and D. R. Brunfeldt, "MARS X-Band Scatterometer," Remote Sensing Laboratory Technical Report 360-14, University of Kansas Center for Research, Inc., Lawrence, KS, 1981.

Hallikainen, M., F. T. Ulaby, M. El-Rayes, and M. C. Dobson, "Microwave Dielectric Behavior of Soil," Remote Sensing Laboratory Technical Report 545-5, University of Kansas Center for Research, Inc., Lawrence, KS, 1983.

Hoekman, D. H., L. Krul, and E. P. W. Attema, "A Multilayer Model for Radar backscattering from Vegetation Canopies," Digest of the 2nd IEEE Intl. Geoscience and Remote Sensing Symp., Munich, West Germany, 1-4 June, 1982.

Huet, M., "Evolution des paramètres de structure et de biomass d'un couvert de blé. Utilisation des techniques de télédétection micro-ondes," Ph.D. dissertation, l'Université Paul Sabatier de Toulouse, 1983.

Large, E. C., "Growth Stages in Cereals, Illustration of the Feekes Scale," Plant Pathology, Vol. 3, pp. 128-129, 1954.

Linville, D. E., R. F. Dale, and H. F. Hodges, "Solar Radiation Weighting for Weather and Corn Growth Models," Agron. J., Vol. 70, pp. 257-263, 1978.

Lopes, A., "Etude expérimentale et théorique de l'attentuation et de la rétrodiffusion des micro-ondes par un couvert de blé. Application à la télédétection," Ph.D. dissertation, l'Université Paul Sabatier de Toulouse, 1983.

Nelson, S. O., "Microwave Dielectric Properties of Insects and Grain Kernels," Journal of Microwave Power, Vol. 11, No. 4, pp. 299-303, 1976.

Nelson, S. O., and L. E. Stetson, "Frequency and Moisture Dependence of the Dielectric Properties of Hard Red Winter Wheat," J. Agric. Engng. Res., pp. 181-192, 1976.

Osman, A. M., "Dry-Matter Production of a Wheat Crop in Relation to Light Interception and Photosynthetic Capacity of Leaves," Ann. Bot., Vol. 35, pp. 1017-1035, 1971.

Peiyu, J., G. Deli, S. Guixiong, and M. Jinyu, "Radar Backscattering Coefficients of Paddy Fields," Digest of the 3rd IEEE Intl. Geoscience and Remote Sensing Symp., San Francisco, CA, August 31-September 2, 1983.

Polder D., and J. H. Van Santen, "The Effective Permeability of Mixtures of Solids," Physica, Vol. 12, p. 257, 1946.

Shibles, R. M., and C. R. Weber, "Leaf Area, Solar Radiation Interception and Dry Matter Production by Soybeans," Crop Science, pp. 575-577, 1965.

Sieber, A. J., "Wind Influence on the Backscattering Coefficient of Crops," Digest of the 2nd IEEE Intl. Geoscience and Remote Sensing Symp., Munich, West Germany, 1-4 June 1982.

Stiles, W. H., and F. T. Ulaby, "The Active and Passive Microwave Response to Snow Parameters, Part I: Wetness," Journal of Geophysical Research, Vol. 85, No. C2, February 1980.

Story, A. G., W. H. Johnson, and R. E. Stewart, "Remote Measurement of Concentration and Height of Heads of Standing Grain with Microwave Energy," Trans. of the ASAE, pp. 28-32, 1970.

Tucker, C. J., B. N. Holben, J. H. Elgin, and J. E. McMurtrey, III, "Remote Sensing of Total Dry-Matter Accumulation in Winter Wheat," Remote Sensing of Environment, Vol. 11, pp. 171-189, 1981.

Ulaby, F. T., "Review of Approaches to the Investigation of the Scattering Properties of Material Media," Digest of the 2nd IEEE Intl. Geoscience and Remote Sensing Symp., Munich, West Germany, 1-4 June, 1982.

Ulaby, F. T., C. T. Allen, G. W. Eger, and E. T. Kanemasu, "Relating the Radar Backscattering Coefficient to Leaf-Area Index," Rem. Sens. Environ., Vol. 14, pp. 113-133, 1984.

Ulaby, F. T., C. T. Allen, G. W. Eger, and E. T. Kanemasu, "Relating the Radar Backscattering Coefficient to Leaf-Area Index," Remote Sensing Laboratory Technical Report 360-20, University of Kansas Center for Research, Inc., Lawrence, KS, 1983.

Ulaby, F. T., P. P. Batlivala, and M. C. Dobson, "Microwave Backscatter Dependence on Surface Roughness, Soil Moisture and Soil Texture, Part I: Bare Soil," IEEE Transactions on Geoscience Electronics, Vol. GE-16, No. 4, pp. 286-295, October 1978.

Ulaby, F. T., and G. Burns, "The Potential Use of Radar for Crop Classification and Yield Estimation," Proceedings Microwave Remote Sensing Symposium, Houston, Texas, December 6-7, 1977.

Ulaby, F. T., M. C. Dobson, and G. A. Bradley, "If You Want to Remotely Sense Soil Moisture, Use a C-Band Radar," Proceedings Microwave Remote Sensing Symposium, Houston, Texas, December 6-7, 1977.

Ulaby, F. T., and R. P. Jedlicka, "Microwave Dielectric Properties of Plant Materials," Remote Sensing Laboratory Technical Report 595-1, University of Kansas Center for Research, Inc., Lawrence, KS, 1984.

Ulaby, F. T., R. K. Moore, and A. K. Fung, Microwave Remote Sensing: Active and Passive, Vol. I, Addison-Wesley Publishing Co., Reading, MA, 1981.

Ulaby, F. T., R. K. Moore, and A. K. Fung, Microwave Remote Sensing: Active and Passive, Vol. II, Addison-Wesley Publishing Co., Reading, MA, 1982.

Van Kastern, H. W. J., and M. K. Smit, "Measurements on the Backscatter of X-Band Radiation of Seven Crops, Throughout the Growing Seasons," NIWARS Publ. No. 47, 1977.

APPENDIX A

Soil Dielectric and Reflectivity

In concert with the 1981 summer experiment, which investigated the σ^o of cropland, soil samples of the various fields were also acquired. A textural analysis was performed to determine the constituent parts by percentage (e.g., sand, silt, and clay). The results are presented in Table A.1. Accompanying the analysis for each field is a classification (e.g., silty loam). Dielectric measurements were made subsequently on five general soil types, into which all of the fields in the 1981 summer experiment could be grouped. The composition of these five soil types is given in Table A.2. The dielectric measurements were made at a number of frequencies from 1.4 GHz to 18 GHz, including 10 GHz, under various soil-moisture conditions. Based upon these experimental data, the dielectric constant as a function of soil moisture at specific frequencies was obtained. An example of this relationship is shown in Figure A.1 for a frequency of 10 GHz. Note that soil types 1 and 5 represent the textural extremes between which all others lie, i.e., they have the highest sand and clay contents, respectively.

The curves in Figure A.1 are the results of polynomial regression fits performed on the measured data. For details on measurement techniques, analysis procedures, etc., see Hallikainen et al. (1983). The polynomials used in obtaining the curves of Figure A.1 are listed in Table A.3.

Based on these equations, it is possible to compute the Fresnel reflectivity, Γ, for each soil type under a wide range of

TABLE A.1

Particle-Size Classification of the 0 - 5-cm Layer for the Summer 1981 Vegetation Experiment

Field No.	% Sand	% Silt	% Clay	Soil Type No.	Classification
1W (11S)	57.7	33.6	8.7	1	Sandy Loam
2W (6S)	53.7	37.9	8.4	1	Sandy Loam
3W	10.1	61.4	27.8	4	Silty Clay Loam
4W	26.0	54.7	19.3	3	Silty Loam
5W	18.0	61.2	22.8	4	Silty Loam
6W (7S)	13.2*	72.4	14.4	4	Silty Loam
7W (8S)	11.4*	76.5	12.1	4	Silty Loam
8W	32.0	53.1	14.9	3	Silty Loam
9W (9S)	59.3	31.1	9.6	1	Sandy Loam
10W (10S)	46.0	41.5	12.5	2	Loam
1C	35.9	51.9	12.2	3	Silty Loam
2C	24.1*	51.1	24.8	3	Silty Loam
3C	29.9	60.5	9.6	3	Silty Loam
4C	40.6	44.3	15.1	2	Loam
5C	36.1	49.9	14.0	3	Loam
6C	31.5	52.4	16.1	3	Silty Loam
7C	31.2	52.2	16.6	3	Silty Loam
8C	30.4	40.9	28.7	3	Clay Loam
9C	56.6	29.9	13.5	1	Sandy Loam
10C	39.7	44.2	16.1	2	Loam
1S	37.2	45.8	17.0	3	Loam
2S	60.9	29.5	9.6	1	Sandy Loam
3S	32.4	56.0	11.6	3	Silty Loam
4S				1	
5S	6.1*	68.3	25.6	4	Silty Loam

*Defoamed

TABLE A.2

Soil Textures of Five Soil Types Used in Dielectric Measurements

Soil Type No.	Designation	Soil Type	Soil Texture (%) Sand	Silt	Clay
1	Field 1	Sandy Loam	51.51	35.06	13.43
2	Field 2	Loam	41.96	49.51	8.53
3	Field 3	Silt Loam	30.63	55.89	13.48
4	Field 4	Silt Loam	17.16	63.84	19.00
5	Field 5	Silty Clay	5.02	47.60	47.38

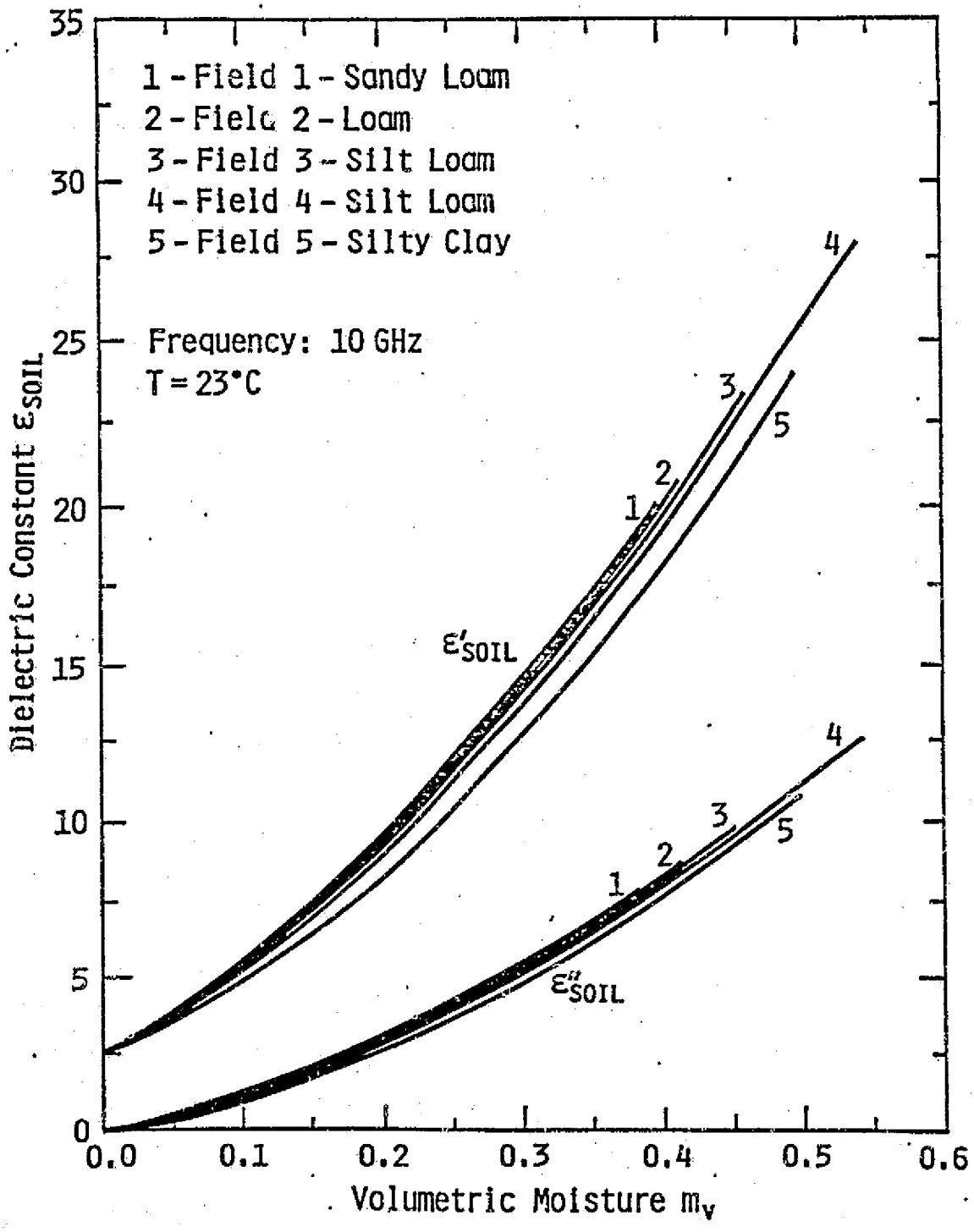

Figure A.1 Dielectric properties of five soil types as a function of volumetric moisture content. From Hallikainen et al. (1983).

TABLE A.3

Polynomial Fits of the Dielectric Constant of Five Soil Types

$\varepsilon_r = \varepsilon' - j\varepsilon''$

Real Part, $\varepsilon' = A_0 + A_1 m_v + A_2 m_v^2$

Soil Type	A_0	A_1	A_2
1	2.453	17.24	88.12
2	2.306	20.29	64.25
3	2.071	27.16	46.25
4	2.657	5.194	101.1
5	2.276	12.57	64.98

Imaginary Part, $\varepsilon'' = B_0 + B_1 m_v + B_2 m_v^2$

Soil Type	B_0	B_1	B_2
1	-0.0346	4.591	47.72
2	-0.1127	8.073	29.43
3	-0.1245	8.234	29.36
4	0.00181	2.698	41.76
5	-0.0563	3.531	36.30

Range of Validity

$0.05 < m_v < 0.50$

f = 10 GHz

moisture conditions, for a given incidence angle, θ. The equations for computing the Fresnel reflectivity are

$$r_H = \left| \frac{\cos\theta - [\varepsilon_r - \sin^2\theta]^{1/2}}{\cos\theta + [\varepsilon_r - \sin^2\theta]^{1/2}} \right|^2$$

$$r_V = \left| \frac{-\varepsilon_r \cos\theta + [\varepsilon_r - \sin^2\theta]^{1/2}}{\varepsilon_r \cos\theta + [\varepsilon_r - \sin^2\theta]^{1/2}} \right|^2 ,$$

where ε_r is the dielectric constant of the medium (which may be complex) and θ is the incident angle of the incoming wave. Plots of the Fresnel reflectivity at a 50° incidence angle for various soil-moisture conditions are presented in Figures A.2 and A.3. The five curves, one for each soil type, show similar though not identical behaviors. The relationship between reflectivity and soil moisture is neither entirely linear nor exponential; however, the linear form is a much more accurate approximation. For this reason Γ was included as computed above directly into the modeling of the σ^o data. A listing of the results of the textural analysis of the observed fields, shown in Table A.1, includes classification into one of the five soil types studied in detail (actually only four soil types were used, because fields having a soil type similar to soil type 5 were not encountered during the 1981 summer experiment).

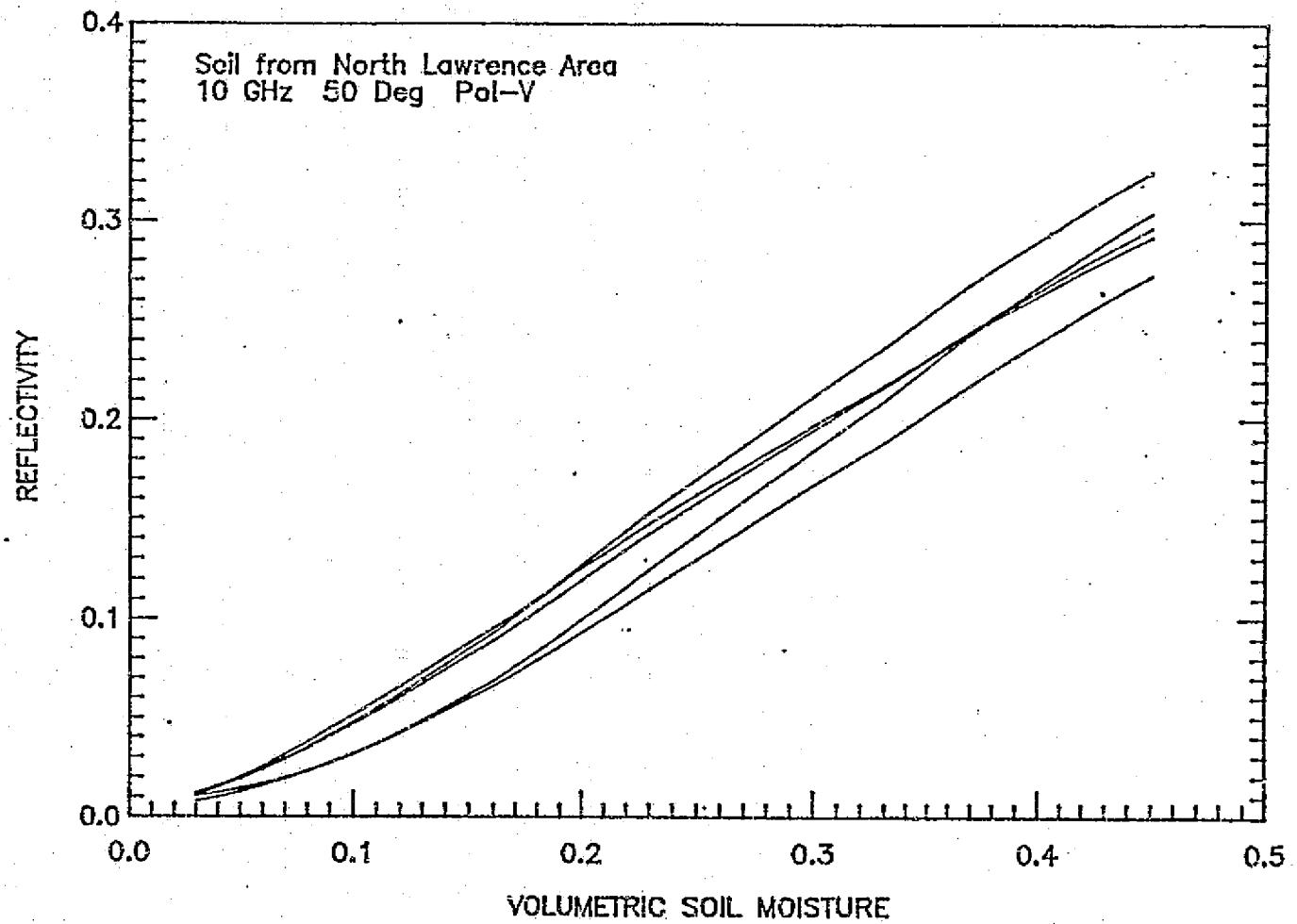

Figure A.2 Computed Fresnel reflectivity for V polarization, at a 50° incidence angle for smooth surfaces of five soil types as a function of volumetric moisture content.

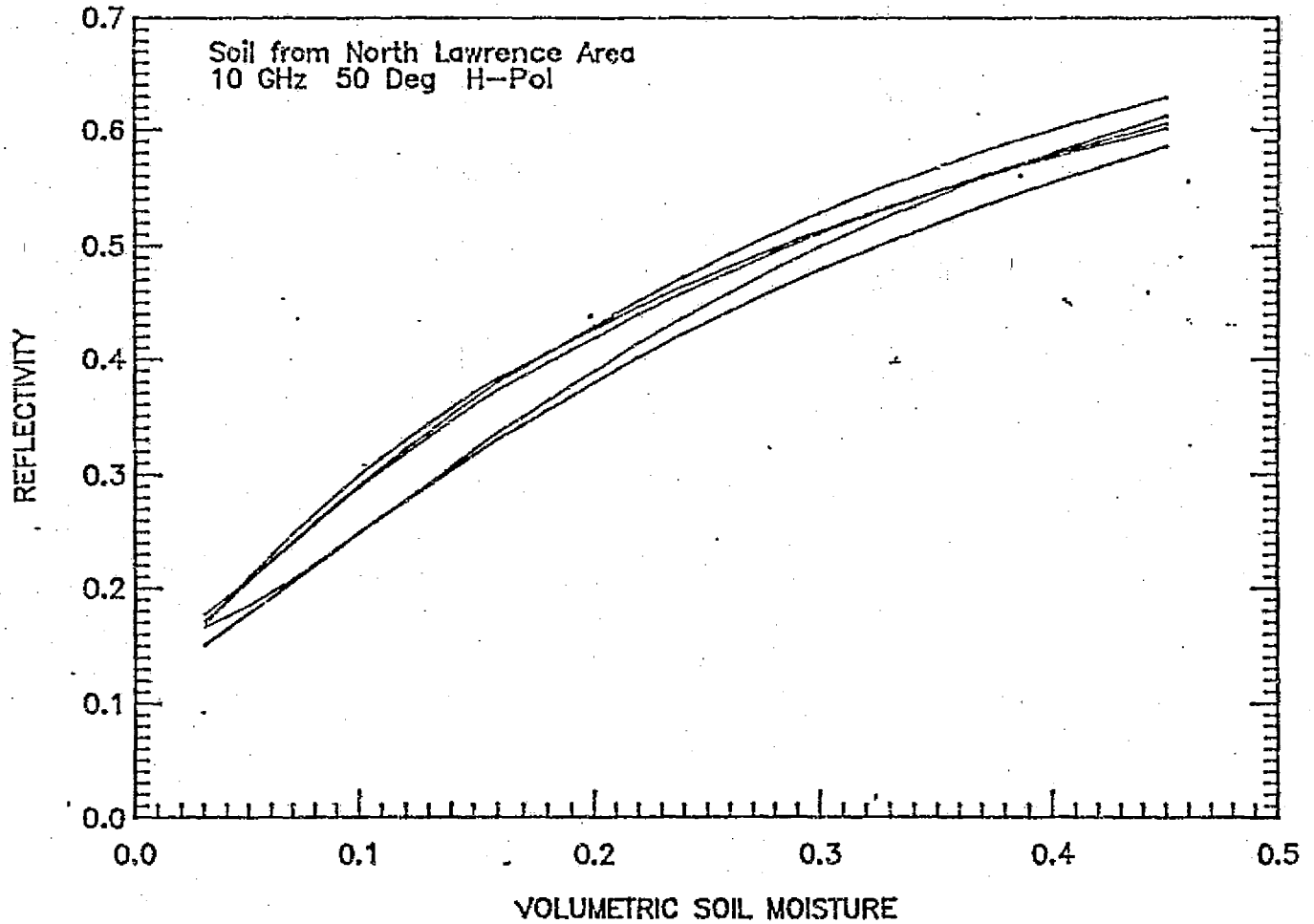

Figure A.3 Computed Fresnel reflectivity for H polarization, at a 50° incidence angle for smooth surfaces of five soil types as a function of volumetric moisture content.

APPENDIX B

What follows is a tabular listing of the data acquired during the 1981 summer experiment. The data are grouped by crop type and field number. A description of each column heading and entry follows.

JULIAN DATE	Day of year in 1981
SIGMAO VV	Backscattering coefficient in decibels (dB) for a frequency of 10.2 GHz, an incidence angle of 50° from nadir, and VV polarization
SIGMAO VH	Same as SIGMAO VV, except VH polarization
SOIL MOIST	Volumetric soil moisture in top 5 cm of soil surface ($cm^3\ cm^{-3} \times 100$)
CANOPY HEIGHT	Height of canopy in meters

Plant Parameters

FRESH BIOMASS	Biomass per unit area of freshly cut plant material ($kg\ m^{-2}$)
DRY BIOMASS	Biomass per unit area of dried plant material ($kg\ m^{-2}$)

Plant Parts

LEAF AND STALK	Combined biomass of leaves and stalks for wheat plants
HEAD	Biomass of wheat head material
STALK	Biomass of corn stalk material
FRUIT	Biomass of corn cob, kernels, and enclosing material
LEAF	Biomass of corn leaves
PLANT	Biomass of all soybean plant parts combined
CODE	Code designating any abnormal conditions affecting the observed canopy. An explanation of the code follows most tables.

This data has undergone a clean-up process in which the plant parameters (height and biomasses) were smoothed to eliminate the rapid variations known to be due to measurement error. Data from Soybean Field No. 7 are not presented because of the limited size of the data sets due to farm-operator problems.

WHEAT FIELD # 1

JULIAN DATE	SIGMA0 VV	SIGMA0 VH	SOIL MOIS	CANOPY HEIGHT	LEAF & STALK BIOMASS FRESH	LEAF & STALK BIOMASS DRY	HEAD BIOMASS FRESH	HEAD BIOMASS DRY	CODE
121.	-16.4	-22.2	3.8	0.689	1.450	0.500	0.000	0.000	0.
124.	-12.1	-15.8	--	0.708	1.491	0.594	0.000	0.000	4.
126.	-15.6	-20.7	7.7	0.718	1.569	0.660	0.000	0.000	0.
128.	-15.4	-20.2	5.7	0.729	1.553	0.687	0.093	0.030	0.
131.	-14.0	-18.0	16.3	0.744	1.416	0.635	0.343	0.153	0.
135.	-13.6	-17.0	17.5	0.759	1.411	0.638	0.623	0.279	0.
139.	-14.3	-18.6	24.4	0.766	1.492	0.668	0.818	0.367	0.
140.	-13.2	-18.5	25.8	0.766	1.521	0.681	0.854	0.383	0.
142.	-12.7	-17.9	20.2	0.766	1.560	0.695	0.911	0.412	0.
147.	-13.4	-19.3	14.0	0.756	1.598	0.717	0.969	0.456	0.
149.	-13.4	-17.5	27.3	0.749	1.585	0.724	0.962	0.465	0.
152.	-13.2	-17.1	19.9	0.736	1.525	0.728	0.923	0.472	0.
154.	-14.6	-18.4	28.7	0.726	1.459	0.725	0.883	0.474	4.
155.	-13.8	-17.8	31.4	0.722	1.410	0.715	0.859	0.474	0.
159.	-10.6	-16.1	26.6	0.703	1.159	0.654	0.754	0.473	3.
161.	-11.3	-16.2	23.1	0.696	0.992	0.591	0.700	0.473	0.
167.	-11.0	-12.6	24.1	0.689	0.722	0.510	0.555	0.485	4.
168.	-10.7	-16.4	25.3	0.691	0.705	0.500	0.536	0.490	0.
169.	-10.1	-16.9	25.1	0.694	0.604	0.455	0.517	0.496	0.
173.	-9.0	-13.8	28.0	0.227	0.272	0.197	0.000	0.000	1.
177.	-8.4	-15.6	22.1	0.227	0.272	0.197	0.000	0.000	1.
180.	-10.9	-18.2	18.4	0.227	0.272	0.197	0.000	0.000	1.
195.	-7.8	-17.3	13.5	0.160	0.272	0.197	0.000	0.000	1.

--- CODE EXPLANATION ---
0 -- NORMAL DATA
1 -- POST-HARVEST
2 -- BLOWN DOWN AREAS
3 -- WINDY DURING DATA ACQUISITION
4 -- RECENT HEAVY RAIN

WHEAT FIELD # 2

JULIAN DATE	SIGMAO VV	SIGMAO VH	SOIL MOIS	CANOPY HEIGHT	LEAF & STALK FRESH BIOMASS	LEAF & STALK DRY BIOMASS	HEAD FRESH BIOMASS	HEAD DRY BIOMASS	CODE
121.	-11.0	-20.1	5.8	0.661	1.723	0.422	0.000	0.000	0.
124.	-14.5	-18.5	--	0.755	1.710	0.514	0.000	0.000	4.
126.	-14.0	-21.0	8.9	0.802	1.703	0.560	0.000	0.000	0.
128.	-18.7	-22.9	6.2	0.828	1.666	0.586	0.000	0.000	0.
131.	-16.8	-19.7	14.9	0.845	1.513	0.590	0.141	0.037	0.
135.	-16.1	-18.3	16.6	0.840	1.319	0.527	0.369	0.148	0.
140.	-18.2	-19.8	23.8	0.815	1.324	0.560	0.436	0.165	0.
142.	-19.6	-18.9	18.0	0.804	1.291	0.552	0.494	0.187	3.
147.	-15.4	-18.9	20.9	0.784	1.149	0.500	0.661	0.262	0.
152.	-16.4	-20.0	22.4	0.779	0.992	0.428	0.780	0.350	0.
159.	-16.5	-20.8	22.8	0.788	0.860	0.381	0.763	0.447	3.
161.	-17.0	-21.9	23.3	0.789	0.836	0.387	0.720	0.460	0.
167.	-5.5	-11.6	--	0.759	0.403	0.239	0.521	0.440	4.
168.	-7.5	-14.7	21.3	0.747	0.339	0.200	0.480	0.425	0.
169.	-8.6	-12.7	26.6	0.731	0.268	0.160	0.439	0.407	0.
173.	-10.7	-13.6	28.5	0.402	0.231	0.191	0.000	0.000	1.
177.	-9.1	-14.0	26.4	0.360	0.231	0.185	0.000	0.000	1.
180.	-7.7	-13.9	28.5	0.340	0.225	0.180	0.000	0.000	1.
195.	-10.8	-18.1	15.5	0.340	0.223	0.165	0.000	0.000	1.

--- CODE EXPLANATION ---
0 -- NORMAL DATA
1 -- POST-HARVEST
2 -- BLOWN DOWN AREAS
3 -- WINDY DURING DATA ACQUISITION
4 -- RECENT HEAVY RAIN

WHEAT FIELD # 3

JULIAN DATE	SIGMA0 VV	SIGMA0 VH	SOIL MOIS	CANOPY HEIGHT	LEAF & STALK FRESH BIOMASS	LEAF & STALK DRY BIOMASS	HEAD FRESH BIOMASS	HEAD DRY BIOMASS	CODE
121.	-11.8	-18.4	16.7	0.754	4.698	0.846	0.000	0.000	0.
124.	-6.1	-16.2	--	0.820	4.774	1.029	0.000	0.000	4.
126.	-11.0	-18.5	18.8	0.853	4.812	1.121	0.000	0.000	0.
128.	-10.3	-18.7	23.6	0.865	4.791	1.188	0.000	0.000	0.
131.	-10.9	-19.2	32.0	0.928	4.636	1.220	0.124	0.041	0.
133.	-14.7	-19.0	--	0.954	4.252	1.145	0.491	0.163	4.
134.	-13.5	-19.3	--	0.962	4.200	1.148	0.537	0.175	4.
135.	-13.9	-18.4	28.8	0.971	4.147	1.151	0.584	0.188	0.
139.	-16.2	-21.1	33.9	0.999	3.904	1.146	0.773	0.243	0.
140.	-16.7	-20.6	34.6	1.004	3.845	1.145	0.817	0.258	0.
142.	-15.4	-19.4	32.2	1.012	3.720	1.133	0.896	0.289	0.
147.	-15.5	-18.9	40.3	1.016	3.445	1.118	1.029	0.367	0.
148.	-12.3	-18.9	--	1.015	3.386	1.112	1.044	0.383	4.
149.	-14.6	-18.8	41.5	1.013	3.331	1.106	1.055	0.398	2.
152.	-16.6	-20.5	33.9	1.002	3.176	1.106	1.067	0.443	0.
154.	-7.5	-17.5	46.1	0.992	3.058	1.098	1.059	0.471	2.
155.	-8.8	-13.1	50.3	0.986	3.002	1.096	1.052	0.485	2.
159.	-16.3	-21.6	40.5	0.958	2.745	1.089	1.001	0.533	0.
161.	-13.6	-14.7	35.0	0.941	2.598	1.079	0.966	0.553	2.
167.	-11.4	-13.3	39.9	0.882	2.026	0.977	0.836	0.592	2.
168.	-13.8	-15.9	34.4	0.872	1.905	0.940	0.812	0.595	0.
169.	-12.6	-15.0	33.2	0.861	1.784	0.902	0.788	0.597	0.
173.	-8.4	-13.6	45.2	0.820	1.182	0.642	0.686	0.591	0.
175.	-10.0	-16.0	43.3	0.799	0.795	0.421	0.633	0.580	2.
177.	-8.3	-13.3	38.2	0.780	0.334	0.115	0.578	0.562	2.
180.	-5.1	-11.2	36.4	0.223	0.200	0.148	0.000	0.000	1.
195.	-8.1	-17.5	23.3	0.223	0.200	0.148	0.000	0.000	1.

--- CODE EXPLANATION ---
0 -- NORMAL DATA
1 -- POST-HARVEST
2 -- BLOWN DOWN AREAS
3 -- WINDY DURING DATA ACQUISITION
4 -- RECENT HEAVY RAIN

WHEAT FIELD # 4

JULIAN DATE	SIGMAO VV	SIGMAO VH	SOIL MOIS	CANOPY HEIGHT	LEAF & STALK FRESH BIOMASS	LEAF & STALK DRY BIOMASS	----HEAD---- FRESH BIOMASS	----HEAD---- DRY BIOMASS	CODE
121.	-11.4	-19.9	18.9	0.753	3.602	0.796	0.000	0.000	0.
124.	-11.4	-17.0	--	0.848	3.745	0.932	0.000	0.000	4.
126.	-14.5	-21.5	24.0	0.896	3.816	1.000	0.000	0.000	0.
128.	-16.3	-21.8	21.8	0.938	3.849	1.043	0.000	0.000	0.
131.	-16.1	-20.5	25.7	0.986	3.787	1.061	0.130	0.040	0.
135.	-17.6	-20.9	29.6	1.029	3.519	0.998	0.479	0.157	0.
140.	-17.7	-20.8	37.8	1.053	3.440	1.016	0.617	0.193	0.
142.	-17.5	-21.0	35.2	1.055	3.373	1.012	0.687	0.218	0.
147.	-16.2	-20.8	35.1	1.047	3.154	0.993	0.845	0.299	0.
152.	-13.1	-17.4	33.4	1.024	2.897	0.978	0.939	0.395	0.
159.	-17.3	-21.0	40.5	0.980	2.453	0.962	0.953	0.523	3.
161.	-14.2	-17.6	39.1	0.966	2.300	0.951	0.936	0.554	2.
168.	-11.4	-16.8	38.5	0.918	1.631	0.825	0.827	0.618	0.
169.	-13.2	-14.2	38.1	0.911	1.520	0.790	0.805	0.621	0.
176.	-10.3	-16.9	--	0.866	0.683	0.560	0.617	0.571	0.
180.	-9.2	-12.0	49.5	0.843	0.556	0.467	0.403	0.373	0.
183.	-8.6	-11.3	50.5	0.825	0.465	0.400	0.388	0.359	0.
196.	-8.0	-16.6	37.3	0.237	0.300	0.229	0.000	0.000	1.

--- CODE EXPLANATION ---
0 -- NORMAL DATA
1 -- POST-HARVEST
2 -- BLOWN DOWN AREAS
3 -- WINDY DURING DATA ACQUISITION
4 -- RECENT HEAVY RAIN

WHEAT FIELD # 5

JULIAN DATE	SIGMAO VV	SIGMAO VH	SOIL MOIS	CANOPY HEIGHT	LEAF & STALK FRESH BIOMASS	LEAF & STALK DRY BIOMASS	HEAD FRESH BIOMASS	HEAD DRY BIOMASS	CODE
121.	-12.2	-24.8	15.4	0.823	3.239	0.865	0.000	0.000	0.
126.	-12.5	-21.5	24.5	0.923	4.177	1.111	0.000	0.000	0.
128.	-13.0	-20.5	22.1	0.950	4.410	1.169	0.000	0.000	0.
131.	-12.5	-20.5	29.8	0.981	4.506	1.183	0.127	0.040	0.
135.	-13.8	-20.3	34.0	1.006	4.377	1.139	0.363	0.117	0.
148.	-16.0	-20.3	32.5	1.017	3.542	1.070	0.635	0.200	0.
149.	-14.3	-19.9	29.2	1.015	3.438	1.055	0.664	0.217	4.
152.	-15.6	-21.0	31.3	1.007	3.129	1.014	0.738	0.270	0.
159.	-15.7	-19.8	36.0	0.976	2.461	0.921	0.821	0.405	3.
161.	-18.5	-20.9	33.1	0.963	2.287	0.896	0.824	0.442	2.
167.	-12.9	-13.7	36.7	0.908	1.827	0.843	0.793	0.533	4.
168.	-15.0	-19.9	36.8	0.896	1.758	0.835	0.782	0.544	0.
169.	-14.4	-16.9	38.0	0.882	1.693	0.830	0.770	0.554	0.
175.	-10.6	-14.0	52.8	0.772	1.343	0.818	0.672	0.573	0.
180.	-6.9	-13.0	49.5	0.631	1.100	0.820	0.554	0.526	0.
183.	-7.7	-12.5	54.0	0.517	0.889	0.772	0.487	0.463	0.
196.	-2.7	-14.3	32.5	0.230	0.350	0.290	0.000	0.000	1.

--- CODE EXPLANATION ---
0 -- NORMAL DATA
1 -- POST-HARVEST
2 -- BLOWN DOWN AREAS
3 -- WINDY DURING DATA ACQUISITION
4 -- RECENT HEAVY RAIN

WHEAT FIELD # 6

JULIAN DATE	SIGMA0 VV	SIGMA0 VH	SOIL MOIS	CANOPY HEIGHT	LEAF & STALK FRESH BIOMASS	LEAF & STALK DRY BIOMASS	----HEAD---- FRESH BIOMASS	----HEAD---- DRY BIOMASS	CODE
121.	-12.1	-18.8	5.7	0.780	2.477	0.860	0.000	0.000	0.
126.	-13.1	-19.7	14.3	0.824	2.874	1.040	0.000	0.000	0.
128.	-14.0	-19.9	9.8	0.861	2.936	1.080	0.062	0.020	0.
131.	-14.3	-18.3	23.5	0.892	2.955	1.112	0.186	0.060	0.
133.	-13.3	-18.9	--	0.896	2.627	1.004	0.581	0.206	4.
134.	-14.1	-18.3	--	0.898	2.572	0.994	0.659	0.229	4.
135.	-15.0	-15.8	30.5	0.899	2.518	0.984	0.735	0.252	0.
140.	-15.3	-18.2	32.7	0.877	2.238	0.927	1.042	0.359	0.
142.	-14.1	-16.8	26.0	0.863	2.140	0.899	1.118	0.398	0.
147.	-15.2	-18.1	32.2	0.831	1.946	0.826	1.191	0.488	0.
148.	-13.2	-16.2	--	0.826	1.911	0.812	1.189	0.504	4.
149.	-15.0	-18.8	35.2	0.821	1.878	0.797	1.184	0.520	0.
152.	-14.8	-19.5	22.5	0.810	1.780	0.758	1.152	0.564	0.
154.	-14.7	-18.3	42.1	0.805	1.706	0.730	1.121	0.590	0.
156.	-15.0	-19.3	36.8	0.803	1.626	0.703	1.085	0.614	0.
159.	-11.0	-15.0	35.2	0.804	1.495	0.663	1.027	0.646	3.
161.	-15.8	-19.7	34.7	0.805	1.392	0.631	0.989	0.664	0.
163.	-15.6	-15.7	39.4	0.807	1.283	0.598	0.950	0.679	0.
166.	-10.9	-15.0	42.4	0.806	1.099	0.542	0.896	0.697	4.
168.	-13.1	-14.8	38.3	0.801	0.961	0.494	0.861	0.705	0.
170.	-9.5	-14.4	37.1	0.792	0.843	0.482	0.828	0.710	0.
173.	-8.1	-14.6	42.1	0.762	0.800	0.477	0.747	0.650	4.
175.	-8.6	-15.1	35.5	0.730	0.747	0.474	0.636	0.560	0.
177.	-8.4	-13.5	37.4	0.684	0.625	0.442	0.543	0.502	0.
180.	-8.2	-14.3	36.3	0.270	0.466	0.435	0.000	0.000	1.
196.	-8.6	-18.2	33.0	0.270	0.466	0.435	0.000	0.000	1.

--- CODE EXPLANATION ---
0 -- NORMAL DATA
1 -- POST-HARVEST
2 -- BLOWN DOWN AREAS
3 -- WINDY DURING DATA ACQUISITION
4 -- RECENT HEAVY RAIN

WHEAT FIELD # 7

JULIAN DATE	SIGMA0 VV	SIGMA0 VH	SOIL MOIS	CANOPY HEIGHT	LEAF & STALK FRESH BIOMASS	LEAF & STALK DRY BIOMASS	----HEAD---- FRESH BIOMASS	----HEAD---- DRY BIOMASS	CODE
126.	-20.8	-24.8	22.0	0.973	4.685	1.691	0.000	0.000	0.
128.	-16.8	-22.0	16.5	0.990	4.717	1.763	0.117	0.035	0.
131.	-16.7	-21.1	30.3	0.999	4.613	1.799	0.331	0.110	0.
135.	-17.8	-18.7	35.0	0.991	4.087	1.657	0.798	0.297	0.
140.	-14.8	-19.0	37.9	0.969	3.596	1.518	0.976	0.375	0.
142.	-13.4	-18.8	36.2	0.960	3.338	1.429	1.057	0.417	0.
147.	-9.5	-13.8	35.2	0.945	2.633	1.159	1.238	0.537	0.
149.	-9.9	-12.6	21.3	0.942	2.368	1.049	1.354	0.608	0.
152.	-8.1	-13.3	26.4	0.940	2.314	1.025	1.520	0.798	0.
156.	-8.4	-12.8	40.5	0.936	2.435	1.120	1.534	0.890	0.
159.	-5.9	-8.3	38.3	0.926	2.188	1.050	1.260	0.820	3.
161.	-9.3	-11.2	38.3	0.913	2.010	1.006	1.099	0.780	0.
163.	-6.8	-8.6	43.3	0.892	1.928	1.022	0.960	0.750	4.
167.	-6.9	-7.9	39.5	0.814	1.600	0.931	0.885	0.740	4.
168.	-7.5	-10.5	41.4	0.785	1.317	0.836	0.810	0.729	0.
170.	-6.0	-9.1	38.5	0.713	0.720	0.475	0.576	0.520	0.
177.	-5.9	-11.1	39.1	0.220	0.404	0.291	0.000	0.000	1.
196.	-6.9	-16.4	22.8	0.187	0.339	0.269	0.000	0.000	1.

--- CODE EXPLANATION ---
0 -- NORMAL DATA
1 -- POST-HARVEST
2 -- BLOWN DOWN AREAS
3 -- WINDY DURING DATA ACQUISITION
4 -- RECENT HEAVY RAIN

WHEAT FIELD # 8

JULIAN DATE	SIGMA0 VV	SIGMA0 VH	SOIL MOIS	CANOPY HEIGHT	LEAF & STALK FRESH BIOMASS	LEAF & STALK DRY BIOMASS	HEAD FRESH BIOMASS	HEAD DRY BIOMASS	CODE
121.	-15.8	-21.0	13.3	0.851	3.173	0.952	0.000	0.000	0.
126.	-17.7	-20.8	22.2	0.974	3.706	1.201	0.000	0.000	0.
128.	-15.4	-19.4	20.7	1.006	3.805	1.259	0.000	0.000	0.
131.	-14.6	-18.1	26.2	1.038	3.717	1.264	0.136	0.046	0.
133.	-16.9	-19.0	--	1.050	3.351	1.159	0.453	0.159	4.
134.	-14.9	-19.0	--	1.054	3.266	1.140	0.521	0.180	4.
135.	-15.5	-19.2	31.3	1.058	3.183	1.123	0.588	0.200	0.
140.	-15.4	-18.7	33.7	1.056	2.650	0.996	0.865	0.297	0.
142.	-15.1	-19.2	25.7	1.049	2.454	0.945	0.937	0.333	0.
148.	-15.3	-20.1	31.0	1.014	1.947	0.794	1.022	0.432	0.
149.	-15.6	-20.1	33.0	1.007	1.879	0.774	1.021	0.447	0.
152.	-16.6	-21.0	27.2	0.984	1.693	0.719	1.003	0.489	0.
154.	-14.2	-18.8	36.9	0.968	1.590	0.691	0.982	0.515	4.
156.	-16.0	-19.4	37.6	0.951	1.496	0.668	0.957	0.539	0.
159.	-14.6	-17.1	33.9	0.926	1.370	0.640	0.914	0.570	3.
161.	-16.2	-15.2	34.9	0.910	1.396	0.670	0.885	0.588	0.
163.	-10.7	-15.5	33.7	0.893	1.298	0.675	0.856	0.603	4.
166.	-11.8	-16.7	41.9	0.867	1.259	0.680	0.813	0.622	4.
168.	-8.3	-14.6	33.3	0.849	1.040	0.677	0.786	0.630	0.
170.	-5.1	-10.5	32.3	0.830	1.210	0.669	0.760	0.636	4.
173.	-6.4	-14.2	40.3	0.801	0.950	0.665	0.723	0.640	0.
175.	-7.0	-13.0	37.3	0.779	0.807	0.665	0.699	0.639	0.
177.	-6.9	-13.5	36.2	0.755	0.732	0.664	0.677	0.634	0.
180.	-8.4	-13.6	35.9	0.714	0.709	0.650	0.656	0.621	0.
183.	-6.6	-11.8	37.0	0.665	0.576	0.550	0.627	0.600	0.
196.	-5.0	-12.4	23.6	0.233	0.205	0.180	0.000	0.000	1.

--- CODE EXPLANATION ---
0 -- NORMAL DATA
1 -- POST-HARVEST
2 -- BLOWN DOWN AREAS
3 -- WINDY DURING DATA ACQUISITION
4 -- RECENT HEAVY RAIN

WHEAT FIELD # 9

JULIAN DATE	SIGMAO VV	SIGMAO VH	SOIL MOIS	CANOPY HEIGHT	LEAF & STALK FRESH BIOMASS	LEAF & STALK DRY BIOMASS	----HEAD---- FRESH BIOMASS	----HEAD---- DRY BIOMASS	CODE
121.	-18.0	-23.6	4.9	0.597	1.537	0.598	0.000	0.000	0.
126.	-18.3	-21.6	12.6	0.716	2.216	0.856	0.000	0.000	0.
128.	-15.6	-20.5	10.4	0.742	2.316	0.908	0.059	0.018	0.
131.	-13.7	-17.1	15.0	0.764	2.338	0.951	0.190	0.060	0.
133.	-14.2	-20.9	--	0.768	2.057	0.852	0.507	0.195	4.
134.	-12.2	-16.7	--	0.770	2.017	0.848	0.559	0.211	4.
135.	-11.3	-15.3	19.6	0.771	1.980	0.845	0.608	0.226	0.
139.	-11.2	-16.1	22.5	0.763	1.755	0.794	0.764	0.279	0.
140.	-11.2	-16.2	22.1	0.760	1.701	0.778	0.791	0.291	0.
142.	-12.2	-17.3	21.1	0.752	1.582	0.735	0.832	0.313	0.
148.	-13.3	-18.0	18.6	0.731	1.264	0.573	0.857	0.371	0.
149.	-14.0	-17.4	18.6	0.728	1.225	0.551	0.851	0.379	0.
152.	-16.1	-19.8	16.8	0.722	1.104	0.475	0.824	0.406	0.
154.	-14.0	-16.9	25.4	0.720	1.126	0.473	0.803	0.424	0.
156.	-11.9	-15.4	26.5	0.719	1.100	0.462	0.780	0.442	0.
159.	-10.0	-15.3	21.3	0.720	1.061	0.454	0.748	0.473	3.
161.	-11.5	-15.5	17.8	0.722	1.047	0.450	0.730	0.495	0.
163.	-8.3	-12.7	24.6	0.723	0.898	0.449	0.715	0.520	4.
166.	-8.5	-13.1	28.2	0.722	0.763	0.448	0.698	0.562	4.
168.	-6.3	-15.1	22.9	0.719	0.688	0.447	0.692	0.594	0.
170.	-4.4	-12.7	22.5	0.302	0.218	0.161	0.000	0.000	1.
173.	-5.6	-15.9	26.7	0.287	0.218	0.162	0.000	0.000	1.
196.	-10.1	-17.6	4.6	0.267	0.184	0.161	0.000	0.000	1.

--- CODE EXPLANATION ---
0 -- NORMAL DATA
1 -- POST-HARVEST
2 -- BLOWN DOWN AREAS
3 -- WINDY DURING DATA ACQUISITION
4 -- RECENT HEAVY RAIN

WHEAT FIELD # 10

JULIAN DATE	SIGMA0 VV	SIGMA0 VH	SOIL MOIS	CANOPY HEIGHT	LEAF & STALK FRESH BIOMASS	LEAF & STALK DRY BIOMASS	----HEAD---- FRESH BIOMASS	----HEAD---- DRY BIOMASS	CODE
121.	-11.2	-19.3	9.5	0.290	0.402	0.173	0.000	0.000	0.
126.	-15.1	-20.3	24.7	0.386	0.823	0.276	0.000	0.000	0.
128.	-13.5	-19.3	16.2	0.417	0.992	0.314	0.000	0.000	0.
131.	-13.7	-18.7	18.2	0.474	1.202	0.359	0.000	0.000	0.
133.	-12.5	-17.3	--	0.525	1.324	0.385	0.000	0.000	4.
134.	-7.6	-14.2	--	0.542	1.364	0.394	0.000	0.000	4.
135.	-14.0	-18.8	29.9	0.559	1.405	0.403	0.000	0.000	0.
140.	-9.6	-18.0	32.1	0.666	1.564	0.450	0.000	0.000	4.
142.	-16.6	-20.5	26.2	0.706	1.531	0.442	0.062	0.021	3.
148.	-16.1	-19.3	22.9	0.807	1.413	0.442	0.184	0.055	0.
149.	-16.0	-20.3	34.7	0.820	1.357	0.432	0.228	0.069	0.
152.	-15.8	-19.0	24.5	0.853	1.207	0.403	0.323	0.106	0.
154.	-15.3	-17.9	26.0	0.869	1.121	0.391	0.362	0.125	4.
156.	-17.2	-21.3	21.5	0.880	1.039	0.380	0.384	0.139	0.
159.	-16.6	-17.8	23.4	0.887	0.925	0.368	0.392	0.155	3.
161.	-17.7	-13.6	13.3	0.886	0.855	0.362	0.384	0.162	0.
163.	-16.8	-14.4	26.4	0.881	0.789	0.360	0.366	0.166	4.
166.	-10.3	-11.5	30.0	0.866	0.698	0.358	0.330	0.170	4.
168.	-10.7	-14.6	28.8	0.853	0.633	0.356	0.303	0.171	0.
170.	-9.1	-12.4	28.8	0.837	0.571	0.353	0.275	0.172	0.
173.	-5.6	-10.8	42.3	0.811	0.473	0.341	0.235	0.173	2.
175.	-6.1	-12.6	29.5	0.794	0.393	0.315	0.212	0.175	0.
177.	-6.6	-10.2	26.9	0.778	0.280	0.252	0.192	0.178	0.
180.	-5.1	-12.5	24.2	0.273	0.239	0.152	0.000	0.000	1.
196.	-7.8	-15.1	--	0.198	0.136	0.093	0.000	0.000	1.

--- CODE EXPLANATION ---
0 -- NORMAL DATA
1 -- POST-HARVEST
2 -- BLOWN DOWN AREAS
3 -- WINDY DURING DATA ACQUISITION
4 -- RECENT HEAVY RAIN

CORN FIELD # 1

JULIAN DATE	SIGMA0 VV	SIGMA0 VH	SOIL MOIS	--STALK--- FRESH BIOMASS	DRY BIOMASS	CANOPY HEIGHT	--FRUIT--- FRESH BIOMASS	DRY BIOMASS	---LEAF--- FRESH BIOMASS	DRY BIOMASS	CODE
139.	-10.2	-19.2	30.5	0.066	0.013	0.168	0.000	0.000	0.090	0.018	0.
141.	-10.2	-17.9	27.0	0.082	0.015	0.257	0.000	0.000	0.105	0.019	0.
146.	-7.5	-14.7	22.8	0.204	0.029	0.504	0.000	0.000	0.213	0.031	4.
147.	-10.2	-17.6	14.0	0.279	0.039	0.557	0.000	0.000	0.279	0.039	0.
149.	-7.0	-14.0	27.5	0.440	0.057	0.664	0.000	0.000	0.406	0.052	0.
154.	-5.6	-13.1	33.5	0.905	0.100	0.943	0.000	0.000	0.683	0.075	4.
155.	-5.0	-12.1	31.7	1.008	0.108	1.000	0.000	0.000	0.730	0.078	4.
156.	-5.7	-13.9	27.4	1.113	0.116	1.056	0.000	0.000	0.774	0.080	4.
160.	-5.9	-13.0	25.0	1.566	0.152	1.281	0.000	0.000	0.920	0.089	0.
163.	-6.8	-12.5	30.0	1.932	0.183	1.446	0.000	0.000	0.996	0.095	0.
167.	-7.4	-12.5	34.1	2.453	0.238	1.658	0.000	0.000	1.051	0.102	4.
169.	-7.5	-16.1	28.4	2.722	0.269	1.759	0.000	0.000	1.058	0.105	4.
170.	-7.4	-15.4	31.0	2.850	0.285	1.808	0.000	0.000	1.064	0.106	4.
175.	-8.9	-13.4	29.9	3.229	0.296	2.037	0.250	0.080	1.078	0.130	0.
176.	-7.4	-13.7	27.8	3.250	0.298	2.079	0.350	0.100	1.079	0.135	0.
183.	-7.0	-12.4	33.7	2.917	0.290	2.338	1.459	0.275	1.180	0.201	0.
194.	-7.5	-14.7	14.3	2.611	0.438	2.599	2.334	0.463	1.274	0.281	0.
196.	-7.6	-14.1	14.4	2.607	0.465	2.627	2.429	0.517	1.258	0.277	0.
198.	-8.2	-14.4	8.9	2.635	0.501	2.649	2.495	0.575	1.232	0.273	0.
201.	-6.9	-12.9	28.4	2.688	0.530	2.671	2.551	0.669	1.173	0.269	4.
204.	-8.9	-16.7	24.6	2.752	0.551	2.681	2.566	0.769	1.098	0.265	0.
209.	-8.6	-15.7	21.6	2.828	0.556	2.672	2.533	0.939	0.951	0.260	0.
210.	-8.4	-14.6	30.8	2.830	0.549	2.667	2.521	0.973	0.921	0.259	0.
211.	-8.1	-14.7	29.9	2.837	0.550	2.660	2.508	1.006	0.890	0.258	0.
216.	-8.4	-13.1	47.3	2.758	0.488	2.616	2.428	1.167	0.745	0.255	0.
218.	-9.0	-16.6	34.7	2.697	0.456	2.593	2.391	1.227	0.691	0.253	0.
222.	-8.8	-15.8	26.7	2.785	0.473	2.541	2.312	1.332	0.593	0.250	0.
224.	-9.1	-16.0	22.3	2.828	0.486	2.514	2.270	1.377	0.549	0.249	0.
225.	-10.1	-16.9	25.4	2.846	0.491	2.500	2.248	1.397	0.528	0.248	0.
236.	-12.4	-17.9	13.6	2.535	0.502	2.370	1.971	1.485	0.343	0.235	0.
240.	-5.0	-13.0	30.0	2.432	0.498	2.349	1.846	1.441	0.292	0.227	0.
242.	-7.5	-13.9	25.8	2.295	0.485	2.348	1.776	1.401	0.269	0.223	0.
244.	-4.8	-12.5	35.0	2.137	0.468	2.348	1.699	1.348	0.247	0.218	4.
246.	-4.8	-12.8	29.5	1.968	0.446	2.348	1.614	1.281	0.227	0.212	0.
249.	-8.7	-14.6	27.8	1.677	0.405	2.348	1.468	1.153	0.203	0.203	0.
251.	-4.4	-12.1	28.7	1.325	0.400	2.348	1.355	1.047	0.195	0.195	4.
256.	-8.3	-15.5	27.2	0.439	0.248	0.440	0.000	0.000	0.000	0.000	1.

--- CODE EXPLANATION ---
0 -- NORMAL DATA
1 -- POST-HARVEST
3 -- WINDY DURING DATA ACQUISITION
4 -- RECENT HEAVY RAIN

CORN FIELD # 2

JULIAN DATE	SIGMAO VV	SIGMAO VH	SOIL MOIS	--STALK--- FRESH BIOMASS	DRY BIOMASS	CANOPY HEIGHT	--FRUIT--- FRESH BIOMASS	DRY BIOMASS	---LEAF--- FRESH BIOMASS	DRY BIOMASS	CODE
139.	-7.5	-18.4	39.9	0.063	0.013	0.350	0.000	0.000	0.086	0.018	4.
141.	-9.6	-18.5	27.9	0.101	0.018	0.362	0.000	0.000	0.129	0.023	0.
147.	-10.3	-19.1	24.0	0.322	0.038	0.540	0.000	0.000	0.321	0.038	0.
149.	-8.0	-14.4	36.1	0.475	0.050	0.636	0.000	0.000	0.438	0.047	0.
154.	-5.2	-11.8	40.6	0.934	0.083	0.929	0.000	0.000	0.704	0.063	4.
155.	-4.6	-10.9	39.6	1.039	0.092	0.994	0.000	0.000	0.752	0.066	4.
156.	-5.1	-12.9	39.7	1.148	0.100	1.061	0.000	0.000	0.797	0.069	4.
160.	-5.1	-13.9	28.5	1.623	0.144	1.335	0.000	0.000	0.953	0.085	4.
163.	-4.1	-12.1	39.9	2.018	0.192	1.542	0.000	0.000	1.040	0.099	4.
167.	-6.8	-12.9	37.7	2.591	0.277	1.809	0.000	0.000	1.110	0.119	4.
169.	-4.4	-11.8	35.3	2.891	0.330	1.935	0.000	0.000	1.124	0.128	4.
170.	-5.7	-12.2	34.7	3.045	0.359	1.996	0.000	0.000	1.126	0.133	4.
175.	-7.3	-11.4	39.6	3.304	0.420	2.270	0.470	0.100	1.130	0.157	0.
176.	-7.0	-13.8	41.8	3.405	0.432	2.319	0.500	0.110	1.135	0.174	0.
183.	-7.8	-12.4	38.3	4.003	0.572	2.587	0.720	0.190	1.138	0.240	0.
194.	-8.3	-14.9	19.4	4.126	0.734	2.763	1.229	0.333	1.109	0.271	0.
196.	-9.7	-16.5	18.1	4.010	0.730	2.767	1.357	0.371	1.097	0.269	0.
197.	-7.8	-14.0	14.8	3.938	0.726	2.766	1.428	0.395	1.091	0.267	0.
201.	-8.5	-13.7	42.8	3.541	0.636	2.752	1.719	0.519	1.062	0.261	4.
204.	-7.0	-13.0	39.9	3.189	0.529	2.733	1.911	0.633	1.039	0.256	0.
209.	-8.0	-14.1	40.1	3.281	0.525	2.703	2.127	0.841	1.003	0.248	4.
210.	-8.6	-14.8	39.2	3.255	0.520	2.699	2.154	0.883	0.996	0.246	0.
211.	-7.6	-13.7	40.1	3.190	0.510	2.697	2.176	0.925	0.989	0.245	0.
216.	-8.7	-15.0	39.2	3.474	0.405	2.697	2.210	1.115	0.963	0.241	4.
223.	-8.7	-15.1	33.2	2.389	0.372	2.697	2.000	1.000	0.951	0.246	0.
224.	-6.3	-17.4	29.7	0.460	0.066	0.243	0.000	0.000	0.000	0.000	1.
225.	-6.3	-16.4	22.2	0.494	0.099	0.198	0.000	0.000	0.000	0.000	1.

--- CODE EXPLANATION ---
0 -- NORMAL DATA
1 -- POST-HARVEST
3 -- WINDY DURING DATA ACQUISITION
4 -- RECENT HEAVY RAIN

CORN FIELD # 3

JULIAN DATE	SIGMAO VV	SIGMAO VH	SOIL MOIS	--STALK--- FRESH BIOMASS	DRY BIOMASS	CANOPY HEIGHT	--FRUIT--- FRESH BIOMASS	DRY BIOMASS	---LEAF--- FRESH BIOMASS	DRY BIOMASS	CODE
139.	-7.4	-18.2	34.2	0.039	0.007	0.277	0.000	0.000	0.055	0.010	4.
141.	-8.7	-17.7	36.4	0.053	0.009	0.276	0.000	0.000	0.068	0.012	0.
146.	-10.5	-18.5	31.2	0.111	0.017	0.363	0.000	0.000	0.116	0.017	0.
147.	-11.9	-18.8	28.8	0.169	0.024	0.393	0.000	0.000	0.168	0.025	0.
149.	-5.3	-13.0	34.1	0.300	0.041	0.405	0.000	0.000	0.277	0.037	4.
154.	-5.4	-12.5	36.8	0.725	0.084	0.696	0.000	0.000	0.547	0.064	4.
155.	-5.9	-12.2	37.0	0.824	0.092	0.750	0.000	0.000	0.597	0.067	4.
156.	-7.3	-14.3	33.5	0.929	0.101	0.805	0.000	0.000	0.646	0.071	0.
160.	-5.9	-12.1	29.0	1.390	0.135	1.040	0.000	0.000	0.816	0.079	4.
163.	-6.1	-12.4	32.1	1.776	0.162	1.226	0.000	0.000	0.915	0.083	4.
167.	-5.9	-12.3	36.6	2.335	0.187	1.477	0.000	0.000	1.001	0.100	4.
169.	-6.6	-12.5	28.9	2.628	0.187	1.602	0.000	0.000	1.022	0.120	4.
170.	-5.5	-12.5	31.7	2.780	0.190	1.663	0.000	0.000	1.028	0.130	4.
176.	-7.1	-12.9	33.7	3.431	0.176	2.013	0.200	0.065	1.078	0.173	0.
183.	-7.1	-12.1	27.7	3.074	0.192	2.356	1.452	0.148	1.114	0.241	0.
194.	-7.9	-14.5	13.7	3.155	0.290	2.704	2.377	0.445	1.223	0.278	0.
196.	-7.9	-14.9	12.3	3.183	0.321	2.740	2.460	0.507	1.258	0.283	0.
197.	-8.5	-14.5	8.2	3.198	0.341	2.754	2.495	0.538	1.276	0.285	0.
201.	-7.1	-13.5	26.8	3.243	0.425	2.791	2.598	0.665	1.345	0.290	4.
204.	-7.7	-14.5	22.6	3.261	0.493	2.798	2.643	0.760	1.387	0.293	0.
209.	-8.5	-16.0	30.2	3.258	0.596	2.775	2.670	0.914	1.410	0.295	4.
210.	-10.3	-17.2	31.0	3.255	0.615	2.765	2.670	0.944	1.404	0.295	4.
211.	-9.1	-16.0	27.2	3.252	0.634	2.755	2.668	0.973	1.394	0.295	0.
216.	-7.8	-14.6	23.4	3.219	0.702	2.685	2.633	1.110	1.285	0.294	4.
217.	-6.4	-12.9	34.5	3.209	0.711	2.669	2.622	1.135	1.252	0.293	4.
223.	-7.1	-14.6	30.1	3.078	0.699	2.566	2.527	1.265	1.002	0.289	0.
225.	-7.3	-14.6	28.6	2.992	0.664	2.533	2.485	1.298	0.911	0.287	0.
236.	-7.9	-14.9	13.1	2.771	0.493	2.520	2.166	1.375	0.490	0.276	0.
240.	-9.3	-15.6	31.0	2.891	0.484	2.502	2.010	1.348	0.387	0.273	0.
242.	-9.1	-16.1	27.5	2.938	0.476	2.500	1.923	1.321	0.345	0.271	0.
244.	-8.6	-13.6	18.3	3.014	0.464	2.500	1.830	1.285	0.308	0.270	4.
246.	-8.9	-13.8	22.7	3.072	0.451	2.500	1.730	1.240	0.276	0.269	0.
249.	-6.6	-12.0	23.5	2.034	0.557	0.440	0.000	0.000	0.000	0.000	1.

--- CODE EXPLANATION ---
0 -- NORMAL DATA
1 -- POST-HARVEST
3 -- WINDY DURING DATA ACQUISITION
4 -- RECENT HEAVY RAIN

CORN FIELD # 4

JULIAN DATE	SIGMAO VV	SIGMAO VH	SOIL MOIS	--STALK--- FRESH BIOMASS	DRY BIOMASS	CANOPY HEIGHT	--FRUIT--- FRESH BIOMASS	DRY BIOMASS	---LEAF--- FRESH BIOMASS	DRY BIOMASS	CODE
139.	-7.8	-19.5	33.9	0.132	0.031	0.302	0.000	0.000	0.183	0.042	4.
141.	-5.6	-15.1	31.9	0.188	0.037	0.350	0.000	0.000	0.239	0.046	0.
147.	-8.3	-14.9	24.6	0.604	0.071	0.602	0.000	0.000	0.603	0.070	0.
149.	-4.8	-12.4	32.0	0.847	0.086	0.713	0.000	0.000	0.782	0.080	4.
154.	-5.3	-12.2	41.5	1.564	0.105	1.028	0.000	0.000	1.179	0.120	4.
155.	-5.3	-11.8	38.3	1.725	0.101	1.096	0.000	0.000	1.250	0.140	4.
156.	-6.2	-13.5	42.5	1.892	0.107	1.164	0.000	0.000	1.314	0.150	4.
160.	-4.6	-12.0	27.1	2.611	0.184	1.442	0.000	0.000	1.534	0.160	4.
163.	-6.0	-11.7	32.0	3.199	0.256	1.650	0.000	0.000	1.648	0.180	4.
167.	-6.5	-12.2	36.0	4.033	0.389	1.917	0.000	0.000	1.728	0.210	4.
169.	-5.4	-11.0	32.9	4.467	0.461	2.043	0.000	0.000	1.737	0.240	4.
170.	-5.3	-12.1	31.0	4.682	0.490	2.105	0.000	0.000	1.732	0.260	4.
176.	-6.3	-12.6	32.8	5.452	0.668	2.434	0.300	0.090	1.820	0.340	0.
183.	-6.7	-12.1	30.2	5.170	0.736	2.721	1.475	0.266	1.898	0.493	0.
194.	-7.9	-15.5	15.0	4.281	0.790	2.940	2.919	0.655	1.818	0.449	0.
196.	-6.9	-14.0	15.4	4.167	0.754	2.951	3.010	0.735	1.793	0.439	0.
197.	-8.5	-14.6	14.5	4.108	0.727	2.954	3.040	0.776	1.780	0.434	0.
201.	-6.2	-13.1	26.8	3.849	0.716	2.949	3.096	0.941	1.724	0.415	4.
204.	-6.7	-14.4	26.4	3.785	0.704	2.931	3.095	1.065	1.681	0.401	0.
209.	-7.2	-14.1	36.1	3.683	0.685	2.887	3.063	1.266	1.617	0.385	4.
210.	-7.1	-14.2	36.9	3.608	0.671	2.877	3.056	1.304	1.606	0.382	4.
211.	-6.5	-13.4	43.8	3.586	0.667	2.868	3.049	1.342	1.596	0.380	0.
216.	-7.7	-15.0	39.6	3.532	0.657	2.831	3.026	1.519	1.562	0.378	4.
217.	-7.2	-13.2	37.4	3.495	0.650	2.828	3.025	1.551	1.543	0.375	4.
219.	-9.0	-17.9	36.7	3.452	0.642	2.826	3.026	1.611	1.504	0.370	4.
223.	-7.0	-15.0	31.6	3.415	0.632	2.825	3.049	1.716	1.457	0.370	0.
225.	-7.0	-13.6	36.9	3.286	0.628	2.824	3.073	1.758	1.415	0.368	0.

--- CODE EXPLANATION ---
0 -- NORMAL DATA
1 -- POST-HARVEST
3 -- WINDY DURING DATA ACQUISITION
4 -- RECENT HEAVY RAIN

CORN FIELD # 5

JULIAN DATE	SIGMAO VV	SIGMAO VH	SOIL MOIS	--STALK--- FRESH BIOMASS	DRY BIOMASS	CANOPY HEIGHT	--FRUIT--- FRESH BIOMASS	DRY BIOMASS	---LEAF--- FRESH BIOMASS	DRY BIOMASS	CODE
139.	-8.8	-17.8	33.2	0.066	0.014	0.301	0.000	0.000	0.090	0.019	4.
141.	-8.0	-15.2	28.6	0.102	0.019	0.336	0.000	0.000	0.129	0.024	0.
146.	-7.1	-15.9	24.7	0.275	0.038	0.489	0.000	0.000	0.287	0.040	0.
147.	-6.7	-14.0	20.1	0.348	0.045	0.529	0.000	0.000	0.348	0.046	0.
149.	-6.0	-12.3	26.6	0.502	0.059	0.617	0.000	0.000	0.464	0.055	0.
154.	-5.7	-12.0	34.3	0.950	0.095	0.873	0.000	0.000	0.717	0.072	4.
155.	-5.7	-12.6	36.9	1.050	0.103	0.928	0.000	0.000	0.760	0.074	4.
156.	-5.0	-14.0	31.5	1.152	0.111	0.985	0.000	0.000	0.801	0.077	0.
160.	-4.2	-12.6	27.0	1.598	0.152	1.219	0.000	0.000	0.939	0.089	0.
163.	-5.8	-13.4	31.2	1.963	0.190	1.398	0.000	0.000	1.011	0.098	4.
167.	-6.7	-12.8	35.9	2.493	0.265	1.634	0.000	0.000	1.069	0.113	4.
169.	-5.2	-11.9	25.9	2.771	0.307	1.748	0.000	0.000	1.078	0.120	4.
170.	-5.4	-13.4	26.6	2.914	0.328	1.804	0.000	0.000	1.078	0.127	4.
175.	-6.3	-12.0	28.2	3.493	0.410	2.066	0.150	0.045	1.078	0.158	0.
176.	-5.6	-12.1	27.5	3.537	0.422	2.115	0.200	0.060	1.078	0.168	0.
183.	-6.6	-11.5	30.6	3.024	0.480	2.408	1.550	0.196	1.079	0.240	0.
194.	-6.8	-13.3	10.5	3.128	0.553	2.680	2.331	0.487	1.079	0.281	0.
196.	-8.7	-15.4	6.0	3.174	0.567	2.703	2.377	0.535	1.080	0.284	0.
197.	-6.7	-13.2	8.5	3.175	0.570	2.712	2.394	0.558	1.095	0.285	0.
201.	-6.9	-12.7	28.9	3.164	0.579	2.729	2.425	0.645	1.154	0.286	4.
204.	-7.6	-15.8	24.1	3.130	0.578	2.723	2.419	0.707	1.191	0.285	0.
209.	-6.8	-14.9	34.5	3.024	0.552	2.684	2.368	0.800	1.216	0.280	4.
210.	-7.1	-14.7	34.8	2.991	0.537	2.672	2.353	0.818	1.213	0.278	4.
211.	-8.1	-16.2	39.3	2.966	0.528	2.660	2.337	0.835	1.206	0.277	0.
216.	-6.9	-12.2	29.6	2.833	0.468	2.585	2.238	0.914	1.114	0.269	4.
217.	-6.4	-12.9	38.2	2.805	0.453	2.568	2.215	0.928	1.084	0.267	4.
219.	-7.5	-14.0	28.9	2.483	0.447	2.535	2.168	0.956	1.017	0.264	4.
223.	-7.2	-14.3	21.0	2.472	0.445	2.470	2.065	1.007	0.861	0.259	0.
225.	-7.3	-15.0	26.6	2.467	0.444	2.441	2.012	1.030	0.780	0.257	0.
240.	-8.1	-13.8	27.3	2.428	0.437	2.440	1.585	1.149	0.324	0.250	0.
242.	-8.7	-14.2	29.9	2.417	0.435	2.435	1.528	1.158	0.285	0.248	0.
244.	-6.2	-12.7	45.3	2.268	0.433	2.430	1.471	1.166	0.259	0.246	4.
246.	-5.1	-10.7	26.9	1.066	0.327	0.660	0.000	0.000	0.000	0.000	1.

--- CODE EXPLANATION ---
0 -- NORMAL DATA
1 -- POST-HARVEST
3 -- WINDY DURING DATA ACQUISITION
4 -- RECENT HEAVY RAIN.

CORN FIELD # 6

JULIAN DATE	SIGMAO VV	SIGMAO VH	SOIL MOIS	--STALK--- FRESH BIOMASS	DRY BIOMASS	CANOPY HEIGHT	--FRUIT--- FRESH BIOMASS	DRY BIOMASS	---LEAF--- FRESH BIOMASS	DRY BIOMASS	CODE
139.	-6.2	-16.5	36.3	0.107	0.018	0.247	0.000	0.000	0.148	0.025	4.
142.	-7.7	-16.0	30.2	0.151	0.023	0.404	0.000	0.000	0.184	0.028	0.
147.	-7.6	-14.2	30.0	0.438	0.057	0.682	0.000	0.000	0.438	0.056	0.
148.	-5.6	-13.1	--	0.537	0.066	0.740	0.000	0.000	0.515	0.064	4.
149.	-7.0	-13.4	34.3	0.639	0.076	0.797	0.000	0.000	0.589	0.071	0.
154.	-5.5	-12.4	34.3	1.185	0.122	1.088	0.000	0.000	0.894	0.092	4.
155.	-5.9	-12.1	34.4	1.300	0.130	1.147	0.000	0.000	0.942	0.094	4.
156.	-6.0	-13.3	31.5	1.419	0.136	1.205	0.000	0.000	0.986	0.100	4.
160.	-6.8	-14.7	42.4	1.906	0.162	1.433	0.000	0.000	1.120	0.107	0.
163.	-5.0	-11.0	33.3	2.289	0.165	1.599	0.000	0.000	1.179	0.130	4.
166.	-6.8	-14.0	37.7	2.681	0.172	1.760	0.000	0.000	1.204	0.150	4.
167.	-7.4	-11.6	38.4	2.677	0.174	1.811	0.000	0.000	1.206	0.190	4.
169.	-5.4	-12.8	25.5	2.794	0.176	1.912	0.000	0.000	1.220	0.200	4.
170.	-6.0	-12.8	29.7	2.950	0.177	1.961	0.000	0.000	1.230	0.210	4.
175.	-6.5	-11.9	25.5	3.111	0.181	2.190	0.620	0.120	1.258	0.243	0.
176.	-5.7	-12.3	23.4	3.009	0.200	2.232	0.820	0.150	1.270	0.254	0.
177.	-5.6	-11.4	31.1	2.677	0.246	2.273	1.235	0.173	1.292	0.265	0.
194.	-6.4	-13.5	17.1	2.363	0.311	2.766	2.861	0.442	1.289	0.270	0.
197.	-8.3	-15.0	10.1	2.525	0.359	2.811	2.835	0.518	1.278	0.271	0.
198.	-7.6	-14.2	15.7	2.580	0.379	2.824	2.824	0.545	1.272	0.271	0.
202.	-7.0	-13.1	--	2.765	0.449	2.860	2.777	0.655	1.235	0.272	0.
204.	-7.1	-13.3	19.0	2.840	0.479	2.871	2.751	0.711	1.208	0.272	0.
209.	-7.6	-14.3	35.7	2.998	0.561	2.877	2.675	0.853	1.120	0.271	4.
210.	-7.6	-15.0	37.2	3.025	0.577	2.875	2.658	0.881	1.098	0.271	4.
211.	-7.0	-14.2	29.0	3.038	0.584	2.872	2.641	0.909	1.076	0.270	0.
216.	-6.3	-12.6	32.6	3.090	0.635	2.845	2.548	1.042	0.954	0.268	4.
217.	-6.8	-13.0	37.8	3.091	0.642	2.837	2.528	1.067	0.929	0.268	4.
220.	-7.8	-14.9	--	3.055	0.642	2.810	2.465	1.137	0.850	0.266	0.
222.	-7.7	-15.5	33.5	3.015	0.638	2.790	2.421	1.180	0.798	0.264	0.
223.	-7.8	-13.7	29.0	2.986	0.629	2.779	2.398	1.200	0.772	0.264	0.
226.	-7.8	-15.2	28.0	2.882	0.597	2.746	2.324	1.254	0.696	0.262	0.
242.	-6.1	-13.6	28.3	2.613	0.468	2.621	1.820	1.317	0.381	0.251	0.
245.	-4.6	-12.6	33.5	2.599	0.455	2.620	1.697	1.274	0.340	0.250	4.
247.	-4.2	-12.8	--	2.586	0.443	2.620	1.608	1.234	0.316	0.249	0.
249.	-4.9	-13.8	29.0	2.576	0.428	2.620	1.514	1.185	0.293	0.249	0.
252.	-4.9	-13.9	33.2	2.529	0.400	2.620	1.359	1.091	0.263	0.248	0.
258.	-9.6	-16.2	--	2.113	0.321	2.620	1.159	0.950	0.249	0.249	0.

--- CODE EXPLANATION ---
0 -- NORMAL DATA
1 -- POST-HARVEST
3 -- WINDY DURING DATA ACQUISITION
4 -- RECENT HEAVY RAIN

CORN FIELD # 7

JULIAN DATE	SIGMA0 VV	SIGMA0 VH	SOIL MOIS	--STALK--- FRESH BIOMASS	DRY BIOMASS	CANOPY HEIGHT	--FRUIT--- FRESH BIOMASS	DRY BIOMASS	---LEAF--- FRESH BIOMASS	DRY BIOMASS	CODE
140.	-12.2	-18.9	36.3	0.037	0.006	0.178	0.000	0.000	0.050	0.009	0.
142.	-10.2	-18.1	23.2	0.069	0.011	0.225	0.000	0.000	0.085	0.014	0.
147.	-13.3	-18.4	21.7	0.084	0.012	0.382	0.000	0.000	0.083	0.012	0.
148.	-9.4	-17.0	--	0.133	0.018	0.420	0.000	0.000	0.128	0.018	4.
149.	-9.6	-16.2	29.2	0.184	0.025	0.458	0.000	0.000	0.170	0.023	0.
154.	-4.4	-12.8	38.1	0.530	0.064	0.672	0.000	0.000	0.399	0.048	4.
155.	-3.8	-11.0	45.2	0.614	0.072	0.718	0.000	0.000	0.444	0.053	4.
156.	-5.1	-12.6	38.3	0.703	0.081	0.765	0.000	0.000	0.488	0.057	4.
160.	-7.0	-13.8	21.2	1.102	0.096	0.957	0.000	0.000	0.647	0.095	0.
163.	-5.2	-12.6	41.0	1.443	0.112	1.105	0.000	0.000	0.743	0.120	4.
166.	-6.6	-13.9	42.1	1.813	0.119	1.253	0.000	0.000	0.815	0.154	4.
167.	-5.4	-12.6	39.4	1.943	0.129	1.302	0.000	0.000	0.833	0.160	4.
169.	-6.4	-13.7	30.1	2.209	0.149	1.399	0.000	0.000	0.859	0.170	4.
170.	-5.3	-12.8	--	2.344	0.158	1.446	0.000	0.000	0.867	0.176	4.
176.	-7.4	-14.1	35.2	2.692	0.185	1.719	0.360	0.050	0.994	0.210	0.
194.	-7.1	-13.4	12.3	2.458	0.267	2.313	2.057	0.381	1.400	0.352	0.
197.	-1.1	-13.7	20.8	2.100	0.272	2.371	2.597	0.504	1.397	0.345	9.
198.	-8.1	-14.7	12.7	2.050	0.276	2.388	2.721	0.541	1.371	0.344	0.
202.	-8.4	-14.6	34.8	2.033	0.318	2.441	2.966	0.672	1.288	0.337	0.
204.	-7.0	-14.2	32.9	2.105	0.351	2.460	2.972	0.727	1.253	0.334	0.
209.	-8.5	-14.7	43.6	2.358	0.437	2.485	2.801	0.843	1.175	0.329	4.
210.	-8.8	-14.2	40.8	2.404	0.452	2.487	2.750	0.862	1.160	0.328	4.
211.	-8.0	-14.3	36.7	2.447	0.465	2.488	2.696	0.880	1.144	0.327	0.
216.	-8.5	-13.3	34.6	2.609	0.542	2.478	2.419	0.957	1.061	0.322	4.
217.	-6.9	-13.8	39.7	2.618	0.547	2.473	2.366	0.970	1.042	0.321	4.
219.	-8.8	-14.4	38.7	2.625	0.561	2.462	2.264	0.993	1.004	0.320	4.
222.	-8.1	-14.7	30.8	2.592	0.572	2.442	2.127	1.024	0.941	0.317	0.
223.	-8.2	-14.0	29.2	2.562	0.566	2.435	2.086	1.033	0.919	0.316	0.
238.	-8.7	-15.0	41.0	2.110	0.435	2.342	1.767	1.160	0.558	0.295	4.
242.	-9.0	-14.3	31.2	2.143	0.445	2.340	1.789	1.204	0.469	0.287	0.
245.	-7.3	-12.9	35.5	2.162	0.455	2.335	1.845	1.244	0.407	0.279	4.
247.	-6.4	-11.6	39.1	2.173	0.462	2.330	1.904	1.275	0.369	0.273	0.
249.	-8.6	-13.7	32.1	2.185	0.470	2.325	1.985	1.309	0.334	0.266	0.
252.	-6.3	-12.1	30.8	2.194	0.485	2.320	2.158	1.370	0.285	0.255	0.
258.	-7.9	-15.1	--	0.368	0.147	0.440	0.000	0.000	0.000	0.000	1.
259.	-9.0	-15.8	22.1	0.402	0.181	0.440	0.000	0.000	0.000	0.000	1.

--- CODE EXPLANATION ---
0 -- NORMAL DATA
1 -- POST-HARVEST
3 -- WINDY DURING DATA ACQUISITION
4 -- RECENT HEAVY RAIN
9 -- ABNORMAL SIGMA0

CORN FIELD # 8

JULIAN DATE	SIGMAO VV	SIGMAO VH	SOIL MOIS	--STALK--- FRESH BIOMASS	DRY BIOMASS	CANOPY HEIGHT	--FRUIT--- FRESH BIOMASS	DRY BIOMASS	---LEAF--- FRESH BIOMASS	DRY BIOMASS	CODE
140.	-9.0	-16.8	31.7	0.027	0.005	0.304	0.000	0.000	0.035	0.007	0.
142.	-9.2	-18.2	35.0	0.047	0.008	0.310	0.000	0.000	0.057	0.009	0.
148.	-7.2	-16.8	23.1	0.120	0.014	0.443	0.000	0.000	0.115	0.013	4.
149.	-7.4	-16.0	29.2	0.151	0.017	0.478	0.000	0.000	0.140	0.015	4.
155.	-4.0	-11.3	43.2	0.425	0.043	0.743	0.000	0.000	0.307	0.031	4.
156.	-4.9	-12.0	39.1	0.484	0.050	0.794	0.000	0.000	0.336	0.034	4.
160.	-7.4	-15.1	44.7	0.759	0.083	1.004	0.000	0.000	0.445	0.049	0.
163.	-5.5	-11.5	43.1	1.002	0.119	1.165	0.000	0.000	0.516	0.062	4.
166.	-5.9	-12.5	44.7	1.274	0.166	1.323	0.000	0.000	0.572	0.074	4.
167.	-5.7	-12.8	40.7	1.370	0.183	1.374	0.000	0.000	0.587	0.079	4.
169.	-6.7	-14.5	34.7	1.571	0.225	1.473	0.000	0.000	0.611	0.087	4.
170.	-5.0	-11.4	41.0	1.674	0.246	1.521	0.000	0.000	0.619	0.091	4.
175.	-6.3	-11.7	36.3	1.691	0.257	1.739	0.510	0.120	0.614	0.094	0.
176.	-6.2	-12.3	39.3	1.711	0.260	1.777	0.710	0.180	0.609	0.100	0.
194.	-6.7	-14.0	23.5	1.822	0.277	2.124	1.994	0.555	0.602	0.174	0.
197.	-6.9	-13.6	14.1	1.890	0.283	2.123	2.050	0.566	0.633	0.180	0.
198.	-6.6	-13.9	14.1	1.902	0.285	2.120	2.071	0.577	0.644	0.183	0.
204.	-8.4	-14.9	31.2	1.925	0.291	2.083	2.152	0.693	0.695	0.193	0.
209.	-6.1	-13.8	--	2.042	0.302	2.045	2.097	0.816	0.692	0.196	4.
210.	-7.2	-14.3	79.9	2.057	0.309	2.039	2.071	0.839	0.684	0.195	4.
211.	-7.4	-13.4	40.7	2.057	0.315	2.034	2.041	0.861	0.673	0.194	0.
216.	-7.1	-13.4	38.3	1.870	0.335	2.033	1.823	0.937	0.576	0.184	4.
217.	-7.7	-14.3	44.3	1.791	0.335	2.030	1.767	0.943	0.549	0.180	4.
222.	-7.6	-14.3	36.6	1.435	0.393	2.025	1.431	0.907	0.390	0.152	0.
223.	-8.2	-15.3	28.9	1.510	0.479	2.020	1.352	0.885	0.356	0.145	0.
238.	-4.7	-12.5	43.0	0.416	0.133	0.605	0.000	0.000	0.000	0.000	1.

--- CODE EXPLANATION ---
0 -- NORMAL DATA
1 -- POST-HARVEST
3 -- WINDY DURING DATA ACQUISITION
4 -- RECENT HEAVY RAIN

C-4

CORN FIELD # 9

JULIAN DATE	SIGMA0 VV	SIGMA0 VH	SOIL MOIS	--STALK--- FRESH BIOMASS	DRY BIOMASS	CANOPY HEIGHT	--FRUIT--- FRESH BIOMASS	DRY BIOMASS	---LEAF--- FRESH BIOMASS	DRY BIOMASS	CODE
140.	-9.3	-20.2	34.1	0.022	0.004	0.199	0.000	0.000	0.028	0.005	4.
142.	-14.0	-22.8	21.3	0.039	0.007	0.229	0.000	0.000	0.048	0.008	0.
148.	-13.0	-20.5	24.4	0.142	0.019	0.408	0.000	0.000	0.137	0.018	0.
149.	-9.8	-17.6	20.0	0.198	0.025	0.448	0.000	0.000	0.182	0.024	4.
155.	-5.2	-12.6	37.2	0.652	0.069	0.740	0.000	0.000	0.473	0.050	4.
156.	-5.7	-13.0	30.8	0.748	0.077	0.794	0.000	0.000	0.519	0.054	4.
161.	-7.0	-13.4	19.0	1.300	0.124	1.083	0.000	0.000	0.732	0.069	0.
163.	-5.7	-12.8	38.8	1.553	0.145	1.202	0.000	0.000	0.800	0.074	4.
167.	-5.9	-10.9	34.6	2.108	0.196	1.443	0.000	0.000	0.904	0.084	4.
170.	-5.0	-12.3	29.8	2.561	0.243	1.621	0.000	0.000	0.947	0.090	4.
175.	-6.1	-11.1	31.8	3.360	0.335	1.902	0.000	0.000	0.950	0.100	0.
176.	-6.7	-12.5	33.1	3.509	0.355	1.956	0.000	0.000	0.958	0.105	0.
177.	-7.5	-12.7	27.0	3.539	0.330	2.008	0.110	0.030	0.966	0.120	0.
194.	-7.4	-13.6	16.0	3.258	0.377	2.647	2.243	0.352	1.110	0.282	0.
197.	-7.2	-14.0	16.3	3.208	0.412	2.704	2.400	0.417	1.196	0.287	0.
198.	-6.8	-13.1	12.6	3.141	0.425	2.720	2.436	0.439	1.281	0.288	0.
205.	-7.3	-14.5	26.4	2.933	0.509	2.776	2.514	0.589	1.593	0.289	0.
209.	-7.5	-14.7	36.8	3.086	0.553	2.770	2.477	0.674	1.441	0.286	4.
210.	-7.5	-13.8	35.6	3.137	0.563	2.765	2.462	0.695	1.379	0.284	4.
212.	-7.4	-13.9	31.4	3.233	0.578	2.752	2.429	0.736	1.244	0.281	0.
216.	-7.3	-13.9	30.7	3.350	0.591	2.710	2.352	0.818	0.980	0.275	4.
217.	-7.0	-14.1	36.5	3.364	0.596	2.697	2.331	0.838	0.921	0.273	4.
222.	-7.5	-15.3	30.1	3.281	0.588	2.626	2.227	0.937	0.683	0.264	0.
223.	-7.4	-14.5	31.2	3.233	0.577	2.610	2.206	0.956	0.646	0.262	0.
226.	-9.0	-16.1	--	3.063	0.551	2.565	2.145	1.012	0.552	0.257	4.
238.	-9.0	-15.8	32.5	2.258	0.438	2.460	1.924	1.217	0.363	0.249	4.
242.	-9.2	-15.3	30.8	2.086	0.457	2.455	1.860	1.276	0.332	0.244	0.
245.	-8.8	-14.9	30.5	1.948	0.471	2.450	1.815	1.318	0.318	0.242	4.
247.	-9.1	-14.7	28.5	1.846	0.480	2.445	1.786	1.343	0.312	0.240	0.
249.	-10.4	-16.0	25.6	1.746	0.490	2.440	1.759	1.368	0.309	0.238	0.
253.	-4.9	-12.5	31.0	0.395	0.213	0.470	0.000	0.000	0.000	0.000	1.
256.	-5.5	-14.7	27.0	0.443	0.261	0.470	0.000	0.000	0.000	0.000	1.

--- CODE EXPLANATION ---
0 -- NORMAL DATA
1 -- POST-HARVEST
3 -- WINDY DURING DATA ACQUISITION
4 -- RECENT HEAVY RAIN

CORN FIELD # 10

JULIAN DATE	SIGMAO VV	SIGMAO VH	SOIL MOIS	--STALK--- FRESH BIOMASS	DRY BIOMASS	CANOPY HEIGHT	--FRUIT--- FRESH BIOMASS	DRY BIOMASS	---LEAF--- FRESH BIOMASS	DRY BIOMASS	CODE
140.	-4.3	-12.7	34.0	0.041	0.008	0.209	0.000	0.000	0.054	0.010	0.
142.	-4.2	-12.6	35.1	0.052	0.009	0.296	0.000	0.000	0.064	0.011	0.
148.	-8.3	-13.1	25.0	0.321	0.045	0.576	0.000	0.000	0.309	0.044	4.
149.	-8.1	-13.8	31.1	0.392	0.053	0.624	0.000	0.000	0.361	0.049	0.
160.	-8.1	-16.5	35.5	1.360	0.137	1.172	0.000	0.000	0.798	0.081	0.
163.	-8.4	-13.9	35.4	1.678	0.163	1.320	0.000	0.000	0.864	0.084	4.
167.	-5.8	-13.1	33.9	2.129	0.202	1.510	0.000	0.000	0.913	0.087	4.
169.	-6.4	-14.0	28.8	2.365	0.217	1.602	0.000	0.000	0.920	0.095	4.
170.	-5.2	-12.4	41.7	2.487	0.227	1.647	0.000	0.000	0.920	0.100	4.
194.	-6.0	-13.6	19.8	2.251	0.346	2.462	2.456	0.385	1.621	0.227	0.
197.	-7.3	-14.1	16.5	2.203	0.414	2.522	2.582	0.457	1.344	0.242	0.
198.	-6.3	-12.9	11.3	2.188	0.426	2.539	2.614	0.485	1.300	0.247	0.
202.	-8.4	-15.5	33.3	2.206	0.498	2.599	2.693	0.606	1.265	0.250	0.
204.	-7.8	-15.0	30.6	2.237	0.520	2.623	2.710	0.673	1.251	0.257	0.
209.	-7.4	-14.0	73.8	2.390	0.571	2.665	2.707	0.849	1.194	0.260	4.
210.	-7.9	-16.1	38.1	2.419	0.570	2.671	2.701	0.886	1.170	0.261	4.
211.	-6.7	-13.8	43.2	2.456	0.578	2.675	2.693	0.922	1.143	0.262	0.
216.	-7.1	-12.4	39.4	2.592	0.577	2.687	2.637	1.100	0.985	0.268	4.
219.	-6.6	-13.8	39.4	2.619	0.551	2.685	2.593	1.201	0.888	0.273	4.
222.	-6.7	-14.2	37.3	2.603	0.535	2.677	2.542	1.293	0.797	0.278	0.
223.	-6.0	-12.8	30.1	2.647	0.532	2.674	2.523	1.322	0.768	0.279	4.
226.	-6.8	-14.3	37.0	2.658	0.529	2.661	2.464	1.398	0.689	0.283	0.
236.	-7.1	-14.3	19.3	2.667	0.528	2.608	2.231	1.428	0.486	0.290	0.
242.	-8.1	-14.2	--	2.687	0.528	2.587	2.195	1.483	0.395	0.284	0.
245.	-7.5	-14.2	36.7	2.723	0.528	2.585	2.160	1.490	0.355	0.277	0.
247.	-7.9	-12.6	--	2.763	0.528	2.585	2.140	1.497	0.330	0.271	0.
249.	-8.0	-14.6	28.2	2.665	0.528	2.585	2.105	1.520	0.305	0.263	0.
252.	-6.5	-13.1	34.0	2.998	0.528	2.585	2.040	1.517	0.270	0.249	0.
258.	-7.6	-14.0	29.7	3.339	0.516	2.585	1.970	1.520	0.208	0.208	0.
259.	-7.1	-13.9	20.8	3.484	0.516	2.585	1.920	1.530	0.199	0.199	0.

--- CODE EXPLANATION ---
0 -- NORMAL DATA
1 -- POST-HARVEST
3 -- WINDY DURING DATA ACQUISITION
4 -- RECENT HEAVY RAIN

SOYBEAN FIELD # 1

JULIAN DATE	SIGMA0 VV	SIGMA0 VH	SOIL MOIS	---PLANT--- FRESH BIOMASS	DRY BIOMASS	CANOPY HEIGHT	CODE
141.	-9.4	-23.6	--	0.046	0.017	0.020	0.
146.	-10.3	-24.3	28.2	0.065	0.019	0.023	0.
147.	-8.1	-17.0	20.4	0.068	0.020	0.023	0.
148.	-8.8	-17.0	22.9	0.072	0.020	0.023	0.
154.	-6.5	-14.3	36.3	0.092	0.020	0.023	4.
155.	-6.6	-14.8	31.4	0.095	0.020	0.028	4.
156.	-10.8	-19.9	28.4	0.099	0.020	0.034	0.
160.	-11.0	-19.5	23.7	0.112	0.020	0.067	0.
163.	-8.3	-15.8	32.3	0.122	0.021	0.102	4.
167.	-5.5	-16.1	36.0	0.136	0.022	0.159	4.
169.	-6.3	-15.0	24.4	0.143	0.022	0.192	4.
170.	-3.7	-12.7	31.8	0.147	0.023	0.208	4.
176.	-8.6	-15.3	25.2	0.178	0.027	0.318	0.
183.	-5.9	-11.8	32.9	0.217	0.034	0.457	0.
194.	-6.3	-12.5	7.7	0.838	0.143	0.672	0.
196.	-6.0	-12.0	10.7	1.091	0.189	0.709	0.
197.	-5.0	-12.7	6.0	1.226	0.215	0.727	0.
201.	-6.3	-11.8	32.1	1.800	0.322	0.795	4.
204.	-5.1	-11.3	27.2	2.262	0.414	0.842	0.
209.	-8.0	-16.4	40.2	3.053	0.571	0.912	4.
210.	-7.4	-16.0	40.7	3.212	0.604	0.925	4.
211.	-6.7	-13.9	34.4	3.367	0.633	0.937	0.
215.	-8.3	-14.5	35.8	3.982	0.757	0.980	0.
218.	-5.9	-13.8	43.7	4.418	0.844	1.008	4.
222.	-6.2	-13.0	34.0	4.954	0.951	1.037	0.
224.	-5.7	-12.6	30.6	5.202	1.004	1.049	0.
225.	-7.2	-14.1	46.9	5.316	1.026	1.054	0.
236.	-5.3	-11.4	14.7	6.255	1.239	1.078	0.
240.	-5.9	-12.8	32.1	6.431	1.299	1.075	0.
242.	-5.2	-12.4	27.3	6.487	1.330	1.071	0.
244.	-6.3	-13.0	--	6.523	1.363	1.066	4.
246.	-5.2	-11.4	33.1	6.538	1.399	1.060	0.
251.	-5.6	-12.1	31.8	6.485	1.498	1.043	4.
253.	-6.3	-12.0	28.4	6.428	1.543	1.035	0.
256.	-4.9	-10.7	26.2	6.304	1.614	1.023	0.
258.	-5.8	-12.4	23.4	6.199	1.668	1.016	0.
259.	-6.9	-13.0	24.7	6.146	1.702	1.012	0.
260.	-5.9	-11.6	16.0	6.076	1.726	1.009	0.
264.	-5.4	-11.5	14.1	5.780	1.855	0.998	0.
266.	-5.9	-10.5	13.2	4.750	1.800	0.994	0.
271.	-5.0	-9.7	26.7	4.095	1.770	0.993	0.
275.	-6.5	-11.2	23.4	2.950	1.750	0.993	4.
278.	-5.4	-10.6	32.0	2.350	1.700	0.993	0.
280.	-7.2	-13.2	26.8	1.823	1.650	0.993	0.
287.	-6.5	-11.7	39.4	1.811	1.520	0.993	4.
292.	-6.8	-14.0	30.7	1.774	1.450	0.993	0.
294.	-7.6	-15.5	27.0	0.068	0.065	0.050	1.
296.	-9.6	-19.7	--	0.100	0.097	0.050	1.

SOYBEAN FIELD # 2

JULIAN DATE	SIGMA0 VV	SIGMA0 VH	SOIL MOIS	---PLANT--- FRESH BIOMASS	DRY BIOMASS	CANOPY HEIGHT	CODE
141.	-3.3	-17.8	--	0.041	0.011	0.010	0.
146.	-8.7	-16.7	27.7	0.061	0.016	0.015	4.
147.	-11.5	-21.4	24.4	0.065	0.017	0.020	0.
148.	-12.0	-21.2	26.3	0.069	0.018	0.023	0.
154.	-8.4	-18.9	31.1	0.093	0.024	0.026	4.
155.	-8.8	-18.9	29.6	0.097	0.025	0.032	4.
156.	-13.9	-22.1	25.2	0.097	0.022	0.040	0.
160.	-10.2	-20.1	21.3	0.109	0.022	0.080	0.
163.	-8.5	-16.5	25.2	0.117	0.021	0.120	4.
167.	-7.6	-14.4	26.6	0.130	0.022	0.182	4.
169.	-6.8	-14.2	24.6	0.137	0.023	0.217	4.
170.	-6.3	-12.6	22.3	0.133	0.016	0.236	4.
176.	-6.4	-12.8	26.7	0.219	0.047	0.353	0.
183.	-4.9	-10.3	28.0	0.352	0.093	0.502	0.
194.	-5.8	-12.5	8.4	1.255	0.282	0.736	0.
196.	-5.7	-12.4	3.4	1.272	0.290	0.776	0.
197.	-7.4	-12.7	6.7	1.300	0.300	0.796	0.
201.	-4.5	-12.3	20.8	1.522	0.330	0.873	4.
204.	-6.6	-13.0	12.5	2.023	0.405	0.926	0.
209.	-6.7	-14.5	6.6	2.818	0.490	1.008	0.
210.	-7.4	-15.0	28.9	2.970	0.505	1.023	0.
211.	-5.7	-13.0	35.8	3.114	0.514	1.037	0.
215.	-5.2	-11.8	30.6	3.661	0.553	1.090	0.
217.	-5.9	-13.8	27.3	3.910	0.571	1.114	0.
219.	-7.1	-12.4	28.0	4.144	0.593	1.135	4.
223.	-6.7	-12.8	30.2	4.564	0.653	1.172	0.
225.	-7.5	-14.2	22.7	4.750	0.693	1.187	0.
236.	-5.2	-11.8	12.2	5.493	1.121	1.233	0.
240.	-5.3	-12.8	19.4	5.651	1.373	1.234	0.
242.	-4.7	-11.1	16.1	5.699	1.510	1.232	0.
244.	-5.2	-11.8	22.8	5.737	1.664	1.229	0.
246.	-5.1	-11.7	16.9	5.758	1.825	1.224	0.
251.	-6.4	-13.1	54.6	5.721	2.243	1.204	4.
256.	-5.2	-10.0	14.5	5.526	2.625	1.178	0.
258.	-5.8	-10.9	16.5	4.281	1.640	1.166	0.
260.	-6.6	-11.5	10.2	2.500	1.400	1.154	0.
264.	-7.4	-11.9	6.4	1.500	1.279	1.128	0.
266.	-9.2	-13.6	7.4	1.330	1.279	1.115	0.
271.	-8.0	-14.5	16.4	1.250	1.157	1.084	0.
275.	-7.9	-14.7	15.2	1.200	1.140	1.063	0.
278.	-7.5	-14.3	21.2	1.190	1.120	1.051	0.
280.	-7.5	-14.9	14.4	1.181	1.103	1.045	0.
287.	-6.8	-14.7	22.7	1.179	1.087	1.044	0.
292.	-7.0	-13.7	23.1	1.099	1.010	1.044	0.
296.	-9.4	-17.5	20.2	0.752	0.667	1.044	0.

SOYBEAN FIELD # 3

JULIAN DATE	SIGMAO VV	SIGMAO VH	SOIL MOIS	---PLANT--- FRESH BIOMASS	DRY BIOMASS	CANOPY HEIGHT	CODE
141.	-6.7	-21.3	45.4	0.024	0.006	0.030	0.
146.	-14.4	-21.7	31.2	0.045	0.012	0.060	0.
147.	-16.8	-24.8	24.4	0.047	0.011	0.090	0.
148.	-15.8	-24.0	26.8	0.049	0.010	0.100	0.
154.	-12.4	-20.3	33.1	0.140	0.016	0.110	4.
155.	-11.3	-18.8	29.0	0.160	0.018	0.120	4.
156.	-13.3	-21.3	31.0	0.180	0.020	0.130	0.
160.	-8.6	-16.3	23.4	0.240	0.025	0.150	0.
163.	-4.7	-12.4	28.4	0.290	0.030	0.160	4.
167.	-6.8	-11.5	32.9	0.360	0.047	0.177	0.
169.	-6.5	-13.6	26.5	0.407	0.054	0.245	0.
170.	-5.2	-10.7	27.4	0.430	0.065	0.278	4.
176.	-5.7	-13.3	24.9	0.500	0.096	0.453	0.
177.	-5.9	-12.5	24.2	0.587	0.106	0.479	0.
194.	-5.0	-12.5	6.3	2.029	0.434	0.805	0.
196.	-5.4	-12.6	6.0	2.100	0.439	0.830	0.
198.	-6.4	-13.5	7.8	2.561	0.531	0.853	0.
203.	-6.5	-13.7	30.4	3.269	0.644	0.901	0.
204.	-6.7	-13.8	22.9	3.528	0.688	0.909	0.
209.	-6.3	-14.9	35.1	4.780	0.884	0.942	4.
210.	-6.5	-14.2	32.2	5.022	0.924	0.948	0.
211.	-6.1	-13.3	32.0	5.253	0.956	0.953	0.
215.	-5.4	-12.4	30.6	6.132	1.092	0.969	4.
218.	-6.5	-12.9	37.9	6.729	1.198	0.978	4.
219.	-7.0	-13.6	34.6	6.909	1.230	0.980	4.
222.	-5.7	-13.0	34.2	7.416	1.342	0.985	0.
223.	-7.0	-13.0	27.7	7.573	1.386	0.987	0.
225.	-6.6	-13.2	26.3	7.855	1.469	0.989	0.
236.	-5.3	-11.9	14.9	8.862	2.118	0.990	0.
240.	-5.7	-11.5	31.0	8.992	2.437	0.988	0.
242.	-4.3	-10.5	23.1	9.011	2.613	0.987	0.
244.	-6.1	-12.3	33.2	8.987	2.786	0.987	4.
246.	-4.8	-11.9	29.0	8.931	2.965	0.987	0.
251.	-5.3	-10.6	--	8.667	3.441	0.987	4.
253.	-4.1	-8.9	28.4	8.481	3.605	0.987	0.
256.	-4.0	-8.6	28.4	4.900	2.800	0.987	0.
258.	-5.0	-10.9	29.0	4.000	2.000	0.987	0.
259.	-5.5	-10.0	16.6	3.511	1.907	0.987	0.
261.	-6.6	-10.4	18.0	2.862	1.700	0.987	0.
264.	-6.1	-11.7	18.2	2.500	1.660	0.987	0.
266.	-6.7	-11.6	15.9	2.300	1.630	0.987	0.
271.	-7.0	-11.3	25.7	2.000	1.600	0.987	0.
275.	-6.6	-11.9	24.1	1.800	1.560	0.987	0.
278.	-5.3	-10.5	28.5	1.700	1.530	0.987	0.
280.	-6.2	-12.0	20.5	1.600	1.500	0.987	0.

SOYBEAN FIELD # 4

JULIAN DATE	SIGMAO VV	SIGMAO VH	SOIL MOIS	---PLANT--- FRESH BIOMASS	DRY BIOMASS	CANOPY HEIGHT	CODE
154.	-9.0	-19.5	30.4	0.077	0.020	0.030	4.
155.	-9.9	-19.8	31.0	0.075	0.015	0.050	4.
156.	-12.0	-22.7	26.0	0.077	0.014	0.060	0.
161.	-15.1	-22.3	15.2	0.093	0.015	0.070	0.
163.	-10.9	-18.5	30.8	0.098	0.014	0.080	4.
166.	-10.9	-18.8	--	0.113	0.020	0.100	4.
167.	-11.1	-17.7	21.2	0.126	0.030	0.110	4.
170.	-7.0	-14.3	22.7	0.141	0.036	0.120	0.
175.	-6.9	-13.3	14.9	0.132	0.031	0.135	0.
176.	-9.3	-17.6	17.0	0.160	0.037	0.131	0.
183.	-5.5	-11.3	25.3	0.402	0.087	0.178	0.
194.	-4.8	-12.4	6.5	1.055	0.232	0.415	0.
196.	-6.2	-13.2	5.8	1.212	0.268	0.469	0.
197.	-5.6	-13.2	5.3	1.429	0.316	0.496	0.
208.	-6.8	-15.3	31.2	4.241	0.929	0.797	4.
209.	-6.2	-14.9	27.3	4.542	0.990	0.822	4.
210.	-5.8	-13.8	24.3	4.843	1.051	0.846	0.
212.	-6.8	-15.3	22.0	5.431	1.162	0.894	0.
215.	-6.3	-13.5	25.6	6.282	1.313	0.959	0.
218.	-6.8	-13.8	30.5	7.073	1.436	1.016	4.
219.	-5.7	-12.8	25.0	7.323	1.472	1.033	4.
222.	-6.1	-13.8	21.0	8.011	1.554	1.079	0.
226.	-7.6	-13.5	19.9	8.793	1.627	1.125	4.
238.	-6.3	-13.6	25.4	10.100	1.707	1.166	0.
242.	-5.9	-11.3	18.5	10.211	1.777	1.151	0.
245.	-5.5	-12.0	24.8	10.195	1.866	1.133	0.
249.	-5.6	-11.7	16.2	10.073	2.075	1.102	0.
253.	-5.5	-10.9	21.7	9.818	2.376	1.069	0.
256.	-4.0	-12.0	18.2	9.561	2.687	1.044	0.
259.	-6.7	-10.9	11.4	9.232	2.700	1.023	0.
260.	-6.0	-11.4	9.8	9.099	2.813	1.017	0.
264.	-4.8	-9.7	7.7	8.000	2.989	1.002	0.
266.	-6.3	-10.5	9.1	6.900	2.900	1.002	0.
271.	-6.6	-10.6	18.6	3.351	2.758	1.002	0.
273.	-6.7	-11.8	15.5	2.944	2.745	1.002	0.
275.	-7.5	-12.4	17.7	2.768	2.650	1.002	4.
278.	-7.1	-12.8	22.3	2.682	2.562	1.002	0.
280.	-10.2	-17.6	18.9	0.067	0.064	0.050	1.

--- CODE EXPLANATION ---
0 -- NORMAL DATA
1 -- POST-HARVEST
3 -- WINDY DURING DATA ACQUISITION
4 -- RECENT HEAVY RAIN

SOYBEAN FIELD # 5

JULIAN DATE	SIGMA0 VV	SIGMA0 VH	SOIL MOIS	---PLANT--- FRESH BIOMASS	DRY BIOMASS	CANOPY HEIGHT	CODE
141.	-7.4	-20.0	--	0.031	0.003	0.030	0.
147.	-12.3	-21.3	30.2	0.050	0.004	0.030	0.
148.	-12.4	-21.3	31.9	0.055	0.005	0.140	0.
154.	-9.6	-17.2	44.2	0.105	0.010	0.180	4.
155.	-7.8	-15.6	50.4	0.116	0.011	0.190	4.
156.	-9.6	-18.8	47.8	0.122	0.012	0.200	0.
160.	-7.3	-15.6	39.2	0.155	0.018	0.230	0.
163.	-4.0	-10.5	58.2	0.172	0.022	0.260	4.
167.	-6.9	-13.4	44.0	0.200	0.030	0.285	0.
169.	-7.8	-17.4	29.6	0.222	0.035	0.298	0.
170.	-4.8	-11.5	45.0	0.251	0.041	0.306	4.
176.	-11.2	-17.2	34.8	0.311	0.060	0.366	0.
183.	-4.3	-9.8	40.4	0.385	0.085	0.456	0.
194.	-4.5	-11.7	13.4	0.457	0.111	0.615	0.
196.	-4.5	-11.4	12.3	0.627	0.154	0.643	0.
197.	-4.9	-11.5	18.7	0.717	0.176	0.657	0.
204.	-4.9	-11.4	37.1	1.433	0.345	0.749	0.
205.	-5.9	-13.3	34.7	1.544	0.370	0.761	0.
208.	-4.4	-12.2	62.2	1.878	0.441	0.795	4.
211.	-5.9	-13.7	50.0	2.210	0.504	0.826	0.
212.	-5.8	-13.8	49.6	2.320	0.524	0.836	0.
215.	-4.6	-12.8	46.1	2.644	0.579	0.862	0.
217.	-5.3	-12.4	51.1	2.851	0.610	0.878	0.
219.	-7.9	-13.6	46.4	3.050	0.638	0.892	4.
224.	-6.1	-12.0	33.6	3.501	0.690	0.920	0.
226.	-6.3	-11.8	45.7	3.666	0.711	0.929	0.
238.	-6.1	-12.3	48.6	4.383	0.872	0.950	0.
242.	-5.0	-9.9	43.8	4.518	0.976	0.947	0.
245.	-5.3	-11.3	42.8	4.589	1.088	0.944	0.
249.	-6.1	-12.3	40.3	4.635	1.284	0.938	0.
252.	-4.9	-10.5	41.3	4.626	1.467	0.934	0.
259.	-5.3	-9.4	28.7	4.000	2.000	0.928	0.
260.	-5.9	-10.4	27.4	3.609	2.024	0.928	0.
264.	-5.4	-9.3	25.3	3.053	2.179	0.928	0.
266.	-7.2	-11.2	26.5	1.983	1.447	0.928	0.
271.	-6.4	-10.7	41.6	1.400	1.100	0.928	0.
273.	-6.7	-11.9	34.6	0.871	0.827	0.979	0.
275.	-9.0	-18.3	33.5	0.107	0.104	0.050	1.

--- CODE EXPLANATION ---
0 -- NORMAL DATA
1 -- POST-HARVEST
3 -- WINDY DURING DATA ACQUISITION
4 -- RECENT HEAVY RAIN

SOYBEAN FIELD # 6

JULIAN DATE	SIGMAO VV	SIGMAO VH	SOIL MOIS	---PLANT--- FRESH BIOMASS	DRY BIOMASS	CANOPY HEIGHT	CODE
201.	-7.1	-13.3	21.9	0.308	0.063	0.312	0.
204.	-6.9	-16.0	19.9	0.441	0.086	0.394	0.
209.	-6.4	-14.7	26.9	0.790	0.149	0.523	4.
210.	-8.3	-17.1	26.2	0.856	0.160	0.547	0.
211.	-6.4	-13.9	26.1	0.923	0.173	0.571	0.
215.	-6.8	-14.7	22.6	1.170	0.218	0.660	0.
217.	-5.8	-12.9	28.5	1.284	0.239	0.701	4.
223.	-6.7	-14.0	18.5	1.581	0.299	0.809	0.
225.	-7.2	-15.0	15.8	1.662	0.316	0.840	0.
236.	-7.6	-12.0	7.9	1.935	0.391	0.958	0.
240.	-7.9	-12.7	20.7	1.959	0.409	0.980	0.
242.	-6.8	-11.7	16.9	1.953	0.414	0.988	0.
244.	-7.1	-11.6	25.0	1.941	0.421	0.993	4.
246.	-6.3	-10.9	22.0	1.919	0.426	0.995	0.
251.	-6.2	-11.1	20.9	1.823	0.434	0.993	0.
256.	-4.9	-10.8	18.8	1.681	0.439	0.981	0.
258.	-6.0	-11.0	11.8	1.611	0.438	0.974	0.
260.	-6.7	-10.6	12.8	1.538	0.440	0.966	0.
261.	-6.4	-11.5	14.8	1.498	0.439	0.961	0.
264.	-6.4	-11.2	10.9	1.376	0.439	0.948	0.
266.	-7.2	-11.4	9.9	1.289	0.437	0.939	0.
271.	-6.3	-10.8	17.6	1.059	0.427	0.919	0.
275.	-7.9	-12.6	20.7	0.862	0.404	0.908	0.
278.	-9.3	-12.9	26.4	0.710	0.375	0.905	0.
280.	-9.0	-13.8	22.7	0.607	0.349	0.905	0.
287.	-7.1	-11.8	33.4	0.428	0.331	0.905	4.
292.	-8.6	-15.5	24.3	0.393	0.362	0.905	0.
294.	-10.6	-16.7	20.9	0.083	0.080	0.050	1.

--- CODE EXPLANATION ---
0 -- NORMAL DATA
1 -- POST-HARVEST
3 -- WINDY DURING DATA ACQUISITION
4 -- RECENT HEAVY RAIN

SOYBEAN FIELD # 8

JULIAN DATE	SIGMAO VV	SIGMAO VH	SOIL MOIS	---PLANT--- FRESH BIOMASS	DRY BIOMASS	CANOPY HEIGHT	CODE
203.	-7.9	-16.2	37.3	0.124	0.024	0.211	4.
205.	-9.8	-17.1	34.0	0.148	0.028	0.220	0.
216.	-6.2	-12.4	--	0.273	0.051	0.351	4.
223.	-6.5	-12.6	31.8	0.416	0.080	0.473	0.
224.	-7.1	-12.8	35.2	0.425	0.083	0.492	0.
226.	-6.8	-13.0	--	0.450	0.088	0.528	0.
242.	-6.3	-12.3	30.6	0.790	0.159	0.776	0.
249.	-5.9	-12.9	27.9	0.926	0.181	0.840	0.
256.	-4.8	-11.0	23.3	1.011	0.191	0.872	0.
259.	-5.6	-12.5	22.1	1.028	0.192	0.876	0.
260.	-6.4	-12.7	19.4	1.031	0.193	0.876	0.
264.	-5.9	-11.6	18.4	1.032	0.195	0.871	0.
266.	-6.0	-11.5	16.7	1.025	0.197	0.866	0.
271.	-5.8	-11.3	27.5	0.988	0.204	0.847	0.
273.	-4.5	-9.1	22.2	0.966	0.210	0.838	0.
275.	-6.6	-11.8	25.7	0.939	0.215	0.828	0.
280.	-6.5	-12.1	23.6	0.860	0.237	0.827	0.
294.	-8.4	-14.3	31.5	0.529	0.297	0.822	0.
296.	-9.4	-14.9	33.0	0.459	0.288	0.822	0.
301.	-8.2	-15.2	31.1	0.343	0.277	0.822	0.
315.	-7.4	-15.8	--	0.030	0.027	0.050	1.

--- CODE EXPLANATION ---
0 -- NORMAL DATA
1 -- POST-HARVEST
3 -- WINDY DURING DATA ACQUISITION
4 -- RECENT HEAVY RAIN

SOYBEAN FIELD # 9

JULIAN DATE	SIGMA0 VV	SIGMA0 VH	SOIL MOIS	---PLANT--- FRESH BIOMASS	DRY BIOMASS	CANOPY HEIGHT	CODE
205.	-9.0	-17.3	9.3	0.193	0.036	0.332	0.
208.	-6.8	-12.1	30.0	0.411	0.080	0.416	4.
210.	-5.8	-14.2	20.7	0.585	0.116	0.471	4.
212.	-6.4	-14.4	18.8	0.733	0.147	0.523	0.
215.	-7.0	-13.3	19.0	0.912	0.187	0.597	0.
218.	-5.9	-14.2	29.1	1.044	0.216	0.666	4.
219.	-6.9	-14.2	--	1.079	0.224	0.688	0.
223.	-6.8	-12.8	12.6	1.175	0.246	0.767	0.
224.	-5.5	-12.6	12.1	1.190	0.249	0.785	0.
226.	-5.5	-12.3	17.8	1.209	0.253	0.819	0.
238.	-6.7	-13.3	21.7	1.131	0.234	0.957	4.
242.	-5.6	-11.3	18.3	1.064	0.222	0.980	0.
245.	-5.1	-11.6	21.7	1.009	0.214	0.989	0.
249.	-5.2	-11.9	15.4	0.934	0.205	0.993	0.
253.	-5.3	-11.0	19.0	0.863	0.199	0.988	0.
256.	-4.5	-11.2	16.7	0.813	0.198	0.980	0.
259.	-5.6	-12.3	15.0	0.769	0.200	0.969	0.
260.	-5.1	-12.0	8.8	0.755	0.201	0.964	0.
264.	-4.9	-11.0	8.5	0.707	0.211	0.946	0.
266.	-4.8	-9.8	5.1	0.687	0.218	0.937	0.
271.	-4.8	-10.4	18.8	0.647	0.245	0.916	0.
273.	-5.0	-8.9	9.7	0.635	0.240	0.910	0.
275.	-6.6	-10.6	16.5	0.624	0.240	0.906	0.
278.	-6.1	-10.6	19.3	0.610	0.230	0.906	0.
280.	-7.1	-12.5	15.7	0.601	0.220	0.906	0.
287.	-6.9	-12.1	22.9	0.531	0.190	0.906	4.
292.	-8.3	-16.6	18.6	0.198	0.178	0.906	0.
294.	-9.6	-18.7	17.1	0.237	0.160	0.906	0.
296.	-12.0	-21.3	14.9	0.136	0.133	0.050	1.

--- CODE EXPLANATION ---
0 -- NORMAL DATA
1 -- POST-HARVEST
3 -- WINDY DURING DATA ACQUISITION
4 -- RECENT HEAVY RAIN

SOYBEAN FIELD # 10

JULIAN DATE	SIGMAO VV	SIGMAO VH	SOIL MOIS	---PLANT--- FRESH BIOMASS	DRY BIOMASS	CANOPY HEIGHT	CODE
204.	-6.8	-12.7	18.5	0.180	0.035	0.220	0.
205.	-8.4	-13.6	23.2	0.200	0.040	0.239	0.
208.	-3.6	-11.2	--	0.240	0.049	0.297	4.
211.	-5.9	-13.5	27.8	0.300	0.052	0.353	0.
212.	-6.2	-13.6	24.2	0.300	0.055	0.372	0.
216.	-6.6	-11.4	22.5	0.320	0.060	0.444	0.
218.	-5.7	-11.3	27.5	0.330	0.063	0.479	4.
219.	-5.4	-11.8	--	0.340	0.066	0.496	4.
224.	-5.9	-12.0	20.0	0.352	0.069	0.577	0.
226.	-5.4	-12.0	26.3	0.364	0.073	0.608	4.
238.	-5.7	-12.4	--	0.476	0.115	0.764	4.
242.	-5.9	-11.0	17.8	0.522	0.131	0.805	0.
245.	-6.8	-12.5	--	0.555	0.141	0.832	0.
249.	-6.5	-13.1	16.3	0.597	0.153	0.863	0.
253.	-7.0	-11.5	19.7	0.632	0.160	0.888	0.
259.	-6.5	-13.0	13.4	0.670	0.164	0.916	0.
260.	-7.0	-13.1	13.4	0.675	0.165	0.919	0.
266.	-6.0	-11.7	13.3	0.689	0.164	0.934	0.
271.	-6.0	-11.8	16.7	0.685	0.166	0.939	0.
273.	-4.8	-10.4	16.7	0.680	0.169	0.939	0.
275.	-6.6	-12.1	15.1	0.673	0.173	0.939	4.
278.	-5.2	-10.8	22.7	0.660	0.183	0.937	0.
280.	-6.6	-12.1	15.2	0.540	0.193	0.935	0.
287.	-5.2	-10.0	29.3	0.420	0.200	0.927	4.
292.	-7.5	-12.5	32.3	0.350	0.210	0.921	0.
294.	-8.3	-15.9	29.3	0.290	0.200	0.920	0.
301.	-8.6	-16.1	21.9	0.131	0.129	0.920	0.

--- CODE EXPLANATION ---
0 -- NORMAL DATA
1 -- POST-HARVEST
3 -- WINDY DURING DATA ACQUISITION
4 -- RECENT HEAVY RAIN

SOYBEAN FIELD # 11

JULIAN DATE	SIGMAO VV	SIGMAO VH	SOIL MOIS	---PLANT--- FRESH BIOMASS	DRY BIOMASS	CANOPY HEIGHT	CODE
203.	-8.6	-17.9	--	0.460	0.060	0.060	0.
215.	-6.6	-13.6	25.5	1.076	0.178	0.603	0.
217.	-5.4	-12.0	28.2	1.452	0.222	0.665	4.
219.	-6.5	-14.2	--	1.453	0.251	0.723	0.
223.	-4.6	-12.9	12.2	1.449	0.287	0.822	0.
240.	-6.9	-12.5	19.3	1.317	0.262	1.044	0.
242.	-6.6	-12.5	30.2	1.291	0.257	1.052	0.
244.	-6.5	-13.1	21.4	1.263	0.254	1.057	0.
246.	-5.0	-11.4	17.1	1.234	0.253	1.059	0.
251.	-6.0	-12.3	22.9	1.153	0.261	1.054	0.
256.	-7.6	-12.1	8.2	1.058	0.278	1.038	0.
258.	-7.5	-13.3	6.2	1.016	0.288	1.029	0.
260.	-7.4	-14.8	5.5	0.971	0.297	1.020	0.
261.	-7.1	-13.3	5.3	0.948	0.303	1.015	0.
264.	-6.2	-11.2	4.7	0.872	0.314	1.002	0.
266.	-5.6	-10.8	3.9	0.817	0.319	0.993	0.
271.	-5.9	-11.4	15.5	0.662	0.317	0.977	0.
275.	-7.3	-12.9	16.5	0.518	0.288	0.974	0.
278.	-7.6	-12.0	25.8	0.399	0.246	0.974	0.
280.	-8.1	-12.9	19.7	0.318	0.209	0.974	0.
287.	-7.3	-13.5	26.1	0.337	0.255	0.974	4.
292.	-8.9	-15.5	22.1	0.296	0.258	0.974	0.
294.	-10.7	-17.0	19.3	0.029	0.026	0.050	1.
296.	-13.7	-22.5	--	0.034	0.031	0.050	1.

--- CODE EXPLANATION ---
0 -- NORMAL DATA
1 -- POST-HARVEST
3 -- WINDY DURING DATA ACQUISITION
4 -- RECENT HEAVY RAIN

APPENDIX C

SIMPLIFICATION OF THEORETICAL MODELS

The backscattering from agricultural targets has been rigorously modeled from the theoretical standpoint in an effort to explain experimental results as well as to determine scattering sources. These models begin with Maxwell's equations and evolve into scattering models using the target's physical properties as inputs. In the course of this evolution, it has been necessary to make certain assumptions to reduce the mathematics to a "reasonable" degree of complexity. As shown below, the resulting models are still far too complex for most users, which renders them largely ineffective. It is for this reason that empirical models of the full theoretical models based upon numerical results are presented.

The case of microwave backscattering from agricultural targets is commonly modeled as a lossy, scattering volume over a rough, lossy surface. For this reason it will be necessary to treat this case in two steps: (1) the surface component and (2) the volume component. In addition, a third component, the surface-volume interaction component is present and must be dealt with as well.

Surface Models

Soil-surface conditions in the microwave portion of the electromagnetic spectrum meet the requirements of three of the theoretical surface scattering models. Below, each is described briefly and in the last one, simplification through

empirical modeling is presented as well. For a more rigorous description as well as a derivation, see Ulaby et al. (1982), Chapter 12. In all cases it is assumed that $\mu_r = 1$, and that only incoherent backscattering is considered, unless otherwise noted.

Small Perturbation Model

The requirements for the application of this model are (i) that the surface height standard deviation be much smaller than the wavelength, i.e., $k\sigma < 0.3$, and (ii) that the RMS slope of the surface be small, i.e., $m < 0.3$. Here, k is the wavenumber in free space and equals $2\pi/\lambda$, σ is the surface height standard deviation, m is the RMS slope of the surface and is defined here as $\sqrt{2}\,\sigma/L$, where L is the surface correlation length. This implies that $L > 4.71\,\sigma$. If a Gaussian correlation coefficient of the form $\exp(-\zeta^2/L^2)$ is assumed, which corresponds to an isotropic roughness spectrum, this model predicts backscattering of the form

$$\sigma^o_{pq} = 4(k\sigma)^2(kL)^2\cos^4\theta \exp[-(kL \sin\theta)^2]|\alpha_{pq}|^2, \qquad (C.1)$$

where p,q denote received and transmitted polarizations, respectively. The incidence angle, relative to nadir is given by θ, and the α's are as follows

$$\alpha_{hh} = R_{\perp} \qquad (C.2a)$$

$$\alpha_{vv} = (\varepsilon_r - 1)\frac{\sin^2\theta - \varepsilon_r(1 + \sin^2\theta)}{[\varepsilon_r\cos\theta + (\varepsilon_r - \sin^2\theta)^{1/2}]^2}$$

$$= - \left[R_{||} + T_{||}^2 \frac{(\varepsilon_r - 1)\tan^2\theta}{2\varepsilon_r}\right] \qquad \text{(C.2b)}$$

$$\alpha_{vh} = \alpha_{hv} = 0, \qquad \text{(C.2c)}$$

where ε_r denotes the relative dielectric constant of the soil surface, $R_{\perp}$ and $R_{||}$ denote the Fresnel reflection coefficients for a plane dielectric surface for perpendicular and parallel polarizations, and $T_{||}$ is the Fresnel transmission coefficient for parallel polarization. At the end of this section a simplified expression for $|\alpha_{VV}|^2$, as well as the original Fresnel reflection coefficients will be presented. Further simplification of the small perturbation model is not required.

Kirchhoff Stationary-Phase Approximation

The remaining two models share the same evolution up to a point, after which differing assumptions were made for different conditions. The Kirchhoff stationary-phase model has two restrictions, namely, that $k\sigma > 2$ and $kL > 6$, which implies a restriction on the RMS slope of $m > 0.47$. This model takes the form for the backscattering case of

$$\sigma^o_{pp} = \frac{|R_{pp}(0)|^2 \, e^{-\tan^2\theta/2m^2}}{2m^2 \cos^4 \theta} \qquad \text{(C.3)}$$

$$\sigma^o_{pq} = 0 \quad \text{for } p \neq q \ ,$$

where p,q denote received and transmitted polarizations, and

$R_{pp}(0)$ is the Fresnel reflection coefficient at normal incidence. Clearly, σ^o_{vv} and σ^o_{hh} could be equivalent. Again, further simplification is not necessary.

Kirchhoff-Scalar Approximation

This model also has certain restrictions that $kL > 6$ and $m < 0.25$, which implies that $\sigma < 0.25L$. If we assume an exponential surface correlation function, $e^{-\zeta/L}$, the expression for backscattering is

$$\sigma^o_{pp} = 2|R_{pp}|^2 \cos^2\theta \exp[-4k^2\sigma^2\cos^2\theta] \sum_{n=1}^{\infty} \frac{(4k^2\sigma^2\cos^2\theta)^n}{n!} \frac{n/kL}{[4\sin^2\theta + \frac{n^2}{(kL)^2}]^{1.5}}, \qquad (C.4)$$

where R_{pp} is the Fresnel reflection coefficient for pp polarization and θ is the angle of incidence. Polarization is the only factor in the R_{pp} term; therefore, $\sigma^o_{pq} = 0$ for $p \neq q$.

Clearly, the infinite summation makes the computation difficult at best; however, upon close examination it is apparent that only the first ten or so terms are significant. Table C.1 lists the RMS error, maximum and minimum error, and the correlation coefficient (r^2) as the summation is made up to eight terms long. The results are from a data set generated by a program that computes σ^o using many more terms, beyond which further terms are insignificant. In establishing the data set, the angles were varied from 5° to 60° in increments of 5° with an

additional angle of 1°, the $k\sigma$ term was varied from 0.1 to 0.9 in increments of 0.1, and kL took on the values 7, 15, 30, and 60. As can be seen in the table, limiting the calculation to the first five terms results in an RMS error of only 0.14 dB and a correlation of nearly 1. The conditions under which the large underestimation by the truncated model occurs were investigated and it was found that the errors are most significant for $5^0 < \theta < 30^0$, with the worst case being at $\theta = 10°$, and that these errors are least significant for small $k\sigma$ and kL, i.e., when $k\sigma$ and kL are both at the maximum (0.9 and 60) the extreme errors appeared. Therefore, as the inputs approach those yielding significant errors, it may be desirable to include additional terms in the summation, whereas for inputs away from this area, few terms are necessary.

Plots of normalized σ^o versus the various parameters for all three models are shown at the end of this appendix along with tabulations of theoretical values used in deriving the empirical model given above.

Coherent Backscattering

So far, all the surface scattering models have dealt with incoherent backscattering. For most cases, this is the only term of significance. However, for sufficiently smooth surfaces near nadir, a term accounting for coherent backscattering is necessary. Because closed-form expressions exist, simplifications will not be necessary. Fung and Eom (1983a) presented the following model for coherent backscattering for small incidence

angles, θ:

$$\sigma^o_{coh}(\theta) \cong \frac{|R_{pp}(\theta)|^2}{\left(\frac{1}{k^2R_o^2\beta_o^2} + \frac{\beta_o^2}{4}\right)} \exp\left[-4k^2\sigma^2 - \frac{\theta^2}{\left(\frac{1}{k^2R_o^2\beta_o^2} + \frac{\beta_o^2}{4}\right)}\right] \quad (C.5)$$

Here R_{pp} represents the Fresnel reflection coefficient, k is the freespace wave number ($2\pi/\lambda$), R_o is the range to the target along the antenna bore sight, and β_o is the one-sided beamwidth of the antenna. The surface roughness is characterized by $k\sigma$ and θ is the incidence angle relative to nadir.

Fresnel Reflection Coefficients

The Fresnel reflection coefficient for a wave impinging on a plane dielectric surface from free space is denoted by R_{pp}, where pp is the wave polarization. For vertical or parallel polarization

$$R_{VV} = \frac{\varepsilon_r \cos\theta + \sqrt{\varepsilon_r - \sin^2\theta}}{\varepsilon_r \cos\theta + \sqrt{\varepsilon_r - \sin^2\theta}} \quad (C.6)$$

and for horizontal or perpendicular polarization

$$R_{HH} = \frac{\cos\theta - \sqrt{\varepsilon_r - \sin^2\theta}}{\cos\theta + \sqrt{\varepsilon_r - \sin^2\theta}}. \quad (C.7)$$

Since ε_r may be complex, the computation of $|R_{VV}|^2$ and $|R_{hh}|^2$ may be complicated; therefore empirical models were derived. For ε_r complex it may be expressed as $\varepsilon_r' - j\varepsilon_r''$ and another quantity loss tangent may now be defined as $\tan\delta = \frac{\varepsilon_r''}{\varepsilon_r'}$. Hence the

following model has as parameters θ, ε_r', and $\tan\delta$. For vertical polarization,

$$|R_{vv}|^2 = g_1(\theta) \cdot g_2(\varepsilon_r') \cdot g_3(\tan\delta) \qquad (C.8)$$

where

$$g_1(\theta) = 0.7031 + 1.385 \times 10^{-3}\theta - 1.223 \times 10^{-4}\theta^2 \qquad (C.9a)$$

(θ in degrees)

$$g_2(\varepsilon_r'') = 6.134 \times 10^{-2} + 3.977 \times 10^{-2}(\varepsilon_r') - 4.336 \times 10^{-4}(\varepsilon_r')^2 \qquad (C.9b)$$

$$g_3(\tan\delta) = 0.7942 + 2.277 \times 10^{-2}(\tan\delta) + 0.2014\ (\tan\delta)^2 \ . \qquad (C.9c)$$

The product of g_1, g_2, and g_3 is the magnitude of the Fresnel reflection coefficient squared, for vertical polarization. The RMS difference error is 0.02 and r^2 is 0.98.

For horizontal polarization

$$|R_{hh}|^2 = h_1(\theta) \cdot h_2(\varepsilon_r') \cdot h_3(\tan\delta), \text{ where} \qquad (C.10)$$

$$h_1(\theta) = 0.6613 - 5.707 \times 10^{-4}\theta + 9.307 \times 10^{-5}\ \theta^2 \qquad (C.11a)$$

(θ in degrees)

$$h_2(\varepsilon_r') = 0.2532 + 3.803 \times 10^{-2}(\varepsilon_r') - 4.525 \times 10^{-4}(\varepsilon_r')^2 \qquad (C.11b)$$

$$h_3(\tan\delta) = 0.7475 + 1.653 \times 10^{-2}(\tan\delta) + 0.1291\ (\tan\delta)^2. \quad \text{(C.11c)}$$

The product of h_1, h_2, and h_3 is the magnitude of the Fresnel reflection coefficient squared for horizontal polarization. the RMS difference error is 0.03 and r^2 is 0.96.

A similar model was derived for $|\alpha_{VV}|^2$ for use in the small perturbation model. This empirical model has the form

$$|\alpha_{VV}|^2 = b_1(\theta) \cdot b_1(\varepsilon_r') + b_2(\tan\delta), \quad \text{(C.12)}$$

where

$$b_1(\theta) = 0.6642 - 2.959 \times 10^{-3}\theta^2 + 8.874 \times 10^{-5}\theta^3 \quad \text{(C.13a)}$$

(θ in degrees)

$$b_2(\varepsilon_r') = 2.988 \times 10^{-4} + 7.790 \times 10^{-2}(\varepsilon_r') - 7.259 \times 10^{-4}(\varepsilon_r')^2 \quad \text{(C.13b)}$$

$$b_3(\tan\delta) = 0.8224 + 2.521 \times 10^{-2}(\tan\delta) + 0.2630\ (\tan\delta)^2. \quad \text{(C.13c)}$$

The product of b_1, b_2, and b_3 is an estimate of $|\alpha_{VV}|^2$ with an RMS difference error of 0.53 and an r^2 of 0.98.

In deriving all three models, the ranges on θ, ε_r', and $\tan\delta$ are $0 \leq \theta \leq 60^0$; $5 \leq \varepsilon_r' \leq 45$; $0 \leq \tan\delta \leq 0.6$.

Volume Backscattering Model

In Chapter 13 of Ulaby et al. (1984) the case of scattering

by a lossy-scattering volume over a surface is treated, and a solution via the radiative transfer approach is given. When applied to a volume having no definable upper surface, as is the case with a vegetation canopy, this theoretical model takes the form of a matrix equation

$$\sigma^o_{pq}(\mu_{SK}, \mu_\ell, \phi_s - \phi) = 4\pi\frac{\mu_k}{w_\ell}\{\sum_{m=0}^{\infty}[S^m \cos m(\phi_s-\phi) + S^{-m}\sin m(\phi_s-\phi)]$$

$$+ \sum_{m=0}^{\infty}[(D^m - S^m_{TO})\cos m(\phi_s - \phi) + (D^{-m} - S^{-m}_{TO})\sin m(\phi_s - \phi)]$$

$$+ E\Gamma E\}_{pq} \qquad (C.14)$$

where S, D, E, and Γ represent matrices. The exact definition and derivation of each term will not be included here; therefore, interested readers are referred to Eom and Fung (1983b). Essentially, the first summation represents the diffuse volume scattering, while the second summation represents the diffuse volume-surface interaction. The last term ($E\Gamma E$) represents direct surface scattering.

Hence, the above equation may be rewritten in terms of individual components as

$$\sigma^o_{total} = \sigma^o_{surface} + \sigma^o_{volume} + \sigma^o_{interaction} . \qquad (C.15)$$

The volume is assumed to have no upper boundary, i.e., $\varepsilon_{vol} \simeq 1$, and is characterized by only its optical depth, τ, and its albedo, ω. For a given surface ($k\sigma$, kL, ε_r, $\tan\delta$) the

contribution to the total is easily computed as

$$\sigma^o_{surface}(k\sigma,kL,\varepsilon_r,\tan\delta;\ \theta,\tau) = \sigma^o_{surface}(k\sigma,kL,\varepsilon_r,\tan\delta;\ \theta,0)/L^2(\theta,\tau) \tag{C.16}$$

where L^2 represents the round-trip loss through the canopy at an angle of θ and is written as

$$L^2(\theta,\tau) = \exp(2\tau/\cos\theta). \tag{C.17}$$

The σ^o_{volume} term is less simple. If we assume that losses due to scattering and absorption are polarization-independent, and that all scattering within the volume behaves in a Rayleigh phase manner, and if we ignore all but single scattering, the following equation is obtained:

$$\sigma^o_{pp} = 0.75\ \omega\ [1-\exp(-2\tau/\cos\theta)]\ \cos\theta$$
and
$$\sigma^o_{pq} = 0 \text{ for } p\neq q, \qquad p,q \text{ are v and h.} \tag{C.18}$$

However, the full theoretical model does not restrict itself to single scattering cases. This, it turns out, has a small impact on pp polarizations and a major impact on pq polarizations, i.e., σ^o_{pq} $(p\neq q)$ is no longer zero.

The single scattering form of σ^o_{pp} was used in deriving an empirical model with the following results:

$$\sigma^o_{vv} \approx \sigma^o_{hh} \doteq 0.742\omega\ (1 + 0.536\omega\tau - 0.237\ (\omega\tau)^2) \qquad (C.19)$$

$$[1 - \exp(-2.119\tau \sec\theta)] \cos\theta$$

and

$$\sigma^o_{vh} \doteq \omega(0.0438\omega\tau - 0.0175(\omega\tau)^2 + 0.006085(\omega\tau)^3)$$

$$[1 - \exp\ (-11.727\tau \sec\theta)] \cos\theta. \qquad (C.20)$$

The RMS errors were found to be 0.174 dB for like polarization (vv, hh) and 2.17 dB for cross polarization (vh). The correlation coefficient associated with each model are for like polarization $r^2 = 0.9994$ and for cross polarization $r^2 = 0.9744$.

The ranges of the input parameters used in deriving these empirical models are as follows: $8.4^0 \leq \theta \leq 84.5^0$; $0.1 \leq \tau \leq 2.2$; $0.01 \leq \omega \leq 0.5$. As a note, the peculiar selection of angles at which σ^o is evaluated in the theoretical model is a result of integration by Gaussian quadrature, which reduces the required processing considerably.

Surface-Volume Interaction Model

The surface-volume interaction backscattering is also computed using Eq. (C.14). As a simple first-order approximation, the following model has been proposed as an estimate

$$\sigma^o_{int}\ (\theta) = 2\sigma^o_{vol}(\theta)\ |R_{pp}(\theta)|^2\ e^{-\tau/\cos\theta}\ , \qquad (C.21)$$

where $\sigma^o_{vol}(\theta)$ is the volume backscattering coefficient, $R_{pp}(\theta)$ is the Fresnel reflection coefficient at polarization pp and incidence angle θ. One factor not accounted for in this simple approach is surface roughness. If we assume that the surface portion of the interaction component is dominated by forward or specular scattering, then we may model the roughness dependence as for coherent backscattering, i.e., with an $\exp[-(k\sigma)^2\cos\theta]$ dependence. Incorporating this dependence into Eq. (C.21) as well as a model of the form of Eq. (C.19) to represent σ^o_{vol}, we have a basis for σ^o_{int}.

Prior to optimization of the free model parameters to obtain a "best fit," an investigation into the significance of σ^o_{int} in σ^o_{tot}, Eq. (C.15), was made. For the ranges of θ, τ, ω, and $k\sigma$ used in obtaining these empirical models, the difference in σ^o_{tot} and $\sigma^o_{vol} + \sigma^o_{surface}$, i.e., σ^o_{tot} neglecting σ^o_{int} for VV polarization rarely exceeds 1 dB, whereas for HH polarization the difference frequently exceeds 3 dB. For VH polarization, σ^o_{int} usually dominates σ^o_{tot}. Therefore it was decided that an empirical model for σ^o_{int} in VV polarization is not necessary. For the remaining polarizations (HH and VH) the model was optimized, and the results are shown below.

$$\sigma^o_{HH} \doteq 1.924\ \omega[1 + 0.924\omega\tau + 0.398(\omega\tau)^2]$$
$$[1 - \exp(-1.925\tau\sec\theta)]\exp(-1.372\tau^{1.12}\sec\theta)$$
$$\exp[-0.836(k\sigma)^2\cos\theta]\ |R_{hh}|^2\cos\theta \qquad \text{(C.22)}$$

$$\sigma^o_{VH} = 0.01284\ \omega[1 + 7.848\omega\tau + 7.896(\omega\tau)^2]$$

$$[1 - \exp(-6.915\tau \sec\theta)] \exp(-1.024\tau^{1.38}\sec\theta)$$
$$\exp(2.892(k\sigma)^2\cos\theta)\ \tfrac{1}{2}[|R_{vv}|^2 + |R_{hh}|^2]\cos\theta \qquad (C.23)$$

The RMS errors were found to be 0.233 dB and 1.247 dB for HH and VH polarizations, respectively, while the correlation coefficients (r^2) were found to be 0.9989 and 0.9775.

The ranges of the input parameters used in deriving these empirical models are as follows: $8.4^0 \leq \theta \leq 62.7^0$; $0.1 \leq \tau \leq 2.2$; $0.01 \leq \omega \leq 0.5$; and $0.1 \leq k\sigma \leq 0.9$. The other necessary input parameters were set to constant values of $\epsilon = 15$ and $kL = 7$. The upper limit on θ was lowered to 62.7° in order to improve the model fits.

Summary of the Empirical Models

Fresnel Reflectivity $|R_{pp}|^2$

$$|R_{vv}|^2 = g_1(\theta) \cdot g_2(\varepsilon_r') \cdot g_3(\tan\delta)$$

where

$g_1(\theta) = 0.7031 + 1.385 \times 10^{-3}\theta - 1.223 \times 10^{-4}\theta^2$ (θ in degrees)

$g_2(\varepsilon_r') = 6.134 \times 10^{-2} + 3.977 \times 10^{-2}(\varepsilon_r') - 4.336 \times 10^{-4}(\varepsilon_r')^2$

$g_3(\tan\delta) = 0.7942 + 2.277 \times 10^{-2}(\tan\delta) + 0.2014\ (\tan\delta)^2$

RMS Error = 0.02 $\quad r^2 = 0.9808$, N = 245

$|R_{vv}|^2 = 0.961 \cdot |R_{vv}|^2 + 0.0144$, standard error = 0.02

Range of validity: $0 < \theta < 60^0$; $5 < \varepsilon_r' < 45$; $0 < \tan\delta < 0.6$

$|\text{Error}|_{max} = 0.059$

$$|R_{hh}|^2 = h_1(\theta) \cdot h_2(\varepsilon_r') \cdot h_3(\tan\delta)$$

where

$h_1(\theta) = 0.6613 - 5.707 \times 10^{-4}\theta + 9.307 \times 10^{-5}\theta^2$ (θ in degrees)

$h_2(\varepsilon_r') = 0.2532 + 3.803 \times 10^{-2}(\varepsilon_r') - 4.525 \times 10^{-4}(\varepsilon_r')^2$

$h_3(\tan\delta) = 0.7475 + 1.653 \times 10^{-2}(\tan\delta) + 0.1291\ (\tan\delta)^2$

RMS Error = 0.03 $\quad r^2 = 0.9647$, N = 245

$|R_{hh}|^2 = 0.946\ |R_{hh}|^2 + 0.0274$, standard error = 0.03

Range of validity: $0 < \theta < 60^0$; $5 < \varepsilon_r' < 45$; $0 < \tan\delta < 0.6$

$|\text{Error}|_{max} = 0.096$

$|\alpha_{vv}|^2$

$|\alpha_{vv}|^2 = b_1(\theta) \cdot b_2(\varepsilon_r') \cdot b_3(\tan\delta)$

where

$b_1(\theta) = 0.6642 - 2.959 \times 10^{-3}\theta^2 + 8.874 \times 10^{-5}\theta^3$ (θ in degrees)

$b_2(\varepsilon_r') = 2.988 \times 10^{-4} + 7.790 \times 10^{-2}(\varepsilon_r') - 7.259 \times 10^{-4}(\varepsilon_r')^2$

$b_3(\tan\delta) = 0.8224 + 2.521 \times 10^{-2}(\tan\delta) + 0.2630\ (\tan\delta)^2$

RMS Error = 0.53, $r^2 = 0.9840$, N = 245

$|\alpha_{vv}|^2 = 0.983\ |\alpha_{vv}|^2 + 0.015$, standard error = 0.52

Range of validity: $0 \leq \theta \leq 60^0$; $5 \leq \varepsilon_r' \leq 45$; $0 \leq \tan\delta \leq 0.6$

$|\text{Error}|_{max} = 1.641$ (occurs for large θ and large ε_r')

Volume Backscattering: σ^o_{vol}

$$\sigma^o_{vv} = \sigma^o_{hh} = 0.742\ \omega[1 + 0.536(\omega\tau) - 0.237(\omega\tau)^2] [1-\exp(-2.119\tau \sec\theta)] \cos\theta$$

RMS Error = 0.174 dB, $r^2 = 0.9994$, N = 416

$\sigma^o_{pp} = 0.991\ \sigma^o_{pp} - 0.110$ dB, standard error = 0.164 dB

Range of validity: $8.4^0 \leq \theta \leq 84.5^0$; $0.1 \leq \tau \leq 2.2$;

$0.01 \leq \omega \leq 0.5$

$|\text{Error}|_{max} = 0.64$ dB

$$\sigma^o_{VH} = \omega[0.0438(\omega\tau) - 0.0175(\omega\tau)^2 + 0.006085(\omega\tau)^3] [1 - \exp(-11.727\tau \sec\theta)] \cos\theta$$

RMS Error = 2.17 dB, $r^2 = 0.9744$, N = 416

$\sigma^o_{vh} = 0.927\ \sigma^o_{vh} - 2.513$ dB, standard error = 1.957 dB

Range of validity: $8.4^0 \leq \theta \leq 84.5^0$; $0.1 \leq \tau \leq 2.2$;

$0.01 \leq \omega \leq 0.5$

$|\text{Error}|_{max} = 8.69$ dB (occurs when θ is large, τ is large)

Surface-Volume Interaction: σ^o_{int}

$$\sigma^o_{hh} = 1.924\ \omega[1 + 0.924(\omega\tau) + 0.398\ (\omega\tau)^2]$$
$$[1 - \exp(-1.925\tau \sec\theta)] \exp(-1.372\ \tau^{1.12}\sec\theta)$$
$$\exp[-0.836(k\sigma)^2\cos\theta]\ |R_{hh}|^2 \cos\theta,$$

RMS Error = 0.233 dB $\quad r^2 = 0.9989$, N = 366

$\sigma^o_{hh} = 0.9970\ \ \sigma^o_{hh} - 0.0901$ dB, standard error = 0.232 dB

Range of validity: $8.4^0 \leq \theta \leq 62.7^0$; $0.1 \leq \tau \leq 2.2$;

$0.01 \leq \omega \leq 0.5$; $0.1 \leq k\sigma \leq 0.9$, $kL = 7$

$|\text{Error}|_{max} = 2.08$ dB (|Error| exceeds 1 dB only when $\theta = 62.5°$ and $\tau > 1.9$)

$$\sigma^o_{vh} = 0.01284\ \omega[1 + 7.848(\omega\tau) + 7.896(\omega\tau)^2]$$
$$[1 - \exp(-6.915\tau \sec\theta)] \exp(-1.024\tau^{1.38}\sec\theta)$$
$$\exp[2.892(k\sigma)^2\cos\theta]\ 1/2\ [|R_{vv}|^2 + |R_{hh}|^2] \cos\theta$$

RMS Error = 1.247 dB, $\quad r^2 = 0.9775$, N = 366

$\sigma^o_{vh} = 0.9763\ \ \sigma^o_{vh} - 0.7592$ dB, standard error = 1.235 dB

Range of validity: $8.4^0 \leq \theta \leq 62.7^0$; $0.1 \leq t \leq 2.2$;

$0.01 \leq \omega \leq 0.5$; $0.1 \leq k\sigma \leq 0.9$; $kL = 7$

$|\text{Error}|_{max} = 5.22$ dB (occur at both $\theta = 8.4°$ and $\theta = 62.5°$, $\tau > 1.6$)

Table C.1

Kirchhoff Scalar Approximation

Exponential Correlation Function: $e^{-\zeta/L}$

$$\sigma^0_{pp} \doteq 2|R_{pp}|^2 \cos^2\theta \exp[-4(k\sigma)^2\cos^2\theta] \sum_{n=1}^{M} \frac{(4(k\sigma)^2\cos^2\theta)^n}{n!} \frac{(n/kL)}{[4\sin^2\theta + \frac{n^2}{(kL)^2}]^{1.5}}$$

Comparison of truncated model with full model ($M = \infty$)

M	RMS error (dB)	MAX error (dB)	MIN error (dB)	r^2
1	4.493	-0.02	-13.37	0.9603
2	1.904	0.02	-7.24	0.9908
3	0.835	0.02	-3.87	0.9980
4	0.356	0.02	-1.97	0.9996
5	0.144	0.02	-0.93	0.9999
6	0.054	0.02	-0.40	1
7	0.019	0.02	-0.15	1
8	0.008	0.02	-0.05	1

Range of Values

$1^0 \leq \theta \leq 60^0$ N = 468

$0.1 \leq k\sigma \leq 0.9$ error = σ^0_{pred} (dB) - σ^0_{true} (dB)

$7 \leq kL \leq \infty$

The following is a tabulation of

(1) The normalized σ^o (dB) computed using the Kirchhoff-Scalar Approximation model for 9 values of $k\sigma$ (0.1 to 0.9) and 4 values of kL (7,15,30,60). To get σ^o_{vv} or σ^o_{hh} in decibels simply add the appropriate Fresnel reflectivity ($|R_{pp}|^2$), expressed in dB.

(2) The computed σ^o (dB) from a volume bounded by a rough ($k\sigma$ = 0.5, kL = 7, ϵ = 15-j0) surface on the bottom for various optical depths τ (0.1, 0.2, 0.4, 0.6, 0.8, 1.2, 1.6, 1.9, 2.2) and albedos ω (0.01, 0.1, 0.2, 0.3, 0.4, 0.5), and incident angles θ (8.4, 19.2, 30.0, 40.9, 51.8, 62,7, 73.6, 84.5°). The total backscattering (σ^o) for a given θ, τ, ω, and polarization is the sum of three components: volume, interaction, and surface. Note that before summation, these values must first be returned to real ($m^2\ m^{-2}$) values. Also note that there is no surface term for cross-polarization values, i.e., $\sigma^o_{vh} = \sigma^o_{hv} = 0$ for the surface component.

(3) The computed σ^o(dB) from a volume (albedo = 0.2, optical depth = 0.2) bounded by a rough surface on the bottom with a fixed correlation length (kL = 7) and various surface RMS heights, $k\sigma$(0.1 to 0.9). Total backscattering is found as described in (2) above.

ksigma = 0.1 NORMALIZED SIGMA0

INCIDENCE ANGLE	SURFACE BACKSCATTER IN DECIBELS kL= 7	kL=15	kL=30	kL=60
1	5.42	10.82	13.62	13.54
5	-0.20	-0.98	-3.30	-6.13
10	-7.00	-9.48	-12.29	-15.26
15	-11.97	-14.88	-17.79	-20.78
20	-15.86	-18.93	-21.90	-24.87
25	-19.13	-22.29	-25.27	-28.27
30	-22.06	-25.26	-28.25	-31.24
35	-24.78	-28.00	-30.99	-34.02
40	-27.41	-30.65	-33.66	-36.66
45	-30.03	-33.26	-36.28	-39.29
50	-32.73	-35.98	-38.99	-41.98
55	-35.56	-38.83	-41.83	-44.84
60	-38.68	-41.94	-44.94	-47.95

ksigma = 0.2 NORMALIZED SIGMA0

INCIDENCE ANGLE	SURFACE BACKSCATTER IN DECIBELS kL= 7	kL=15	kL=30	kL=60
1	10.97	16.41	19.26	19.30
5	5.47	4.82	2.64	-0.12
10	-1.19	-3.52	-6.29	-9.23
15	-6.07	-8.89	-11.79	-14.76
20	-9.91	-12.92	-15.87	-18.87
25	-13.18	-16.29	-19.25	-22.25
30	-16.07	-19.25	-22.23	-25.23
35	-18.79	-21.99	-24.98	-27.98
40	-21.40	-24.63	-27.62	-30.63
45	-24.02	-27.26	-30.25	-33.26
50	-26.71	-29.96	-32.96	-35.97
55	-29.54	-32.81	-35.81	-38.81
60	-32.65	-35.92	-38.92	-41.93

ksigma = 0.3 NORMALIZED SIGMA0

INCIDENCE ANGLE	SURFACE BACKSCATTER IN DECIBELS kL= 7	kL=15	kL=30	kL=60
1	13.75	19.21	22.15	22.41
5	8.39	8.01	6.04	3.36
10	1.97	-0.14	-2.81	-5.73
15	-2.75	-5.42	-8.28	-11.24
20	-6.52	-9.44	-12.36	-15.35
25	-9.73	-12.79	-15.74	-18.73
30	-12.61	-15.74	-18.71	-21.72
35	-15.30	-18.48	-21.45	-24.46
40	-17.91	-21.12	-24.11	-27.11
45	-20.51	-23.75	-26.74	-29.74
50	-23.19	-26.44	-29.44	-32.44
55	-26.03	-29.29	-32.29	-35.29
60	-29.14	-32.40	-35.40	-38.39

ksigma = 0.4 NORMALIZED SIGMA0

INCIDENCE ANGLE	SURFACE BACKSCATTER IN DECIBELS kL= 7	kL=15	kL=30	kL=60
1	15.20	20.71	23.76	24.31
5	10.07	10.03	8.34	5.81
10	3.97	2.17	-0.37	-3.25
15	-0.57	-3.02	-5.81	-8.75
20	-4.22	-7.00	-9.88	-12.84
25	-7.37	-10.32	-13.24	-16.23
30	-10.20	-13.28	-16.22	-19.22
35	-12.88	-16.00	-18.97	-21.97
40	-15.45	-18.63	-21.62	-24.61
45	-18.04	-21.25	-24.24	-27.25
50	-20.73	-23.95	-26.94	-29.94
55	-23.55	-26.80	-29.78	-32.80
60	-26.65	-29.89	-32.90	-35.91

ksigma = 0.5 NORMALIZED SIGMA0

INCIDENCE ANGLE	SURFACE BACKSCATTER IN DECIBELS kL= 7	kL=15	kL=30	kL=60
1	15.83	21.38	24.59	25.49
5	10.96	11.35	10.00	7.64
10	5.27	3.84	1.48	-1.33
15	0.96	-1.22	-3.92	-6.83
20	-2.54	-5.14	-7.96	-10.92
25	-5.61	-8.43	-11.32	-14.30
30	-8.39	-11.36	-14.29	-17.28
35	-11.01	-14.06	-17.03	-20.04
40	-13.58	-16.71	-19.68	-22.66
45	-16.15	-19.32	-22.30	-25.31
50	-18.81	-22.01	-25.00	-28.01
55	-21.63	-24.86	-27.85	-30.86
60	-24.72	-27.97	-30.97	-33.97

ksigma = 0.6 NORMALIZED SIGMA0

INCIDENCE ANGLE	SURFACE BACKSCATTER IN DECIBELS kL= 7	kL=15	kL=30	kL=60
1	15.80	21.42	24.84	26.14
5	11.29	12.16	11.23	9.11
10	6.03	5.07	2.95	0.22
15	2.02	0.18	-2.37	-5.26
20	-1.32	-3.66	-6.41	-9.35
25	-4.26	-6.91	-9.76	-12.72
30	-6.97	-9.82	-12.72	-15.70
35	-9.54	-12.52	-15.46	-18.44
40	-12.07	-15.14	-18.10	-21.10
45	-14.62	-17.76	-20.73	-23.73
50	-17.27	-20.44	-23.42	-26.42
55	-20.07	-23.28	-26.27	-29.27
60	-23.15	-26.38	-29.38	-32.39

ksigma = 0.7 NORMALIZED SIGMA0

INCIDENCE ANGLE	SURFACE BACKSCATTER IN DECIBELS kL= 7	kL=15	kL=30	kL=60
1	15.31	20.98	24.63	26.38
5	11.17	12.58	12.12	10.29
10	6.42	5.99	4.13	1.52
15	2.73	1.28	-1.12	-3.95
20	-0.41	-2.47	-5.12	-8.02
25	-3.21	-5.66	-8.44	-11.38
30	-5.84	-8.54	-11.38	-14.37
35	-8.36	-11.22	-14.15	-17.11
40	-10.84	-13.83	-16.76	-19.77
45	-13.34	-16.43	-19.39	-22.40
50	-15.98	-19.11	-22.09	-25.09
55	-18.77	-21.95	-24.94	-27.94
60	-21.83	-25.05	-28.05	-31.05

ksigma = 0.8 NORMALIZED SIGMA0

INCIDENCE ANGLE	SURFACE BACKSCATTER IN DECIBELS kL= 7	kL=15	kL=30	kL=60
1	14.38	20.15	24.04	26.29
5	10.69	12.67	12.74	11.24
10	6.48	6.62	5.07	2.62
15	3.14	2.14	-0.05	-2.80
20	0.22	-1.48	-4.02	-6.87
25	-2.44	-4.61	-7.32	-10.23
30	-4.94	-7.45	-10.25	-13.21
35	-7.38	-10.12	-12.97	-15.95
40	-9.80	-12.69	-15.62	-18.59
45	-12.30	-15.30	-18.24	-21.22
50	-14.87	-17.97	-20.92	-23.93
55	-17.65	-20.79	-23.78	-26.79
60	-20.70	-23.90	-26.88	-29.89

ksigma = 0.9 NORMALIZED SIGMA0

INCIDENCE ANGLE	SURFACE BACKSCATTER IN DECIBELS kL= 7	kL=15	kL=30	kL=60
1	13.12	19.00	23.18	25.93
5	9.93	12.50	13.11	12.01
10	6.27	6.99	5.86	3.56
15	3.29	2.80	0.85	-1.81
20	0.62	-0.70	-3.05	-5.87
25	-1.87	-3.74	-6.33	-9.23
30	-4.25	-6.52	-9.25	-12.20
35	-6.58	-9.15	-11.97	-14.94
40	-8.95	-11.72	-14.60	-17.58
45	-11.38	-14.30	-17.22	-20.21
50	-13.92	-16.96	-19.91	-22.91
55	-16.66	-19.78	-22.76	-25.75
60	-19.70	-22.88	-25.86	-28.86

FOR ALL CASES: SURFACE DIELECTRIC = 15 - j0, ksigma = 0.5, kL = 7

BACKSCATTER COMPONENTS IN DECIBELS

ANGLE			------VOLUME-----			---INTERACTION---			--SURFACE--	
(DEG)	TAU	ALBEDO	VV	HH	VH	VV	HH	VH	VV	HH
8.4	0.1	0.01	-28.7	-28.7	-65.5	-31.4	-31.1	-41.6	1.4	1.5
19.2	0.1	0.01	-28.7	-28.7	-65.7	-32.9	-30.6	-43.9	-7.8	-7.3
30.0	0.1	0.01	-28.7	-28.7	-66.2	-35.9	-30.2	-44.9	-14.7	-13.4
40.9	0.1	0.01	-28.8	-28.8	-66.8	-40.7	-29.7	-45.5	-21.3	-18.7
51.8	0.1	0.01	-28.9	-28.9	-67.7	-42.9	-29.1	-46.4	-28.8	-24.1
62.7	0.1	0.01	-29.1	-29.1	-68.7	-42.4	-28.7	-48.4	-39.2	-30.6
73.6	0.1	0.01	-29.7	-29.7	-69.9	-52.8	-28.8	-51.9	-63.6	-40.4
84.5	0.1	0.01	-32.0	-32.0	-72.9	-41.3	-34.0	-59.8	-71.4	-64.9

BACKSCATTER COMPONENTS IN DECIBELS

ANGLE			------VOLUME-----			---INTERACTION---			--SURFACE--	
(DEG)	TAU	ALBEDO	VV	HH	VH	VV	HH	VH	VV	HH
8.4	0.1	0.10	-18.6	-18.6	-45.4	-21.3	-20.9	-31.3	1.4	1.5
19.2	0.1	0.10	-18.6	-18.6	-45.7	-22.8	-20.5	-33.5	-7.8	-7.3
30.0	0.1	0.10	-18.7	-18.7	-46.1	-25.8	-20.1	-34.4	-14.7	-13.4
40.9	0.1	0.10	-18.7	-18.8	-46.8	-30.5	-19.5	-35.0	-21.3	-18.7
51.8	0.1	0.10	-18.9	-18.9	-47.6	-32.6	-19.0	-36.0	-28.8	-24.1
62.7	0.1	0.10	-19.1	-19.1	-48.5	-32.2	-18.6	-37.9	-39.2	-30.6
73.6	0.1	0.10	-19.6	-19.6	-49.8	-41.8	-18.7	-41.3	-63.6	-40.4
84.5	0.1	0.10	-21.9	-22.0	-52.8	-31.1	-23.9	-48.6	-71.4	-64.9

BACKSCATTER COMPONENTS IN DECIBELS

ANGLE			------VOLUME-----			---INTERACTION---			--SURFACE--	
(DEG)	TAU	ALBEDO	VV	HH	VH	VV	HH	VH	VV	HH
8.4	0.1	0.20	-15.6	-15.6	-39.3	-18.2	-17.8	-28.0	1.4	1.5
19.2	0.1	0.20	-15.6	-15.6	-39.5	-19.7	-17.4	-30.0	-7.8	-7.3
30.0	0.1	0.20	-15.6	-15.6	-40.0	-22.7	-17.0	-30.9	-14.7	-13.4
40.9	0.1	0.20	-15.7	-15.7	-40.6	-27.3	-16.5	-31.5	-21.3	-18.7
51.8	0.1	0.20	-15.8	-15.8	-41.4	-29.2	-15.9	-32.5	-28.8	-24.1
62.7	0.1	0.20	-16.0	-16.1	-42.4	-28.9	-15.5	-34.4	-39.2	-30.6
73.6	0.1	0.20	-16.5	-16.6	-43.6	-37.9	-15.6	-37.6	-63.6	-40.4
84.5	0.1	0.20	-18.9	-18.9	-46.7	-28.0	-20.8	-44.5	-71.4	-64.9

BACKSCATTER COMPONENTS IN DECIBELS

ANGLE			------VOLUME-----			---INTERACTION---			--SURFACE--	
(DEG)	TAU	ALBEDO	VV	HH	VH	VV	HH	VH	VV	HH
8.4	0.1	0.30	-13.8	-13.8	-35.7	-16.4	-16.0	-25.9	1.4	1.5
19.2	0.1	0.30	-13.8	-13.8	-35.9	-17.8	-15.6	-27.8	-7.8	-7.3
30.0	0.1	0.30	-13.8	-13.8	-36.4	-20.8	-15.1	-28.7	-14.7	-13.4
40.9	0.1	0.30	-13.9	-13.9	-37.0	-25.2	-14.6	-29.3	-21.3	-18.7
51.8	0.1	0.30	-14.0	-14.0	-37.8	-27.2	-14.1	-30.3	-28.8	-24.1
62.7	0.1	0.30	-14.2	-14.3	-38.8	-27.0	-13.7	-32.2	-39.2	-30.6
73.6	0.1	0.30	-14.7	-14.8	-40.0	-35.3	-13.8	-35.3	-63.6	-40.4
84.5	0.1	0.30	-17.0	-17.1	-43.0	-26.1	-19.0	-41.7	-71.4	-64.9

FOR ALL CASES: SURFACE DIELECTRIC = 15 - j0, ksigma = 0.5, kL = 7

BACKSCATTER COMPONENTS IN DECIBELS

ANGLE			------VOLUME-----			---INTERACTION---			--SURFACE--	
(DEG)	TAU	ALBEDO	VV	HH	VH	VV	HH	VH	VV	HH
8.4	0.1	0.40	-12.5	-12.5	-33.1	-15.0	-14.6	-24.4	1.4	1.5
19.2	0.1	0.40	-12.5	-12.5	-33.3	-16.4	-14.2	-26.1	-7.8	-7.3
30.0	0.1	0.40	-12.5	-12.5	-33.8	-19.4	-13.8	-27.0	-14.7	-13.4
40.9	0.1	0.40	-12.6	-12.6	-34.4	-23.7	-13.3	-27.6	-21.3	-18.7
51.8	0.1	0.40	-12.7	-12.7	-35.2	-25.6	-12.8	-28.6	-28.8	-24.1
62.7	0.1	0.40	-12.9	-13.0	-36.2	-25.5	-12.3	-30.5	-39.2	-30.6
73.6	0.1	0.40	-13.4	-13.5	-37.4	-33.3	-12.4	-33.5	-63.6	-40.4
84.5	0.1	0.40	-15.7	-15.8	-40.4	-24.7	-17.6	-39.6	-71.4	-64.9

BACKSCATTER COMPONENTS IN DECIBELS

ANGLE			------VOLUME-----			---INTERACTION---			--SURFACE--	
(DEG)	TAU	ALBEDO	VV	HH	VH	VV	HH	VH	VV	HH
8.4	0.1	0.50	-11.5	-11.5	-31.1	-14.0	-13.5	-23.1	1.4	1.5
19.2	0.1	0.50	-11.5	-11.5	-31.3	-15.3	-13.1	-24.8	-7.8	-7.3
30.0	0.1	0.50	-11.5	-11.5	-31.8	-18.3	-12.7	-25.6	-14.7	-13.4
40.9	0.1	0.50	-11.5	-11.6	-32.4	-22.5	-12.2	-26.2	-21.3	-18.7
51.8	0.1	0.50	-11.6	-11.7	-33.2	-24.4	-11.7	-27.2	-28.8	-24.1
62.7	0.1	0.50	-11.8	-11.9	-34.1	-24.3	-11.3	-29.1	-39.2	-30.6
73.6	0.1	0.50	-12.3	-12.5	-35.3	-31.6	-11.4	-32.0	-63.6	-40.4
84.5	0.1	0.50	-14.7	-14.8	-38.3	-23.6	-16.5	-37.8	-71.4	-64.9

BACKSCATTER COMPONENTS IN DECIBELS

ANGLE			------VOLUME-----			---INTERACTION---			--SURFACE--	
(DEG)	TAU	ALBEDO	VV	HH	VH	VV	HH	VH	VV	HH
8.4	0.2	0.01	-26.1	-26.1	-60.7	-29.4	-29.0	-39.7	0.6	0.6
19.2	0.2	0.01	-26.1	-26.1	-61.0	-30.9	-28.6	-42.2	-8.7	-8.2
30.0	0.2	0.01	-26.2	-26.2	-61.4	-34.1	-28.3	-43.3	-15.7	-14.4
40.9	0.2	0.01	-26.3	-26.3	-62.1	-39.2	-27.9	-44.1	-22.4	-19.8
51.8	0.2	0.01	-26.5	-26.5	-62.9	-41.7	-27.6	-45.3	-30.2	-25.5
62.7	0.2	0.01	-27.0	-27.0	-64.0	-41.4	-27.7	-47.7	-41.1	-32.5
73.6	0.2	0.01	-27.9	-27.9	-65.6	-52.9	-29.1	-52.1	-66.7	-43.5
84.5	0.2	0.01	-31.5	-31.5	-70.6	-47.5	-40.4	-64.2	-80.6	-74.1

BACKSCATTER COMPONENTS IN DECIBELS

ANGLE			------VOLUME-----			---INTERACTION---			--SURFACE--	
(DEG)	TAU	ALBEDO	VV	HH	VH	VV	HH	VH	VV	HH
8.4	0.2	0.10	-16.0	-16.0	-40.6	-19.2	-18.8	-29.3	0.6	0.6
19.2	0.2	0.10	-16.0	-16.0	-40.8	-20.8	-18.5	-31.5	-8.7	-8.2
30.0	0.2	0.10	-16.1	-16.1	-41.3	-23.9	-18.1	-32.6	-15.7	-14.4
40.9	0.2	0.10	-16.2	-16.3	-41.9	-29.0	-17.8	-33.3	-22.4	-19.8
51.8	0.2	0.10	-16.5	-16.5	-42.8	-31.2	-17.5	-34.6	-30.2	-25.5
62.7	0.2	0.10	-16.9	-16.9	-43.8	-31.1	-17.6	-36.9	-41.1	-32.5
73.6	0.2	0.10	-17.8	-17.9	-45.5	-41.6	-18.9	-41.0	-66.7	-43.5
84.5	0.2	0.10	-21.4	-21.4	-50.4	-37.2	-30.2	-51.9	-80.6	-74.1

FOR ALL CASES: SURFACE DIELECTRIC = 15 - j0, ksigma = 0.5, kL = 7

BACKSCATTER COMPONENTS IN DECIBELS

ANGLE			------VOLUME-----			---INTERACTION---			--SURFACE--	
(DEG)	TAU	ALBEDO	VV	HH	VH	VV	HH	VH	VV	HH
8.4	0.2	0.20	-12.9	-12.9	-34.4	-16.1	-15.7	-25.8	0.6	0.6
19.2	0.2	0.20	-12.9	-13.0	-34.7	-17.6	-15.3	-27.8	-8.7	-8.2
30.0	0.2	0.20	-13.0	-13.0	-35.1	-20.7	-15.0	-28.8	-15.7	-14.4
40.9	0.2	0.20	-13.1	-13.2	-35.7	-25.6	-14.6	-29.6	-22.4	-19.8
51.8	0.2	0.20	-13.3	-13.4	-36.6	-27.8	-14.4	-30.8	-30.2	-25.5
62.7	0.2	0.20	-13.8	-13.8	-37.6	-27.8	-14.5	-33.0	-41.1	-32.5
73.6	0.2	0.20	-14.7	-14.8	-39.2	-37.4	-15.8	-36.9	-66.7	-43.5
84.5	0.2	0.20	-18.3	-18.4	-44.2	-33.9	-26.9	-47.1	-80.6	-74.1

BACKSCATTER COMPONENTS IN DECIBELS

ANGLE			------VOLUME-----			---INTERACTION---			--SURFACE--	
(DEG)	TAU	ALBEDO	VV	HH	VH	VV	HH	VH	VV	HH
8.4	0.2	0.30	-11.1	-11.1	-30.7	-14.2	-13.8	-23.5	0.6	0.6
19.2	0.2	0.30	-11.1	-11.1	-31.0	-15.6	-13.4	-25.4	-8.7	-8.2
30.0	0.2	0.30	-11.2	-11.2	-31.4	-18.7	-13.1	-26.3	-15.7	-14.4
40.9	0.2	0.30	-11.3	-11.3	-32.0	-23.4	-12.7	-27.1	-22.4	-19.8
51.8	0.2	0.30	-11.5	-11.6	-32.9	-25.5	-12.5	-28.3	-30.2	-25.5
62.7	0.2	0.30	-11.9	-12.0	-33.9	-25.7	-12.6	-30.5	-41.1	-32.5
73.6	0.2	0.30	-12.8	-13.0	-35.5	-34.5	-13.9	-34.2	-66.7	-43.5
84.5	0.2	0.30	-16.4	-16.6	-40.4	-31.8	-24.9	-43.8	-80.6	-74.1

BACKSCATTER COMPONENTS IN DECIBELS

ANGLE			------VOLUME-----			---INTERACTION---			--SURFACE--	
(DEG)	TAU	ALBEDO	VV	HH	VH	VV	HH	VH	VV	HH
8.4	0.2	0.40	-9.3	-9.8	-28.1	-12.8	-12.3	-21.8	0.6	0.6
19.2	0.2	0.40	-9.8	-9.8	-28.3	-14.2	-12.0	-23.5	-8.7	-8.2
30.0	0.2	0.40	-9.8	-9.9	-28.7	-17.3	-11.7	-24.4	-15.7	-14.4
40.9	0.2	0.40	-9.9	-10.0	-29.4	-21.8	-11.3	-25.2	-22.4	-19.8
51.8	0.2	0.40	-10.1	-10.2	-30.2	-23.9	-11.1	-26.4	-30.2	-25.5
62.7	0.2	0.40	-10.5	-10.7	-31.2	-24.1	-11.2	-28.5	-41.1	-32.5
73.6	0.2	0.40	-11.5	-11.6	-32.8	-32.3	-12.5	-32.0	-66.7	-43.5
84.5	0.2	0.40	-15.1	-15.2	-37.7	-30.3	-23.4	-41.3	-80.6	-74.1

BACKSCATTER COMPONENTS IN DECIBELS

ANGLE			------VOLUME-----			---INTERACTION---			--SURFACE--	
(DEG)	TAU	ALBEDO	VV	HH	VH	VV	HH	VH	VV	HH
8.4	0.2	0.50	-8.7	-8.7	-26.0	-11.6	-11.2	-20.4	0.6	0.6
19.2	0.2	0.50	-8.7	-8.7	-26.2	-13.0	-10.9	-21.9	-8.7	-8.2
30.0	0.2	0.50	-8.8	-8.8	-26.6	-16.0	-10.5	-22.7	-15.7	-14.4
40.9	0.2	0.50	-8.9	-9.0	-27.2	-20.4	-10.2	-23.5	-22.4	-19.8
51.8	0.2	0.50	-9.0	-9.2	-28.0	-22.4	-10.0	-24.8	-30.2	-25.5
62.7	0.2	0.50	-9.4	-9.6	-29.1	-22.8	-10.1	-26.8	-41.1	-32.5
73.6	0.2	0.50	-10.4	-10.6	-30.6	-30.5	-11.4	-30.2	-66.7	-43.5
84.5	0.2	0.50	-14.0	-14.2	-35.5	-29.0	-22.2	-39.2	-80.6	-74.1

FOR ALL CASES: SURFACE DIELECTRIC = 15 - j0, ksigma = 0.5, kL = 7

BACKSCATTER COMPONENTS IN DECIBELS

ANGLE			------VOLUME-----			---INTERACTION---			--SURFACE--	
(DEG)	TAU	ALBEDO	VV	HH	VH	VV	HH	VH	VV	HH
8.4	0.4	0.01	-23.8	-23.8	-56.8	-28.2	-27.9	-38.7	-1.2	-1.1
19.2	0.4	0.01	-23.9	-23.9	-57.1	-29.9	-27.6	-41.4	-10.5	-10.0
30.0	0.4	0.01	-24.1	-24.1	-57.5	-33.4	-27.4	-42.8	-17.7	-16.4
40.9	0.4	0.01	-24.3	-24.3	-58.2	-39.2	-27.4	-44.0	-24.7	-22.1
51.8	0.4	0.01	-24.7	-24.7	-59.1	-42.1	-27.6	-45.7	-33.0	-28.3
62.7	0.4	0.01	-25.5	-25.5	-60.5	-42.3	-28.7	-49.0	-44.9	-36.3
73.6	0.4	0.01	-27.0	-27.0	-62.8	-55.9	-32.5	-55.1	-72.9	-49.6
84.5	0.4	0.01	-31.4	-31.4	-69.8	-62.5	-55.4	-74.0	-98.9	-92.3

BACKSCATTER COMPONENTS IN DECIBELS

ANGLE			------VOLUME-----			---INTERACTION---			--SURFACE--	
(DEG)	TAU	ALBEDO	VV	HH	VH	VV	HH	VH	VV	HH
8.4	0.4	0.10	-13.7	-13.7	-36.6	-18.0	-17.6	-28.2	-1.2	-1.1
19.2	0.4	0.10	-13.8	-13.8	-36.9	-19.7	-17.4	-30.5	-10.5	-10.0
30.0	0.4	0.10	-13.9	-14.0	-37.3	-23.1	-17.2	-31.8	-17.7	-16.4
40.9	0.4	0.10	-14.2	-14.2	-38.0	-28.7	-17.2	-32.9	-24.7	-22.1
51.8	0.4	0.10	-14.6	-14.6	-38.9	-31.5	-17.5	-34.6	-33.0	-28.3
62.7	0.4	0.10	-15.3	-15.4	-40.2	-31.9	-18.5	-37.6	-44.9	-36.3
73.6	0.4	0.10	-16.8	-16.9	-42.5	-44.3	-22.3	-43.1	-72.9	-49.6
84.5	0.4	0.10	-21.3	-21.4	-49.5	-51.2	-43.9	-58.4	-98.9	-92.3

BACKSCATTER COMPONENTS IN DECIBELS

ANGLE			------VOLUME-----			---INTERACTION---			--SURFACE--	
(DEG)	TAU	ALBEDO	VV	HH	VH	VV	HH	VH	VV	HH
8.4	0.4	0.20	-10.6	-10.6	-30.3	-14.8	-14.4	-24.5	-1.2	-1.1
19.2	0.4	0.20	-10.7	-10.7	-30.6	-16.4	-14.2	-26.5	-10.5	-10.0
30.0	0.4	0.20	-10.8	-10.8	-31.0	-19.8	-14.0	-27.7	-17.7	-16.4
40.9	0.4	0.20	-11.0	-11.1	-31.7	-25.1	-14.0	-28.7	-24.7	-22.1
51.8	0.4	0.20	-11.4	-11.5	-32.6	-27.8	-14.2	-30.4	-33.0	-28.3
62.7	0.4	0.20	-12.1	-12.2	-33.9	-28.5	-15.3	-33.2	-44.9	-36.3
73.6	0.4	0.20	-13.7	-13.8	-36.1	-39.7	-19.0	-38.3	-72.9	-49.6
84.5	0.4	0.20	-18.2	-18.3	-43.2	-46.9	-39.4	-52.3	-98.9	-92.3

BACKSCATTER COMPONENTS IN DECIBELS

ANGLE			------VOLUME-----			---INTERACTION---			--SURFACE--	
(DEG)	TAU	ALBEDO	VV	HH	VH	VV	HH	VH	VV	HH
8.4	0.4	0.30	-8.7	-8.7	-26.6	-12.8	-12.4	-22.0	-1.2	-1.1
19.2	0.4	0.30	-8.8	-8.8	-26.8	-14.4	-12.2	-23.8	-10.5	-10.0
30.0	0.4	0.30	-8.9	-8.9	-27.2	-17.7	-12.0	-24.9	-17.7	-16.4
40.9	0.4	0.30	-9.1	-9.2	-27.8	-22.8	-12.0	-25.9	-24.7	-22.1
51.8	0.4	0.30	-9.5	-9.6	-28.7	-25.4	-12.3	-27.5	-33.0	-28.3
62.7	0.4	0.30	-10.2	-10.3	-30.0	-26.3	-13.3	-30.2	-44.9	-36.3
73.6	0.4	0.30	-11.7	-11.9	-32.3	-36.5	-17.0	-35.1	-72.9	-49.6
84.5	0.4	0.30	-16.3	-16.5	-39.4	-43.9	-36.5	-48.3	-98.9	-92.3

FOR ALL CASES: SURFACE DIELECTRIC = 15 - j0, ksigma = 0.5, kL = 7

BACKSCATTER COMPONENTS IN DECIBELS

ANGLE			------VOLUME-----			---INTERACTION---			--SURFACE--	
(DEG)	TAU	ALBEDO	VV	HH	VH	VV	HH	VH	VV	HH
8.4	0.4	0.40	-7.3	-7.3	-23.8	-11.3	-10.9	-20.1	-1.2	-1.1
19.2	0.4	0.40	-7.4	-7.4	-24.0	-12.9	-10.7	-21.7	-10.5	-10.0
30.0	0.4	0.40	-7.5	-7.5	-24.4	-16.1	-10.5	-22.7	-17.7	-16.4
40.9	0.4	0.40	-7.7	-7.8	-25.0	-21.0	-10.5	-23.7	-24.7	-22.1
51.8	0.4	0.40	-8.1	-8.2	-25.9	-23.6	-10.8	-25.3	-33.0	-28.3
62.7	0.4	0.40	-8.8	-9.0	-27.2	-24.6	-11.8	-27.8	-44.9	-36.3
73.6	0.4	0.40	-10.3	-10.5	-29.4	-34.0	-15.5	-32.5	-72.9	-49.6
84.5	0.4	0.40	-15.0	-15.1	-36.6	-41.5	-34.1	-45.2	-98.9	-92.3

BACKSCATTER COMPONENTS IN DECIBELS

ANGLE			------VOLUME-----			---INTERACTION---			--SURFACE--	
(DEG)	TAU	ALBEDO	VV	HH	VH	VV	HH	VH	VV	HH
8.4	0.4	0.50	-6.2	-6.2	-21.5	-10.1	-9.7	-18.4	-1.2	-1.1
19.2	0.4	0.50	-6.3	-6.3	-21.8	-11.6	-9.5	-19.9	-10.5	-10.0
30.0	0.4	0.50	-6.4	-6.4	-22.2	-14.8	-9.3	-20.8	-17.7	-16.4
40.9	0.4	0.50	-6.6	-6.7	-22.8	-19.4	-9.3	-21.8	-24.7	-22.1
51.8	0.4	0.50	-6.9	-7.1	-23.7	-21.9	-9.6	-23.3	-33.0	-28.3
62.7	0.4	0.50	-7.6	-7.8	-24.9	-23.1	-10.6	-25.8	-44.9	-36.3
73.6	0.4	0.50	-9.1	-9.4	-27.1	-31.8	-14.3	-30.3	-72.9	-49.6
84.5	0.4	0.50	-13.9	-14.1	-34.3	-39.5	-32.2	-42.6	-98.9	-92.3

BACKSCATTER COMPONENTS IN DECIBELS

ANGLE			------VOLUME-----			---INTERACTION---			--SURFACE--	
(DEG)	TAU	ALBEDO	VV	HH	VH	VV	HH	VH	VV	HH
8.4	0.6	0.01	-22.8	-22.8	-55.1	-28.2	-27.9	-38.9	-3.0	-2.9
19.2	0.6	0.01	-22.9	-22.9	-55.3	-30.0	-27.7	-41.9	-12.4	-11.9
30.0	0.6	0.01	-23.1	-23.1	-55.8	-33.9	-27.8	-43.5	-19.7	-18.4
40.9	0.6	0.01	-23.4	-23.4	-56.5	-40.4	-28.1	-44.9	-27.0	-24.4
51.8	0.6	0.01	-24.0	-24.0	-57.5	-43.9	-28.8	-47.1	-35.8	-31.1
62.7	0.6	0.01	-25.0	-25.0	-59.1	-44.4	-30.8	-51.2	-48.7	-40.1
73.6	0.6	0.01	-26.8	-26.8	-61.8	-60.1	-37.0	-58.9	-79.1	-55.8
84.5	0.6	0.01	-31.4	-31.4	-69.8	-76.9	-68.9	-81.4	-117.	-111.

BACKSCATTER COMPONENTS IN DECIBELS

ANGLE			------VOLUME-----			---INTERACTION---			--SURFACE--	
(DEG)	TAU	ALBEDO	VV	HH	VH	VV	HH	VH	VV	HH
8.4	0.6	0.10	-12.7	-12.7	-34.8	-18.1	-17.7	-28.3	-3.0	-2.9
19.2	0.6	0.10	-12.8	-12.8	-35.0	-19.8	-17.5	-30.7	-12.4	-11.9
30.0	0.6	0.10	-13.0	-13.0	-35.5	-23.5	-17.5	-32.2	-19.7	-18.4
40.9	0.6	0.10	-13.3	-13.3	-36.2	-29.6	-17.8	-33.5	-27.0	-24.4
51.8	0.6	0.10	-13.8	-13.9	-37.2	-32.9	-18.6	-35.6	-35.8	-31.1
62.7	0.6	0.10	-14.8	-14.8	-38.7	-34.0	-20.6	-39.3	-48.7	-40.1
73.6	0.6	0.10	-16.6	-16.7	-41.5	-47.8	-26.6	-46.1	-79.1	-55.8
84.5	0.6	0.10	-21.3	-21.4	-49.4	-60.2	-51.8	-62.3	-117.	-111.

FOR ALL CASES: SURFACE DIELECTRIC = 15 - j0, ksigma = 0.5, kL = 7

BACKSCATTER COMPONENTS IN DECIBELS

ANGLE			------VOLUME-----			---INTERACTION---			--SURFACE--	
(DEG)	TAU	ALBEDO	VV	HH	VH	VV	HH	VH	VV	HH
8.4	0.6	0.20	-9.5	-9.5	-28.5	-14.8	-14.4	-24.5	-3.0	-2.9
19.2	0.6	0.20	-9.6	-9.6	-28.7	-16.5	-14.2	-26.5	-12.4	-11.9
30.0	0.6	0.20	-9.8	-9.8	-29.1	-20.1	-14.3	-27.8	-19.7	-18.4
40.9	0.6	0.20	-10.1	-10.1	-29.8	-25.9	-14.5	-29.1	-27.0	-24.4
51.8	0.6	0.20	-10.6	-10.7	-30.8	-29.1	-15.3	-31.1	-35.8	-31.1
62.7	0.6	0.20	-11.6	-11.7	-32.3	-30.5	-17.3	-34.6	-48.7	-40.1
73.6	0.6	0.20	-13.4	-13.6	-35.1	-42.7	-23.3	-40.8	-79.1	-55.8
84.5	0.6	0.20	-18.2	-18.3	-43.1	-53.9	-45.6	-55.5	-117.	-111.

BACKSCATTER COMPONENTS IN DECIBELS

ANGLE			------VOLUME-----			---INTERACTION---			--SURFACE--	
(DEG)	TAU	ALBEDO	VV	HH	VH	VV	HH	VH	VV	HH
8.4	0.6	0.30	-7.6	-7.6	-24.6	-12.8	-12.3	-21.9	-3.0	-2.9
19.2	0.6	0.30	-7.7	-7.7	-24.8	-14.4	-12.2	-23.7	-12.4	-11.9
30.0	0.6	0.30	-7.8	-7.9	-25.2	-17.9	-12.2	-24.8	-19.7	-18.4
40.9	0.6	0.30	-8.2	-8.2	-25.9	-23.4	-12.5	-26.1	-27.0	-24.4
51.8	0.6	0.30	-8.7	-8.8	-26.9	-26.5	-13.3	-28.0	-35.8	-31.1
62.7	0.6	0.30	-9.6	-9.8	-28.4	-28.2	-15.3	-31.3	-48.7	-40.1
73.6	0.6	0.30	-11.5	-11.6	-31.2	-39.2	-21.1	-37.2	-79.1	-55.8
84.5	0.6	0.30	-16.4	-16.5	-39.2	-49.9	-41.7	-51.1	-117.	-111.

BACKSCATTER COMPONENTS IN DECIBELS

ANGLE			------VOLUME-----			---INTERACTION---			--SURFACE--	
(DEG)	TAU	ALBEDO	VV	HH	VH	VV	HH	VH	VV	HH
8.4	0.6	0.40	-6.2	-6.2	-21.7	-11.2	-10.8	-19.8	-3.0	-2.9
19.2	0.6	0.40	-6.3	-6.3	-21.9	-12.8	-10.6	-21.4	-12.4	-11.9
30.0	0.6	0.40	-6.4	-6.5	-22.4	-16.2	-10.7	-22.4	-19.7	-18.4
40.9	0.6	0.40	-6.7	-6.8	-23.0	-21.4	-10.9	-23.6	-27.0	-24.4
51.8	0.6	0.40	-7.2	-7.4	-24.0	-24.4	-11.7	-25.5	-35.8	-31.1
62.7	0.6	0.40	-8.2	-8.4	-25.5	-26.3	-13.7	-28.6	-48.7	-40.1
73.6	0.6	0.40	-10.0	-10.3	-28.2	-36.3	-19.4	-34.3	-79.1	-55.8
84.5	0.6	0.40	-15.0	-15.1	-36.3	-46.7	-38.7	-47.8	-117.	-111.

BACKSCATTER COMPONENTS IN DECIBELS

ANGLE			------VOLUME-----			---INTERACTION---			--SURFACE--	
(DEG)	TAU	ALBEDO	VV	HH	VH	VV	HH	VH	VV	HH
8.4	0.6	0.50	-5.0	-5.0	-19.4	-9.9	-9.5	-18.0	-3.0	-2.9
19.2	0.6	0.50	-5.1	-5.1	-19.6	-11.5	-9.4	-19.4	-12.4	-11.9
30.0	0.6	0.50	-5.2	-5.3	-20.0	-14.8	-9.4	-20.3	-19.7	-18.4
40.9	0.6	0.50	-5.5	-5.6	-20.7	-19.6	-9.7	-21.5	-27.0	-24.4
51.8	0.6	0.50	-6.0	-6.2	-21.6	-22.6	-10.4	-23.3	-35.8	-31.1
62.7	0.6	0.50	-6.9	-7.2	-23.1	-24.7	-12.4	-26.3	-48.7	-40.1
73.6	0.6	0.50	-8.8	-9.1	-25.8	-33.8	-18.0	-31.8	-79.1	-55.8
84.5	0.6	0.50	-13.9	-14.1	-34.0	-44.1	-36.3	-44.8	-117.	-111.

FOR ALL CASES: SURFACE DIELECTRIC = 15 - j0, ksigma = 0.5, kL = 7

BACKSCATTER COMPONENTS IN DECIBELS

ANGLE			------VOLUME-----			---INTERACTION---			--SURFACE--	
(DEG)	TAU	ALBEDO	VV	HH	VH	VV	HH	VH	VV	HH
8.4	0.8	0.01	-22.2	-22.2	-54.1	-28.9	-28.6	-39.6	-4.7	-4.6
19.2	0.8	0.01	-22.4	-22.4	-54.3	-30.8	-28.4	-42.6	-14.2	-13.7
30.0	0.8	0.01	-22.6	-22.6	-54.8	-34.7	-28.6	-44.5	-21.7	-20.4
40.9	0.8	0.01	-23.0	-23.0	-55.6	-41.6	-29.2	-46.2	-29.3	-26.7
51.8	0.8	0.01	-23.7	-23.7	-56.7	-45.5	-30.4	-48.9	-38.6	-33.9
62.7	0.8	0.01	-24.8	-24.8	-58.4	-47.0	-33.4	-53.7	-52.5	-43.9
73.6	0.8	0.01	-26.7	-26.7	-61.5	-64.5	-41.9	-63.0	-85.2	-62.0
84.5	0.8	0.01	-31.4	-31.4	-69.7	-84.0	-75.1	-85.4	-135.	-129.

BACKSCATTER COMPONENTS IN DECIBELS

ANGLE			------VOLUME-----			---INTERACTION---			--SURFACE--	
(DEG)	TAU	ALBEDO	VV	HH	VH	VV	HH	VH	VV	HH
8.4	0.8	0.10	-12.1	-12.1	-33.8	-18.6	-18.2	-28.9	-4.7	-4.6
19.2	0.8	0.10	-12.2	-12.2	-34.0	-20.5	-18.1	-31.4	-14.2	-13.7
30.0	0.8	0.10	-12.4	-12.5	-34.5	-24.3	-18.4	-33.0	-21.7	-20.4
40.9	0.8	0.10	-12.8	-12.9	-35.2	-30.9	-18.9	-34.6	-29.3	-26.7
51.8	0.8	0.10	-13.5	-13.5	-36.3	-34.6	-20.2	-37.1	-38.6	-33.9
62.7	0.8	0.10	-14.6	-14.6	-38.0	-36.5	-23.2	-41.4	-52.5	-43.9
73.6	0.8	0.10	-16.6	-16.6	-41.1	-51.2	-31.4	-49.3	-85.2	-62.0
84.5	0.8	0.10	-21.3	-21.4	-49.4	-63.8	-55.0	-64.9	-135.	-129.

BACKSCATTER COMPONENTS IN DECIBELS

ANGLE			------VOLUME-----			---INTERACTION---			--SURFACE--	
(DEG)	TAU	ALBEDO	VV	HH	VH	VV	HH	VH	VV	HH
8.4	0.8	0.20	-8.9	-8.9	-27.3	-15.3	-14.9	-25.0	-4.7	-4.6
19.2	0.8	0.20	-9.0	-9.0	-27.6	-17.1	-14.8	-27.1	-14.2	-13.7
30.0	0.8	0.20	-9.2	-9.2	-28.1	-20.9	-15.0	-28.5	-21.7	-20.4
40.9	0.8	0.20	-9.6	-9.7	-28.8	-27.0	-15.6	-30.0	-29.3	-26.7
51.8	0.8	0.20	-10.3	-10.3	-29.9	-30.7	-16.8	-32.4	-38.6	-33.9
62.7	0.8	0.20	-11.4	-11.4	-31.6	-32.9	-19.8	-36.4	-52.5	-43.9
73.6	0.8	0.20	-13.4	-13.5	-34.7	-45.6	-27.8	-43.6	-85.2	-62.0
84.5	0.8	0.20	-18.2	-18.3	-43.0	-57.1	-48.5	-57.9	-135.	-129.

BACKSCATTER COMPONENTS IN DECIBELS

ANGLE			------VOLUME-----			---INTERACTION---			--SURFACE--	
(DEG)	TAU	ALBEDO	VV	HH	VH	VV	HH	VH	VV	HH
8.4	0.8	0.30	-6.9	-6.9	-23.4	-13.2	-12.8	-22.3	-4.7	-4.6
19.2	0.8	0.30	-7.1	-7.1	-23.7	-15.0	-12.7	-24.1	-14.2	-13.7
30.0	0.8	0.30	-7.3	-7.3	-24.1	-18.6	-12.9	-25.3	-21.7	-20.4
40.9	0.8	0.30	-7.6	-7.7	-24.8	-24.4	-13.5	-26.8	-29.3	-26.7
51.8	0.8	0.30	-8.3	-8.4	-25.9	-28.0	-14.8	-29.1	-38.6	-33.9
62.7	0.8	0.30	-9.4	-9.5	-27.6	-30.5	-17.6	-32.8	-52.5	-43.9
73.6	0.8	0.30	-11.4	-11.6	-30.7	-41.7	-25.5	-39.6	-85.2	-62.0
84.5	0.8	0.30	-16.3	-16.5	-39.1	-52.8	-44.4	-53.4	-135.	-129.

FOR ALL CASES: SURFACE DIELECTRIC = 15 - j0, ksigma = 0.5, kL = 7

BACKSCATTER COMPONENTS IN DECIBELS

ANGLE			------VOLUME-----			---INTERACTION---			--SURFACE--	
(DEG)	TAU	ALBEDO	VV	HH	VH	VV	HH	VH	VV	HH
8.4	0.8	0.40	-5.5	-5.5	-20.5	-11.6	-11.2	-20.1	-4.7	-4.6
19.2	0.8	0.40	-5.6	-5.6	-20.7	-13.3	-11.1	-21.6	-14.2	-13.7
30.0	0.8	0.40	-5.8	-5.9	-21.2	-16.8	-11.3	-22.8	-21.7	-20.4
40.9	0.8	0.40	-6.2	-6.3	-21.9	-22.3	-11.9	-24.2	-29.3	-26.7
51.8	0.8	0.40	-6.8	-6.9	-22.9	-25.8	-13.1	-26.4	-38.6	-33.9
62.7	0.8	0.40	-7.9	-8.1	-24.6	-28.5	-16.0	-30.0	-52.5	-43.9
73.6	0.8	0.40	-10.0	-10.2	-27.7	-38.6	-23.6	-36.4	-85.2	-62.0
84.5	0.8	0.40	-15.0	-15.1	-36.3	-49.4	-41.3	-49.8	-135.	-129.

BACKSCATTER COMPONENTS IN DECIBELS

ANGLE			------VOLUME-----			---INTERACTION---			--SURFACE--	
(DEG)	TAU	ALBEDO	VV	HH	VH	VV	HH	VH	VV	HH
8.4	0.8	0.50	-4.3	-4.3	-18.1	-10.2	-9.8	-18.1	-4.7	-4.6
19.2	0.8	0.50	-4.4	-4.4	-18.3	-11.9	-9.8	-19.5	-14.2	-13.7
30.0	0.8	0.50	-4.6	-4.7	-18.8	-15.3	-10.0	-20.5	-21.7	-20.4
40.9	0.8	0.50	-5.0	-5.1	-19.4	-20.3	-10.5	-21.9	-29.3	-26.7
51.8	0.8	0.50	-5.6	-5.8	-20.5	-23.8	-11.8	-24.0	-38.6	-33.9
62.7	0.8	0.50	-6.7	-6.9	-22.1	-26.7	-14.6	-27.4	-52.5	-43.9
73.6	0.8	0.50	-8.7	-9.0	-25.3	-35.8	-21.9	-33.6	-85.2	-62.0
84.5	0.8	0.50	-13.9	-14.1	-33.9	-46.6	-38.8	-46.7	-135.	-129.

BACKSCATTER COMPONENTS IN DECIBELS

ANGLE			------VOLUME-----			---INTERACTION---			--SURFACE--	
(DEG)	TAU	ALBEDO	VV	HH	VH	VV	HH	VH	VV	HH
8.4	1.2	0.01	-21.7	-21.7	-53.1	-30.6	-30.4	-41.6	-8.2	-8.1
19.2	1.2	0.01	-21.8	-21.8	-53.4	-32.8	-30.4	-45.0	-17.9	-17.4
30.0	1.2	0.01	-22.1	-22.1	-53.9	-37.3	-31.0	-47.2	-25.7	-24.4
40.9	1.2	0.01	-22.6	-22.6	-54.7	-45.2	-32.2	-49.5	-33.9	-31.3
51.8	1.2	0.01	-23.4	-23.4	-56.0	-50.1	-34.4	-53.1	-44.2	-39.5
62.7	1.2	0.01	-24.6	-24.7	-57.9	-52.8	-39.3	-59.3	-60.0	-51.4
73.6	1.2	0.01	-26.7	-26.7	-61.3	-73.4	-52.3	-71.3	-97.6	-74.3
84.5	1.2	0.01	-31.4	-31.4	-69.8	-90.0	-80.5	-90.6	-172.	-166.

BACKSCATTER COMPONENTS IN DECIBELS

ANGLE			------VOLUME-----			---INTERACTION---			--SURFACE--	
(DEG)	TAU	ALBEDO	VV	HH	VH	VV	HH	VH	VV	HH
8.4	1.2	0.10	-11.5	-11.5	-32.7	-20.4	-20.0	-30.8	-8.2	-8.1
19.2	1.2	0.10	-11.6	-11.6	-33.0	-22.4	-20.2	-33.4	-17.9	-17.4
30.0	1.2	0.10	-11.9	-12.0	-33.5	-26.7	-20.7	-35.4	-25.7	-24.4
40.9	1.2	0.10	-12.4	-12.5	-34.3	-34.0	-21.8	-37.5	-33.9	-31.3
51.8	1.2	0.10	-13.2	-13.2	-35.6	-38.7	-24.1	-40.7	-44.2	-39.5
62.7	1.2	0.10	-14.5	-14.5	-37.5	-42.2	-28.9	-46.2	-60.0	-51.4
73.6	1.2	0.10	-16.6	-16.6	-41.0	-57.6	-41.0	-55.5	-97.6	-74.3
84.5	1.2	0.10	-21.3	-21.4	-49.4	-69.2	-60.0	-69.6	-172.	-166.

FOR ALL CASES: SURFACE DIELECTRIC = 15 - j0, ksigma = 0.5, kL = 7

BACKSCATTER COMPONENTS IN DECIBELS

ANGLE			------VOLUME-----			---INTERACTION---			--SURFACE--	
(DEG)	TAU	ALBEDO	VV	HH	VH	VV	HH	VH	VV	HH
8.4	1.2	0.20	-8.3	-8.3	-26.2	-17.1	-16.6	-26.7	-8.2	-8.1
19.2	1.2	0.20	-8.4	-8.4	-26.5	-19.0	-16.7	-28.9	-17.9	-17.4
30.0	1.2	0.20	-8.7	-8.7	-27.0	-23.1	-17.3	-30.6	-25.7	-24.4
40.9	1.2	0.20	-9.2	-9.2	-27.8	-29.9	-18.4	-32.5	-33.9	-31.3
51.8	1.2	0.20	-10.0	-10.0	-29.1	-34.5	-20.6	-35.6	-44.2	-39.5
62.7	1.2	0.20	-11.2	-11.3	-31.0	-38.4	-25.3	-40.6	-60.0	-51.4
73.6	1.2	0.20	-13.4	-13.5	-34.5	-51.1	-36.6	-49.0	-97.6	-74.3
84.5	1.2	0.20	-18.2	-18.3	-43.0	-62.3	-53.3	-62.3	-172.	-166.

BACKSCATTER COMPONENTS IN DECIBELS

ANGLE			------VOLUME-----			---INTERACTION---			--SURFACE--	
(DEG)	TAU	ALBEDO	VV	HH	VH	VV	HH	VH	VV	HH
8.4	1.2	0.30	-6.3	-6.3	-22.2	-14.9	-14.5	-23.9	-8.2	-8.1
19.2	1.2	0.30	-6.4	-6.4	-22.5	-16.8	-14.6	-25.7	-17.9	-17.4
30.0	1.2	0.30	-6.7	-6.8	-23.0	-20.8	-15.1	-27.2	-25.7	-24.4
40.9	1.2	0.30	-7.2	-7.3	-23.8	-27.0	-16.2	-29.1	-33.9	-31.3
51.8	1.2	0.30	-8.0	-8.1	-25.0	-31.5	-18.4	-31.9	-44.2	-39.5
62.7	1.2	0.30	-9.2	-9.4	-27.0	-35.7	-23.0	-36.6	-60.0	-51.4
73.6	1.2	0.30	-11.4	-11.6	-30.5	-46.6	-33.6	-44.5	-97.6	-74.3
84.5	1.2	0.30	-16.3	-16.5	-39.1	-57.8	-49.0	-57.5	-172.	-166.

BACKSCATTER COMPONENTS IN DECIBELS

ANGLE			------VOLUME-----			---INTERACTION---			--SURFACE--	
(DEG)	TAU	ALBEDO	VV	HH	VH	VV	HH	VH	VV	HH
8.4	1.2	0.40	-4.8	-4.8	-19.2	-13.1	-12.7	-21.5	-8.2	-8.1
19.2	1.2	0.40	-4.9	-4.9	-19.4	-15.0	-12.9	-23.0	-17.9	-17.4
30.0	1.2	0.40	-5.2	-5.3	-19.9	-18.8	-13.4	-24.4	-25.7	-24.4
40.9	1.2	0.40	-5.7	-5.8	-20.7	-24.6	-14.5	-26.2	-33.9	-31.3
51.8	1.2	0.40	-6.4	-6.6	-21.9	-29.0	-16.6	-28.9	-44.2	-39.5
62.7	1.2	0.40	-7.7	-7.9	-23.9	-33.4	-21.1	-33.3	-60.0	-51.4
73.6	1.2	0.40	-9.9	-10.1	-27.4	-42.9	-31.1	-40.8	-97.6	-74.3
84.5	1.2	0.40	-15.0	-15.1	-36.2	-54.2	-45.7	-53.6	-172.	-166.

BACKSCATTER COMPONENTS IN DECIBELS

ANGLE			------VOLUME-----			---INTERACTION---			--SURFACE--	
(DEG)	TAU	ALBEDO	VV	HH	VH	VV	HH	VH	VV	HH
8.4	1.2	0.50	-3.6	-3.6	-16.6	-11.6	-11.3	-19.3	-8.2	-8.1
19.2	1.2	0.50	-3.7	-3.7	-16.9	-13.5	-11.4	-20.7	-17.9	-17.4
30.0	1.2	0.50	-4.0	-4.1	-17.4	-17.1	-11.9	-21.9	-25.7	-24.4
40.9	1.2	0.50	-4.4	-4.6	-18.1	-22.4	-13.0	-23.6	-33.9	-31.3
51.8	1.2	0.50	-5.2	-5.4	-19.4	-26.7	-15.1	-26.2	-44.2	-39.5
62.7	1.2	0.50	-6.5	-6.7	-21.3	-31.1	-19.5	-30.5	-60.0	-51.4
73.6	1.2	0.50	-8.7	-9.0	-24.9	-39.7	-28.8	-37.6	-97.6	-74.3
84.5	1.2	0.50	-13.9	-14.1	-33.8	-51.0	-42.9	-50.2	-172.	-166.

FOR ALL CASES: SURFACE DIELECTRIC = 15 - j0, ksigma = 0.5, kL = 7

BACKSCATTER COMPONENTS IN DECIBELS

ANGLE			------VOLUME-----			---INTERACTION---			--SURFACE--	
(DEG)	TAU	ALBEDO	VV	HH	VH	VV	HH	VH	VV	HH
8.4	1.6	0.01	-21.4	-21.4	-52.7	-33.1	-32.8	-44.1	-11.7	-11.6
19.2	1.6	0.01	-21.6	-21.6	-53.0	-35.4	-33.0	-47.6	-21.6	-21.1
30.0	1.6	0.01	-22.0	-22.0	-53.5	-40.1	-33.8	-50.2	-29.7	-28.4
40.9	1.6	0.01	-22.5	-22.5	-54.4	-48.6	-35.6	-53.1	-38.5	-35.9
51.8	1.6	0.01	-23.3	-23.3	-55.8	-54.4	-38.8	-57.5	-49.8	-45.1
62.7	1.6	0.01	-24.6	-24.6	-57.8	-59.1	-45.6	-65.2	-67.5	-58.9
73.6	1.6	0.01	-26.7	-26.7	-61.3	-81.5	-62.8	-79.0	-110.	-86.4
84.5	1.6	0.01	-31.4	-31.4	-69.7	-95.2	-85.1	-95.2	-207.	-201.

BACKSCATTER COMPONENTS IN DECIBELS

ANGLE			------VOLUME-----			---INTERACTION---			--SURFACE--	
(DEG)	TAU	ALBEDO	VV	HH	VH	VV	HH	VH	VV	HH
8.4	1.6	0.10	-11.2	-11.2	-32.2	-22.7	-22.3	-33.2	-11.7	-11.6
19.2	1.6	0.10	-11.4	-11.4	-32.5	-24.9	-22.6	-36.0	-21.6	-21.1
30.0	1.6	0.10	-11.8	-11.8	-33.1	-29.5	-23.5	-38.2	-29.7	-28.4
40.9	1.6	0.10	-12.3	-12.3	-34.0	-37.5	-25.1	-40.7	-38.5	-35.9
51.8	1.6	0.10	-13.1	-13.2	-35.3	-43.0	-28.4	-44.7	-49.8	-45.1
62.7	1.6	0.10	-14.4	-14.5	-37.4	-48.3	-35.0	-51.2	-67.5	-58.9
73.6	1.6	0.10	-16.6	-16.6	-40.9	-63.2	-49.4	-61.0	-110.	-86.4
84.5	1.6	0.10	-21.3	-21.4	-49.4	-74.4	-64.4	-74.0	-207.	-201.

BACKSCATTER COMPONENTS IN DECIBELS

ANGLE			------VOLUME-----			---INTERACTION---			--SURFACE--	
(DEG)	TAU	ALBEDO	VV	HH	VH	VV	HH	VH	VV	HH
8.4	1.6	0.20	-8.0	-8.0	-25.7	-19.3	-18.9	-29.0	-11.7	-11.6
19.2	1.6	0.20	-8.2	-8.2	-26.0	-21.4	-19.2	-31.3	-21.6	-21.1
30.0	1.6	0.20	-8.5	-8.5	-26.6	-25.9	-20.0	-33.2	-29.7	-28.4
40.9	1.6	0.20	-9.1	-9.1	-27.4	-33.1	-21.7	-35.6	-38.5	-35.9
51.8	1.6	0.20	-9.9	-10.0	-28.8	-38.6	-24.8	-39.2	-49.8	-45.1
62.7	1.6	0.20	-11.2	-11.3	-30.8	-44.2	-31.2	-45.1	-67.5	-58.9
73.6	1.6	0.20	-13.4	-13.5	-34.4	-56.1	-43.8	-53.9	-110.	-86.4
84.5	1.6	0.20	-18.2	-18.3	-43.0	-67.3	-57.6	-66.6	-207.	-201.

BACKSCATTER COMPONENTS IN DECIBELS

ANGLE			------VOLUME-----			---INTERACTION---			--SURFACE--	
(DEG)	TAU	ALBEDO	VV	HH	VH	VV	HH	VH	VV	HH
8.4	1.6	0.30	-6.0	-6.0	-21.6	-17.0	-16.6	-26.0	-11.7	-11.6
19.	1.6	0.30	-6.2	-6.2	-21.9	-19.1	-16.9	-27.9	-21.6	-21.1
30.0	1.6	0.30	-6.5	-6.5	-22.5	-23.4	-17.7	-29.6	-29.7	-28.4
40.9	1.6	0.30	-7.0	-7.1	-23.3	-30.0	-19.4	-31.9	-38.5	-35.9
51.8	1.6	0.30	-7.9	-8.0	-24.7	-35.4	-22.5	-35.3	-49.8	-45.1
62.7	1.6	0.30	-9.2	-9.3	-26.8	-41.2	-28.6	-40.8	-67.5	-58.9
73.6	1.6	0.30	-11.4	-11.5	-30.4	-51.3	-40.0	-49.0	-110.	-86.4
84.5	1.6	0.30	-16.3	-16.5	-39.1	-62.6	-53.2	-61.5	-207.	-201.

FOR ALL CASES: SURFACE DIELECTRIC = 15 - j0, ksigma = 0.5, kL = 7

BACKSCATTER COMPONENTS IN DECIBELS

ANGLE			------VOLUME-----			---INTERACTION---			--SURFACE--	
(DEG)	TAU	ALBEDO	VV	HH	VH	VV	HH	VH	VV	HH
8.4	1.6	0.40	-4.5	-4.5	-18.5	-15.2	-14.9	-23.5	-11.7	-11.6
19.2	1.6	0.40	-4.6	-4.7	-18.8	-17.2	-15.1	-25.1	-21.6	-21.1
30.0	1.6	0.40	-5.0	-5.0	-19.4	-21.3	-16.0	-26.6	-29.7	-28.4
40.9	1.6	0.40	-5.5	-5.6	-20.2	-27.4	-17.6	-28.7	-38.5	-35.9
51.8	1.6	0.40	-6.3	-6.5	-21.5	-32.5	-20.6	-32.0	-49.8	-45.1
62.7	1.6	0.40	-7.7	-7.9	-23.6	-38.4	-26.4	-37.1	-67.5	-58.9
73.6	1.6	0.40	-9.9	-10.1	-27.3	-47.2	-36.8	-44.9	-110.	-86.4
84.5	1.6	0.40	-14.9	-15.1	-36.2	-58.8	-49.7	-57.4	-207.	-201.

BACKSCATTER COMPONENTS IN DECIBELS

ANGLE			------VOLUME-----			---INTERACTION---			--SURFACE--	
(DEG)	TAU	ALBEDO	VV	HH	VH	VV	HH	VH	VV	HH
8.4	1.6	0.50	-3.2	-3.2	-15.9	-13.7	-13.3	-21.1	-11.7	-11.6
19.2	1.6	0.50	-3.4	-3.4	-16.2	-15.6	-13.6	-22.5	-21.6	-21.1
30.0	1.6	0.50	-3.7	-3.8	-16.7	-19.4	-14.4	-23.9	-29.7	-28.4
40.9	1.6	0.50	-4.2	-4.4	-17.6	-25.0	-16.0	-25.9	-38.5	-35.9
51.8	1.6	0.50	-5.1	-5.3	-18.9	-29.9	-18.9	-29.0	-49.8	-45.1
62.7	1.6	0.50	-6.4	-6.7	-21.0	-35.6	-24.5	-33.9	-67.5	-58.9
73.6	1.6	0.50	-8.7	-9.0	-24.8	-43.6	-34.0	-41.3	-110.	-86.4
84.5	1.6	0.50	-13.9	-14.1	-33.7	-55.3	-46.7	-53.7	-207.	-201.

BACKSCATTER COMPONENTS IN DECIBELS

ANGLE			------VOLUME-----			---INTERACTION---			--SURFACE--	
(DEG)	TAU	ALBEDO	VV	HH	VH	VV	HH	VH	VV	HH
8.4	1.9	0.10	-11.2	-11.2	-32.1	-24.7	-24.2	-35.1	-14.4	-14.3
19.2	1.9	0.10	-11.3	-11.3	-32.4	-26.9	-24.6	-38.0	-24.3	-23.8
30.0	1.9	0.10	-11.7	-11.7	-33.0	-31.8	-25.7	-40.5	-32.7	-31.4
40.9	1.9	0.10	-12.3	-12.3	-33.9	-40.2	-27.9	-43.4	-41.9	-39.3
51.8	1.9	0.10	-13.1	-13.2	-35.2	-46.4	-31.8	-47.9	-54.0	-49.3
62.7	1.9	0.10	-14.4	-14.5	-37.4	-53.0	-39.6	-54.9	-73.2	-64.6
73.6	1.9	0.10	-16.6	-16.6	-40.9	-67.1	-54.3	-64.7	-119.	-95.7
84.5	1.9	0.10	-21.3	-21.4	-49.4	-78.1	-67.6	-77.3	-234.	-228.

BACKSCATTER COMPONENTS IN DECIBELS

ANGLE			------VOLUME-----			---INTERACTION---			--SURFACE--	
(DEG)	TAU	ALBEDO	VV	HH	VH	VV	HH	VH	VV	HH
8.4	1.9	0.20	-7.9	-7.9	-25.5	-21.2	-20.8	-30.9	-14.4	-14.3
19.2	1.9	0.20	-8.1	-8.1	-25.8	-23.4	-21.1	-33.3	-24.3	-23.8
30.0	1.9	0.20	-8.4	-8.5	-26.4	-28.1	-22.2	-35.3	-32.7	-31.4
40.9	1.9	0.20	-9.0	-9.1	-27.3	-35.7	-24.3	-38.0	-41.9	-39.3
51.8	1.9	0.20	-9.9	-9.9	-28.7	-41.8	-28.1	-42.1	-54.0	-49.3
62.7	1.9	0.20	-11.2	-11.3	-30.8	-48.6	-35.6	-48.5	-73.2	-64.6
73.6	1.9	0.20	-13.3	-13.4	-34.4	-59.7	-47.9	-57.3	-119.	-95.7
84.5	1.9	0.20	-18.2	-18.3	-43.0	-70.9	-60.6	-69.7	-234.	-228.

FOR ALL CASES: SURFACE DIELECTRIC = 15 - j0, ksigma = 0.5, kL = 7

BACKSCATTER COMPONENTS IN DECIBELS

ANGLE			------VOLUME-----			---INTERACTION---			--SURFACE--	
(DEG)	TAU	ALBEDO	VV	HH	VH	VV	HH	VH	VV	HH
8.4	1.9	0.30	-5.9	-5.9	-21.4	-18.9	-18.5	-27.8	-14.4	-14.3
19.2	1.9	0.30	-6.1	-6.1	-21.7	-21.0	-18.9	-29.8	-24.3	-23.8
30.0	1.9	0.30	-6.4	-6.5	-22.3	-25.5	-19.9	-31.6	-32.7	-31.4
40.9	1.9	0.30	-7.0	-7.1	-23.2	-32.4	-22.0	-34.2	-41.9	-39.3
51.8	1.9	0.30	-7.9	-8.0	-24.6	-38.3	-25.7	-38.0	-54.0	-49.3
62.7	1.9	0.30	-9.2	-9.3	-26.7	-45.2	-32.7	-43.9	-73.2	-64.6
73.6	1.9	0.30	-11.4	-11.5	-30.4	-54.7	-43.7	-52.1	-119.	-95.7
84.5	1.9	0.30	-16.3	-16.4	-39.1	-66.1	-56.1	-64.5	-234.	-228.

BACKSCATTER COMPONENTS IN DECIBELS

ANGLE			------VOLUME-----			---INTERACTION---			--SURFACE--	
(DEG)	TAU	ALBEDO	VV	HH	VH	VV	HH	VH	VV	HH
8.4	1.9	0.40	-4.4	-4.4	-18.3	-17.0	-16.6	-25.2	-14.4	-14.3
19.2	1.9	0.40	-4.5	-4.6	-18.6	-19.1	-17.0	-26.8	-24.3	-23.8
30.0	1.9	0.40	-4.9	-4.9	-19.1	-23.3	-18.1	-28.5	-32.7	-31.4
40.9	1.9	0.40	-5.5	-5.5	-20.0	-29.6	-20.1	-30.9	-41.9	-39.3
51.8	1.9	0.40	-6.3	-6.5	-21.4	-35.3	-23.7	-34.5	-54.0	-49.3
62.7	1.9	0.40	-7.6	-7.9	-23.6	-41.9	-30.3	-40.1	-73.2	-64.6
73.6	1.9	0.40	-9.9	-10.1	-27.3	-50.4	-40.2	-47.9	-119.	-95.7
84.5	1.9	0.40	-14.9	-15.1	-36.1	-62.0	-52.6	-60.2	-234.	-228.

BACKSCATTER COMPONENTS IN DECIBELS

ANGLE			------VOLUME-----			---INTERACTION---			--SURFACE--	
(DEG)	TAU	ALBEDO	VV	HH	VH	VV	HH	VH	VV	HH
8.4	1.9	0.50	-3.1	-3.1	-15.6	-15.4	-15.0	-22.7	-14.4	-14.3
19.2	1.9	0.50	-3.3	-3.3	-15.9	-17.4	-15.4	-24.1	-24.3	-23.8
30.0	1.9	0.50	-3.6	-3.7	-16.5	-21.3	-16.4	-25.6	-32.7	-31.4
40.9	1.9	0.50	-4.2	-4.3	-17.4	-27.0	-18.4	-27.9	-41.9	-39.3
51.8	1.9	0.50	-5.0	-5.2	-18.8	-32.4	-21.8	-31.3	-54.0	-49.3
62.7	1.9	0.50	-6.4	-6.7	-20.9	-38.7	-28.1	-36.6	-73.2	-64.6
73.6	1.9	0.50	-8.7	-9.0	-24.7	-46.5	-37.2	-44.0	-119.	-95.7
84.5	1.9	0.50	-13.8	-14.1	-33.7	-58.3	-49.4	-56.3	-234.	-228.

BACKSCATTER COMPONENTS IN DECIBELS

ANGLE			------VOLUME-----			---INTERACTION---			--SURFACE--	
(DEG)	TAU	ALBEDO	VV	HH	VH	VV	HH	VH	VV	HH
8.4	2.2	0.10	-11.1	-11.1	-32.0	-26.7	-26.3	-37.2	-17.0	-16.9
19.2	2.2	0.10	-11.3	-11.3	-32.3	-29.1	-26.8	-40.2	-27.1	-26.6
30.0	2.2	0.10	-11.7	-11.7	-32.9	-34.2	-28.1	-42.8	-35.7	-34.4
40.9	2.2	0.10	-12.2	-12.3	-33.8	-42.9	-30.6	-46.1	-45.4	-42.8
51.8	2.2	0.10	-13.1	-13.1	-35.2	-49.8	-35.3	-51.1	-58.2	-53.5
62.7	2.2	0.10	-14.4	-14.5	-37.3	-57.7	-44.2	-58.7	-78.9	-70.3
73.6	2.2	0.10	-16.6	-16.6	-40.9	-70.9	-58.2	-68.2	-128.	-105.
84.5	2.2	0.10	-21.3	-21.4	-49.4	-81.7	-70.7	-80.5	-261.	-255.

FOR ALL CASES: SURFACE DIELECTRIC = 15 - j0, ksigma = 0.5, kL = 7

BACKSCATTER COMPONENTS IN DECIBELS

ANGLE			------VOLUME-----			---INTERACTION---			--SURFACE--	
(DEG)	TAU	ALBEDO	VV	HH	VH	VV	HH	VH	VV	HH
8.4	2.2	0.20	-7.9	-7.9	-25.4	-23.2	-22.8	-32.9	-17.0	-16.9
19.2	2.2	0.20	-8.0	-8.1	-25.7	-25.5	-23.3	-35.3	-27.1	-26.6
30.0	2.2	0.20	-8.4	-8.4	-26.3	-30.4	-24.6	-37.6	-35.7	-34.4
40.9	2.2	0.20	-9.0	-9.0	-27.2	-38.3	-27.0	-40.6	-45.4	-42.8
51.8	2.2	0.20	-9.9	-9.9	-28.6	-45.0	-31.5	-45.1	-58.2	-53.5
62.7	2.2	0.20	-11.2	-11.3	-30.8	-52.9	-39.9	-51.9	-78.9	-70.3
73.6	2.2	0.20	-13.4	-13.5	-34.4	-63.3	-51.4	-60.5	-128.	-105.
84.5	2.2	0.20	-18.2	-18.3	-43.0	-74.4	-63.7	-72.8	-261.	-255.

BACKSCATTER COMPONENTS IN DECIBELS

ANGLE			------VOLUME-----			---INTERACTION---			--SURFACE--	
(DEG)	TAU	ALBEDO	VV	HH	VH	VV	HH	VH	VV	HH
8.4	2.2	0.30	-5.8	-5.8	-21.3	-20.8	-20.4	-29.7	-17.0	-16.9
19.2	2.2	0.30	-6.0	-6.0	-21.6	-23.1	-20.9	-31.8	-27.1	-26.6
30.0	2.2	0.30	-6.4	-6.4	-22.2	-27.7	-22.2	-33.8	-35.7	-34.4
40.9	2.2	0.30	-7.0	-7.0	-23.1	-34.9	-24.6	-36.6	-45.4	-42.8
51.8	2.2	0.30	-7.9	-7.9	-24.5	-41.3	-29.0	-40.8	-58.2	-53.5
62.7	2.2	0.30	-9.2	-9.3	-26.7	-49.0	-36.7	-47.1	-78.9	-70.3
73.6	2.2	0.30	-11.4	-11.5	-30.4	-58.0	-46.9	-55.2	-128.	-105.
84.5	2.2	0.30	-16.3	-16.5	-39.1	-69.5	-59.1	-67.4	-261.	-255.

BACKSCATTER COMPONENTS IN DECIBELS

ANGLE			------VOLUME-----			---INTERACTION---			--SURFACE--	
(DEG)	TAU	ALBEDO	VV	HH	VH	VV	HH	VH	VV	HH
8.4	2.2	0.40	-4.3	-4.3	-18.1	-18.9	-18.5	-27.0	-17.0	-16.9
19.2	2.2	0.40	-4.5	-4.5	-18.4	-21.1	-19.0	-28.7	-27.1	-26.6
30.0	2.2	0.40	-4.8	-4.9	-19.0	-25.5	-20.3	-30.5	-35.7	-34.4
40.9	2.2	0.40	-5.4	-5.5	-20.0	-31.9	-22.6	-33.2	-45.4	-42.8
51.8	2.2	0.40	-6.3	-6.4	-21.4	-38.0	-26.8	-37.1	-58.2	-53.5
62.7	2.2	0.40	-7.6	-7.9	-23.6	-45.3	-34.0	-43.0	-78.9	-70.3
73.6	2.2	0.40	-9.9	-10.1	-27.3	-53.5	-43.3	-50.7	-128.	-105.
84.5	2.2	0.40	-15.0	-15.1	-36.2	-65.2	-55.4	-63.0	-261.	-255.

BACKSCATTER COMPONENTS IN DECIBELS

ANGLE			------VOLUME-----			---INTERACTION---			--SURFACE--	
(DEG)	TAU	ALBEDO	VV	HH	VH	VV	HH	VH	VV	HH
8.4	2.2	0.50	-3.0	-3.0	-15.5	-17.2	-16.8	-24.4	-17.0	-16.9
19.2	2.2	0.50	-3.2	-3.2	-15.8	-19.3	-17.3	-25.8	-27.1	-26.6
30.0	2.2	0.50	-3.6	-3.6	-16.3	-23.4	-18.6	-27.5	-35.7	-34.4
40.9	2.2	0.50	-4.1	-4.2	-17.3	-29.2	-20.8	-30.0	-45.4	-42.8
51.8	2.2	0.50	-5.0	-5.2	-18.7	-34.9	-24.8	-33.7	-58.2	-53.5
62.7	2.2	0.50	-6.4	-6.7	-20.9	-41.7	-31.5	-39.2	-78.9	-70.3
73.6	2.2	0.50	-8.7	-9.0	-24.7	-49.4	-40.1	-46.7	-128.	-105.
84.5	2.2	0.50	-13.9	-14.1	-33.7	-61.3	-52.1	-58.9	-261.	-255.

FOR ALL CASES: SURFACE DIELECTRIC = 15 - j0, kL = 7
OPTICAL DEPTH (TAU) = 0.2, ALBEDO = 0.2

BACKSCATTER COMPONENTS IN DECIBELS

ANGLE		------VOLUME-----			---INTERACTION---			--SURFACE--	
(DEG)	ksigma	VV	HH	VH	VV	HH	VH	VV	HH
8.4	0.1	-12.9	-12.9	-34.4	-15.1	-14.7	-32.1	-11.4	-11.3
19.2	0.1	-12.9	-12.9	-34.7	-16.9	-14.5	-32.9	-22.0	-21.5
30.0	0.1	-13.0	-13.0	-35.1	-20.4	-14.3	-33.6	-29.4	-28.1
40.9	0.1	-13.1	-13.2	-35.7	-26.0	-14.0	-34.6	-36.3	-33.7
51.8	0.1	-13.3	-13.4	-36.6	-27.8	-13.9	-36.0	-44.1	-39.4
62.7	0.1	-13.8	-13.8	-37.6	-27.5	-14.1	-38.0	-55.0	-46.4
73.6	0.1	-14.7	-14.8	-39.2	-38.1	-15.6	-41.1	-80.4	-57.4
84.5	0.1	-18.3	-18.4	-44.2	-33.9	-27.0	-49.6	-94.3	-87.8

BACKSCATTER COMPONENTS IN DECIBELS

ANGLE		------VOLUME-----			---INTERACTION---			--SURFACE--	
(DEG)	ksigma	VV	HH	VH	VV	HH	VH	VV	HH
8.4	0.2	-12.9	-12.9	-34.4	-15.3	-14.8	-30.2	-5.6	-5.5
19.2	0.2	-12.9	-12.9	-34.7	-17.0	-14.6	-31.6	-16.0	-15.5
30.0	0.2	-13.0	-13.0	-35.1	-20.5	-14.4	-32.5	-23.4	-22.1
40.9	0.2	-13.1	-13.2	-35.7	-26.0	-14.1	-33.4	-30.3	-27.7
51.8	0.2	-13.3	-13.4	-36.6	-27.8	-13.9	-34.8	-38.1	-33.4
62.7	0.2	-13.8	-13.8	-37.6	-27.5	-14.1	-36.9	-49.0	-40.4
73.6	0.2	-14.7	-14.8	-39.2	-38.0	-15.7	-40.2	-74.4	-51.4
84.5	0.2	-18.3	-18.4	-44.2	-33.9	-27.0	-49.1	-88.3	-81.7

BACKSCATTER COMPONENTS IN DECIBELS

ANGLE		------VOLUME-----			---INTERACTION---			--SURFACE--	
(DEG)	ksigma	VV	HH	VH	VV	HH	VH	VV	HH
8.4	0.3	-12.9	-12.9	-34.4	-15.5	-15.0	-28.3	-2.5	-2.4
19.2	0.3	-12.9	-12.9	-34.7	-17.1	-14.8	-30.2	-12.7	-12.1
30.0	0.3	-13.0	-13.0	-35.1	-20.5	-14.5	-31.2	-19.9	-18.6
40.9	0.3	-13.1	-13.2	-35.7	-25.9	-14.2	-32.0	-26.8	-24.2
51.8	0.3	-13.3	-13.4	-36.6	-27.8	-14.0	-33.4	-34.5	-29.9
62.7	0.3	-13.8	-13.8	-37.6	-27.6	-14.2	-35.6	-45.4	-36.9
73.6	0.3	-14.7	-14.8	-39.2	-37.8	-15.7	-39.2	-70.9	-47.8
84.5	0.3	-18.3	-18.4	-44.2	-33.9	-26.9	-48.5	-84.8	-78.2

BACKSCATTER COMPONENTS IN DECIBELS

ANGLE		------VOLUME-----			---INTERACTION---			--SURFACE--	
(DEG)	ksigma	VV	HH	VH	VV	HH	VH	VV	HH
8.4	0.4	-12.9	-12.9	-34.4	-15.8	-15.3	-26.9	-0.6	-0.5
19.2	0.4	-12.9	-12.9	-34.7	-17.3	-15.0	-28.9	-10.4	-9.9
30.0	0.4	-13.0	-13.0	-35.1	-20.6	-14.7	-29.9	-17.5	-16.2
40.9	0.4	-13.1	-13.2	-35.7	-25.7	-14.4	-30.7	-24.3	-21.7
51.8	0.4	-13.3	-13.4	-36.6	-27.8	-14.2	-32.0	-32.1	-27.4
62.7	0.4	-13.8	-13.8	-37.6	-27.7	-14.3	-34.2	-43.0	-34.4
73.6	0.4	-14.7	-14.8	-39.2	-37.6	-15.7	-38.0	-68.4	-45.3
84.5	0.4	-18.3	-18.4	-44.2	-33.9	-26.9	-47.8	-82.3	-75.7

FOR ALL CASES: SURFACE DIELECTRIC = 15 - j0, kL = 7
OPTICAL DEPTH (TAU) = 0.2, ALBEDO = 0.2

BACKSCATTER COMPONENTS IN DECIBELS

ANGLE		------VOLUME-----			---INTERACTION---			--SURFACE--	
(DEG)	ksigma	VV	HH	VH	VV	HH	VH	VV	HH
8.4	0.6	-12.9	-12.9	-34.4	-16.5	-16.1	-25.0	1.2	1.3
19.2	0.6	-12.9	-12.9	-34.7	-17.9	-15.7	-26.9	-7.5	-7.0
30.0	0.6	-13.0	-13.0	-35.1	-20.8	-15.3	-27.9	-14.3	-13.0
40.9	0.6	-13.1	-13.2	-35.7	-25.4	-14.9	-28.6	-20.9	-18.3
51.8	0.6	-13.3	-13.4	-36.6	-27.7	-14.6	-29.8	-28.6	-23.9
62.7	0.6	-13.8	-13.8	-37.6	-27.9	-14.6	-32.0	-39.5	-30.9
73.6	0.6	-14.7	-14.8	-39.2	-37.1	-15.9	-35.9	-64.9	-41.8
84.5	0.6	-18.3	-18.4	-44.2	-33.9	-26.9	-46.3	-78.8	-72.2

BACKSCATTER COMPONENTS IN DECIBELS

ANGLE		------VOLUME-----			---INTERACTION---			--SURFACE--	
(DEG)	ksigma	VV	HH	VH	VV	HH	VH	VV	HH
8.4	0.7	-12.9	-12.9	-34.4	-16.9	-16.5	-24.5	1.4	1.5
19.2	0.7	-12.9	-12.9	-34.7	-18.2	-16.0	-26.2	-6.6	-6.1
30.0	0.7	-13.0	-13.0	-35.1	-21.0	-15.6	-27.1	-13.1	-11.8
40.9	0.7	-13.1	-13.2	-35.7	-25.2	-15.2	-27.7	-19.7	-17.1
51.8	0.7	-13.3	-13.4	-36.6	-27.7	-14.8	-28.9	-27.3	-22.6
62.7	0.7	-13.8	-13.8	-37.6	-28.0	-14.8	-31.0	-38.1	-29.6
73.6	0.7	-14.7	-14.8	-39.2	-36.9	-16.0	-34.9	-63.6	-40.5
84.5	0.7	-18.3	-18.4	-44.2	-33.9	-26.9	-45.6	-77.4	-70.8

BACKSCATTER COMPONENTS IN DECIBELS

ANGLE		------VOLUME-----			---INTERACTION---			--SURFACE--	
(DEG)	ksigma	VV	HH	VH	VV	HH	VH	VV	HH
8.4	0.8	-12.9	-12.9	-34.4	-17.3	-16.9	-24.2	1.4	1.4
19.2	0.8	-12.9	-12.9	-34.7	-18.5	-16.4	-25.7	-6.0	-5.5
30.0	0.8	-13.0	-13.0	-35.1	-21.1	-15.9	-26.4	-12.2	-10.9
40.9	0.8	-13.1	-13.2	-35.7	-25.1	-15.5	-27.1	-18.6	-16.0
51.8	0.8	-13.3	-13.4	-36.6	-27.6	-15.1	-28.2	-26.2	-21.5
62.7	0.8	-13.8	-13.8	-37.6	-28.2	-15.1	-30.2	-37.0	-28.4
73.6	0.8	-14.7	-14.8	-39.2	-36.6	-16.1	-34.1	-62.4	-39.3
84.5	0.8	-18.3	-18.4	-44.2	-33.9	-26.9	-44.9	-76.2	-69.7

BACKSCATTER COMPONENTS IN DECIBELS

ANGLE		------VOLUME-----			---INTERACTION---			--SURFACE--	
(DEG)	ksigma	VV	HH	VH	VV	HH	VH	VV	HH
8.4	0.9	-12.9	-12.9	-34.4	-17.7	-17.4	-24.0	1.0	1.1
19.2	0.9	-12.9	-12.9	-34.7	-18.9	-16.8	-25.3	-5.7	-5.1
30.0	0.9	-13.0	-13.0	-35.1	-21.3	-16.3	-25.9	-11.6	-10.2
40.9	0.9	-13.1	-13.2	-35.7	-24.9	-15.8	-26.5	-17.7	-15.2
51.8	0.9	-13.3	-13.4	-36.6	-27.5	-15.4	-27.5	-25.2	-20.6
62.7	0.9	-13.8	-13.8	-37.6	-28.3	-15.3	-29.5	-36.0	-27.4
73.6	0.9	-14.7	-14.8	-39.2	-36.4	-16.2	-33.4	-61.4	-38.3
84.5	0.9	-18.3	-18.4	-44.2	-33.9	-26.8	-44.2	-75.2	-68.7

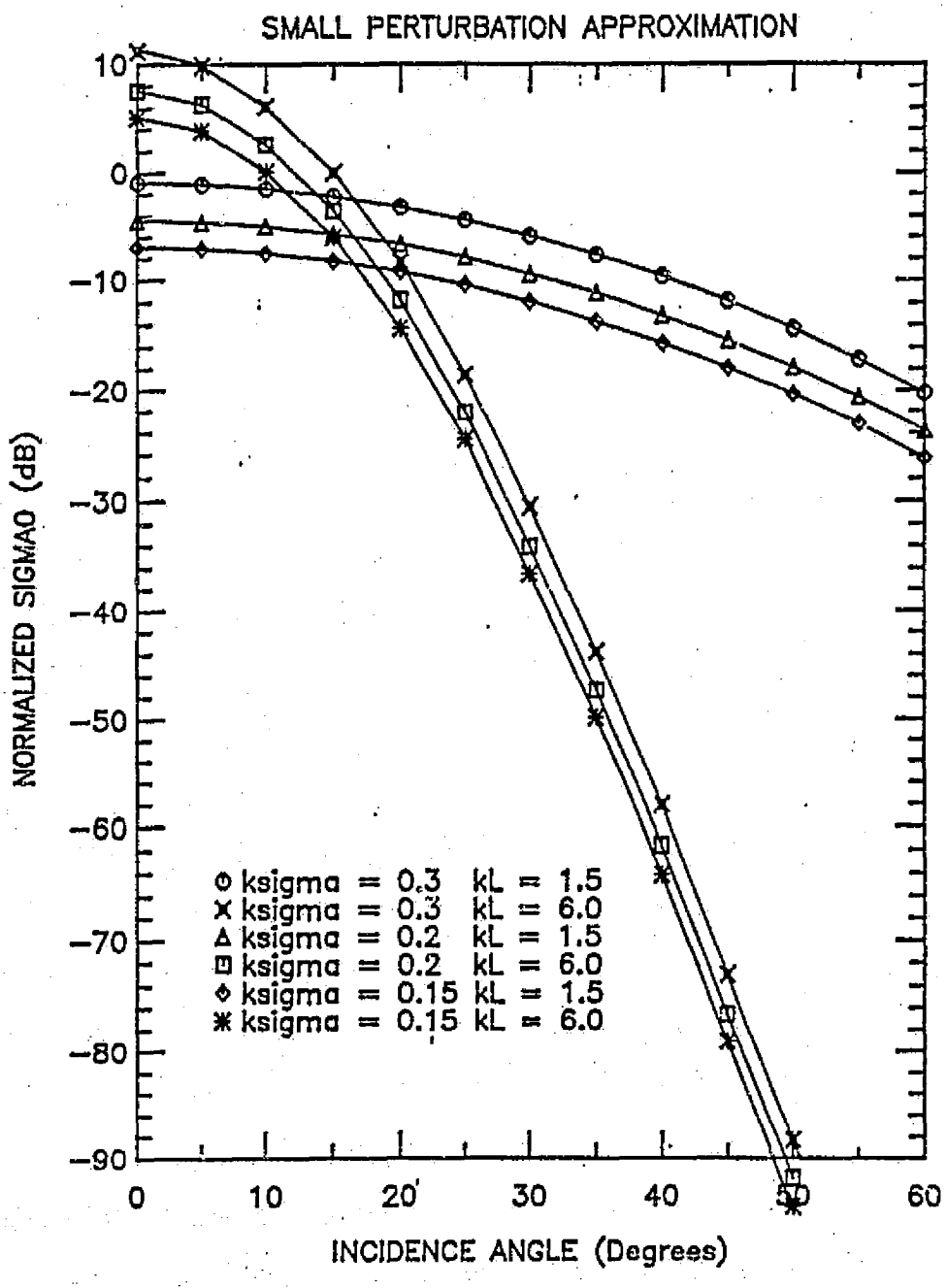

Figure C.1 Computed normalized backscattering using the small perturbation approximation as a function of (a) incidence angle, (b) kσ, and (c) kL under various conditions.

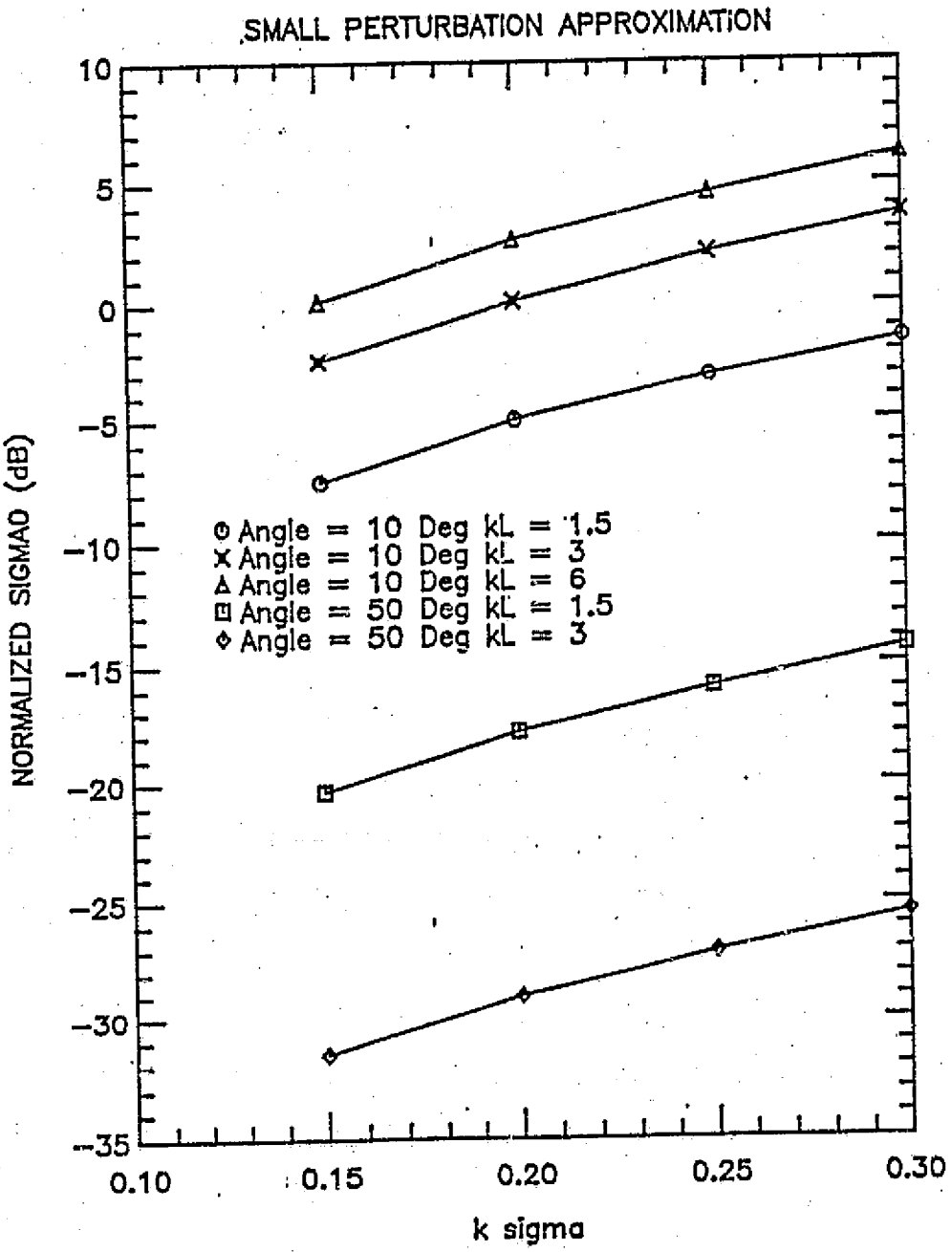
SMALL PERTURBATION APPROXIMATION
NORMALIZED SIGMA0 (dB)
10
5
0
-5
-10
-15
-20
-25
-30
-35
0.10
0.15
0.20
0.25
0.30
k sigma
Angle = 10 Deg kL = 1.5
Angle = 10 Deg kL = 3
Angle = 10 Deg kL = 6
Angle = 50 Deg kL = 1.5
Angle = 50 Deg kL = 3

Figure C.1(b)

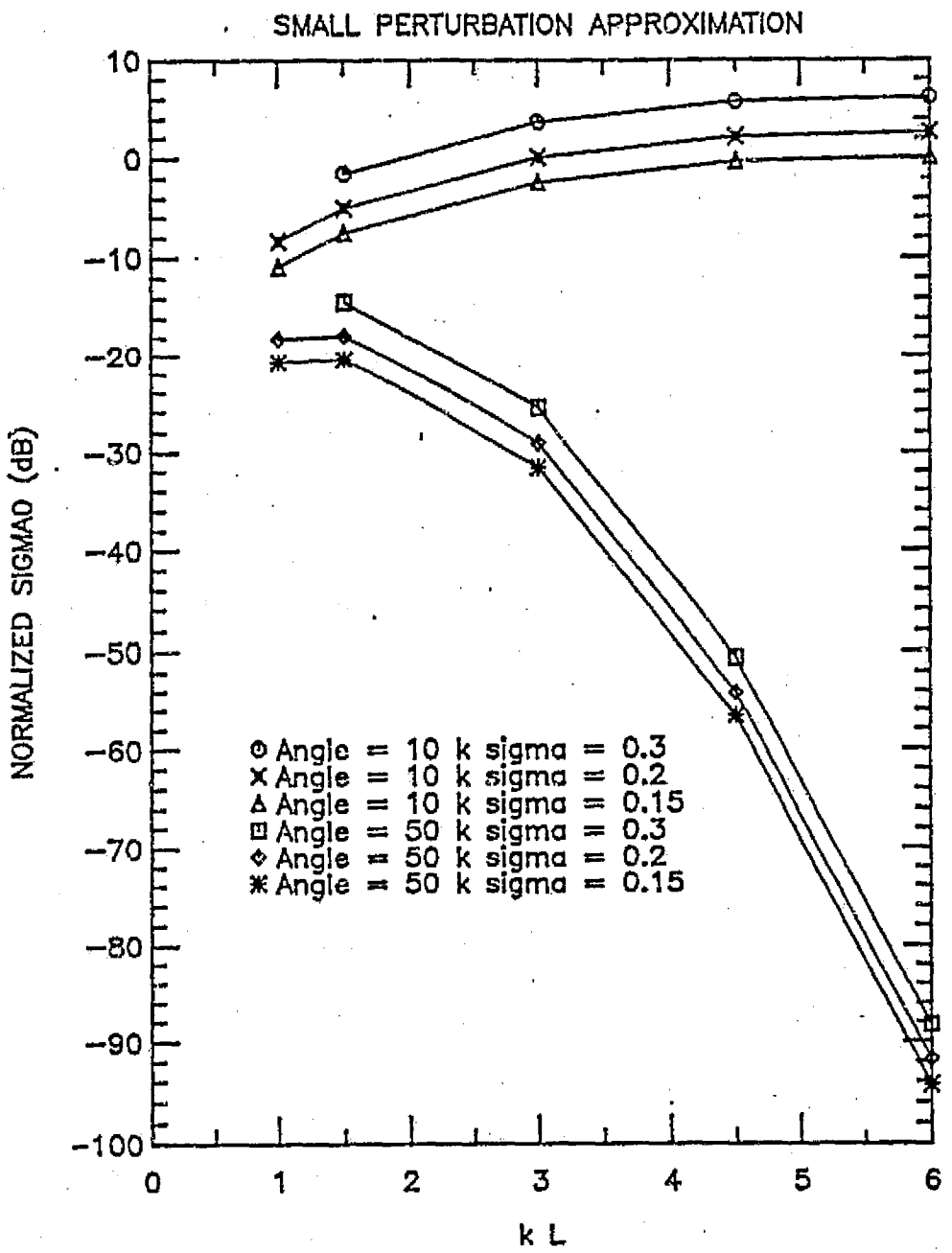
SMALL PERTURBATION APPROXIMATION
NORMALIZED SIGMA0 (dB)
10
0
-10
-20
-30
-40
-50
-60
-70
-80
-90
-100
0
1
2
3
4
5
6
k L
Angle = 10 k sigma = 0.3
Angle = 10 k sigma = 0.2
Angle = 10 k sigma = 0.15
Angle = 50 k sigma = 0.3
Angle = 50 k sigma = 0.2
Angle = 50 k sigma = 0.15

Figure C.1(c)

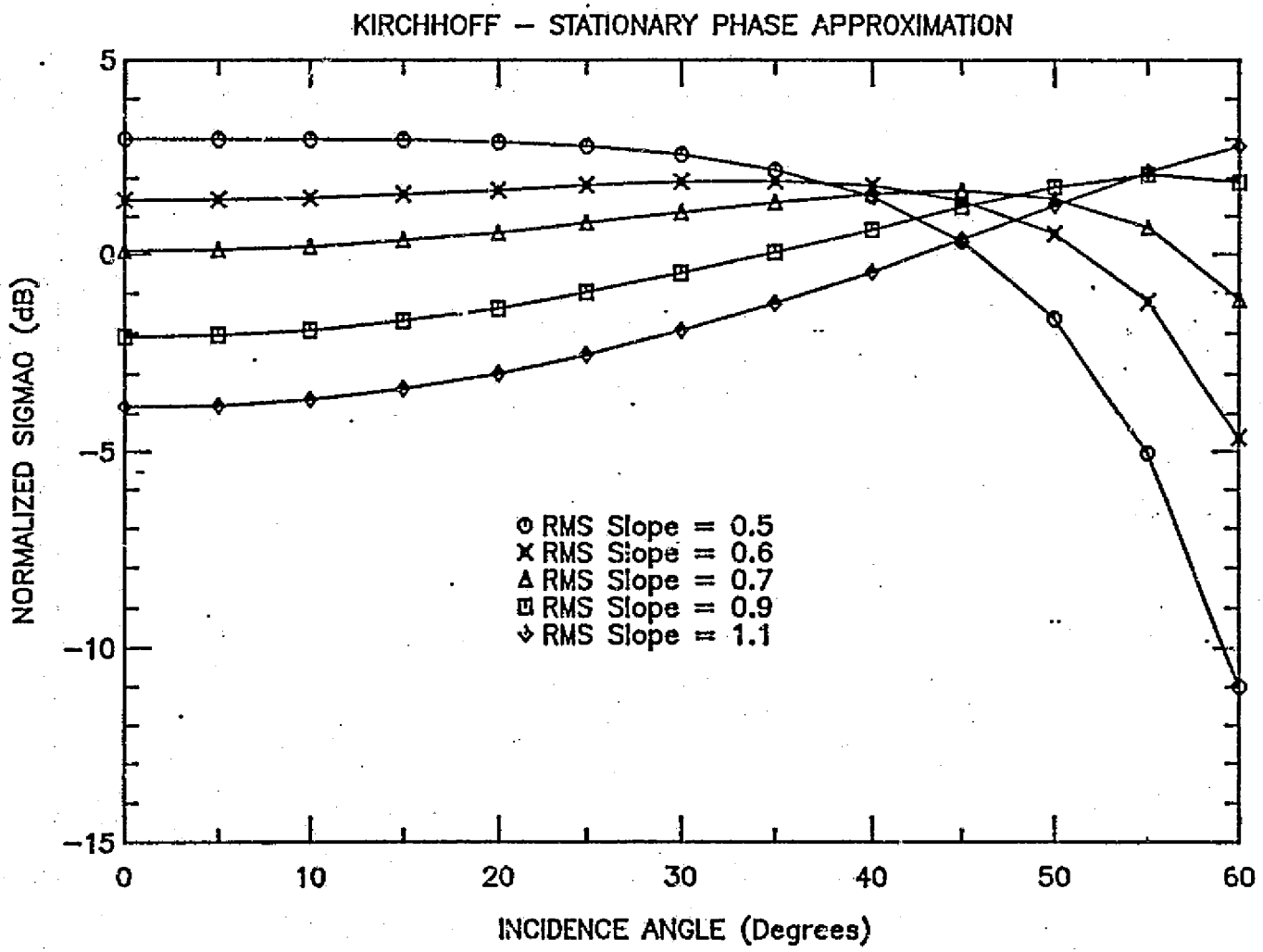

Figure C.2 Computed normalized backscattering using the stationary phase approximation as a function of (a) incidence angle and (b) RMS slope under various conditions.

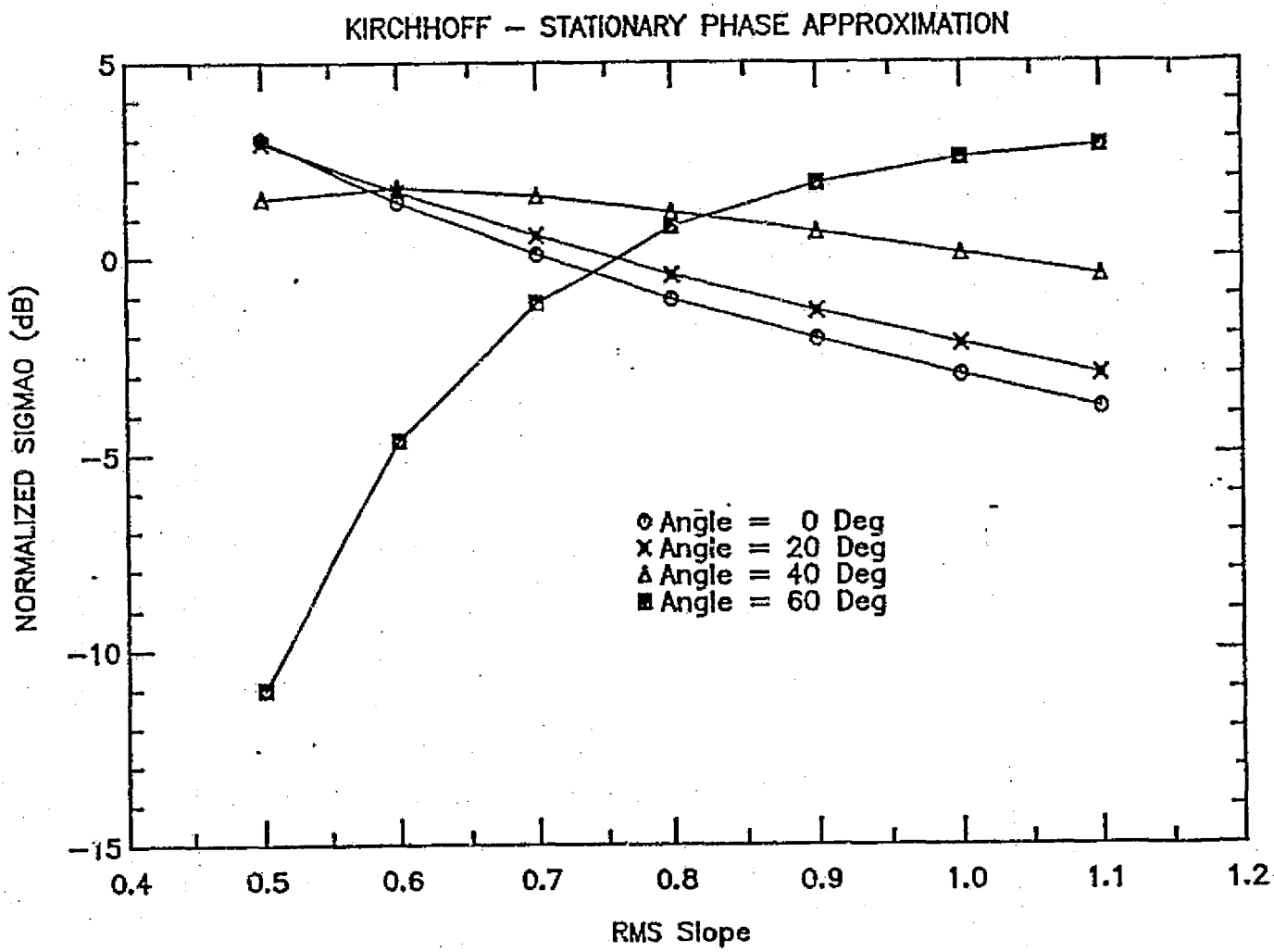
KIRCHHOFF – STATIONARY PHASE APPROXIMATION
NORMALIZED SIGMA0 (dB)
5
0
−5
−10
−15
0.4
0.5
0.6
0.7
0.8
0.9
1.0
1.1
1.2
RMS Slope
Angle = 0 Deg
Angle = 20 Deg
Angle = 40 Deg
Angle = 60 Deg

Figure C.2(b)

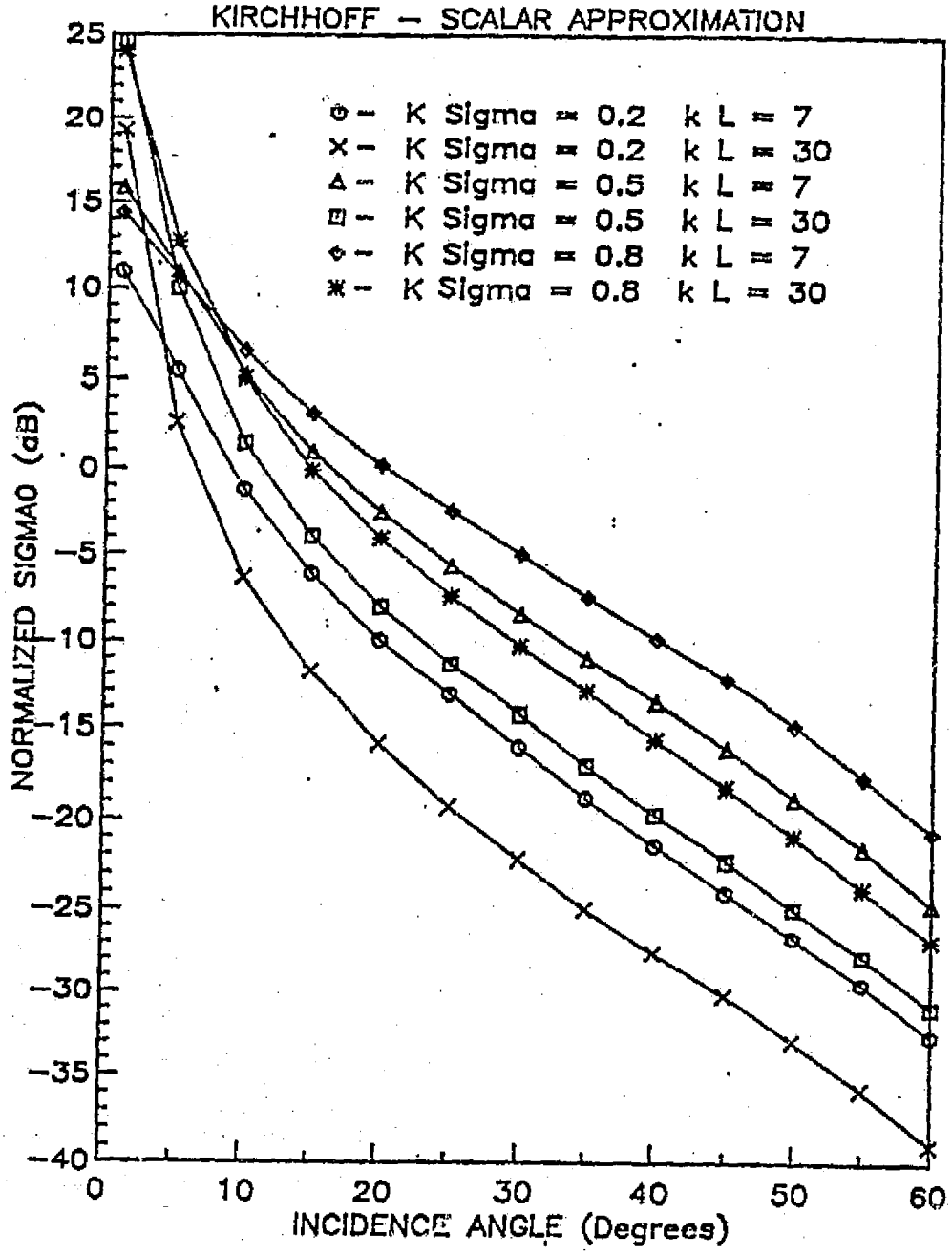

Figure C.3 Computed normalized backscattering using the scalar approximation as a function of (a) incidence angle, (b) $k\sigma$, and (c) kL under various conditions.

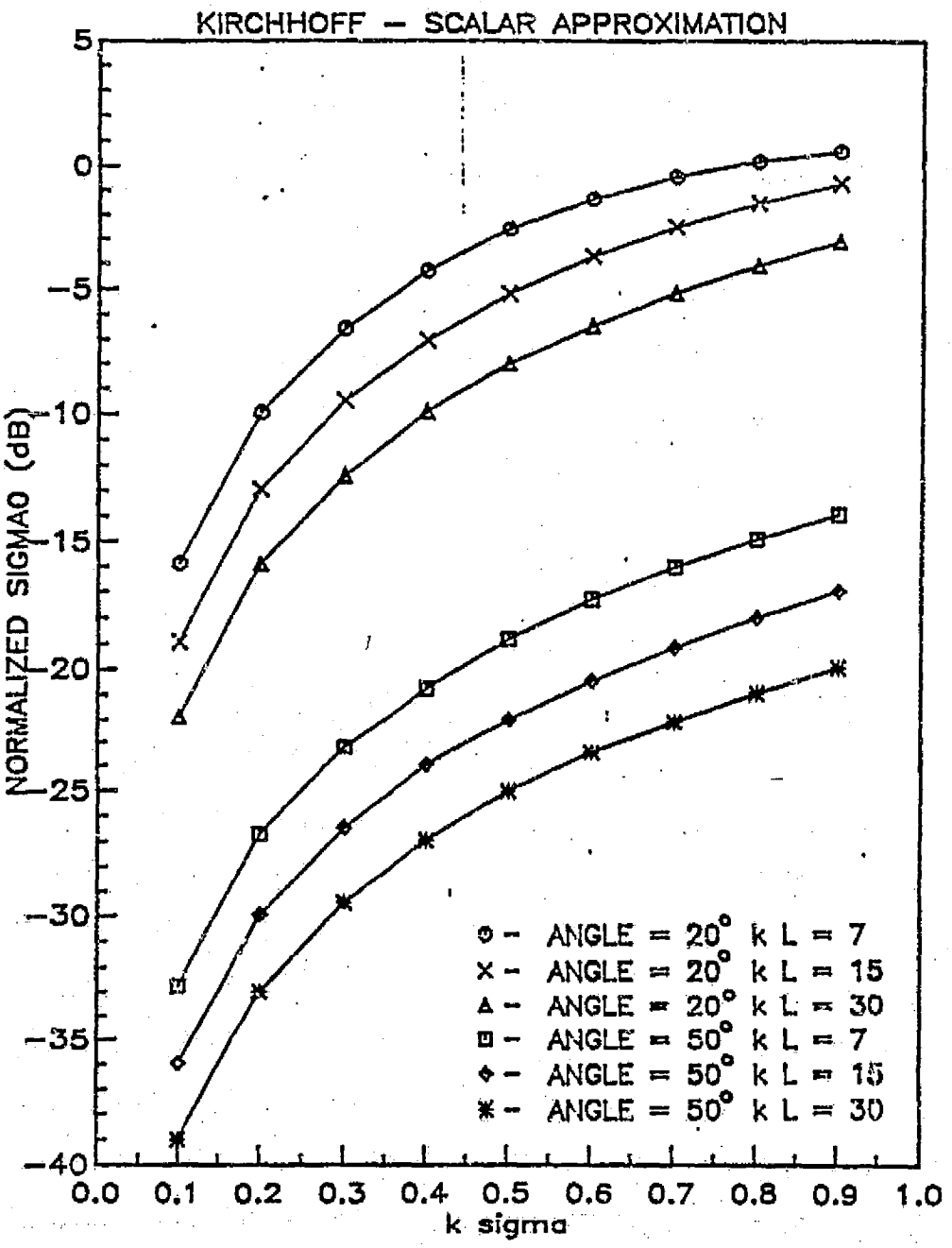
KIRCHHOFF — SCALAR APPROXIMATION
NORMALIZED SIGMA0 (dB)
5
0
-5
-10
-15
-20
-25
-30
-35
-40
0.0
0.1
0.2
0.3
0.4
0.5
0.6
0.7
0.8
0.9
1.0
k sigma
⊙ - ANGLE = 20° k L = 7
× - ANGLE = 20° k L = 15
△ - ANGLE = 20° k L = 30
⊡ - ANGLE = 50° k L = 7
◇ - ANGLE = 50° k L = 15
✳ - ANGLE = 50° k L = 30

Figure C.3(b)

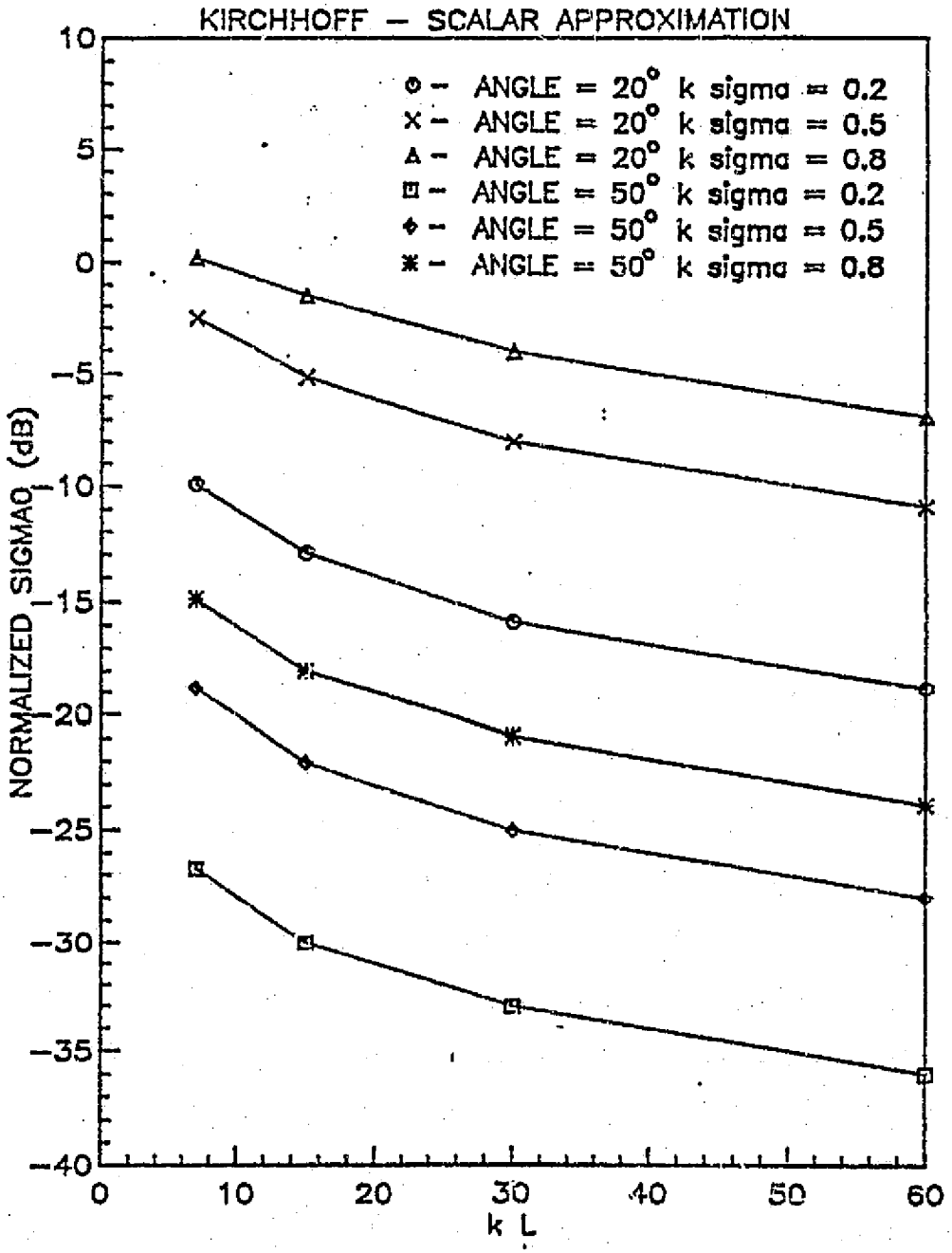
KIRCHHOFF — SCALAR APPROXIMATION
o — ANGLE = 20° k sigma = 0.2
× — ANGLE = 20° k sigma = 0.5
Δ — ANGLE = 20° k sigma = 0.8
□ — ANGLE = 50° k sigma = 0.2
◇ — ANGLE = 50° k sigma = 0.5
✱ — ANGLE = 50° k sigma = 0.8
NORMALIZED SIGMA0 (dB)
10
5
0
−5
−10
−15
−20
−25
−30
−35
−40
0
10
20
30
40
50
60
k L

Figure C.3(c)

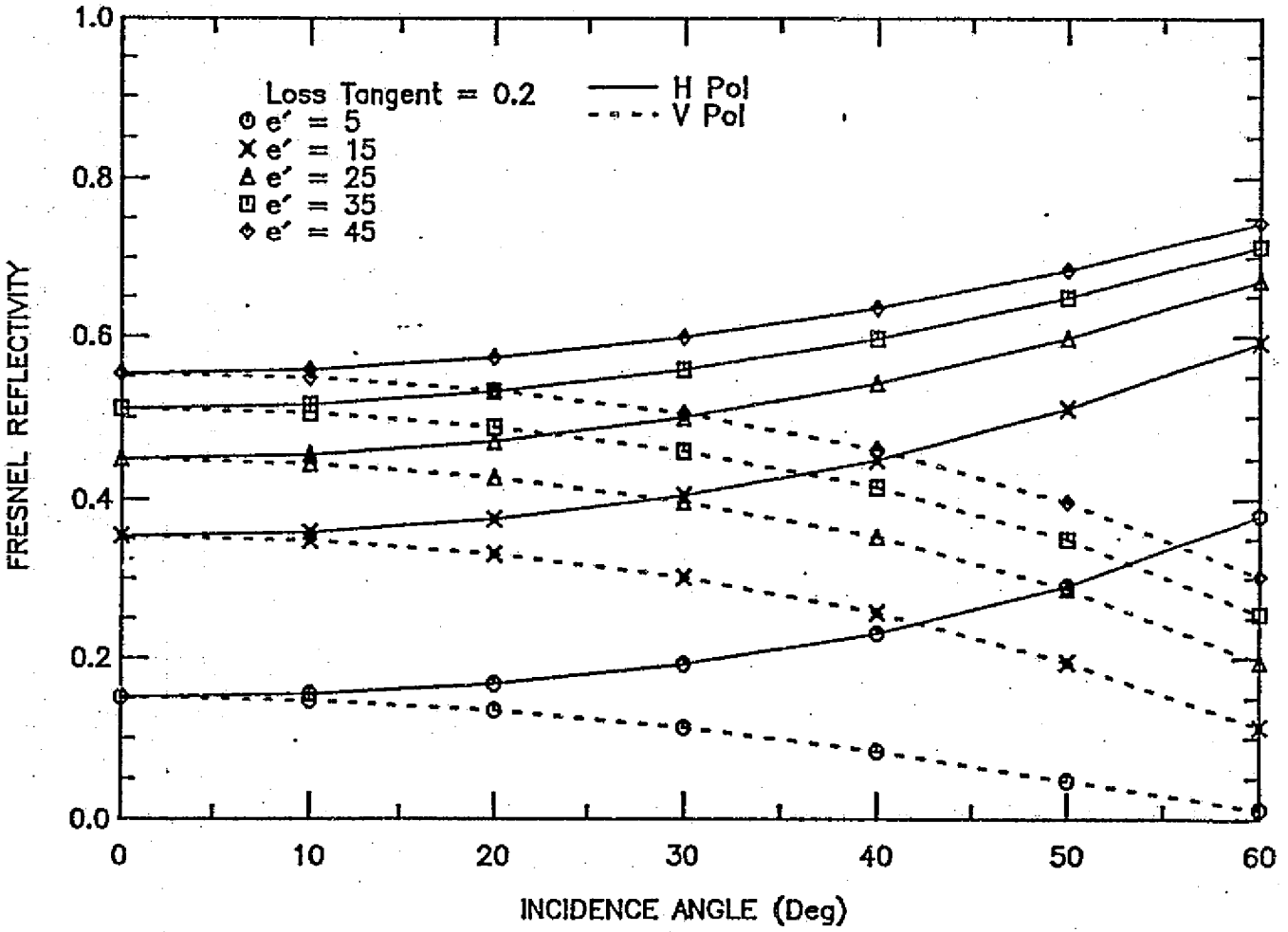

Figure C.4 Computed Fresnel reflectivity as a function of (a) incidence angle, (b) ε', and (c) loss tangent (tan δ) under various conditions.

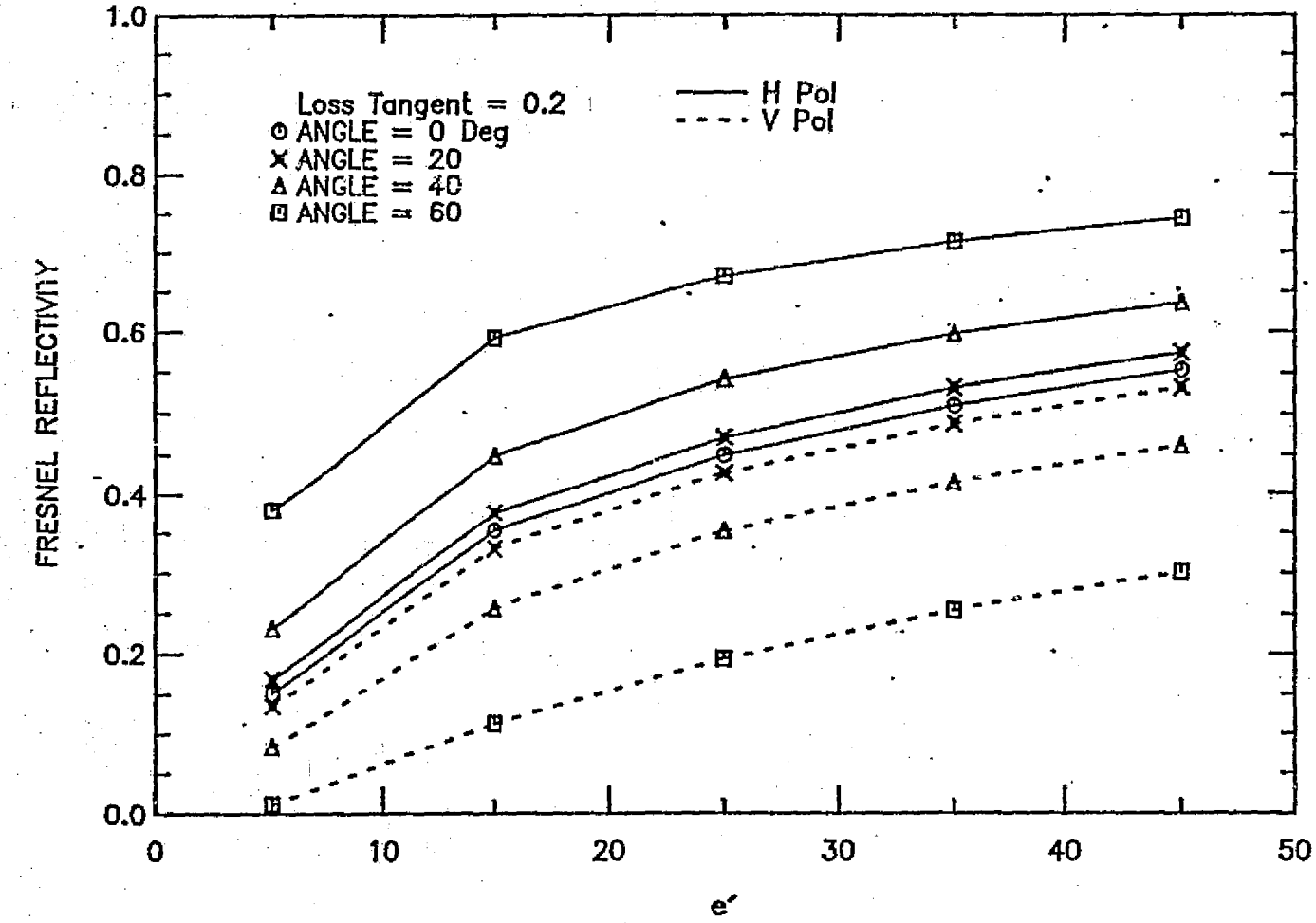
Loss Tangent = 0.2
⊙ ANGLE = 0 Deg
× ANGLE = 20
△ ANGLE = 40
⊡ ANGLE = 60
H Pol
V Pol
FRESNEL REFLECTIVITY
1.0
0.8
0.6
0.4
0.2
0.0
0
10
20
30
40
50
e'

Figure C.4(b)

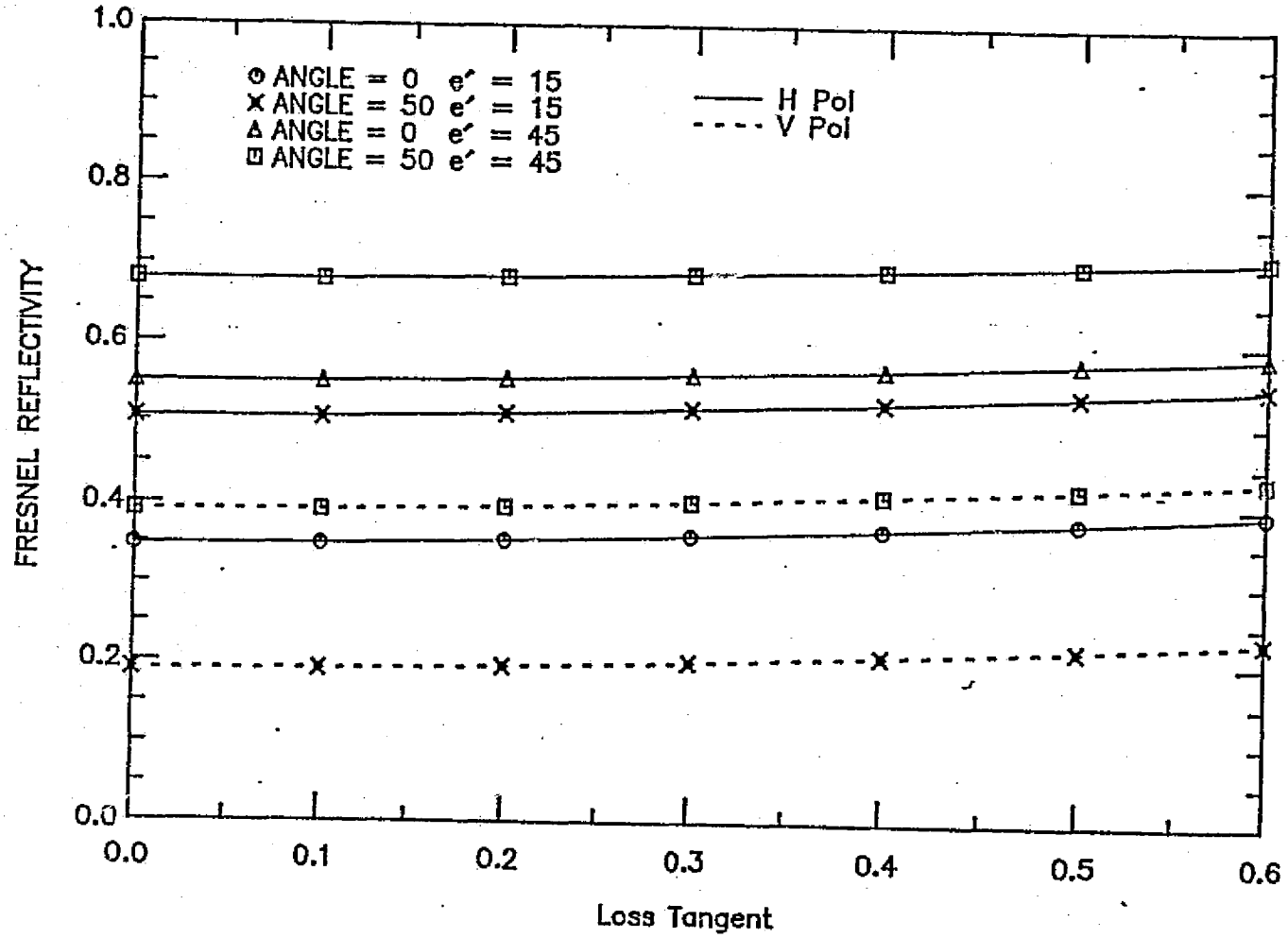
1.0
0.8
0.6
0.4
0.2
0.0
FRESNEL REFLECTIVITY
ANGLE = 0 e' = 15
ANGLE = 50 e' = 15
ANGLE = 0 e' = 45
ANGLE = 50 e' = 45
H Pol
V Pol
0.0
0.1
0.2
0.3
0.4
0.5
0.6
Loss Tangent

Figure C.4(c)

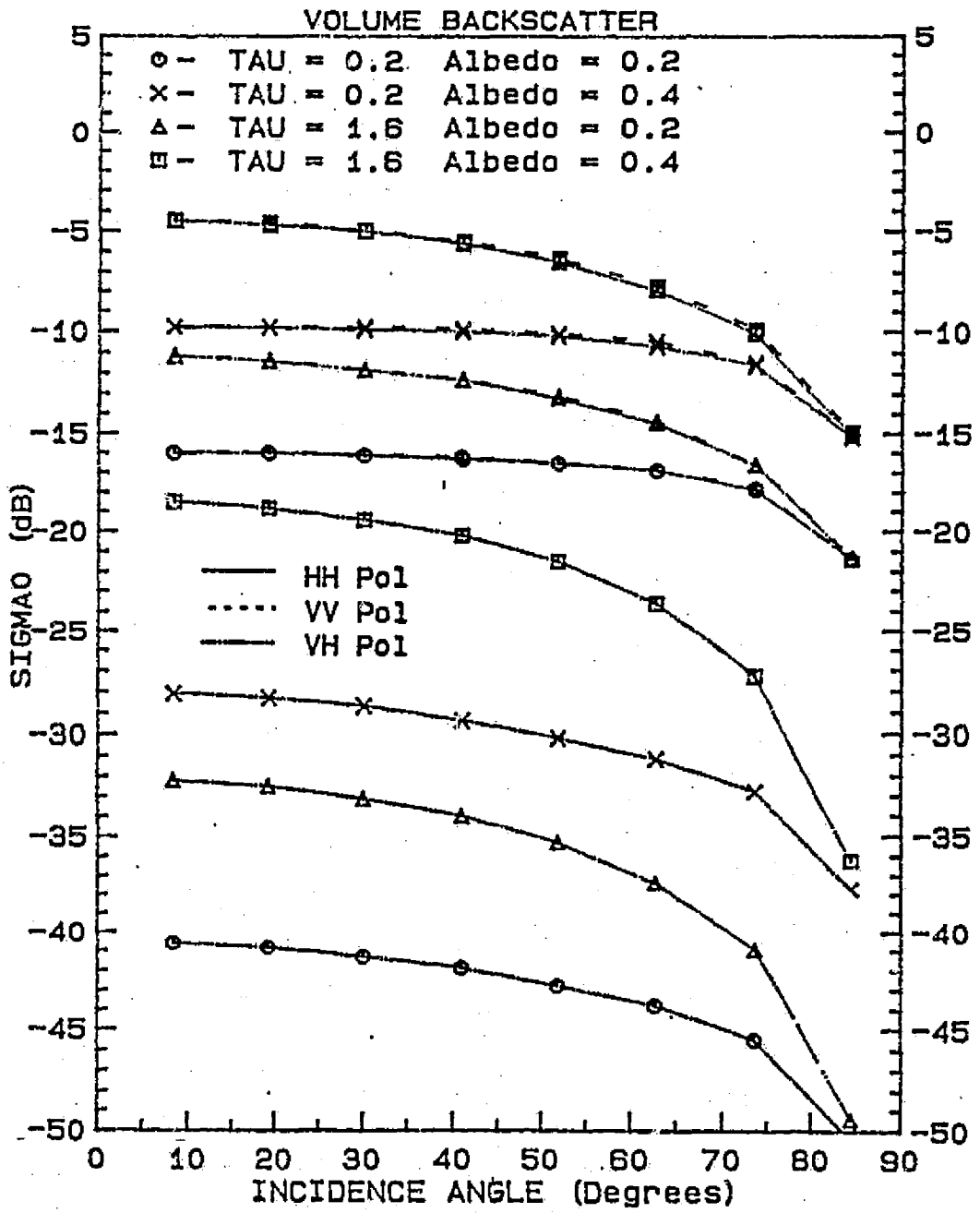

Figure C.5 Computed volume backscattering as a function of (a) incidence angle, (b) optical thickness (τ), and (c) albedo (ω) under various conditions.

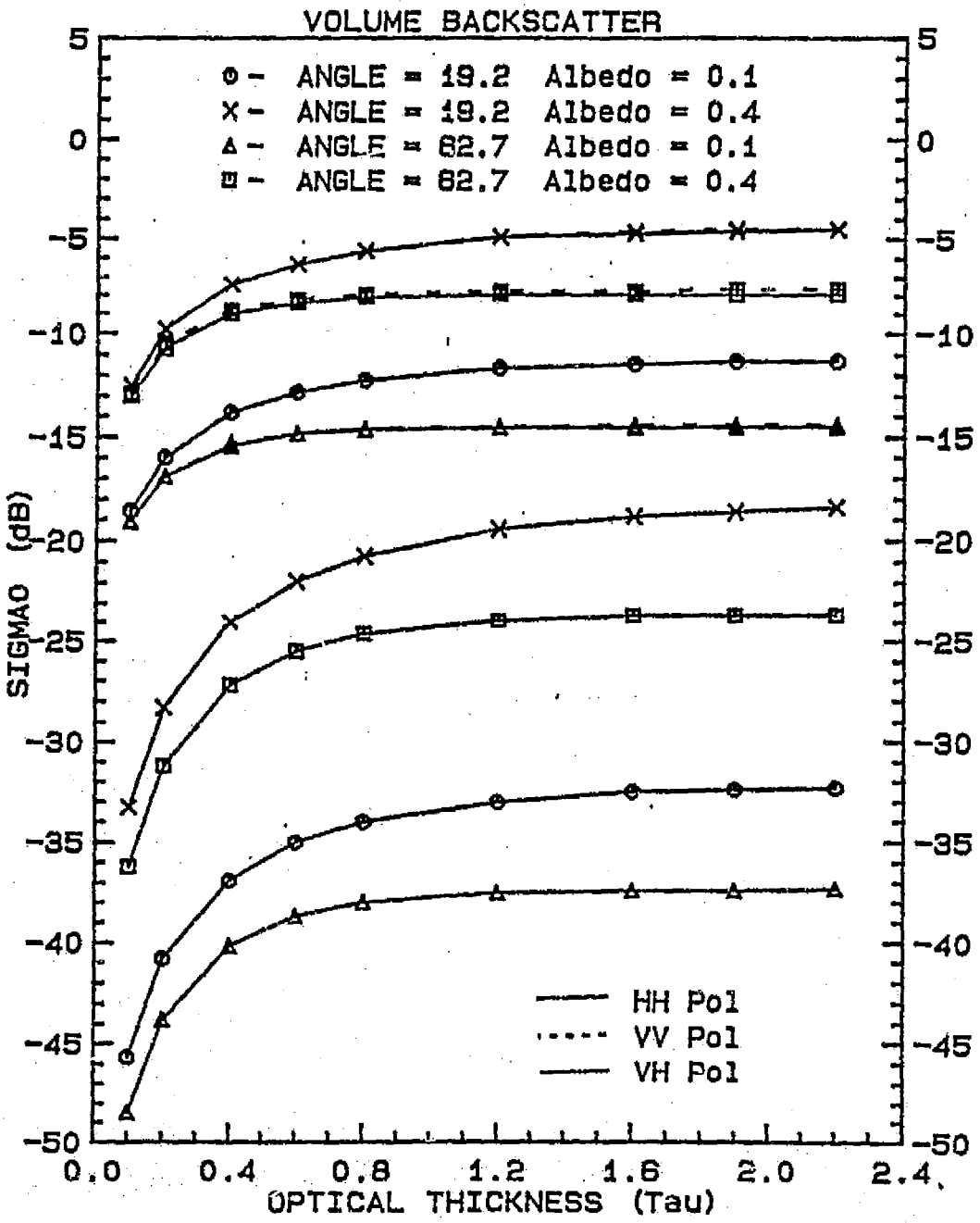
VOLUME BACKSCATTER
o - ANGLE = 19.2 Albedo = 0.1
X - ANGLE = 19.2 Albedo = 0.4
Δ - ANGLE = 62.7 Albedo = 0.1
□ - ANGLE = 62.7 Albedo = 0.4
HH Pol
VV Pol
VH Pol
SIGMA0 (dB)
OPTICAL THICKNESS (Tau)
5
0
-5
-10
-15
-20
-25
-30
-35
-40
-45
-50
0.0
0.4
0.8
1.2
1.6
2.0
2.4

Figure C.5(b)

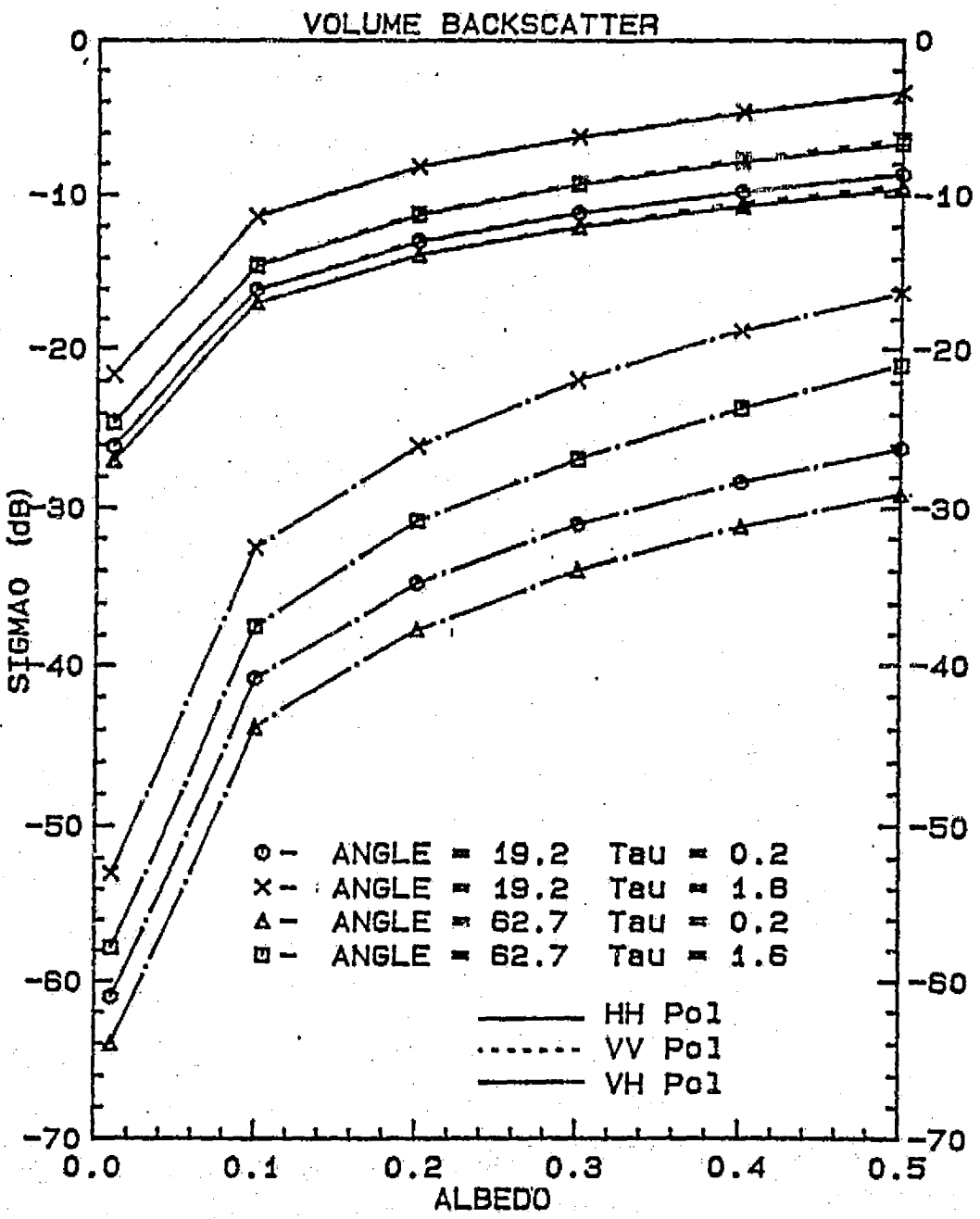
VOLUME BACKSCATTER
SIGMA0 (dB)
0
-10
-20
-30
-40
-50
-60
-70
0.0
0.1
0.2
0.3
0.4
0.5
ALBEDO
ANGLE = 19.2 Tau = 0.2
ANGLE = 19.2 Tau = 1.8
ANGLE = 62.7 Tau = 0.2
ANGLE = 62.7 Tau = 1.6
HH Pol
VV Pol
VH Pol

Figure C.5(c)

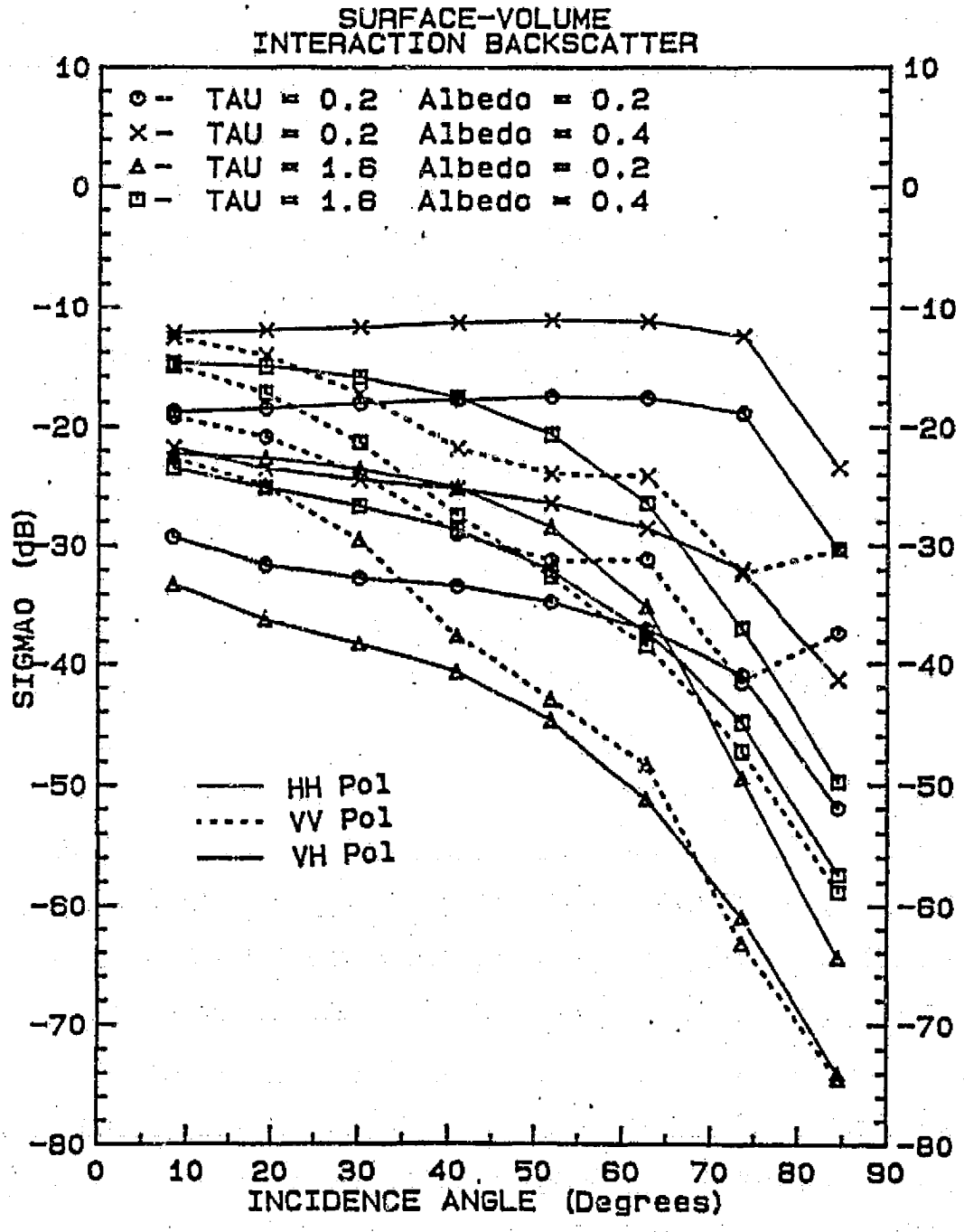

Figure C.6 Computed surface-volume interaction backscattering as a function of (a) incidence angle, (b) optical thickness (τ), (c) albedo (ω), and (d) $k\sigma$ under various conditions.

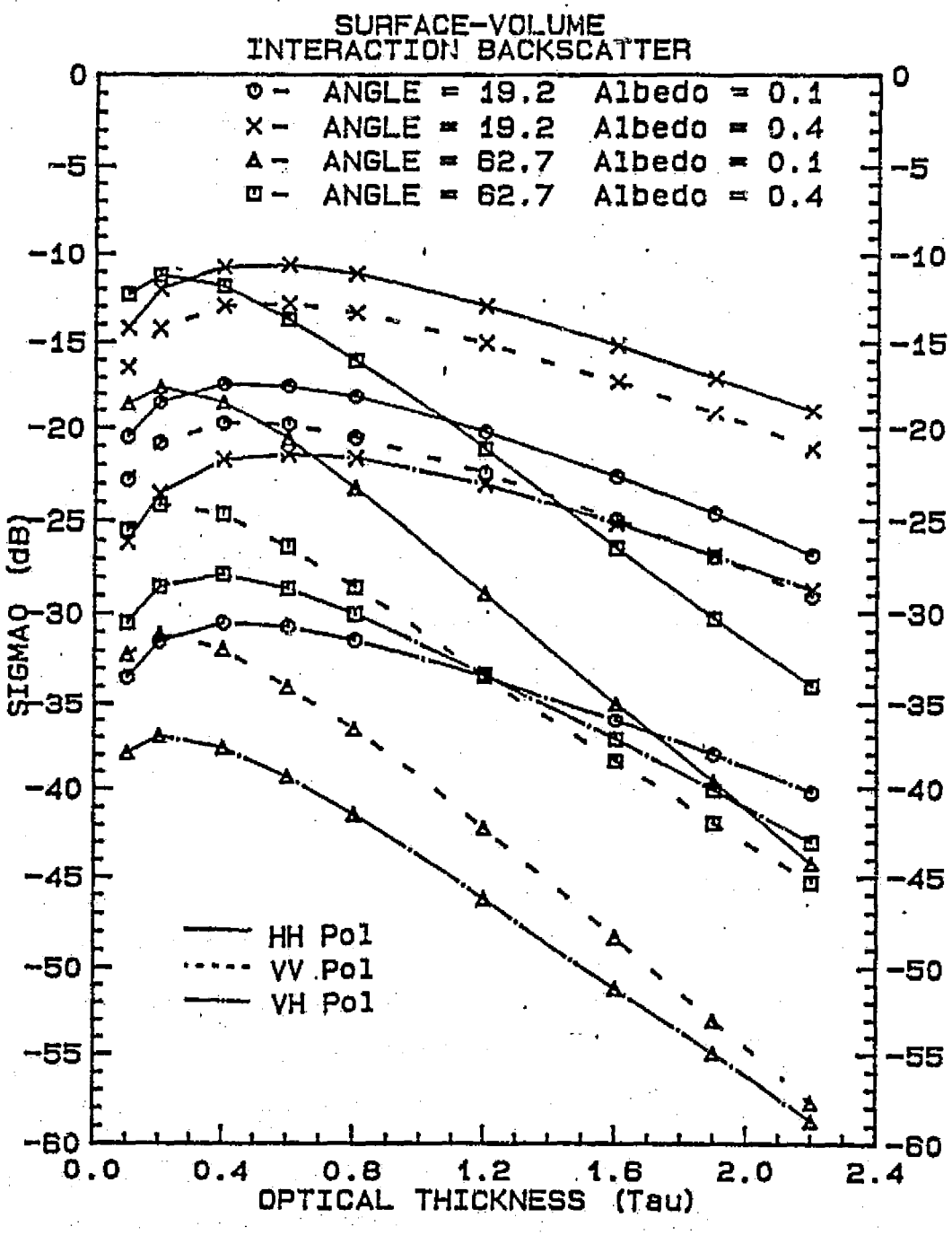
SURFACE-VOLUME
INTERACTION BACKSCATTER
ANGLE = 19.2 Albedo = 0.1
ANGLE = 19.2 Albedo = 0.4
ANGLE = 62.7 Albedo = 0.1
ANGLE = 62.7 Albedo = 0.4
HH Pol
VV Pol
VH Pol
SIGMA0 (dB)
OPTICAL THICKNESS (Tau)
0
-5
-10
-15
-20
-25
-30
-35
-40
-45
-50
-55
-60
0.0
0.4
0.8
1.2
1.6
2.0
2.4

Figure C.6(b)

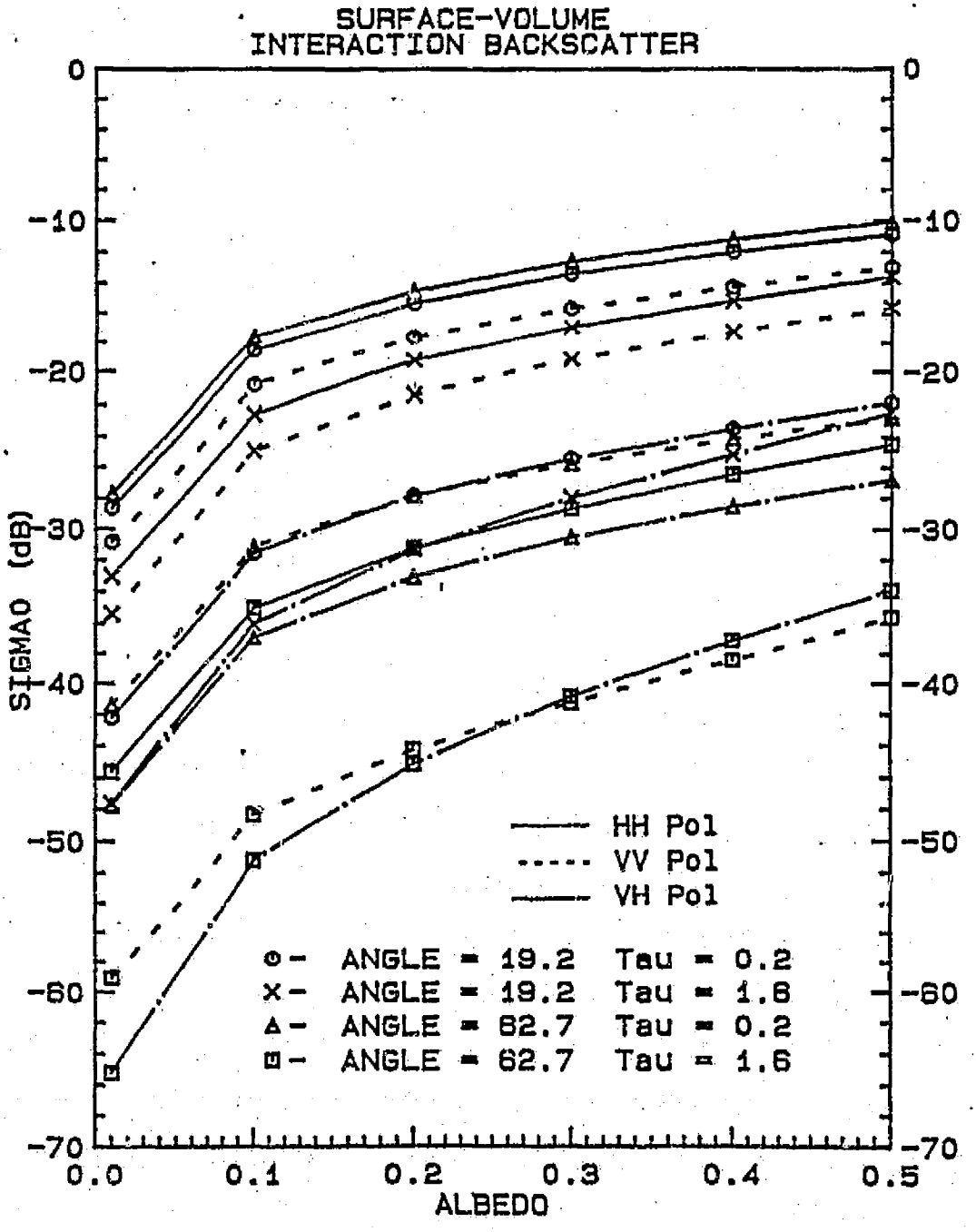
SURFACE-VOLUME
INTERACTION BACKSCATTER
SIGMA0 (dB)
ALBEDO
0
-10
-20
-30
-40
-50
-60
-70
0.0
0.1
0.2
0.3
0.4
0.5
HH Pol
VV Pol
VH Pol
ANGLE = 19.2 Tau = 0.2
ANGLE = 19.2 Tau = 1.6
ANGLE = 62.7 Tau = 0.2
ANGLE = 62.7 Tau = 1.6

Figure C.6(c)

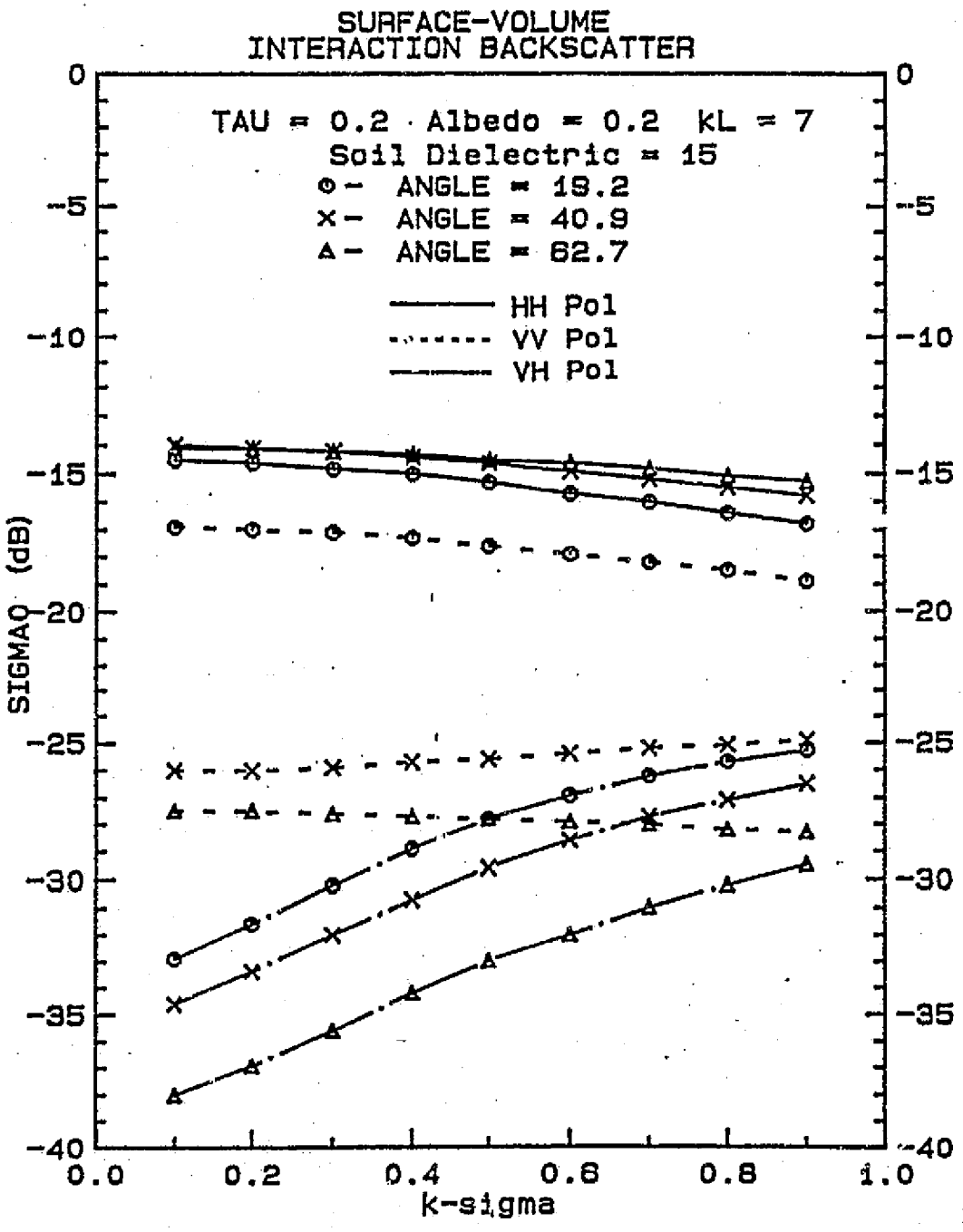
SURFACE-VOLUME
INTERACTION BACKSCATTER
TAU = 0.2 · Albedo = 0.2 kL = 7
Soil Dielectric = 15
ANGLE = 18.2
ANGLE = 40.9
ANGLE = 62.7
HH Pol
VV Pol
VH Pol
SIGMA0 (dB)
k-sigma
0
-5
-10
-15
-20
-25
-30
-35
-40
0.0
0.2
0.4
0.6
0.8
1.0

Figure C.6(d)